Optimal Control of Regulated and Liberalized Power Systems: A Passivity-based Approach

Zur Erlangung des akademischen Grades eines
DOKTORS DER INGENIEURWISSENSCHAFTEN (Dr.-Ing.)
von der KIT-Fakultät für
Elektrotechnik und Informationstechnik
des Karlsruher Instituts für Technologie (KIT)
angenommene

DISSERTATION

von
Pol Jané Soneira, M.Sc.
geb. am 19.12.1994 in Barcelona, Spanien

Tag der mündlichen Prüfung:	24.11.2025
Hauptreferent:	Prof. Dr.-Ing. Sören Hohmann
Korreferent:	Assoc. Prof. Dr. Ionela Prodan

Preface

First and foremost, I would like to thank my supervisor, Prof. Dr.-Ing. Sören Hohmann, for his continuous support, guidance, and encouragement throughout my doctoral studies. The trust placed in me since the very beginning of this journey has been invaluable, and I am grateful for the opportunities to grow both personally and professionally under his mentorship. Also, I would like to thank Ionela Prodan for giving me the opportunity to work in his research group in France, for showing me the ropes of the research world, and for her continuous, incredible support and guidance in both professional and personal matters.

Furthermore, I would like to express my gratitude to the entire IRS team for the filling the everyday with a positive and collaborative atmosphere. Bertus, Armin and Felix, thank you for the countless enriching discussions over the finest mathematical details, and for the hours spent together in and outside the office. I owe them, and also Lukas, a special thanks for the careful proofreading of the thesis.

This journey would not have been possible without the unwavering support of my family and friends. I am deeply grateful to everyone who stood by me and brought joy to my everyday life. Special thanks to Claudio, Jm, Nico and Ankush for all the memorable moments and laughter; to Marc, Edu, Kilian, Cata, Nadine, and Joanna for their constant presence and being there for me; and to Aina, Clara, Carlota, and Claudio for their ongoing support and shared laughter throughout these years. I am especially thankful to my entire family, in particular to my parents, sister and brother, whose belief in me and steadfast support have guided me from the very beginning, and to my grandparents, whose influence during my childhood I believe to have shaped who I am today. Finally, I would like to thank you, Maya, for your love, for endless proofreading, and for the unwavering support basically everywhere as much as you could, and even more, every single day during all these years. Thank you all for providing the necessary control input to my life in order to create a robust and attractive positive invariant set called day-to-day life.

Karlsruhe, 2nd December 2025

Pol Jané Soneira

Abstract

Optimization has played a central role in the planning and operation of power systems since the inception of electric energy. Nowadays, the ongoing transition towards renewable energy introduces significant challenges for current power system operations. The unpredictable nature of renewable sources, combined with existing market regulations, has led to declining system stability and operational inefficiencies. This thesis develops optimization-based control frameworks specifically designed to address these emerging challenges in both present and future power systems. The contributions span from formal theoretical advancements to practical implementations. On one hand, the thesis presents fundamental contributions to optimization algorithms, employing passivity theory to establish local design criteria for optimality and convergence in distributed optimization. On the other hand, it proposes two distinct control frameworks tailored to future power systems. The first framework envisions a regulated power system, where individual agents do not pursue profit-driven objectives. The second framework introduces the novel concept of passivity-based economic ports, enabling a liberalized power system. These frameworks are compared, and their respective strengths and weaknesses in various scenarios are discussed. All control frameworks and theoretical results presented in this dissertation leverage passivity theory. The integration of passivity theory and optimization, which forms the core of this work, provides a pathway toward efficient and stable control of future power systems.

Kurzfassung

Optimierung ist seit Beginn der Verbreitung elektrischer Energie ein zentrales Werkzeug für die Planung und den Betrieb von Energiesystemen. Der aktuell stattfindende Übergang zu erneuerbaren Energien, motiviert durch den Wunsch nach Klimaneutralität, stellt jedoch erhebliche Herausforderungen für den Betrieb von Energiesystemen dar. Die Volatilität erneuerbarer Energien führt zusammen mit den bestehenden Marktregulierungen, die auf vorhersehbare Einspeisungen ausgelegt sind, zu immer größer werdenden Stabilitätsproblemen und einer ineffizienten Betriebsweise. Diese Dissertation zielt darauf ab, optimierungsbasierte Regelungskonzepte zu entwickeln, die speziell darauf ausgelegt sind, die Herausforderungen zukünftiger Energiesysteme zu bewältigen. Die Beiträge dieser Dissertation reichen von formalen theoretischen Methoden bis hin zu deren Anwendung in elektrischen Energiesystemen. Zum einen werden grundlegende Beiträge zu Optimierungstheorie präsentiert, in denen lokale Designanforderungen für Optimalität und Konvergenz in der verteilten Optimierung entwickelt werden. Zum anderen werden zwei konkrete Regelungskonzepte für Stromnetze vorgeschlagen, die die Herausforderungen zukünftiger Energiesysteme adressieren. Diese Regelungskonzepte unterscheiden sich konzeptuell: Das erste Regelungskonzept führt zu einem vollständig regulierten Energiesystem, in dem einzelne Akteure keine eigenen Ziele verfolgen. Das zweite Regelungskonzept führt das im Rahmen dieser Dissertation entwickelte, neuartige Konzept der passivitätsbasierten ökonomischen (engl. economic) Ports ein und resultiert in einem liberalisierten Energiesystem. Diese beiden Regelungskonzepte werden verglichen und ihre Vorteile und Nachteile werden in verschiedenen Szenarien diskutiert. Alle entwickelten theoretischen Methoden und praktischen Regelungskonzepte dieser Dissertation nutzen die Passivitätstheorie. Die Kombination von Passivitätstheorie und Optimierung, die im Kern dieser Dissertation verankert ist, liefert einen Beitrag hin zu einer effizienten und stabilen Regelung zukünftiger Energiesysteme.

Resumen

La optimización ha sido una herramienta fundamental en la planificación y operación de la red eléctrica desde el comienzo de la proliferación de la energía eléctrica. Sin embargo, la actual transición hacia las energías renovables presenta desafíos significativos para la operación de la red eléctrica. La naturaleza impredecible de las energías renovables junto con las regulaciones existentes del mercado eléctrico actual, concebidas para organizar generación planificable, crean problemas de estabilidad y una operación ineficiente. Esta tesis tiene como objetivo desarrollar nuevos conceptos de control para la red eléctrica basados en la optimización, diseñados específicamente para operar una gran cantidad de generación renovable. Las contribuciones de esta tesis abarcan tanto el desarrollo de métodos matemáticos teóricos como su aplicación práctica en conceptos de control. Por un lado, esta tesis presenta contribuciones fundamentales en el área de optimización, utilizando la teoría de pasividad para establecer por primera vez requisitos de los algoritmos para garantizar optimalidad y convergencia en la optimización distribuida. Por otro lado, esta tesis propone dos conceptos de control para la red eléctrica del futuro. El primer concepto de control resulta en un sistema eléctrico regulado, donde cada agente implementa un controlador predefinido en lugar de perseguir objetivos propios. En contraste, el segundo concepto de control introduce la noción de puertos económicos basados en la pasividad, desarrollada en esta tésis, creando un sistema eléctrico liberalizado. Todos los conceptos de control desarrollados en esta tésis, así como los resultados teóricos, utilizan la teoría de pasividad. La combinación de la teoría de pasividad y la optimización, que forma la base de esta tesis, pretende allanar el camino hacia un control eficiente y estable de los sistemas eléctricos del futuro.

Contents

1 Introduction

Optimization lies at the very core of power systems. Since the deployment of interconnected power systems in the first half of the last century, practitioners have asked themselves how to properly allocate the load economically among the available generating units [Hap77]. Prior to the 1930s, heuristic methods were used, such as the base load method, where units are successively loaded up to maximum capacity starting from the most efficient unit [Sta30]. A similar heuristic method is called best point loading, where the units are successively loaded only up to their most efficient operating point, again starting from the most efficient unit [Sta31; Hap77]. Thereafter, simplified versions of the economic dispatch optimization problem were proposed [Hah31; SS+43], culminating years later in the precise formulation of the optimal power flow (OPF) problem by Carpentier in 1962 [Car62]. The main novelty was considering constraints on the node voltages and transmission line capacities by employing the Karush-Kuhn-Tucker (KKT) conditions, which had first been published a few years before, to characterize the optimal solution. Nowadays, the OPF problem forms the basis for the planning and safe operation of power systems all around the globe [COC+12].

After the shift from *regulated* to *liberalized* power systems in the 1980s, new profit-driven actors and energy markets emerged. Despite this fundamental change of the power system structure, *optimization* has remained the core principle behind power system operation. The bidding and offering mechanism employed in energy markets is aimed at ensuring that all generators operate at marginal cost,[1] thus serving the loads by minimizing the generation costs [KS04; Tay15; Pin23; PZP10]. It can be shown that all operating points resulting from an appropriate energy market can be traced back to solving an optimization problem to minimize the generation costs under the constraint of serving the loads in a power system.[2] Both the importance and scale of this kind of optimization becomes apparent when taking into account that the electrical energy generated each year in the EU is around 2800 TWh [Eur24]. Lowering the electric power generation by just $1\,\%$ using a suitable optimization would thus reduce the cost of energy generation by 13 billion euros each year based on the electricity prices in 2022 [Eur23; Age23], or the tons of CO_2 emissions by 7 million.

The last example shows that optimizing electric power generation also plays a role in reducing CO_2 emissions, a task that is becoming increasingly important for humanity. After decades of using fossil fuels to satisfy our energy requirements, it has become

[1] This means that the generators maximize their own profit, see [KS04, p. 28].

[2] Such an operating point is often called Pareto efficient in the literature primarily focusing on an economic perspective. It is a well-known result of microeconomic theory that market equilibria are Pareto efficient, which results from the first and second fundamental theorems of social welfare [KS04; MCWG+95; Var92].

clear that the resulting human-induced climate change is one of the major threats to humanity. To provide remedy, governments around the globe have set up agendas for a transition to a sustainable energy supply [EC16; HZZ20; Con22; Nor17; Int20]. One example is the European Climate Law [Cou21], which obliges all EU member states to reduce their net greenhouse gas emissions to zero by 2050[3] and is informally known as the European Green Deal. This ambitious goal brings along major technological disruptions:

- A shift from conventional, fossil fuel-driven large power plants towards distributed generation units (DGUs), based on renewable energy sources like wind power, biomass, photovoltaic or green hydrogen is observed. The majority of these DGUs are strongly weather-dependent and have to be placed where favorable local conditions are expected, i.e., potentially far from industrial load centers. This *volatility* severely complicates the fundamental task of ensuring that the power generation meets the demand at all times and locations.
- The majority of the DGUs are interfaced via power electronics to the main grid. This creates a physical separation of the inertia, e.g., the rotating masses in wind power plants or other generators, from the main grid. The reduction of grid inertia inevitably leads to a power system with *smaller time constants*, more prone to large state deviations and instability when disturbances occur [Mil+18].
- The large number of DGUs in future power systems together with their intrinsic volatility implies that power systems experience frequent *changing network configurations* and power flows. Typical examples are disconnections of DGUs due to lack of power, or of battery storages, such as electric vehicles, due to user preferences.

As a direct consequence of these developments, many adverse phenomena have been reported. For example, a significant increase of deterministic frequency deviations closely linked to the volatile injection of renewable energy sources [KSW21; WRL18; Eur20; HMDB21], resonance problems between converter controls and power lines [Buc+15; Aeb+12], or new types of instabilities due to converter control interactions at small time scales [Mar+21; KCRC24]. All these stability issues are due to power electronics and have not been observed in traditional, synchronous generator-dominated systems.

From a system theoretical perspective, the large number of small DGUs required to meet the energy demands of modern societies transforms the power grid into a large-scale, multi-agent dynamic system.[4] Furthermore, the networked dynamic system has to cope with increasingly frequent variations in its system dynamics due to network changes as outlined above, which further challenges a stable system operation. Since the

[3] Germany committed to further reducing emissions and impose climate neutrality for the year 2045 after a sentence from the Federal Constitutional Court in 2021 [Deu19; Deu21].

[4] Assuming an average capacity of 1 MW for renewable energy sources (only wind or solar photovoltaic), compared to 1 GW for a conventional synchronous generator, there are currently approximately 3,000 renewable units per conventional generator in the grid – a ratio that continues to rise [Umw25].

mathematical analysis of large-scale power systems is prohibitive due to the problem size and due to the combinatorial explosion of network configurations to analyze, *local stability certificates* for assessing stability of the networked power system turn out to be crucial for future power systems. Furthermore, *distributed operation* strategies are imperative in such a networked system with a large number of actuators pertaining to different, competitive entities. In particular, distributed coordination and optimization algorithms, where the optimizing agents can leave or rejoin the optimization, are necessary for the vital task of power system optimization.

The consequences of the transition to a sustainable power system are, however, not only affecting the technical side of power systems. The current regulations and structure of the optimization in power systems, comprising energy market and normative interventions originally set up in order to ensure a secure operation, are not designed for such a *volatile* power system. Rather, the current optimization structure and regulations are designed for a system with predictable loads and controllable generation reliably participating in the energy market. Due to the already ongoing increasing penetration of volatile, renewable energy sources, the cost of *normative interventions* in the energy market solution has grown from 0.5 billion euros in 2013 to 4.5 billion euros in 2022 in Germany [Bun20; Bun24b]. These normative interventions lead to increasingly strong deviations from the optimal, Pareto-efficient solution resulting from the energy market, making it ineffective. Nevertheless, experts agree that an effective optimization is an essential part of a sustainable power system [SNG20; PFV16; BZ11; Tay15], calling urgently for new approaches tailored to the novel challenges arising in future power systems.

The fundamental problems that are behind the challenges in future power systems as described above are, and have been, widely studied in automatic control theory from a theoretical perspective, in particular in the areas of networked control systems and distributed optimization [Mol+17; Yan+19; Lun19]. Thus, contributions from automatic control are expected to play a central role in the development of operation and control strategies for future power systems. Bridging this gap, the thesis at hand is devoted to designing optimization-based control frameworks that are tailored to the novel challenges of future power systems. This dissertation develops and explores different optimization-based control frameworks; one considering the principles of a *liberalized* market with competitive agents, and another considering a fully *regulated* system in which the agents cooperatively solve a network-wide optimization problem in a distributed manner. Throughout the work, *local stability and optimality* certificates play an important role. Motivated by the specific needs of future power systems, this thesis also presents original contributions to automatic control theory in the field of distributed optimization. Thus, the thesis at hand aims to bridge the gap between automatic control theory and the challenges arising in current and future power systems. The overall objective of this work can be summarized as follows:

Objective of the Thesis
Design distributed control frameworks allowing for an optimal operation of future, large-scale and networked power systems that are volatile, undergo frequent changing network configurations and have fast and nonlinear dynamics.

1.1 Structure of the Thesis

A visual overview of the structure of the thesis is shown in Figure 1.1. The thesis is structured as follows: Chapter 2 gives an overview of the existing methods addressing the Objective of the Thesis. At the end of the chapter, the research gaps in the existing literature are identified and the contributions of this dissertation are stated. Chapter 3 introduces the necessary theoretical background to develop the novel theory in Chapters 4 – 6, which constitute the main part of this work. Chapter 4 presents a centralized control framework for optimal control of networked power systems based on Model Predictive Control (MPC). Chapter 5 presents a novel distributed optimization algorithm suited for solving the global MPC problem arising in the previous chapter (Chapter 4) in a distributed manner. Chapter 6 presents a novel control framework based on a control theory-inspired price-forming mechanism, which is especially suited for volatile and highly dynamic power systems. Lastly, Chapter 7 compares the control frameworks presented in Chapter 4 (using the distributed optimization method presented in Chapter 5) and Chapter 6 via simulations. Chapter 8 closes this thesis with a conclusion.

1.2 Notation

The set of natural numbers is denoted by $\mathbb{N}$, the set of real numbers by $\mathbb{R}$, and the set of positive real numbers by $\mathbb{R}_{\geq 0}$. The set of n-dimensional real-valued vectors is denoted by $\mathbb{R}^n$ and the set of $n \times n$ real-valued matrices by $\mathbb{R}^{n \times n}$. The set of k times continuously differentiable functions is denoted by $\mathfrak{C}^k$. All other sets are described by calligraphic letters $\mathcal{A}$. The interior and boundary of a set $\mathcal{A}$ is denoted by $\text{int}\{\mathcal{A}\}$ and $\text{bnd}\{\mathcal{A}\}$, respectively. The cardinality of a set $\mathcal{A}$ is denoted by $|\mathcal{A}|$. Consider some $x_{\min} < x_{\max}$. The set $\{x \in \mathbb{R} \mid x_{\min} \leq x \leq x_{\max}\}$ is denoted in shorthand notation as $[x_{\min}, x_{\max}]$.

The transpose of a vector $\boldsymbol{x} \in \mathbb{R}^n$ is written as $\boldsymbol{x}^\top$. The vector $\boldsymbol{x} = \text{col}\{x_i\}$ and matrix $\boldsymbol{X} = \text{diag}\{x_i\}$ are the $n \times 1$ column vector and $n \times n$ diagonal matrix of the elements x_i, $i = 1, \ldots, n$, respectively. The operator $\text{col}\{\cdot\}$ describes also the vertical concatenation of vectors, i.e., $\boldsymbol{x} = \text{col}\{\boldsymbol{x}_i\} \in \mathbb{R}^{nN}$ with $x_i \in \mathbb{R}^N$, $i = 1, \ldots, n$. Let $\boldsymbol{I}_n$ denote the $n \times n$

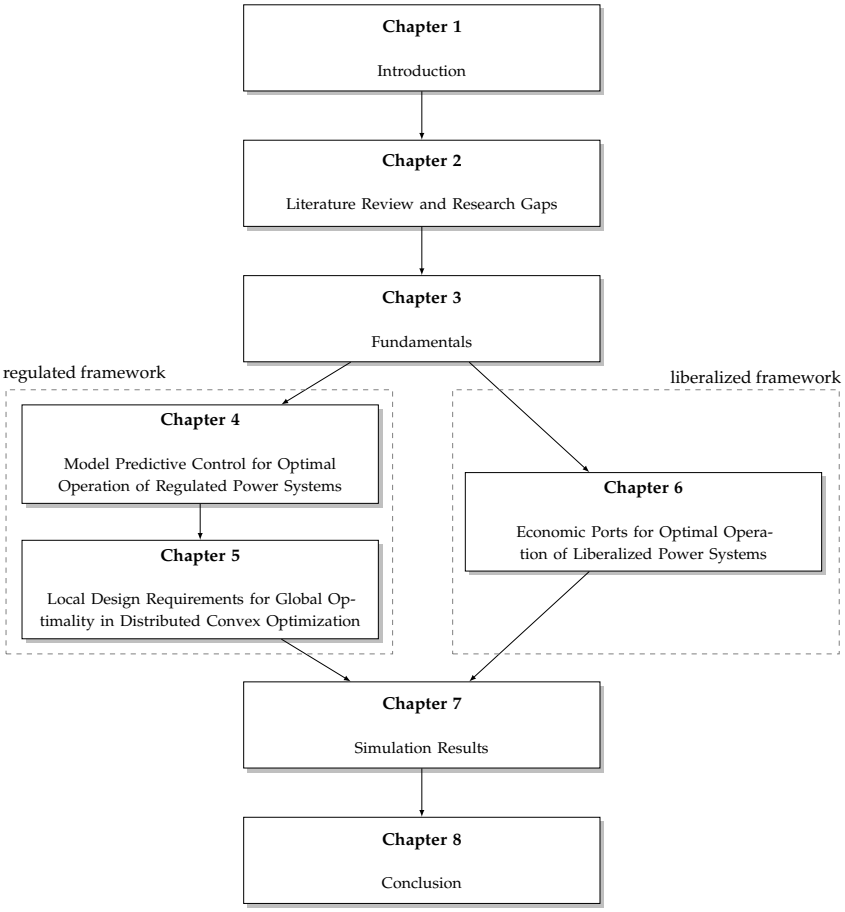

Figure 1.1: Outline and structure of this thesis.

identity matrix, and $\mathbf{1}_n \in \mathbb{R}^n$ a vector of ones. The $n \times l$ matrix of zeros is denoted by $\mathbf{0}_{n\times l}$. A vector of zeros is denoted by $\mathbf{0}$, and $\mathbb{1}_n^k$ denotes a vector of zeros of length n with a 1 in the k-th entry. When clear from the context, the subscripts indicating the dimension of the vectors and matrices $\mathbf{0}$ and $\mathbf{1}$ are omitted. The maximum and minimum eigenvalues of $\boldsymbol{X}$ are denoted as $\mathrm{eigmax}\{\boldsymbol{X}\}$ and $\mathrm{eigmin}\{\boldsymbol{X}\}$. The maximum and minimum entry of a matrix is denoted as $\max\{\boldsymbol{X}\}$ and $\min\{\boldsymbol{X}\}$, respectively.

The euclidean norm of a vector x is denoted by $\|\boldsymbol{x}\|$. The $\boldsymbol{P}$-weighted norm of a vector $\boldsymbol{x}$ is $\|\boldsymbol{x}\|_{\boldsymbol{P}} \coloneqq \boldsymbol{x}^\top \boldsymbol{P}\boldsymbol{x}$, where $\boldsymbol{P}$ is a positive definite matrix. The Kronecker product of $\boldsymbol{x}$ and $\boldsymbol{y}$ is denoted by $\boldsymbol{x} \otimes \boldsymbol{y}$. The Kronecker product of a matrix $\boldsymbol{A}$ with the identity matrix $\boldsymbol{I}_n$ is denoted in shorthand notation by $\boldsymbol{A}_\circ$. The Hadamard product of vectors $\boldsymbol{x}$ and $\boldsymbol{y}$ is denoted by $\boldsymbol{x} \circ \boldsymbol{y}$.

The gradient $\nabla_x f : \mathbb{R}^n \to \mathbb{R}^n$ of a scalar, multivariable function $f : \mathbb{R}^n \to \mathbb{R}$ is defined

as the column vector. The subscript indicates with respect to which variables the partial derivative is taken, if the function has multiple variables. The time derivative of a function $V(t)$ is denoted by $\dot{V} \coloneqq \frac{\mathrm{d}V}{\mathrm{d}t}$.

Graphs are described with the calligraphic letter $\mathcal{G}$. A directed graph is denoted by $\mathcal{G}(\mathcal{A}, \mathcal{E})$, where $\mathcal{A}$ is the set of agents and $\mathcal{E} \subset \mathcal{A} \times \mathcal{A}$ the set of edges. The incidence matrix $\boldsymbol{E} \in \mathbb{R}^{|\mathcal{A}| \times |\mathcal{E}|}$ is defined as $\boldsymbol{E} = (m_{ij})$ with $m_{ij} = -1$ if edge $e_j \in \mathcal{E}$ leaves node $v_i \in \mathcal{A}$, $m_{ij} = 1$ if edge $e_j \in \mathcal{E}$ enters node $v_i \in \mathcal{A}$, and $m_{ij} = 0$ otherwise.

Consider a time-dependent variable $x(t)$. An equilibrium point (or steady state) of this variable is denoted by $\bar{x}$, and $\tilde{x}(t) \coloneqq x(t) - \bar{x}$. The time dependence of variables is omitted when clear from the context.

2 Literature Review and Research Gaps

In this chapter, a detailed review of the existing work considering optimization and control tailored to future power systems is presented. Building upon the existing work, the contributions of this dissertation are stated after identifying research gaps in the current literature. AC and DC systems are considered throughout the chapter, since the focus of this thesis lies rather in the conceptual control framework design and structure than in the type of power system studied.

This chapter is structured as follows. Section 2.1 reviews the control and optimization used in current power systems to provide the basis for the subsequent literature review and for the contributions of this dissertation. In Section 2.2, a classification of control methods for power systems is proposed and important terms within this work are introduced. In Sections 2.3-2.5, a detailed review of the current research considering optimization-based control tailored to future power systems is presented and five major research gaps are identified. Section 2.6 concludes the chapter with the main contributions of this dissertation in the light of the research gaps identified in the preceding sections.

2.1 Current Power Systems Optimization and Control

In this section, the hierarchical control structure and optimization in current power systems is reviewed in Section 2.1.1 and Section 2.1.2, respectively. In particular, the focus lies on how control and optimization are interconnected and what implications the current trend to renewables entails for the existing control and optimization structure. Section 2.1.3 concludes the section with a discussion of the findings from a control-theoretic perspective.

2.1.1 Hierarchical Control of Power Systems

In power systems, two important variables are controlled, the frequency and the voltage [Mac+20; GECC18]. In the following, the control hierarchy for both control loops is reviewed. At a power system level, the transmission system operator is responsible for maintaining both of these variables in an admissible range. Considering a small resistance to reactance ratio in transmission lines,[5] the frequency is strongly related

[5] Note that this is not a valid assumption for medium and low voltage lines and cannot be neglected when many controllable devices are installed at those voltage levels.

to the active power and the voltage to the reactive power. Therefore, both control loops are assumed 'virtually decoupled' [GECC18], and are organized in a hierarchical structure.

The goal of the voltage control is to maintain admissible voltage magnitudes during operation. The voltage magnitudes have to be adjusted such that the required reactive power flow is achieved in order to serve the loads requiring reactive power, e.g., induction motors, under-excited synchronous machines, transformers, etc [GECC18]. In order to avoid large voltage drops and to control the power system efficiently, reactive power should be handled locally to the possible extent [GECC18]. The main possibilities practitioners have are the excitation of the synchronous generators, tap changing transformers, and flexible AC transmission systems (known as FACTSs) [GECC18; Mac+20]. Typically, the voltage control structure has two layers. The primary control is responsible for maintaining a constant voltage at some nodes of the system, typically at the generator nodes using the excitation system. The secondary control is then responsible for the proper selection of these reference values at the controller nodes in order to achieve a certain voltage amplitude level on predefined 'pilot nodes' [GECC18]. All in all, the voltage control is an exclusive responsibility of the transmission system operator and is not directly connected to any market, but handled completely with regulations. The goal of each transmission system operator is to fulfill the requirements of maintaining safe voltage levels and stability throughout the transmission system in a cost-efficient manner.

The goal of the frequency control is to ensure that the frequency is kept in an admissible range despite varying loads or volatile generation. For that, the active power generation is changed according to the frequency variations. This is done in a hierarchical structure comprising three layers, viz. primary, secondary and tertiary control. The primary control is also called frequency containment reserve in the grid codes [Eur16; Dö+19]. It defines a static, linear relation between the frequency deviation and the change in power generation, which is inspired by the dynamics of a grid-connected synchronous generator. It acts instantaneously and has to feed in the increased power generation defined by the droop[6] curve after a maximum of $30\,\mathrm{s}$ [Eur16, Table 5]. The secondary control, also called automatic frequency restoration reserve, is described in Articles 143-145 in the Commission Regulation (EU) 2017/1485 [Eur17a]. The control target of the secondary control is to 'regulate the frequency control error towards zero within the time to restore frequency' [Eur17a, Article 143, §1 (a)]. The time to restore frequency is set to $15\,\mathrm{min}$ in the Central Europe area of ENTSO-E, and it must 'have a proportional-integral behavior' and an anti-windup [Eur17a, Article 145, §4 (b)-(c)].[7] Further, it is specified that the frequency error is the control input, and the setpoint for the droop

[6] The droop curve defines a linear relation between frequency deviation and increased power generation, and is standard in power systems [Mac+20, p. 32].

[7] Note that more advanced control strategies are not allowed within the current European operational regulation framework. Similarly, more advanced automation technologies, e.g., to consider various measurements and divide an averaged control error over various controllers as very popular in current research [Oli+14; SP+15], are not envisaged in the regulations.

controllers the output. The tertiary control, also called manual frequency restoration reserve, has a similar goal as the secondary control, i.e., to regulate the frequency deviation to zero. However, this is done manually by the transmission system operator depending on the actual load situation to achieve other goals such as to minimize costs or maintain the scheduled power imports or exports. Also, both the activation time and the maximal duration of the control action, i.e., the additional power generation, may vary with respect to the secondary control. Every transmission system operator is obliged to implement such a strongly regulated hierarchical control structure, but has the freedom to decide how much capacity is allocated in each layer. This has to be done in order to comply with the frequency quality requirements based on a probabilistic methodology [Eur17a, Article 128, 157 (c)].

All in all, the frequency control is a strongly regulated control architecture, with regulations on both economic and operational aspects. This considerably limits the possibilities for more advanced control methods to be applied. However, the frequency control has also a tight connection to optimization over the European electricity balancing market as detailed in [Eur17b, Title II]. This is further explored in the next section.

2.1.2 Optimization in Power Systems

The optimization in current power systems is achieved through the energy market [Eur19] and the energy balancing market [Eur17b]. In the energy market, producers can offer a certain power generation for imbalance settlement periods of $15\,\mathrm{min}$. Consumers submit bids for every time period and a corresponding maximal price, which they are willing to pay. All offers and bids are submitted $24\,\mathrm{h}$ in advance. The energy market computes then the intersection of the price curves resulting from the aggregated offers and bids, respectively, and a price is set for the market clearing. This has been shown to, theoretically, represent a Cournot competition model, and thus result in Pareto-efficient market equilibria [KS04; Tay15], [Koe22, p. 52ff.], provided that no producer is large enough to exercise market power and the trading structure fulfills the requirements of a perfect market with perfect competition (see [Koe22, Definition A.24]).

A major challenge with this approach is that both the load and a significant portion of the generation, i.e. renewable generation, are considered in the energy market based on forecasts for each imbalance settlement period. As a result, discrepancies between predicted and actual values are common, especially in systems with a high share of renewable energy resources. These imbalances are covered with balancing energy traded at the balancing market. Concretely, the balancing services are traded in two separate market schemes, the balancing capacity and the balancing energy markets. Procuring balancing capacity means that the availability of a certain balancing power over a certain time period is secured. The balancing energy market decides which of the available balancing capacity is actually used. The transmission system operators are responsible for the procurement of sufficient balancing capacity in advance using merit-order, similar as with the energy market. This balancing capacity is activated

by following a new merit-order list [Eur17b, Article 29 §7], possibly including offers corresponding to unforeseen, low-cost, short-term power generation capacities, e.g., pumped-storage power plants after unforeseen rainfalls. This scheme is designed to improve the overall efficiency by including less predictable balancing capacities, but at the same remunerating the market participants that reserved balancing capacity. The result of the balancing market is again a Pareto-efficient allocation of the balancing capacity. The balancing power control structure can be understood as a Pareto-efficient correction for the energy market.

2.1.3 Discussion

In this subsection, the overall structure of control and optimization in current power systems as outlined in the two past sections is discussed from a control-theoretical point of view. This allows illustrating the limitations of the current optimization and control structure, especially when considering a large share of renewable generation, which emphasizes the need for novel methods tackling these shortcomings.

The connection between optimization and control in power systems relies on the balancing market.[8] The different balancing capacity offers correspond to the primary, secondary and tertiary control, depending on their 'mode of activation' [Eur17b, Article 2 §34], i.e., closed-loop or manual, and other requirements specific to each control layer.[9] The balancing market can thus be understood as a market for the different control actions, resulting in a Pareto-efficient allocation of control actions.

From a control-theoretical perspective, the energy market together with the balancing market represents a combination of a feedback and a feedforward structure (see Figure 2.1). The power generations scheduled in the energy market based on predictions (i.e., the optimization) bring the system near to an admissible steady state and can be seen as the feedforward part. The balancing energy is activated when deviations are measured via a frequency deviation, which corresponds to feedback control. Such a combined feedforward and feedback control is a well-known structure in control theory. The effectiveness of such a structure strongly relies on the quality of the feedforward control [Lun13], which is nowadays compromised by the volatile and weather-dependent generation of renewable energy resources. This raises the question whether a feedforward structure, which proved to be effective for power systems with low uncertainty during the last century, is still an efficient method for the optimization of power systems with a high share of renewable energies.

In addition, the increase of renewable generation is compromising the efficiency of the feedforward structure itself, i.e., the energy market. For every generation schedule

[8] Both balancing markets (capacity and energy), since one determines the commitment of holding balancing power ready and the other the activation, together representing the control action. From here on, we refer to both as the balancing market.

[9] For example, the maximum activation time or the maximum and minimum duration of the delivery period [Eur17b, Article 25].

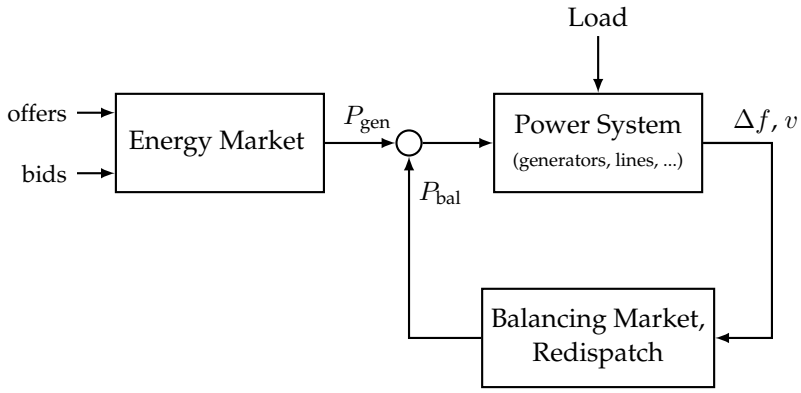

Figure 2.1: Schematic representation of the control and optimization structure in current power systems. The optimization is done in the energy market as a feedforward control.

resulting from the energy market, the transmission system operators have to verify that the technical feasibility constraints, i.e., the maximum and minimum voltage limits or transmission line capacities, are respected. If the safety constraints are not met, a so-called redispatch is invoked. The redispatch is a normative intervention commanding some generators to deviate from the energy market result.[10] This mechanism is necessary because in the energy market, no information of the network characteristics (such as power flow constraints, voltage levels, etc) is considered for computing the generation schedule, i.e., the feedforward control.[11] The volume of the redispatch has increased considerably in the last years: from 14.5 TWh on average in 2016-2019 [Bun20, p. 9], to 34.3 TWh in 2023 [Bun24a, p. 7]. This corresponds to costs of 293 million euro in average for 2016-2019, and 3086 million euro in 2023, as specified in the reports of the Federal Network Regulatory Agency [Bun20; Bun24a].[12]

To put it in a nutshell, optimization and control in power systems are largely decoupled by using a feedforward control structure. However, the recent developments are strongly deteriorating the efficiency of the optimization, i.e., the feedforward control structure. Furthermore, this phenomenon is expected to worsen, since the predictable generators based on fossil fuels are scheduled to be disconnected from the grid in the next few years [Com; Deu19]. Thus, the need for a more efficient optimization arises. In particular, the *small time constants* and *volatility* in future power system call

[10] In 2021, a new Redispatch 2.0 was introduced in Germany, which allows transmission system operators to control also small generators from the distribution system operators.

[11] This is also known as the copper plate assumption.

[12] Notably, the annual report of the Federal Network Regulatory Agency includes a color-coded map of the German transmission system, where five colors indicate the duration of redispatch interventions in hours. In 2017, the highest category was $'\geq 500'$ h; by 2023, this had increased to $'\geq 3000'$ h, clearly illustrating the growing extent of redispatch.

for an optimization in feedback with the system, reacting better to changes and integrating optimization and control in a more efficient way. However, a closed-loop optimization in power systems implies a completely new conception of the control structure, since the optimization in the energy market has always been a feedforward structure (see Figure 2.1).

Before reviewing the existing work in Sections 2.3-2.5, a classification of control methods for power systems along with some important terms for this work are introduced in the next section. The literature review is then structured according to those terms and the proposed classification.

2.2 Introduction of Important Terminology

This section is devoted to defining important terminology for this dissertation. It is composed of two subsections. Section 2.2.1 introduces a classification of power system control philosophies and the necessary terms. Section 2.2.2 introduces the terminology regarding distributed systems used in the rest of the dissertation.

2.2.1 Classification of Power System Control Philosophies

In the following, the meaning of the terms *regulated* and *liberalized* are defined in the context of this dissertation. Furthermore, the term *grid* as used in this work is introduced. In this work, the terms *regulated* and *liberalized* power system are employed from a multi-agent systems or control-theoretical perspective. The terms are used to compare the freedom that the agents in a power system have in comparison with an unbundled[13] power system as nowadays. It is mainly distinguished if the individual agents that are part of a power system may freely take rational actions that are distinct of those of other agents, or if the agents are obliged to utilize a given, specific calculation rule for determining their own controllable variables or system inputs. It is important to mention that the terms *regulated* and *liberalized*, even if there are evident connections, should not be understood from a purely economic perspective; the scope of this work is not to provide the legal and economic framing for these methods to be successfully implemented.

With the word *agents* in the following definitions, the entities which are not responsible for the power system operation are denoted. In the current power systems, these agents are, e.g., the producers and consumers that participate in the energy market.

Term 2.1 (technically regulated power system)

[13] Key aspects are the legal, operational and informational unbundling in power systems, see [Bru+14] for details.

A power system is called technically regulated, if the individual agents have to choose their controllable variables, e.g., typically the generated or consumed power, using a specific calculation formula given by a superior or supervising authority, instead of choosing their variables in order to pursue own interests.

Term 2.2 (liberalized power system)
A power system is called liberalized, if the individual agents can freely implement control strategies to pursue own objectives, i.e., to maximize their revenue. In particular, no superior authority may determine the controllable variables of the agents.

Next, the term *grids* is introduced.

Term 2.3 (grid)
An electrical system is called a grid when it fulfills the following conditions:

1. *It is a connected subset of an electric power system.*
2. *It gathers a group of controllable DGUs and uncontrollable loads or generators.*
3. *It can be operated either electrically connected to the remaining power system (connected mode) or as an independent grid (islanded mode).*
4. *In connected mode, it exchanges some kind of information with the other grids forming the power system to achieve global optimality.*[14]
5. *In islanded mode, it does not exchange information with other grids and optimizes itself.*

While a grid is a single entity, a group of interconnected grids is denoted as a *power system* in this work. Similar concepts for describing a decentralized power system structure have been proposed in literature. The web-of-cells concept divides the power system into cells and independent cell coordinators, with the goal of eliminating any superordinate instance gathering information and coordinating the cells [Mar+17; LHK19]. The virtual power plant concept groups several DGUs of different nature as a single, large, dispatchable generator [Hä+23; He+24]. Finally, the microgrid concept originally

[14] The type of information strongly depends on the concrete control approach and especially on the type of power system, regulated or liberalized as in Term 2.1 and 2.2.

proposed in [Las02] has received much attention in the literature. It was originally defined as a small grid in remote areas with a single point of connection to the main grid [Hat+07]. However, alternative definitions describe it as an active distribution network comprising flexibilities [Sch+16; Dan19, Definition 3.1]. A power system is then often described as a network of microgrids [Che+20; WL20; IYA21; ACG18]. Albeit proposing a similar concept in this thesis, the term *grid* as in Term 2.3 is used to avoid confusion.

2.2.2 Important Terminology of Distributed Systems

In the following, the terms *decentralized*, *distributed* and *centralized* control are introduced. Since these terms are sometimes used with different meanings across literature, they are defined here for avoiding confusion.

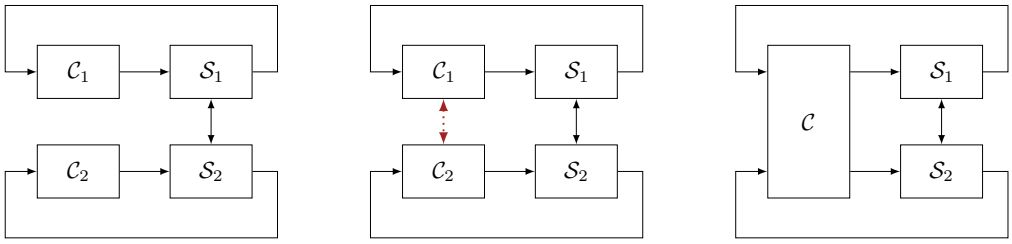

(a) decentralized (b) distributed (c) centralized

Figure 2.2: Decentralized (a), distributed (b) and centralized (c) control structures.

A schematic representation of decentralized, distributed and centralized control is provided in Figure 2.2 for an example with two subsystems $\mathcal{S}_1$ and $\mathcal{S}_2$. A physical interconnection is represented by black lines, and communication is represented by red dotted lines. In decentralized control, each subsystem $\mathcal{S}_1$ and $\mathcal{S}_2$ has an independent controller. The controllers $\mathcal{C}_1$ and $\mathcal{C}_2$ control their subsystem without any communication or information exchange. They rely only on their physical connection (e.g., measurements, control input, etc.) to the subsystem for the control. In distributed control, the independent controllers $\mathcal{C}_1$ and $\mathcal{C}_2$ can additionally exchange information to coordinate their control actions (see red dotted line). In centralized control, only one controller gathering all the information and computing all control actions exists.

In this work, distributed controllers are designed. The subsystems represent the physical grids with all their components. The coordination of the controllers is then designed such that optimality is achieved in order to contribute towards the objective of this thesis stated in Chapter 1.

In the following, the literature review is presented. It is organized as follows. First, in Section 2.3, the control methods for technically regulated power systems are reviewed. Afterwards, since the main limitations of the approaches in the literature arise from the distributed optimization algorithm employed, the existing distributed optimization algorithms are reviewed in Section 2.4. The literature review ends with the control methods for liberalized power systems in Section 2.5.

2.3 Control Methods for Regulated Power Systems

In this section, control approaches in which the producers and consumers have to adopt a given control strategy determining their controllable variables are considered. The vast majority of the control approaches for future power systems proposed in the last years fall into this category. The approaches can be categorized in droop-based, passivity-based, steady-state optimal control approaches, and approaches based on MPC.

Droop-based Approaches

The first category of approaches is droop-based approaches [Gue+10; ZW10; SPDB13; SPDB17; Teg+16; Sch+14]. Droop is an approach widely used in large hydro or steam generators and automatic generation control in traditional AC systems [Mac+20]. It is a proportional controller which provides a fast response in terms of power generation when frequency deviations occur. It is decentralized by nature and establishes a linear relation between the deviation of a desired quantity (frequency or voltage) and the injected power (active or reactive, respectively), called droop slope. Due to the lack of an integral part, droop controllers show a steady-state frequency error, which is compensated via the secondary control. Advantages are a fast response and a flexibly configurable power-sharing capabilities through simple modification of the droop coefficients. Inspired by these ideas, droop control has been transferred to the control of AC and DC power electronics [SPDB13; SPDB17; Teg+16; Sch+14; Oli+14]. Several improvements such as nonlinear [SPDB17], adaptive or dead-band droop have also been proposed to achieve better control performance (see review in [Gao+19]). In [SPDB12; SPDB13], it is shown that a radial lossless power system with droop-controlled inverters and the assumption of constant voltage amplitudes at all nodes and static lines are coupled Kuramoto oscillators. Furthermore, conditions for synchronization, i.e., asymptotic stability of the phase angle variations, are given. In [Sch+14], the assumptions of constant voltage amplitudes and radial networks are relaxed and analytic conditions for the stability are derived by means of Lyapunov theory instead of relying on analogies to the Kuramoto oscillators.

In order to compensate the steady-state deviations from droop control and to achieve a desired power sharing or economic dispatch, various approaches to build on top of

the droop controllers have been proposed [SPDB13; SP+15; DSPB16; SGV14; Kha+20; ZD15]. The work in [SPDB13] proposes a coordination for power setpoints via a consensus algorithm. The authors in [DSPB16] propose a coordination to achieve economic dispatch for AC systems. However, these works rely on assumptions like a radial network, static lines, and static voltages without dynamics. Furthermore, only static power loads are considered, instead of the typical combination of power, current and impedance. The results were extended also to DC systems with voltage droop in [ZD15] employing similar assumptions. In [SGV14], the effectiveness of a secondary control approach for frequency restoration and reactive power sharing is practically demonstrated making use of hardware-in-the-loop. However, stability is only analyzed via simulations. Note that all these methods, built on top of droop-controllers, form a regulated power system as in Term 2.1, since all generators have to implement the given control method rather than being allowed to design a control method for pursuing own objectives.

Remark 2.1. *Note that in current power systems, droop control is also used and is traded in the balancing market. However, the current power system is liberalized. The current power system is liberalized because the setpoints of the generating units arise in the energy market, where every agent takes only into account their own objectives. In the droop-based approaches reviewed above, there exists no energy market, but a (centrally organized) coordination to achieve power sharing or economic dispatch. Clearly, these approaches correspond to a regulated system as in Term 2.1.*

Passivity-based Approaches

Passivity theory (see [SJK12; SP18]) is a powerful approach to the stability analysis of large-scale networked systems. Since power systems are evolving towards large-scale networked, multi-agent systems, passivity theory is finding fruitful applications in the context of power systems, in particular for the stabilization of systems composed of power electronics [Lai+23; Nah+20; Str+21; Wat+21], the coordination of energy sources [Gui+18b; Mal+23; MS20], price-based control [SDPS16b; Köl+21b], or MPC [KA17; Lon+23]. In this subsection, the methods for stabilization and coordination are reviewed. For price-based control (using passivity theory) there is a dedicated section, since it falls into the category of liberalized control methods.

The passivity-based stabilization of power electronics-based DGUs networked with power lines is a mature research topic [Har+16]. The works [Tuc+16; TRFT17] explore separable Lyapunov functions for DC grids, the latter providing conditions that are independent of line parameters. With a separable Lyapunov function the authors are implicitly using the essence of passivity and separable storage functions. However, the controller design requires solving a linear matrix inequality (LMI) every time when a change occurs, e.g., in the load. In [TFT20], the authors extend their methods to AC grids, and in [Nah+20], it is embedded into a formalized passivity-based framework. At the

same time, in [Str+20], similar results are achieved making use of the port Hamiltonian formalism, also for AC grids [Str+19; Str+21]. At the same time, the works in [Lai+21; Wat+19; Wat+21] were proposed by another research group achieving decentralized voltage stabilization also using passivity theory.

Although passivity-based approaches are powerful methods for the stabilization of networked systems, these methods provide no means for the coordination of the individual DGUs. For that, setpoints from a higher level control are typically required. These setpoints are often provided by receding horizon optimization-based controllers [Nah+21; Gie+23; JS+25b], or by passivity-based coordination algorithms [Gui+18b; Mal+23]. In [Gui+18b], the voltage modulated direct power control from [Gui+18a], which is a controller for achieving maximum point power tracking,[15] is cast as a port Hamiltonian controller. They show that each controlled renewable energy source connected to the grid via an inductance is passive w.r.t. the voltage modulated inputs [Gui+18b, Eq. (7)] and the active and reactive power as output. Furthermore, due to the maximum power point tracking, it can be argued that an optimal operation w.r.t. power generation is achieved. Further, the authors show that such a scheme has improved performance when connecting and disconnecting renewable energy resources such as a wind power plant and a photovoltaic plant, but a rigorous consideration of the stability of the networked system (including the battery storage and power lines) is not provided. In [CKS19], current-sharing is achieved based on consensus-like algorithm in grids with constant current loads. In [Mal+23], power sharing is achieved considering a similar scenario but more general constant impedance Z, constant current I, constant power P (ZIP) loads. However, all DGUs use the averaged voltage error, which may lead to voltage configurations with large deviations, when some node voltages with large negative and positive errors compensate each other. In [MS20], a passivity-based power-voltage droop controller is proposed, achieving power sharing. However, only constant impedance loads are considered, and the power-sharing performance is strongly dependent on the load configuration, which hampers an efficient coordination.

All in all, these methods provide powerful tools for stabilization of networked systems. However, the methods for achieving an efficient coordination for the DGUs are limited. In particular, optimization-based approaches have not been proposed so far.

Remark 2.2. *One could argue that passivity-based approaches allow for a liberalized power system, as any controller fulfilling the passivity conditions may be used, and the agents have the freedom to choose their own controller complying with the requirements. However, when it comes to controlling the power injections, all existing methods, as shown above, propose centrally designed power sharing or distributed averaging approaches, giving each agent a specific setpoint to follow, which complies again with technically regulated power systems as in Term 2.1.*

[15] Maximum point power tracking, often called MPPT, is a very popular control method with the goal of operating the renewable energy source always at the operating point with maximum power injection, i.e., the most efficient in terms of power generation.

Steady-state Optimal Control Approaches

In another line of research, authors design controllers steering the power system to steady-state optimal equilibria. In [Hau+16], a feedback optimization constrained to the power flow manifold is first proposed. Instead of periodically computing new OPF solutions and applying the optimal setpoints to the generators, the feedback optimization measures the current state and computes, in real-time using gradient descent, new variables that are closer to the optimizer, eventually converging to an optimal steady state. Such a scheme has two main advantages. Firstly, it can react in real-time to load disturbances. Secondly, it avoids unfeasible states in the transition between two OPF solutions that may arise due to the unconnected and discontinuous nature of the solution set of the nonlinear OPF problem. However, the power system is modeled with the static power flow equations, and the stability of the system including the feedback optimization is not analyzed. This is extended in [Hau+21], with an analysis based on timescale separation, which may not be valid with the trend of smaller time constants in power system dynamics. A survey can be found in [Hau+24].

In [LSM21], the authors propose a system-theoretical framework that recovers various steady-state optimal controllers proposed in the literature as a special case. Similar to the approaches described above, the optimization is a dynamic system in feedback with the plant. This approach derives the controller via an optimality model [LSM21, Definition 3.1]. It is shown that the droop-based approaches [SPDB13; DSPB16] described in Section 2.3, and others like [DG17; ZMD15], are special cases of the proposed method. However, as stated with the droop-based methods, the network model is restricted to simple oscillators connected via lossless power lines, which is insufficient[16] to capture the dynamics occurring in future power systems based on power electronic devices.

There exist other steady-state optimal controllers which correspond, however, to technically liberalized power systems as in Term 2.2 and are thus covered in Section 2.5. They correspond to liberalized power systems because, in contrast to the methods described above, they build a framework consisting of different agents with diverging interests in power systems, such as network operators, market participants, or retail consumers.

Model Predictive Control Approaches

MPC has been extensively studied in the context of power systems, see the surveys [Sul+17; Hu+21]. The objectives are typically to maximize economic welfare or to minimize losses. The constraints ensure power balance through the static power flow equations or even through a simpler power balance equation [Vel+19a; Vel+19b; Ana+20; AOM21]. This procedure assumes an energy system with negligible, stable and non-varying dynamics, such that a simple power balance equation describes the network

[16] An example of issues in a real case is described [Buc+15], where undamped oscillations set equipment on fire in an offshore wind farm.

adequately. Those assumptions, albeit standard in traditional power system analysis with large-scale thermal generators, are questionable for power systems based on power electronics.

To provide remedy, MPC schemes have been proposed considering the dynamics of the underlying power system. The approaches in [Lou+17; Vu+15] consider a droop-controlled microgrid and replace the typical proportional-integral controller necessary to circumvent steady-state deviations with MPC strategies. While in [Vu+15] a central MPC architecture is designed and is thus not suitable for large-scale systems, in [Lou+17] a distributed scheme is proposed. However, both use strongly simplified grid dynamics, including an independent design of the voltage and frequency restoration control. The voltage-frequency decoupling is an assumption valid only for small voltage angles, and only in the case of lossless power lines [Mac+20, p. 8]. Other approaches attempt to directly control the converter voltage without an underlying primary controller [NTG18]. However, the filter dynamics necessitate a sampling time in the range of microseconds, which makes an online solution of the MPC optimization problem feasible only for small grids and short optimization horizons.

To avoid that all agents have to share their private information (such as their objective function) and to alleviate the computational burden in large-scale systems, distributed MPC approaches tailored to power systems have been proposed. One of the first approaches is [Ven+08], which is based on the distributed MPC framework proposed in [VRW05] for regulating a given setpoint of a linear system. Thus, in [Ven+08], a linearized model of the power system describing the frequency deviations depending on the load and generation, also called automatic generation control, is used. The authors show stability of the closed-loop system using the distributed MPC framework with an arbitrary number of iterations larger than one. At convergence, they show to recover the same solution as a centralized MPC. However, the individual agents require information about the system dynamics and objective function of all other agents. The method represents thus merely a mathematical parallelization. Other approaches have been presented in [Par+17; XXM19; Raz+20], however all considering only a static power balance equation describing the power system instead of voltage or frequency dynamics. With such simplified dynamics, the focus of the approaches is the distributed or parallel solution of the optimization problem.

Economic MPC schemes have also been proposed in connection to power systems, see the recent review in [Hu+24]. Economic MPC has the intrinsic advantage that no steady state has to be computed in advance, in contrast to the traditional setpoint-tracking MPC framework [FGM+18; Jia+20] (see Figure 3.2 in Section 3.2). In [Jia+19b], a distributed economic MPC is designed for the combined economic dispatch and load frequency control of interconnected power systems is proposed. The distributed computation is based on the Jacobi iteration [BT97, p. 131], which is merely a mathematical parallelization and assumes that all agents have full information about the other agents. In particular, all agents need full information about the objective functions of other agents. The authors show that the distributed scheme has a comparable performance to the central economic

MPC. However, no stability considerations are provided. In [Jia+20], the results are extended. Detailed algorithms, which the agents have to follow, are provided as well as a stability proof. However, for that the authors assume that the system at hand is dissipative w.r.t. a special supply rate, which automatically provides stability, without showing or arguing why the assumption is valid. In [Jia+19a], a dual-mode economic MPC is designed for a microgrid with a wind power plant, a photovoltaic generator, and a battery storage system. In this method, a fallback stabilizing control action is assumed to be known in advance and applied whenever the system leaves a predefined region. Although the optimization may be computed in a distributed manner, it becomes clear that to check if the system leaves a predefined set around (the whole) network state, information from the whole system is required. This makes the approach not well suited for large-scale systems.

All in all, there exist plenty of methods for the optimization-based control of power systems via MPC. All the approaches allowing a distributed operation — both setpoint-tracking or economic — rely on distributed optimization algorithms to solve the central optimization in a distributed manner. The information the individual agents have to share thus depends on the particular distributed optimization algorithm. As these algorithms are an essential part of these approaches, Section 2.4 reviews the current state of research on these distributed optimization algorithms in more detail.

2.3.1 Summary and Research Gap

There exist plenty of methods for distributed control of regulated power systems. The coordination is achieved through consensus strategies or distributed optimization. All optimization-based approaches in the categories droop, steady-state optimal or MPC consider either very simplified dynamics or rely on centralized computation. The passivity-based methods consider accurate system models, i.e., dynamic models for the lines and power electronic devices allowing for considering varying voltage amplitudes. However, there exist only few passivity-based approaches achieving a coordination between producers, and these approaches can neither consider objective functions for the producers or consumers, nor any state or input constraints, vital for safety-critical systems like power systems. Thus, the following research gap exists:

Research Gap 1

There exist no optimization-based distributed control methods for regulated power systems that simultaneously account for detailed nonlinear models, enforce state and input constraints, and ensure asymptotic stability based on individual subsystem requirements.[17]

2.4 Distributed Optimization Algorithms

As has been shown in Section 2.3, distributed optimization algorithms are widely used in the current research concerning control of future power systems. These algorithms form the basis of, e.g., distributed MPC algorithms, steady-state optimization or consensus-like algorithms (see Section 2.3). The distributed optimization algorithm defines how and which information the individual agents have to exchange, which is central within this thesis. Hence, distributed optimization algorithms are reviewed in this section.

Distributed optimization considers the problem of solving distributed optimization problems with particular structures in a distributed manner. This means that various agents solve parts of the optimization problem and communicate the result in an iterative process, with the goal of cooperatively finding the global minimizer. The approaches can be divided in two categories: methods based on Lagrangian relaxation, i.e., dual decomposition [Con+06], and methods based on multi-agent systems, typically borrowing methods from control theory [Yan+19].

Lagrangian Decomposition Algorithms

The first approaches for distributed optimization are due to Dantzig, Wolfe and Benders [DW60; Ben62] in the 1960s and are known by dual decomposition.[18] It considers optimization problems with a *separable* structure, e.g., for two agents

$$\min_{\boldsymbol{x}_1,\boldsymbol{x}_2} \; J_1(\boldsymbol{x}_1) + J_2(\boldsymbol{x}_2) \tag{2.1a}$$

$$\text{s.t. } \boldsymbol{A}_1\boldsymbol{x}_1 + \boldsymbol{A}_2\boldsymbol{x}_2 = \boldsymbol{b}, \tag{2.1b}$$

[17] Individual subsytem requirements are requirements that have not to be coordinated with the other agents or with some central authority. These are also called local conditions in this dissertation.

[18] The name is due to duality in convex optimization [BV04], which these methods are exploiting. The methods originated from distributed allocation of production capacity in economics.

with objective function $J_1 : \mathbb{R}^{n_1} \to \mathbb{R}$ and $J_2 : \mathbb{R}^{n_2} \to \mathbb{R}$, and matrices $\boldsymbol{A}_1 \in \mathbb{R}^{n_{\text{EQ}} \times n_1}$, $\boldsymbol{A}_2 \in \mathbb{R}^{n_{\text{EQ}} \times n_2}$, $\boldsymbol{b} \in \mathbb{R}^{n_{\text{EQ}}}$ for the $n_{\text{EQ}} \in \mathbb{N}$ equality constraints.[19] Optimization problem (2.1) has a separable structure, because the objective function is composed of a sum of the objective functions of the individual agents. The constraint in (2.1b) couples the optimization problems and prevents a separated computation of the minimizer by each agent. The Lagrange function for (2.1) is

$$L(\boldsymbol{x}_1, \boldsymbol{x}_2, \boldsymbol{\lambda}) = J_1(\boldsymbol{x}_1) + J_2(\boldsymbol{x}_2) + \boldsymbol{\lambda}^\top (\boldsymbol{A}_1 \boldsymbol{x}_1 + \boldsymbol{A}_2 \boldsymbol{x}_2 - \boldsymbol{b}), \tag{2.2}$$

which can be rearranged by separating the terms corresponding to the individual agents to obtain

$$L(\boldsymbol{x}_1, \boldsymbol{x}_2, \boldsymbol{\lambda}) = L_1(\boldsymbol{x}_1, \boldsymbol{\lambda}) + L_2(\boldsymbol{x}_2, \boldsymbol{\lambda}) \tag{2.3}$$

with $L_1(\boldsymbol{x}_1, \boldsymbol{\lambda}) = J_1(\boldsymbol{x}_1) + \boldsymbol{\lambda}^\top (\boldsymbol{A}_1 \boldsymbol{x}_1 - \frac{1}{2}\boldsymbol{b})$ and $L_1(\boldsymbol{x}_1, \boldsymbol{\lambda}) = J_2(\boldsymbol{x}_2) + \boldsymbol{\lambda}^\top (\boldsymbol{A}_2 \boldsymbol{x}_2 - \frac{1}{2}\boldsymbol{b})$. In the dual decomposition algorithm, each agent minimizes a subproblem corresponding to its part of the Lagrange function separately with respect to its own variables, and then the central dual ascent step follows. Concretely, at time step k, it reads

$$\boldsymbol{x}_1^* = \arg\min_{\boldsymbol{x}_1} L_1(\boldsymbol{x}_1, \boldsymbol{\lambda}(k)) \tag{2.4a}$$

$$\boldsymbol{x}_2^* = \arg\min_{\boldsymbol{x}_2} L_2(\boldsymbol{x}_2, \boldsymbol{\lambda}(k)) \tag{2.4b}$$

$$\boldsymbol{\lambda}(k+1) = \boldsymbol{\lambda}(k) + \alpha(\boldsymbol{A}_1 \boldsymbol{x}_1^* + \boldsymbol{A}_2 \boldsymbol{x}_2^* - \boldsymbol{b}). \tag{2.4c}$$

This procedure is repeated, and is shown to converge to the global optimizer for $k \to \infty$ [BNO03, Ch. 8].[20] This is established by standard duality theory, since minimizing the Lagrange function (2.2) centrally or in a decentralized manner as in (2.4) does not alter the result. The disadvantages of the dual decomposition are the need of a central coordination (2.4c) and that each agent has to solve a convex optimization problem (2.4a) every iteration, which may time consuming.

Today, the dual decomposition lays the foundation for many more advanced techniques, such as augmented Lagrangian methods, optimality condition decomposition, or alternating direction method of multipliers (ADMM), see the standard textbooks [Ber99, Ch. 6], [LY16, Ch. 14], [Con+06, Ch. 5]. The augmented Lagrangian methods improve convergence by introducing an additional quadratic term penalizing the constraint error [Con+06, Ch. 5.4]. It confers the optimization better convergence properties because the Lagrange function has better convexity properties [Con+06, Fig. 5.7]. However, it comes at the cost of nonseparable quadratic terms in the augmented Lagrangian function, which have to be considered in both agents. ADMM also utilizes an augmented Lagrange function, but the optimization is sequential in its classical form [Boy+11;

[19] Convex constraints only involving variables from a specific agent can be considered without loss of generality, but are neglected in this presentation for simplicity. See [Con+06, Ch. 5] for a more general presentation.

[20] This result also holds for nondifferentiable objective functions using subgradients under minor conditions on the step size [BNO03, Prop. 8.2.4].

Han22; Yan+22]. There exist variants for solving nonconvex problems, or for avoiding the centralized dual ascent step (2.4c), see the surveys [Yan+22; Han22]. Most notably, the authors in [Fal+20] propose using distributed averaging in order to avoid the centralized dual ascent and guarantee convergence in the convex case. Optimality condition decomposition is similar to the dual decomposition, but assigns all constraints to a single agent. It can thus be seen as a 'particular implementation' of the dual decomposition [CNP02]. The dual ascent step is performed then by the agent in charge of the particular constraint instead of a central coordinator, for which he needs to receive the optimization variables of the other agents which are affected by the constraint. Such a scheme is particularly useful when the coupling constraints are sparse. Otherwise, all agents having a constraint have to exchange variables with almost all other agents, which may be less efficient than having a central coordinator. Sparse constraint structures are common in power systems, since the physical network is typically described with a sparse graph.[21] Therefore, optimality condition decomposition has been widely applied to power systems [NPC03; AKA07; CNP02], coupled power and gas systems [Arn+10], and coupled power and district heating systems [Mau+22]. The main disadvantage particular to optimality condition decomposition is that the convergence to the optimizer is only shown formally in an open neighborhood of the optimizer [CNP02, Theorem 2], without the possibility of analytically computing this neighborhood. However, optimality condition decomposition is shown to have adequate convergence properties in practice [CNP02, Table 2-4].

All in all, Lagrangian relaxation methods are mature and well-studied algorithms for distributed optimization. The original algorithms required a central coordinator, but there exist a wide range of advanced methods with a fully distributed communication. The main disadvantage that remains throughout all methods is the necessity of solving a convex optimization problem every iteration (e.g., (2.4a)), which is inefficient. To provide remedy in this regard, a wide range of methods based on multi-agent systems and control theory have been proposed recently and are reviewed in the next section.

Multi-Agent Distributed Optimization

The combination of distributed optimization with multi-agent systems and graph theory originated with the incremental strategy [Ber97; NB01; BHG07; Li+10; Say14]. In this method, a cyclic path is first defined such that it covers all agents in the network in succession, one after another. Then, in every optimization iteration k, each agent i performs sequentially a gradient descent step with its own objective function J_i, always using the variable it receives from its predecessor $\boldsymbol{x}_{i-1}(k)$ to obtain its own optimizer $\boldsymbol{x}_i(k)$, i.e.,

$$\boldsymbol{x}_i(k) = \boldsymbol{x}_{i-1}(k) - \alpha \nabla J_i(\boldsymbol{x}_{i-1}(k)), \tag{2.5}$$

[21] An exception are networks described by a single power balance equation, since then a single equation couples all variables in the optimization problem.

according to the cyclic path previously defined. Thus, at every optimization iteration k, the optimizer is passed through all the agents, which sequentially perform (2.5). When the cyclic path is completed, a new optimization iteration $k+1$ begins. In this method, each agent must only know its own objective function and the optimizer from the previous agent according to the cyclic path. This scheme is shown to converge to the global optimizer for various problem classes, e.g., nondifferentiable objective functions or using constant step sizes (see the surveys in [Say14] or [Ber99, p. 107ff.]).

However, incremental methods also have considerable disadvantages. First, they are very sensitive to agent or link failures, since then the information flow along the cyclic path is interrupted. In addition, the computation of a cyclic path covering all agents is an NP-hard problem [Kar72] and requires network-wide information, which hampers a true distributed optimization. Furthermore, the cooperation among agents is limited to having a single predecessor and a single successor. Also, the computation (2.5) of the agents is sequential, leading to long, inefficient waiting times for the agents, especially in large networks, since the agents need to wait for each cycle to complete.

To circumvent these issues, in particular to allow receiving and passing information to more than a single agent, and to avoid sequential computation, consensus or diffusion strategies have been developed [NO09; CS13; CS12a; CS12b; Say14]. In these methods, each agent performs a consensus step followed by a gradient descent with their own objective function, i.e., for agent i

$$\boldsymbol{x}_i(k+1) = \underbrace{\sum_{j\in\mathcal{N}_i} a_{ij}\boldsymbol{x}_j(k)}_{\text{consensus step}} - \alpha \underbrace{\nabla J_i(\boldsymbol{x}_i(k))}_{\substack{\text{decentralized}\\ \text{gradient descent}}}, \tag{2.6}$$

where $\mathcal{N}_i$ is the set of neighbors of agent i. Such algorithms are widely known as distributed gradient descent (DGD). There exist several variations of the DGD algorithm. The variations differ on when the weighted average is done, before or after the gradient descent step, or both times [Say14]. The DGD algorithm circumvents both disadvantages of the incremental methods: it relies on communication over a network rather than over a cyclic path covering all agents, and the gradient steps can be performed by the agents in parallel. However, the main limitation of this method is that it does not converge to the global optimum, but only to a neighborhood of it [NO09, Prop. 3], [CS13; MB11]. This is because in (2.6), at steady state, a trade-off between the consensus and the decentralized gradient descent results, neither reaching consensus nor optimality. The size of the neighborhood is proportional to the step size, thus smaller step sizes lead to smaller errors. For achieving convergence with DGD algorithms, diminishing step sizes have to be used, e.g., $\alpha(k) = \frac{1}{k}$, which then leads to slow convergence [Yan+22; NO09].

To provide remedy, concepts from control theory have been applied. The first control-theoretic approach to distributed optimization has been proposed in [WE10]. It consists

in combining a simple gradient descent algorithm (2.7a) with distributed consensus-based algorithms inducing a distributed proportional-integral action (2.7b),

$$\dot{\boldsymbol{x}}_i = -\alpha \nabla J_i(x_i) + \sum_{j \in \mathcal{N}_i} a_{ij} \left(\boldsymbol{z}_j - \boldsymbol{z}_i \right) \tag{2.7a}$$

$$\dot{\boldsymbol{z}}_i = \sum_{j \in \mathcal{N}_i} a_{ij} \left(\boldsymbol{x}_j - \boldsymbol{x}_i \right), \tag{2.7b}$$

where $a_{ij} > 0$ are scalar communication weights according to some connected graph. This algorithm was later named distributed PI algorithm [Yan+19]. In the original version [WE10], the agents communicate the two variables $\boldsymbol{x}_i$ and $\boldsymbol{z}_i$ over an undirected graph. Compared to the first-order DGD algorithm in (2.6), the distributed PI algorithm achieves consensus at steady state due to the integral part in (2.7b) and optimality due to (2.7a), instead of a trade-off between consensus and optimality.

Since then, several extensions of this algorithm have been proposed. The authors in [GC13] show that an immediate extension to directed communication topologies is not possible and propose a variant capable of handling a directed graph as communication network and non-differentiable objective functions. In [Hat+18], the algorithm is analyzed with passivity theory in order to extend the framework to communication delays and constraints. In [LCF16], the algorithm is cast in a discrete-time setting and extended to handle compact, convex constraints. The authors in [KCM15] propose a modification such that the agents exchange only a single variable in order to achieve coordination, in contrast to the previous works. To achieve that, a global initialization condition for all agents has to be imposed. Furthermore, they develop a framework based on Lyapunov theory in order to allow discrete-time communication. Extensions to the method in [KCM15] have been proposed, transferring it to a discrete-time setting in [Yao+18], or analyzing convergence with passivity theory and time-varying parameters [LCH20; LSL20].

Parallel to that line of research, other distributed optimization algorithms without an evident control-theoretical interpretation have been developed. The exact first-order algorithm (EXTRA) algorithm presented in [Shi+15] is shown to converge with a linear rate[22] when the objective functions of the agents are strongly convex. Furthermore, it is shown in [Yao+18], that the discrete-time version of the distributed PI algorithm is a special case of the EXTRA algorithm when the mixing matrices are properly chosen, bringing back again the control perspective. The convergence of the EXTRA algorithm is ensured independently of the network topology and the agents only need to exchange a single variable. However, as in the case of the distributed PI, a global initialization step is necessary. Another algorithm is the distributed gradient tracking (DiGing), proposed in [NOS17; QL17], which tracks the average gradient by using dynamic average consensus. The algorithm only requires a special local initialization, but, similarly

[22] In control theory, convergence with a linear rate is known by the name of 'converges exponentially'. With linear rate it is meant in mathematics that the distance to the optimizer is reduced with the same rate at every iteration [NW99], which is an exponential behavior in the time domain.

to the original version of the distributed PI in [WE10], the agents need to exchange two variables. Recently, a control-theoretical interpretation for the DiGing algorithm has been presented [Not+23]. The authors construct the DiGing algorithm by adding a distributed servomechanism to compensate the steady-state error of decentralized gradient descent. Exploiting the control-theoretical perspective, exponential stability is proven by means of Lyapunov theory. Nevertheless, the global initialization or the necessity of exchanging two variables still remains.

Another class of distributed optimization algorithms exploits second-order derivatives and solves an approximate Newton-Raphson algorithm in a distributed manner by means of average consensus [Var+15; Zan+11; Bof+18; MK22]. First proposed in [Zan+11; Var+15], it introduces the idea of tracking the gradient of the global cost function, serving as precedent of the DiGing algorithms described before. It is extended to lossy communication networks in [Bof+18], and modified in [MK22] in order to achieve a comparable convergence rate to the centralized Newton-Raphson algorithm while using less communication and memory compared to existing methods. Although powerful, these methods require exchanging multiple additional variables and, in some cases, a special global initialization. Thus, these methods are well suited for solving an optimization problem in a parallel manner, but not for the multi-agent systems setting, where privacy of the objective functions of the agents is crucial and flexibility for continuously leaving or (re)joining the network optimization problem is required.

2.4.1 Summary and Research Gaps

In recent years, very powerful algorithms for distributed optimization have been proposed both from the mathematical and control perspective. Lagrangian methods require the agents to solve a general convex optimization problem at every iteration, which is inefficient, and are thus not further considered in this thesis. With respect to the multi-agent methods, all existing algorithms require either a global initialization step or the communication of multiple variables in order to achieve convergence and optimality. Thus, the following research gap exists:

Research Gap 2

There exist no multi-agent distributed optimization algorithms without global initialization which guarantee convergence to the global optimizer while communicating a single variable.

However, this is not the only shortcoming of the existing methods. Despite the high research attention distributed optimization has experienced, the exiting algorithms are still on an early research phase and suffer from fundamental drawbacks. Most notably, up to now, there exist no requirements that enable the constructive design of such algorithms and ensure their interoperability. All the existing works only propose

specific algorithms and, provided that all agents follow their specific algorithm, derive conditions on the tuning parameters for achieving global optimality and convergence. Thus, with the existing methods, agents cannot leave or (re)join the networked optimization without jeopardizing convergence to the correct[23] global optimizer. Hence, with the existing methods, no plug-and-play of agents is possible. Furthermore, the lack of design requirements does not allow agents to use different optimization dynamics. With local design requirements, each agent may individually design their own algorithm such that global optimality and convergence are achieved, even when agents leave or (re)join the networked optimization. The preceding line of arguments is summarized in the following research gap.

Research Gap 3

There exist no local design requirements for the individual agents for ensuring optimality and convergence in distributed optimization algorithms.

In power system applications, addressing Research Gap 2 and 3 regarding distributed optimization algorithms is especially important. Due to the large scale of power systems, it is desirable that the individual agents may use different optimization algorithms as long as complying with local conditions that guarantee convergence to a global optimum. Likewise, it is desirable that the agents communicate as few information as possible for privacy reasons. In addition, the possibility for an agent to leave or rejoin the optimization is fundamental in power systems. Examples for leaving or (re)joining the optimization are when a battery storage runs empty or again has enough energy to feed in power, when an electric vehicle disconnects from the grid, or when a DGU cannot inject power due to changing weather conditions.

2.5 Control Methods for Liberalized Power Systems

So far, methods in which all generators or consumers in a power system apply a predefined computation rule or controller, e.g., in droop-based or distributed MPC-based approaches, have been reviewed. In this section, approaches in which the individual agents act such that they minimize their own (and freely chosen) objective function are considered. For this, most approaches introduce a price variable, and use it to close the gap between a stable system operation and optimization.

It is important to note that there exist game-theoretical approaches dealing exclusively with the economic optimization of power systems (see the surveys in [Nav+20; CY19]), which are not covered in this work. These approaches neglect the network dynamics,

[23] By correct it is meant the new global optimizer considering also the objective function of the agent that joined the networked optimization.

implicitly adopting the copper plate assumption, which leads to the issues described in Section 2.1.

Among the methods considering the system dynamics, many approaches achieve important theoretical results by considering a simplified system model. In [Ste+19] and [Che+21], a Bertrand competition scheme for frequency control in networks of synchronous generators is proposed. In [Che+21], a real-time market for frequency regulation is proposed. The generators implement a continuous-time bidding scheme, and get in return the power generation level, also in continuous time. To satisfy constraints, the theory of projected dynamic systems is used. The authors establish important theoretical results, such as the existence and uniqueness of Nash equilibria and asymptotic stability. In [Ste+19; Ste+18], the authors propose a hybrid system combining the discrete nature of iterative bidding with the continuous nature of frequency dynamics in power systems. Asymptotic stability is shown by first establishing the robust input-to-state stability of the power system, and regarding the time-triggered bidding as an approximation of continuous-time dynamics, interpreting the mismatch as a disturbance. Although providing important theoretical results, the analysis relies on simplified system models, such as constant voltage amplitudes, radial networks, and omits power line and synchronous generator dynamics.

Another class of approaches proposes a price-forming mechanism that arises from the active power imbalance [SDPS16b; SDPS16a; Köl+20b; Köl+20a]. The network is composed of synchronous generators interconnected by power lines. In [SDPS16b; SDPS16a], the network is assumed to be lossless. The price is the Lagrange multiplier corresponding to the power balance constraint, and its continuous-time dynamics are determined by the dual ascent in primal-dual dynamics for finding the optimizer of an optimization problem of economic dispatch. Using passivity theory, asymptotic stability is established by showing that the power system and the primal-dual optimization dynamics, comprising the price and the producers responding to that price, form a skew-symmetric interconnection as in Figure 2.3. In [Köl+20b; Köl+20a], this scheme is extended to lossy networks. In [Köl+21b], it is extended proposing zonal prices and a congestion management to avoid normative interventions, e.g., redispatch, after market clearing. Furthermore, it is shown that the solution converges to the same solution as if the individual producers or consumers maximize their own revenue, showing that the approach is compatible with a liberalized power system as in Term 2.2. Asymptotic stability is proven also by showing that the closed-loop system can be posed as a skew-symmetric interconnection as in Figure 2.3. Albeit achieving important theoretical results, the network is reduced to an interconnection of idealized synchronous generators with static power lines, which does not hold for systems with a large penetration of renewable energy sources connected via power electronics.

Furthermore, although all approaches described can be implemented in a distributed manner, they rely on a centralized analysis as is suggested by Figure 2.3. The aggregated controllers in Figure 2.3 are composed of all individual controllers and the communication between these. The controllers are the primal-dual dynamics comprising the price

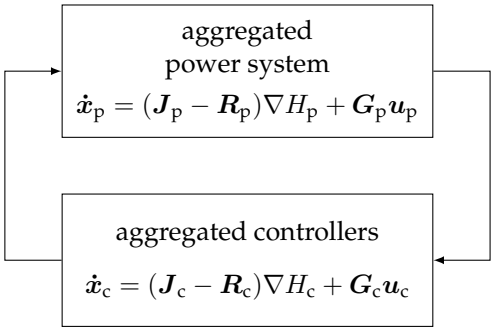

Figure 2.3: Schematic representation of the method proposed in [SDPS16b; SDPS16a; Köl+20b; Köl+20a; Köl+21b].

dynamics and the dynamics of the producers responding to that price. In addition, the communication between the individual controllers couples all individual systems forming the aggregated controllers. To analyze the passivity of the aggregated controllers, the dynamics of all producers must be known. In all proposed approaches it is thus assumed that all producers react in a certain manner — described by a certain dynamic system — to the price. The producers can merely adjust a parameter of the given dynamics. Using different (i.e., unknown) controllers would impede the passivity analysis of the aggregated controller system, which may compromise the operation of the liberalized power system in more realistic scenarios.

2.5.1 Summary and Research Gaps

As presented above, the existing methods fall short in several aspects. Firstly, all existing approaches require the network to be composed of interconnected synchronous generators with static power lines, in some cases with the additional assumption of constant amplitude voltages or radial networks. Thus, the following research gap exists:

Research Gap 4
There exists no control method for liberalized power systems as in Term 2.2 compatible for future power systems based on power electronics instead of synchronous generators.

Furthermore, all the existing methods use the frequency deviation as a proxy for the active power imbalance, which is the key in the price-forming mechanism. For future power systems based on power electronics, where the swing equation may not describe the frequency dynamics adequately or even parts of the system may be DC networks,

the frequency deviation may not be a suitable price-forming mechanism. Therefore, novel price-forming mechanisms are necessary, and the following research gap exists:

Research Gap 5
There exists no price-forming mechanism appropriate for achieving stability and optimality in future power systems based on power electronics.

Lastly, the aforementioned problem of a centralized stability analysis arises from the choice of the system boundaries and the ports as shown in Figure 2.3. The aggregated controllers comprise different producers corresponding to different areas. The passivity analysis requires information about all controller dynamics, which is impractical. Thus, the following research gap exists:

Research Gap 6
There exists no control framework providing stability guarantees with local conditions compatible with liberalized power systems as in Term 2.2.

In this work, we refrain from a control structure as in Figure 2.3 and define novel ports at grid level leading to local conditions allowing for an optimal operation.

2.6 Summary and Statement of Contributions

To overcome the limitations of the existing methods, this thesis is devoted to designing optimization-based control structures for future power systems based on power electronics. Throughout the thesis, passivity theory plays a central role to guarantee stability and optimality with local conditions on the subsystems. Passivity theory is applied to MPC and to distributed optimization algorithms. Likewise, passivity theory is used to propose a control framework for liberalized power systems. The structure of the contributions, illustrated within the concepts of Terms 2.1 and 2.2, is given in Figure 2.4 and outlined in the following.

Complying with regulated power systems as in Term 2.1, a distributed MPC framework with stability guarantees which are independent of the network topology is developed. The first step is to design the MPC problem such that the stability conditions are local conditions. This is summarized in the following contribution, which addresses Research Gap 1.

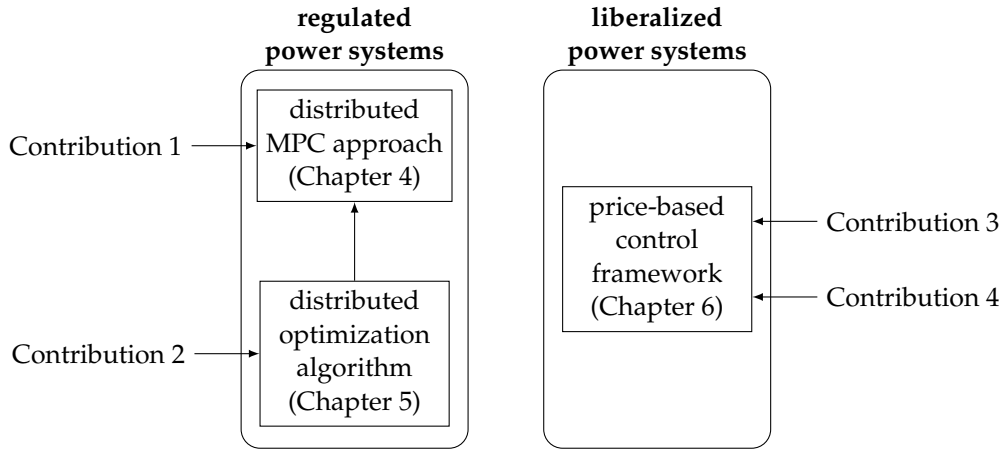

Figure 2.4: Structure and organization of the contributions in this thesis.

Contribution 1

This dissertation develops a MPC framework for future power systems taking into account detailed, nonlinear system dynamics, and where asymptotic stability and optimality is certified only with local conditions on the subsystems.

The MPC problem of Contribution 1 is thus designed such that the stability conditions only affect local variables of each subsystem that can be checked individually by each subsystem. However, from the computation perspective, Contribution 1 results in a centralized MPC problem despite the local stability conditions. For solving the centralized MPC problem in a distributed manner, a distributed optimization algorithm is necessary. For optimization in large-scale systems such as power systems, it is important that privacy is preserved, that communication requirements are low, and that different optimization dynamics as well as plug-and-play of agents is possible. Thus, in this dissertation, a distributed optimization algorithm is proposed exploiting passivity and addressing Research Gaps 2 and 3. This is summarized in the following contribution.

Contribution 2

This dissertation develops a novel passivity-based distributed optimization algorithm capable of handling different optimization dynamics, requiring less communication than existing methods and offering plug-and-play capabilities.

Implementing the methods for regulated power systems implies abolishing the current competitive, liberalized power system. Since this may not be the path chosen by the policymakers, approaches intending to maintain the separation of the roles of a liberalized power system are also explored. In particular, a control framework for liberalized power

systems (see the right-hand side of Figure 2.4) is developed. Novel passivity-based ports at grid level are introduced for the optimal operation of networked grids complying with the roles and information barriers in liberalized power systems. These novel ports allow refraining from the control structure in Figure 2.3, which requires global information to assess passivity. With the following contribution, Research Gaps 4 and 6 are addressed.

Contribution 3
This dissertation develops a distributed control framework for liberalized, future power systems based on power electronics, where asymptotic stability is certified with local conditions and without assumptions on producer behavior.

An essential part of this control framework is a novel control theory-inspired price-forming mechanism. In future power systems with low inertia, the frequency deviation is not expected to be mainly linked to a power shortage [Mil+18] and may thus not be an appropriate price signal as suggested in literature. Instead of relying on frequency deviations, it modifies the price according to the control effort of a set of stabilizing DGUs to maintain stable system variables. Hence, it is compatible with future power systems based on power electronics, possibly also involving DC grids. Since the mechanism is based on control theory principles, it is applicable to other energy domains and networked multi-energy systems. With the following contribution, Research Gap 5 is addressed.

Contribution 4
This dissertation introduces a control theory-inspired price-forming mechanism taking into account the volatile nature of power systems with a high share of renewable energy sources connected via power electronics.

All the contributions of this dissertation are developed exemplary for networked DC grids. An extension of the proposed methodology to AC systems is straightforward modelling the system in the dq reference frame [SB09; Bai+17], which is standard for modelling and control of power electronics. An AC grid model is then mathematically identical to a DC grid model, but with two variables for each voltage and current, i.e., the d and q components. However, all controllers can be designed in a mathematically identical way, for each dq component independently. This connection between DC and AC system modelling has already been noted and exploited in the past. Typically, approaches have been first developed for DC systems and have been later transferred to AC systems, using the same theory. Prominent examples for this procedure are the methods in [Nah+20] for DC and [NFT19] for AC, or [Str+20] for DC and [Str+19] for AC. Thus, in this dissertation, the novel, conceptual approaches are developed for DC systems. In the context of this dissertation, one of the proposed approaches has also

been successfully applied for AC grids using the described procedure [JSDH23].

3 Fundamentals

This chapter provides the relevant mathematical and system-theoretical fundamentals which are essential for understanding and developing the main contributions in Chapters 4-6.

Section 3.1 provides key concepts of networked systems and passivity theory. The relevant matrices for graph representations, along with their properties, are presented. In addition, passivity theory including relevant supply rates and properties are introduced. These concepts are used throughout all remaining chapters.

Section 3.2 provides the basic theory of MPC, which is used in Chapter 4 for developing local stability conditions. Section 3.3 provides basic concepts of convex optimization which form the basis for developing the novel distributed optimization algorithm in Chapter 5. Lastly, in Section 3.4, the power system component models employed throughout this work are presented.

3.1 Networked Systems and Passivity Theory

Throughout the work, networked systems in different forms are considered, e.g., in power systems or agents cooperating for a distributed optimization. All these networked systems are described with dynamic systems networked as defined by a *graph*. After giving a formal definition of a graph, the term networked system is introduced.

Definition 3.1 (directed graph)
A directed graph is a pair $\mathcal{G}(\mathcal{B}, \mathcal{E})$ composed of a set of nodes $\mathcal{B} = \{\mathfrak{v}_1, \dots, \mathfrak{v}_{|\mathcal{B}|}\}$ and a set of ordered pairs of nodes called edges $\mathcal{E} \subseteq \mathcal{B} \times \mathcal{B}$, with $\mathcal{E} = \{\mathfrak{e}_1, \dots, \mathfrak{e}_{|\mathcal{E}|}\}$. An edge $\mathfrak{e}_j = (\mathfrak{v}_i, \mathfrak{v}_l) \in \mathcal{E}$ starts from $\mathfrak{v}_i$ and ends in $\mathfrak{v}_l$.

A graph is undirected if $(\mathfrak{v}_i, \mathfrak{v}_l) \in \mathcal{E}$ implies $(\mathfrak{v}_l, \mathfrak{v}_i) \in \mathcal{E}$. If a graph has weights at each edge it is a weighted graph and is described additionally with an adjacency matrix $\boldsymbol{A}_\mathcal{G} \in \mathbb{R}^{|\mathcal{B}|\times|\mathcal{B}|}$, where for the elements a_{il} of $\boldsymbol{A}_\mathcal{G}$ holds $a_{il} \neq 0$ if $(\mathfrak{v}_i, \mathfrak{v}_l) \in \mathcal{E}$ and $a_{il} = 0$ otherwise. If the graph is undirected, the adjacency matrix is symmetric. A graph without self-loops can also be associated with an incidence matrix $\boldsymbol{E} \in \mathbb{R}^{|\mathcal{B}|\times|\mathcal{E}|}$ relating the individual edges and nodes. The column of the incidence matrix corresponding to edge $\mathfrak{e}_j = (\mathfrak{v}_i, \mathfrak{v}_l)$ has an entry 1 in row i and an entry -1 in row l, and all other entries are zero. For an undirected graph, an incidence matrix can be defined by arbitrarily

choosing an orientation for each edge. The next lemma is essential for Chapter 5 and is adapted from [BH12, Ch. 1.3.7] and [GR01, Ch. 8].

Lemma 3.1 (properties of the incidence matrix)
The incidence matrix $\boldsymbol{E}$ of a graph has the following properties:

- *All column sums equal to zero, i.e.*

$$\boldsymbol{E}^\top \mathbf{1}_{|\mathcal{B}|} = \mathbf{0}_{|\mathcal{E}|}. \tag{3.1}$$

- *The rank of $\boldsymbol{E}$ is equal to the number of nodes minus the number of connected components n_{cc}, i.e.*

$$\operatorname{rank}\{\boldsymbol{E}\} = |\mathcal{B}| - n_{cc}. \tag{3.2}$$

- *For connected graphs (i.e., $n_{cc} = 1$), the kernel of the transpose is spanned by the $\mathbf{1}_{|\mathcal{B}|}$, i.e.,*

$$\ker\{\boldsymbol{E}^\top\} = \{\theta \mathbf{1}_{|\mathcal{B}|} \mid \theta \in \mathbb{R}\}. \tag{3.3}$$

Next, using the definitions of a graph and the incidence matrix, the definition and structure of a networked system as used throughout this work is introduced.

Term 3.1 (networked system)
An autonomous, networked system is a system which can be described with two sets of (dynamic) systems, the node systems Σ_i with $i \in \mathcal{B}$ and the edge systems Π_j with $j \in \mathcal{E}$, together with a graph $\mathcal{G}(\mathcal{B}, \mathcal{E})$ describing the interconnection between the node and edge systems. Each node system $i \in \mathcal{B}$ has a dynamic system of the form

$$\Sigma_i : \begin{aligned} \dot{\boldsymbol{x}}_i &= \boldsymbol{f}_i(\boldsymbol{x}_i, \boldsymbol{u}_i) \\ \boldsymbol{y}_i &= \boldsymbol{c}_i(\boldsymbol{x}_i, \boldsymbol{u}_i), \end{aligned} \tag{3.4}$$

and to edge system $j \in \mathcal{E}$

$$\Pi_k : \begin{aligned} \dot{\boldsymbol{x}}_j &= \boldsymbol{f}_j(\boldsymbol{x}_j, \boldsymbol{u}_j) \\ \boldsymbol{y}_j &= \boldsymbol{c}_j(\boldsymbol{x}_j, \boldsymbol{u}_j), \end{aligned} \tag{3.5}$$

with $\boldsymbol{f}_i : \mathbb{R}^{n_i} \times \mathbb{R}^{m_i} \to \mathbb{R}^{n_i}$, $\boldsymbol{f}_j : \mathbb{R}^{n_j} \times \mathbb{R}^{m_j} \to \mathbb{R}^{n_j}$, $c_i : \mathbb{R}^{n_i} \times \mathbb{R}^{m_i} \to \mathbb{R}^{n_i}$ and $c_j : \mathbb{R}^{n_i} \times \mathbb{R}^{m_i} \to \mathbb{R}^{n_j}$ Lipschitz continuous, and $\boldsymbol{x}_i \in \mathbb{R}^{n_i}$, $\boldsymbol{u}_i \in \mathbb{R}^{m_i}$, $\boldsymbol{y}_i \in \mathbb{R}^{n_i}$, $\boldsymbol{x}_j \in \mathbb{R}^{n_j}$, $\boldsymbol{u}_j \in \mathbb{R}^{m_j}$, $\boldsymbol{y}_j \in \mathbb{R}^{n_j}$. These systems are interconnected according to the graph $\mathcal{G}$ with incidence matrix $\boldsymbol{E}$, with the interconnection structure

$$\begin{bmatrix} \boldsymbol{u}_\Sigma \\ \boldsymbol{u}_\Pi \end{bmatrix} = \begin{bmatrix} 0 & -\boldsymbol{E} \\ \boldsymbol{E}^\top & 0 \end{bmatrix} \otimes \boldsymbol{I}_n \begin{bmatrix} \boldsymbol{y}_\Sigma \\ \boldsymbol{y}_\Pi \end{bmatrix}, \tag{3.6}$$

where $\boldsymbol{u}_\Sigma = \mathrm{col}\{\boldsymbol{u}_i\}$, $\boldsymbol{u}_\Pi = \mathrm{col}\{\boldsymbol{u}_j\}$, *and* $\boldsymbol{y}_\Sigma$, $\boldsymbol{y}_\Pi$, *respectively.*

The structure of a networked system is shown in Figure 3.1. In such a structure, the edge systems Π_k always receive the difference of two outputs of the node systems Σ_i, as the incidence matrix $\boldsymbol{E}$ computes the difference of two outputs of the node systems. In turn, again by definition of the incidence matrix $\boldsymbol{E}$, the output of the edge systems Π_k is given positive and negative to the input of the node systems which the edge system interconnects, according to a predefined flow direction. In power systems, for example, this relates to Kirchhoff's current conservation law, since the edge systems typically represent the power lines with the line current as output [HWL23; Str24].

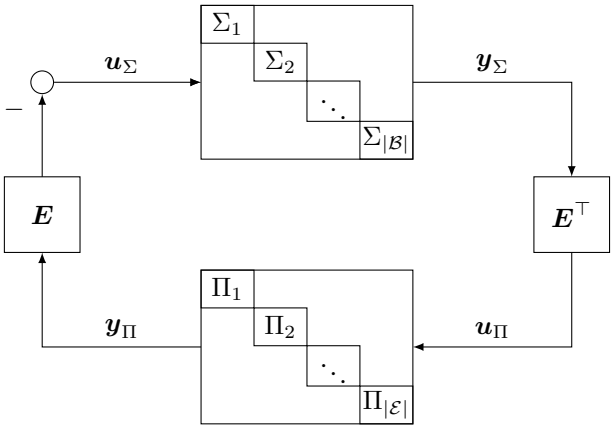

Figure 3.1: Structure of a networked system with node systems Σ_i, edge systems Π_j and a graph described by the incidence matrix $\boldsymbol{E}$.

In Chapters 4 and 6, a networked system with structure as in Figure 3.1 is used for describing networked power systems. In Chapter 5, the same structure is used to propose a novel class of distributed optimization algorithms that exploit the skew-symmetric interconnection (3.6) using passivity theory. In the next section, passivity theory is introduced, which is the basis for the stability results in most contributions of this work.

3.1.1 Passivity Theory

Passivity theory is a mature framework for studying the stability properties of nonlinear systems [Wil72; Kha02; SJK12]. It combines the notion of an energy function, also used in Lyapunov theory, with the inputs and outputs of a system via a supply rate. Passivity

is a property of an individual state-space system[24]

$$\dot{\boldsymbol{x}} = \boldsymbol{f}(\boldsymbol{x}, \boldsymbol{u}) \tag{3.7a}$$

$$\boldsymbol{y} = \boldsymbol{c}(\boldsymbol{x}, \boldsymbol{u}), \tag{3.7b}$$

with $\boldsymbol{x} \in \mathbb{X} \subseteq \mathbb{R}^n$, $\boldsymbol{u} \in \mathbb{U} \subseteq \mathbb{R}^m$, $\boldsymbol{y} \in \mathbb{Y} \subseteq \mathbb{R}^n$, $\boldsymbol{f} : \mathbb{X} \times \mathbb{U} \to \mathbb{R}^n$ and $\boldsymbol{c} : \mathbb{X} \times \mathbb{U} \to \mathbb{R}^n$. Passivity theory provides useful means for assessing stability of the resulting system when (3.7) is interconnected with other systems. Passivity plays an important role in this work, since it allows providing local stability certificates and therefore enables a flexible, plug-and-play operation while ensuring stability.

In standard passivity theory, it is assumed without loss of generality, that all systems have an equilibrium at zero, and thus (asymptotic) stability of the global equilibrium $\bar{\boldsymbol{x}} = \boldsymbol{0}_n$ can be certified. This is, in general, not restrictive for studying any nonzero equilibrium $\bar{\boldsymbol{x}} \neq 0$, since a simple coordinate shift leads to the set-up with an equilibrium at zero. However, in such a set-up, it is not possible to study *multiple* equilibria, or even the set of all equilibria. In many applications, such as power systems [NI23] or internet congestion [WA04], the equilibrium may vary during system operation due to disturbances in a system or due to a system disconnecting from the network. In power systems, for example, a load variation in a single system may induce a completely new equilibrium in the networked power system, e.g., when many generators compensate the load variation. Likewise, the disconnection of a single generator may induce a new equilibrium in the entire network. The formal analysis of such a scenario requires to examine the passivity properties of the subsystems for any feasible equilibria. This motivated the development of equilibrium-independent passivity (EIP), first introduced in [HAP11] and further developed in [AMP16; SP18]. In the following, the formal definition of equilibrium-independent dissipativity is given first in order to introduce later the definition of EIP. The definitions are adopted from [SP18; HAP11].

Definition 3.2 (equilibrium-independent dissipativity)
Let the pair $(\bar{\boldsymbol{x}}, \bar{\boldsymbol{u}})$ denote an equilibrium of (3.7) *and $\bar{\mathbb{X}}$ the set of all equilibrium states. The system* (3.7) *is called equilibrium-independent dissipative w.r.t. supply rate $w : \mathbb{U} \times \mathbb{Y} \to \mathbb{R}$, if there exists a storage function $V : \mathbb{X} \times \bar{\mathbb{X}} \to \mathbb{R}_{\geq 0}$ such that $V(\bar{\boldsymbol{x}}, \bar{\boldsymbol{x}}) = 0$ and*

$$\dot{V} \leq w(\boldsymbol{u} - \bar{\boldsymbol{u}}, \boldsymbol{y} - \bar{\boldsymbol{y}}) \tag{3.8}$$

holds for all $t \geq 0$.

For convenience, define the error variables $\tilde{\boldsymbol{x}} = \boldsymbol{x} - \bar{\boldsymbol{x}}$, $\tilde{\boldsymbol{u}} = \boldsymbol{u} - \bar{\boldsymbol{u}}$ and $\tilde{\boldsymbol{y}} = \boldsymbol{y} - \bar{\boldsymbol{y}}$. The following definition introduces EIP along with some common variants, which are used in this work.

[24] This is a main difference with Lyapunov stability, which is not a system property including input and output, but a property of a differential equation (or autonomous system) describing the behavior of the solutions around a specific equilibrium point.

Definition 3.3 (EIP and its variants)
If system (3.7) *is equilibrium-independent dissipative w.r.t. supply rate*

$$w(\tilde{\boldsymbol{u}}, \tilde{\boldsymbol{y}}, \tilde{\boldsymbol{x}}) = \tilde{\boldsymbol{u}}^\top \tilde{\boldsymbol{y}} - \rho \tilde{\boldsymbol{y}}^\top \tilde{\boldsymbol{y}} - \nu \tilde{\boldsymbol{u}}^\top \tilde{\boldsymbol{u}} - \Psi(\tilde{\boldsymbol{x}}) \tag{3.9}$$

it is called

- *EIP, if* $\rho, \nu \geq 0$ *and the function* $\Psi : \mathbb{R}^n \to \mathbb{R}$ *is positive semidefinite*
- *strictly EIP, if* Ψ *is positive definite and* $\rho, \nu \geq 0$
- *output feedback EIP (OFEIP) with index* $\rho \in \mathbb{R}$*, if* $\nu, \Psi \equiv 0$
- *input feedforward EIP (IFEIP) with index* $\nu \in \mathbb{R}$*, if* $\rho, \Psi \equiv 0$
- *input feedforward-output feedback EIP (IF-OFEIP) with indices* $\nu, \rho \in \mathbb{R}$*, if* $\Psi \equiv 0$
- *state-input-output EIP (SIOEIP) with indices* $\nu, \rho \in \mathbb{R}$*, if* Ψ *positive definite*

In short, it is said a system is OFEIP(ρ) or IFEIP(ν) in the remainder of this dissertation. If $\nu, \rho > 0$, the system has an excess of passivity[25]. If the indices are negative, the system has a lack of passivity.

Remark 3.1. *Strictly speaking, a system can only be EIP w.r.t. a specific input-output pair, i.e.,* $(\boldsymbol{u}, \boldsymbol{y})$ *for system* (3.7)*. However, if a system has a single (possibly vector-valued) input and output, we say in short that the system is EIP, meaning that it is EIP with respect to the only available input-output pair.*

The next definition introduces an important property of nonlinear systems for certifying stability using EIP theorems. The property is called equilibrium-independent observability (EIO) and is a generalization of the classic zero-state observability and zero-state detectability in nonlinear system theory (see, e.g., [vdS17]) to the equilibrium-independent setting. It was first introduced in [SP18].

Definition 3.4 (EIO)
System (3.7) *is called EIO, if for all equilibria* $(\bar{\boldsymbol{x}}, \bar{\boldsymbol{y}}, \bar{\boldsymbol{u}})$ *no trajectory exists that can remain in the set* $\{\boldsymbol{x} \in \mathbb{X} \mid \boldsymbol{c}(\boldsymbol{x}, \bar{\boldsymbol{u}} = \bar{\boldsymbol{y}})\}$ *other than* $\boldsymbol{x}(t) = \bar{\boldsymbol{x}}$*.*

Next, an original condition for computing the SIOEIP properties of a nonlinear input affine system is presented, which is important for the analysis in Chapter 6. It is inspired by the analysis of nonlinear systems by casting it as a linear parameter variant system as in [SW00, Ch. 9.4.1], but transferred to an EIP analysis.

[25] Technically, the system has an excess of EIP. However, the term excess of passivity is more common in the literature, [LCH20; SJK12].

Proposition 3.2 (EIP conditions of an input affine system)
Consider the nonlinear input affine system shifted to an equilibrium $(\bar{\boldsymbol{x}}, \bar{\boldsymbol{u}}) \in \bar{\mathbb{X}} \times \bar{\mathbb{U}}$

$$\dot{\tilde{\boldsymbol{x}}} = \boldsymbol{f}(\tilde{\boldsymbol{x}}, \bar{\boldsymbol{x}}) + \boldsymbol{B}\tilde{\boldsymbol{u}} \tag{3.10}$$
$$\tilde{\boldsymbol{y}} = \boldsymbol{C}\tilde{\boldsymbol{x}} + \boldsymbol{D}\tilde{\boldsymbol{u}} \tag{3.11}$$

where $\boldsymbol{f} : \mathbb{R}^n \times \mathbb{R}^n \to \mathbb{R}^n$, $\boldsymbol{B} \in \mathbb{R}^{n\times m}$, $\boldsymbol{C} \in \mathbb{R}^{m\times n}$ *and* $\boldsymbol{D} \in \mathbb{R}^{m\times m}$. *Let* $\boldsymbol{f}(\tilde{\boldsymbol{x}}, \bar{\boldsymbol{x}}) = \boldsymbol{A}(\tilde{\boldsymbol{x}}, \bar{\boldsymbol{x}})\tilde{\boldsymbol{x}}$ *with* $\boldsymbol{A} : \mathbb{R}^n \times \mathbb{R}^n \to \mathbb{R}^{n\times n}$ *hold. Consider the storage function* $V(\tilde{\boldsymbol{x}}) = \frac{1}{2}\tilde{\boldsymbol{x}}^\top \boldsymbol{S}\tilde{\boldsymbol{x}}$, *the function* $\Psi(\tilde{\boldsymbol{x}}) = \varrho\tilde{\boldsymbol{x}}^\top\tilde{\boldsymbol{x}}$ *and scalars* ρ, ϱ, $\nu \in \mathbb{R}$. *System* (3.10) *is EIP w.r.t. input-output port* $(\tilde{\boldsymbol{u}}, \tilde{\boldsymbol{y}})$ *if there exist scalars* ρ, ϱ, ν *and a matrix* $\boldsymbol{S}$ *such that the LMIs*

$$\boldsymbol{S} > \boldsymbol{0} \tag{3.12a}$$
$$\begin{bmatrix} \boldsymbol{S}\boldsymbol{A}(\tilde{\boldsymbol{x}}, \bar{\boldsymbol{x}}) + \boldsymbol{A}(\tilde{\boldsymbol{x}}, \bar{\boldsymbol{x}})^\top \boldsymbol{S} + 2\rho\boldsymbol{C}^\top\boldsymbol{C} + 2\varrho\boldsymbol{I}_n & \boldsymbol{S}\boldsymbol{B} - \boldsymbol{C}^\top + 2\rho\boldsymbol{C}^\top\boldsymbol{D} \\ \boldsymbol{B}^\top\boldsymbol{S} - \boldsymbol{C} + 2\rho\boldsymbol{D}^\top\boldsymbol{C} & 2(\nu\boldsymbol{I}_n + \rho\boldsymbol{D}^\top\boldsymbol{D}) - \boldsymbol{D} - \boldsymbol{D}^\top \end{bmatrix} \leq \boldsymbol{0} \tag{3.12b}$$
$$\varrho \geq 0 \tag{3.12c}$$

holds for all $\tilde{\boldsymbol{x}} \in \tilde{\mathbb{X}}$ *and* $\bar{\boldsymbol{x}} \in \bar{\mathbb{X}}$, *where* $\tilde{\mathbb{X}}$ *is the set of allowed deviations.*

Proof. The EIP condition as in (3.8) with supply rate (3.9) is

$$\dot{\boldsymbol{S}} = \frac{1}{2}(\tilde{\boldsymbol{x}}^\top\boldsymbol{S}\dot{\tilde{\boldsymbol{x}}} + \dot{\tilde{\boldsymbol{x}}}^\top\boldsymbol{S}\tilde{\boldsymbol{x}}) \leq \tilde{\boldsymbol{u}}^\top\tilde{\boldsymbol{y}} - \rho\tilde{\boldsymbol{y}}^\top\tilde{\boldsymbol{y}} - \nu\tilde{\boldsymbol{u}}^\top\tilde{\boldsymbol{u}} - \varrho\tilde{\boldsymbol{x}}^\top\tilde{\boldsymbol{x}}. \tag{3.13}$$

Substituting the system equations (3.10) in both sides of (3.13) and rewriting the term in vector matrix notation by extracting $(\tilde{\boldsymbol{x}}^\top\tilde{\boldsymbol{u}}^\top)^\top$ in both sides yields the set of LMIs in (3.12). □

Remark 3.2. *Note that Proposition 3.2 allows not only for checking if a system as in* (3.10) *is EIP, but also all its variants in Definition 3.3 by just modifying the scalar constraints* (3.12c).

Remark 3.3. *Condition* (3.12) *can be efficiently solved via semidefinite programming, if* $\boldsymbol{A} : \mathbb{R}^n \times \mathbb{R}^n \to \mathbb{R}^{n\times n}$ *is, element-wise, linear in* $\tilde{\boldsymbol{x}}$ *and* $\mathbb{X}$ *is a polytopic set. Then, using the continuity of the eigenvalues w.r.t. to the matrix entries [HJ12, p. 387], only the vertices of the polytopic set have to be taken into account, see [Boy+94, Ch. 5] or [SW00, Ch. 9.2].*

Remark 3.4. *Note that there may be different ways to split the system dynamics* $\boldsymbol{f}(\tilde{\boldsymbol{x}}, \bar{\boldsymbol{x}}) = \boldsymbol{A}(\tilde{\boldsymbol{x}}, \bar{\boldsymbol{x}})\tilde{\boldsymbol{x}}$. *Hence, the feasibility of the LMI depends on the choice of* $\boldsymbol{A}(\tilde{\boldsymbol{x}}, \bar{\boldsymbol{x}})$.

Regarding the stability analysis of networked EIP systems, there exist plenty of theorems forming the backbone of a mature theory. In the textbook [AMP16], a stability theorem

is given, assuming that an equilibrium of the networked system exists. In [Str24], it is extended for asymptotic stability using Lasalle's Invariance Principle. Furthermore, the paper [SP18] forms the backbone for the EIP theory. Important terms like equilibrium-independent observability, the analog equilibrium-independent counterpart of zero-state detectability, are defined, conditions for the asymptotic, incremental and absolute stability of EIP systems are given, the equilibrium-independent circle criterion is presented, and conditions for the existence of equilibria in networked systems are given, both in continuous and discrete-time versions. These results are not presented here explicitly and are cited when necessary.

After introducing the basic concepts regarding networked systems in this work, in the next section the fundamental concepts from MPC theory are described. The MPC concept represents a link between control theory and optimization.

3.2 MPC Theory

Optimal control problems have attracted great attention in control theory since the seminal publication by Kalman [Kal+60], in which he first established the stability condition he termed as *controllability*. This dissertation also deals with optimal control problems, but with the focus on distributed, optimal operation of future power systems.

Since computing optimal feedback laws is not feasible when considering nonlinear systems or systems with any kind of state or input constraints, MPC was proposed as a solution. In MPC, the infinite horizon is replaced by a finite horizon and the optimization problem (and/or the system) is discretized. That way the dynamic optimization problem of the optimal control formulation is converted to a static open-loop optimization problem. The loop is closed by repeatedly solving the open-loop static optimization problem with a receding horizon. MPC theory then studies under which conditions such a control scheme, where the loop is closed implicitly by repeatedly solving an open loop optimization problem instead of a classical feedback law, results in asymptotic stability.

In this work, the MPC formulation is exploited to enable a distributed control. The MPC formulation, intrinsically, converts the dynamic optimization problem into a static optimization problem.[26] Then, by applying distributed optimization algorithms [Yan+22], it is possible to solve a static optimization problem in a distributed manner, which is not possible when dealing directly with dynamic optimization problems. This path is taken in this work, and contributions to the stability of the closed-loop system are provided in Chapter 4 and to distributed optimization algorithms in Chapter 5.

In MPC, the controller computes the next control action by solving, at every time step t, an open-loop control problem of the form

[26] A static optimization problem is also called sometimes a parameter optimization problem.

$$\text{MPC}(t) := \begin{cases} \min & \displaystyle\int_t^{t+T} l(\boldsymbol{x}(\tau), \boldsymbol{u}(\tau))\mathrm{d}\tau + V_T(\boldsymbol{x}(T)) \\ \text{s. t.} & \dot{x} = f(\boldsymbol{x}(\tau), \boldsymbol{u}(\tau)), \\ & x(\tau) \in \mathbb{X} \\ & x(T) \in \mathbb{X}_T \\ & u(\tau) \in \mathbb{U} \\ & \tau \in [t, t+T]\,, \end{cases} \tag{3.14}$$

where $l : \mathbb{R}^n \times \mathbb{R}^m \to \mathbb{R}$ and $V_T : \mathbb{R}^n \to \mathbb{R}$ are the stage cost and terminal cost, and $\mathbb{X} \subset \mathbb{R}^{n_x}$, $\mathbb{X}_T \subset \mathbb{R}^{n_x}$ and $\mathbb{U} \subset \mathbb{R}^{n_u}$ the constraints of the state $\boldsymbol{x} \in \mathbb{R}^{n_x}$ and the input $\boldsymbol{u} \in \mathbb{R}^{n_u}$. Time T is the optimization horizon. The control law is obtained by applying the optimal input for the time period $\tau \in [t, t+\mu]$ with $\mu << T$, i.e., $\boldsymbol{u}(t) = \boldsymbol{u}^*(\tau)$, where $\boldsymbol{u}^*(\tau)$ is the optimizer of (3.14), to the system and repeating that procedure after the time period μ. The stability of the closed-loop system is well studied in literature for nonlinear systems with state and input constraints in a discrete and continuous-time setting [May+00; RMD17; CA98]. It is generally necessary to assume that $\mathbb{X}$, $\mathbb{X}_T$ and $\mathbb{U}$ are compact sets which contain the optimal steady state. Conditions for stability heavily depend on the form of the objective function, which determines the type of MPC problem. In the following, the two most common types of MPC, setpoint-tracking and economic MPC, are presented. Additionally, an introduction to distributed MPC is given.

3.2.1 Setpoint-tracking MPC

The classical way to operate an MPC is by means of a control hierarchy as in Figure 3.2 (left). A steady-state optimization computes economically optimal setpoints which are passed as a reference for the setpoint-tracking MPC[27] [Eng07; RMD17]. The setpoint is then regulated by the MPC with a stage cost of the form[28]

$$l(\boldsymbol{x}(t), \boldsymbol{u}(t)) = \|\boldsymbol{x}(t) - \boldsymbol{x}_{\text{opt}}\|_{\boldsymbol{Q}}^2 + \|\boldsymbol{u}(t) - \boldsymbol{u}_{\text{opt}}\|_{\boldsymbol{R}}^2. \tag{3.15}$$

The objective function (3.15) penalizes the state and input deviations weighted by the positive definite matrices $\boldsymbol{Q} \in \mathbb{R}^{n \times n}$ and $\boldsymbol{R} \in \mathbb{R}^{m \times m}$. Stability of the setpoint-tracking MPC is typically assessed by using the value function[29] $V^*(\boldsymbol{x}(t))$ as a Lyapunov function candidate for the closed-loop system. Standard results in MPC theory state that the value function is a Lyapunov function for the closed-loop receding horizon operation, if

[27] Time-varying setpoints which change much slower than the system dynamics are assumed, such that piecewise-constant setpoints are tracked. It is shown later that this assumption is typically fulfilled in power systems.

[28] Alternatively, a reference may be given only for the output y. In that case, a stabilizability assumption (related to observability) for the system is necessary for ensuring stability [RMD17].

[29] The value function describes the minimal cost of (3.14) at state $\boldsymbol{x}(t)$ and is a standard definition in optimal control theory. See, e.g., [RMD17, Sec. 2.2].

(i) the terminal constraint set $\mathbb{X}_T$ is positively invariant for the system with a stabilizing control law $\kappa(\boldsymbol{x}(t))$, (ii) the terminal costs V_T are chosen as a Lyapunov function for the system in the terminal constraint set $\mathbb{X}_T$, together with the assumptions of closed and compact constraint sets [May+00].

Remark 3.5. *The setpoint-tracking MPC considers thus the typical regulation problem with picewise-constant setpoints. In particular, a time-varying trajectory-tracking problem is not part of the setpoint-tracking MPC and is not considered in this work.*

Note that the objective function form (3.15) is the key for the value function to fulfill the Lyapunov conditions, since it decreases with the (weighted) distance to the optimal setpoint. Furthermore, this optimal setpoint is the unique minimizer (due to the definiteness of $\boldsymbol{Q}$ and $\boldsymbol{R}$) and lies inside the state and input constraints.

3.2.2 Economic MPC

In economic MPC, general cost functions for the stage cost $l(\cdot)$ and the terminal cost $V_T(\cdot)$ can be used. Convexity is not required, and in general, the minimum of the objective function (if it exists) is neither a steady state of the system nor does it lie inside the state and input constraints. In particular, an admissible steady state $\left(\boldsymbol{x}_{\text{opt}}, \boldsymbol{u}_{\text{opt}}\right)$ is not part of the objective function and must not be given in advance. In fact, it must not even exist [Raw+08]. In Figure 3.2, setpoint-tracking and economic MPC are compared from a procedural perspective. The steady-state optimization in setpoint-tracking MPC corresponds to the economic optimization. It can be observed, that economic MPC avoids computing a steady state in advance and uses instead the economic objective function in the MPC. This is a great advantage when considering networked systems, where computing the steady state requires network-wide information.

Remark 3.6. *The term 'economic' in economic MPC should not be understood literally. It just denotes that the objective function is a general, possibly nonconvex function. The most important difference with setpoint-tracking MPC, is that the minimizer of the objective function does not need to be the optimal steady state (cf.* (3.15)*). The name stems from utilizing an economic objective function (e.g., depending on a time-varying price, possibly nonconvex) in chemical processes [RMD17, p. 153], but is not limited to it [FGM+18; ARA11; AAR11; DAR10]. Any MPC formulation with an objective function where the minimizer is not the optimal steady state is called economic MPC.*

Since in economic MPC the minimum of the objective function does not need to be a steady state, it becomes clear that the value function of (3.14) cannot serve as a

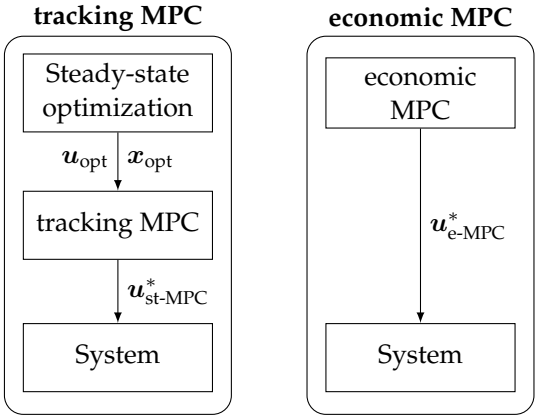

Figure 3.2: Comparison of setpoint-tracking and economic MPCs from a procedural perspective.

Lyapunov function,[30] and the classic MPC stability conditions do not hold [RMD17, p. 153],[FGM+18].

In the next section, the requirements for distributed MPC — which are independent of the type of objective function — are presented.

3.2.3 Distributed MPC

In distributed MPC, problem (3.14) is solved in a distributed manner by a set of agents $\mathcal{A} = \{1, \dots, |\mathcal{A}|\}$. Each agent $m \in \mathcal{A}$ is responsible for a subset of the state and input variables $\boldsymbol{x}^m$ and $\boldsymbol{u}^m$, where $\boldsymbol{x} = \text{col}\{\boldsymbol{x}^m\}$ and $\boldsymbol{u} = \text{col}\{\boldsymbol{u}^m\}$ are the system states and inputs. Thus, each agent is responsible for a part of the system dynamics. The system is partitioned into a set of interconnected dynamic systems

$$\dot{\boldsymbol{x}}^m = \boldsymbol{f}^m(\boldsymbol{x}^m, \boldsymbol{u}^m) + \sum_{\substack{j \in \mathcal{A} \\ j \neq m}} \boldsymbol{f}^{mj}(\boldsymbol{x}_j, \boldsymbol{u}_j) \tag{3.16a}$$

$$\boldsymbol{y}^m = \boldsymbol{c}^m(\boldsymbol{x}^m, \boldsymbol{u}^m). \tag{3.16b}$$

The second term in (3.16a) describes the influence of other systems to the system dynamics of agent $m \in \mathcal{A}$. Note that by combining all systems $m \in \mathcal{A}$, the system dynamics of the whole system as in (3.14) are obtained. Each agent $m \in \mathcal{A}$ solves then

[30] This is because the positive definite condition for the Lyapunov function [Kha02, Chapter 4], i.e., that the value of the function is zero at the desired equilibrium and greater zero elsewhere, is not fulfilled. The positive definite condition is only fulfilled when the objective function is chosen to be the distance to a desired setpoint, as in setpoint-tracking MPC.

the optimization problem

$$\mathrm{MPC}^m(t) := \begin{cases} \min & \int_t^T l^m(\boldsymbol{x}^m(\tau), \boldsymbol{u}^m(\tau))\mathrm{d}\tau + V_T(\boldsymbol{x}(T)) \\ \text{s. t.} & \dot{\boldsymbol{x}}^m = \boldsymbol{f}^m(\boldsymbol{x}^m, \boldsymbol{u}^m) + \sum_{\substack{j\in\mathcal{A} \\ j\neq m}} \boldsymbol{f}^{mj}(\boldsymbol{x}^j, \boldsymbol{u}^j), \\ & \boldsymbol{x}^m(\tau) \in \mathbb{X}^m \\ & \boldsymbol{x}^m(T) \in \mathbb{X}_T^m \\ & \boldsymbol{u}^m(\tau) \in \mathbb{U}^m \\ & \tau \in [t, T]\,, \end{cases} \tag{3.17}$$

where $\mathbb{X}^m$, $\mathbb{X}_T^m$ and $\mathbb{U}$ are the input and state constraints of agent $m \in \mathcal{A}$. Note that the individual optimization problems $m \in \mathcal{A}$ are coupled. The terms that induce such a coupling are highlighted in purple and blue. The purple terms require information about the dynamics of the other agents $m \in \mathcal{A}$. The information is necessary to compute a global Lyapunov function V_T and terminal constraints $\mathbb{X}_T^m$ (see explanation below). The blue terms require communication of the states $\boldsymbol{x}^m$ of the other agents $m \in \mathcal{A}$. This is summarized in the following two main challenges to solve within distributed MPC:

- A Lyapunov function is necessary: as pointed out in Section 3.2.1, the current MPC stability theory builds upon a Lyapunov function. This Lyapunov function is used in the terminal cost V_T, and the positive invariant set corresponding to that Lyapunov function in the terminal constraint $\mathbb{X}_T^m$. In general, for constructing such a global (i.e., system-wide) Lyapunov function, information of the whole system is necessary. This hampers the distributed implementation, especially when systems are disconnecting or rejoining, since every time a new global Lyapunov function has to be computed.
- A distributed optimization algorithm: it becomes clear from (3.17), that agent m needs to receive, at every time step, the coupling states $\boldsymbol{x}^j$ and inputs $\boldsymbol{u}^j$ to calculate its optimizer. The MPC problems (3.17) form, for all $m \in \mathcal{A}$, a distributed optimization problem.

Solving these two challenges forms the basis of distributed MPC. In Figure 3.3, the requirements for distributed MPC are illustrated graphically.

Some distributed MPC methods, consider only one of both aspects. For example, one of the first distributed MPC approaches with guaranteed stability exploits only the aspect of a distributed computation [VRW05]. It formulates a mathematical parallelization in which all agents perform computations and there is no central computation unit, but all the agents need to have full knowledge about the dynamics, constraints and objectives of all other agents.

More recent methods propose algorithms for the synthesis of terminal costs and constraints, i.e., a Lyapunov function, using only local information and communication with neighbors [Con+16; DEL20; HLJ14; Zei+13; Con+12]. That way, the need of sharing the system dynamics among all agents $m \in \mathcal{A}$ is reduced to few neighbors. A focus is also

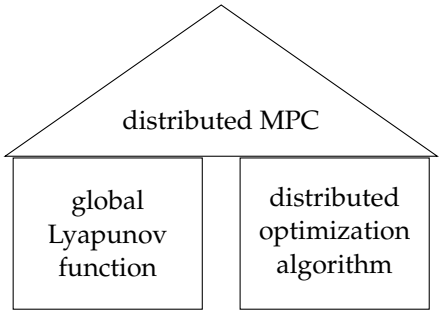

Figure 3.3: Requirements for distributed MPC

the structure of the Lyapunov function itself. The goal is to have a *separable*[31] Lyapunov function, i.e., $V_T(\boldsymbol{x}) = \sum_{i=1}^{|\mathcal{A}|} V_T^m(\boldsymbol{x}^m)$ and $\mathbb{X}_T$ is polytopic. Then, the communication of state variables for evaluating the terminal costs V_T in (3.17) is reduced, and each agent $m \in \mathcal{A}$ can evaluate its terminal costs and constraints without further communication. This is, however, not always possible [Con+16]. In this thesis, passivity is exploited in order to obtain a Lyapunov function with such a suitable structure in Chapter 4.

3.3 Convex Optimization

In this section, the fundamental concepts about convex optimization are presented. All these fundamental concepts are essential for the derivation of the novel distributed optimization framework presented in Chapter 5. First, in Section 3.3.1, the relevant basic definitions and characterizations of convexity and convex functions are stated. In Section 3.3.2, the classical optimality conditions characterizing an optimizer of an unconstrained or constrained network optimization problem are presented.

3.3.1 Basic Definitions

The following definitions of convex sets and functions are taken from [BV04, p. 23] and [BV04, p. 67], respectively.

Definition 3.5 (convex set)
A set $\mathcal{S}$ is convex if for any $\boldsymbol{x}, \boldsymbol{y} \in \mathcal{S}$ and any scalar θ with $0 \leq \theta \leq 1$

$$\theta \boldsymbol{x} + (1 - \theta)\, \boldsymbol{y} \in \mathcal{S} \tag{3.18}$$

[31] See Section A.1 for a concise definition.

holds. Graphically, all points on the line connecting any two points in $\mathcal{S}$ must also lie in $\mathcal{S}$.

Definition 3.6 (convex function)
A function $f : \mathcal{S} \subseteq \mathbb{R}^n \to \mathbb{R}$ with a convex set $\mathcal{S}$ as domain which satisfies

$$f(\theta \boldsymbol{x} + (1-\theta)\boldsymbol{y}) \leq \theta f(\boldsymbol{x}) + (1-\theta) f(\boldsymbol{y}) - \frac{1}{2} M_{\text{conv}} \theta (1-\theta)(\boldsymbol{y}-\boldsymbol{x})^\top (\boldsymbol{y}-\boldsymbol{x}) \tag{3.19}$$

for all $\theta \in [0,1]$ and all $\boldsymbol{x}, \boldsymbol{y} \in \mathbb{R}^n$ is called

a) convex, if $M_{\text{conv}} = 0$.

b) strictly convex, if $M_{\text{conv}} = 0$ and the inequality holds strictly.

c) M_{conv}-strongly convex, if $M_{\text{conv}} > 0$.

For a differentiable function, a first order condition for convexity exists [BV04, Sec. 3.1.3]. A differentiable function $f : \mathbb{R}^n \to \mathbb{R}$ which satisfies

$$\left(\nabla f(\boldsymbol{y}) - \nabla f(\boldsymbol{x})\right)^\top (\boldsymbol{y}-\boldsymbol{x}) \geq M_{\text{conv}} (\boldsymbol{y}-\boldsymbol{x})^\top (\boldsymbol{y}-\boldsymbol{x}) \tag{3.20}$$

for all $\boldsymbol{x}, \boldsymbol{y} \in \mathbb{R}^n$ is called

a) convex, if $M_{\text{conv}} = 0$.

b) strictly convex, if $M_{\text{conv}} = 0$ and the inequality holds strictly.

c) M_{conv}-strongly convex, if $M_{\text{conv}} > 0$.

Furthermore, for any convex function f, the inequalities [Hat+18]

$$\begin{aligned} f(\boldsymbol{x}_1) - f(\boldsymbol{x}_2) &\leq \nabla f(\boldsymbol{x}_1)^\top (\boldsymbol{x}_1 - \boldsymbol{x}_2) \\ f(\boldsymbol{x}_1) - f(\boldsymbol{x}_2) &\geq \nabla f(\boldsymbol{x}_2)^\top (\boldsymbol{x}_1 - \boldsymbol{x}_2) \end{aligned} \tag{3.21}$$

hold for any $\boldsymbol{x}_1, \boldsymbol{x}_2 \in \mathbb{R}^n$.

Lastly, an important inequality for a Lipschitz continuous function is introduced [BC17, Def. 1.47]. For a Lipschitz continuous function $f : \mathbb{R}^n \to \mathbb{R}$, there exists a $M_{\text{Lip},} \in \mathbb{R}_{>0}$ such that

$$\|f(\boldsymbol{x}) - f(\boldsymbol{y})\| \leq M_{\text{Lip},} \|\boldsymbol{x} - \boldsymbol{y}\| \tag{3.22}$$

holds.

3.3.2 Optimality Conditions in Convex Optimization

In the following, the classical optimality conditions for a network optimization problem as defined below are presented. The optimality conditions are taken from [BV04].

Consider a set of agents $\mathcal{A} = \{1, \dots, n_{\mathcal{A}}\}$, $n_{\mathcal{A}} \in \mathbb{N}$. Define the network optimization problem

$$\min \sum_{i \in \mathcal{A}} f_i(\mathbf{y}) \tag{3.23a}$$

$$\text{s.t. } g_{il}(\mathbf{y}) \leq 0, \quad \forall l \in \mathcal{C}_{\text{in},i}, \forall i \in \mathcal{A} \tag{3.23b}$$

$$h_{ij}(\mathbf{y}) = 0, \quad \forall j \in \mathcal{C}_{\text{eq},i}, \forall i \in \mathcal{A} \tag{3.23c}$$

with $\mathbf{y} \in \mathbb{R}^n$. The objective function $f_i : \mathbb{R}^n \to \mathbb{R}$ and the constraints $g_{il} : \mathbb{R}^n \to \mathbb{R}$ and $h_{ij} : \mathbb{R}^n \to \mathbb{R}$ belong to agent $i \in \mathcal{A}$. The variable $\mathbf{y} \in \mathbb{R}^n$ is a global variable of the agents. The sets $\mathcal{C}_{\text{in},i} = \{1, \dots, n_{\text{IC},i}\}$ and $\mathcal{C}_{\text{eq},i} = \{1, \dots, n_{\text{EQ},i}\}$ are the sets of inequality and equality constraints of agent $i \in \mathcal{A}$. The functions $g_{il} : \mathbb{R}^n \to \mathbb{R}$ are assumed to be convex, the functions $h_{ij} : \mathbb{R}^n \to \mathbb{R}$ to be affine, i.e., $h_{ij}(\mathbf{y}) = \boldsymbol{a}_{ij}^\top \mathbf{y} + c_{ij}$. The network optimization problem (3.23) describes the sum of objective functions of all agents, i.e., its solution is a Pareto optimum [Lei74, p. 8].

In the unconstrained case, i.e., h_{ij}, $g_{il} \equiv 0$, it holds the following optimality condition [BV04, p. 140].

Proposition 3.3 (unconstrained optimization)
Assume the optimization problem (3.23) *is convex and there are no constraints. Then,* $\mathbf{y}^*$ *is an optimizer if and only if*

$$\sum_{i \in \mathcal{A}} \nabla f_i(\mathbf{y}^*) = 0 \tag{3.24}$$

holds. If (3.23) *is strictly convex,* $\mathbf{y}^*$ *is unique.*

In the constrained case, the optimality conditions are known as the KKT conditions. Since Slater's condition[32] is assumed to hold, the KKT conditions are necessary and sufficient [BV04, p. 244]. Further, the Lagrange function of agent $i \in \mathcal{A}$ is defined as

$$L_i = f_i(\mathbf{y}) + \sum_{l \in \mathcal{C}_{\text{in},i}} \lambda_{il} g_{il}(\mathbf{y}) + \sum_{j \in \mathcal{C}_{\text{eq},i}} \mu_{ij} h_{ij}(\mathbf{y}), \tag{3.25}$$

[32] Slater's Condition says that the constraints (3.23b) are such that there exist a feasible interior, i.e., a $\boldsymbol{y} \in \mathbb{R}^n$ such that all inequality constraints are strictly satisfied [BV04, p. 226].

with $\lambda_{il}, \mu_{ij} \in \mathbb{R}$, and the global Lagrange function of optimization problem (3.23) as $L = \sum_{i \in \mathcal{A}} L_i$. For convenience, denote $\boldsymbol{\lambda}_i = \mathrm{col}\{\lambda_{il}\} \in \mathbb{R}^{n_{\mathrm{IC},i}}$ as the multipliers of agent i, and analogously for $\boldsymbol{\mu}_i \in \mathbb{R}^{n_{\mathrm{EQ},i}}$. The following proposition can be found in [BV04, p. 243].

Proposition 3.4 (KKT conditions)
Assume the optimization problem (3.23) *is convex and let Slater's condition hold. Then, $\mathbf{y}^*$ is an optimizer if and only if there exist multipliers $\boldsymbol{\lambda}_i^*, \boldsymbol{\mu}_i^*$ such that the conditions*

$$\sum_{i \in \mathcal{A}} \nabla_{\mathbf{y}} L_i(\mathbf{y}^*, \lambda_i^*, \mu_i^*) = 0 \tag{3.26a}$$

$$g_{il}(\mathbf{y}^*) \leq 0 \tag{3.26b}$$

$$h_{ij}(\mathbf{y}^*) = 0 \tag{3.26c}$$

$$\lambda_{il}^* \geq 0 \tag{3.26d}$$

$$\lambda_{il}^* \, g_{il}(\mathbf{y}^*) = 0 \tag{3.26e}$$

are fulfilled for all $i \in \mathcal{A}$, $j \in \mathcal{C}_{\mathrm{in},i}$ and $l \in \mathcal{C}_{\mathrm{eq},i}$. If problem (3.23) *is strictly convex, the optimizer $\mathbf{y}^*$ is unique.*

3.4 Power System Component Models

In the following, the models of the power system components used in Chapters 4 and 6 are presented. Throughout this work, a set of grids $m \in \mathcal{M} = \{1, \ldots, n_{\mathrm{mg}}\}$ is considered, each comprising a set $\mathcal{B}^m$ of $n_{\mathcal{B}}^m = |\mathcal{B}^m|$ electrical buses or nodes[33] connected via a set $\mathcal{E}^m$ of $n_{\mathcal{E}}^m = |\mathcal{E}^m|$ electrical lines. In the next subsections, models of the components of the DC grid are derived, i.e., electrical buses, power lines and loads. These component models are used in Chapter 4 and 6 for forming appropriate power system models in each chapter. The models derived here are not new; they are widely used for modelling meshed DC systems, see the references reviewed in Chapter 2.

The grid index m (always displayed as superscript) is omitted for simplicity in the remainder of this section, since only the individual components are described. Furthermore, all grids $m \in \mathcal{M}$ are composed of the same components (although grids may have different sizes, topologies and parameters).

[33] The terms *buses* and *nodes* are both used in the literature. The term *buses* is more common in the power systems literature, and *nodes* in the control theory literature. Both terms are used equivalently in this dissertation.

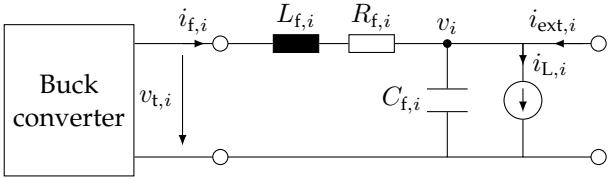

Figure 3.4: Electric scheme of a bus including a DGU and a load.

3.4.1 Distributed Generation Units

DGUs are located on the buses $i \in \mathcal{B}_{\mathrm{DGU}}$, which are a subset of the buses of a grid, i.e., $\mathcal{B}_{\mathrm{DGU}} \subseteq \mathcal{B}$. A graphical representation of a bus including a DGU is shown in Figure 3.4. It is composed of a buck converter supplying a voltage $v_{\mathrm{t},i} \in \mathbb{R}_{\geq 0}$, a load with current $i_{\mathrm{L},i} \in \mathbb{R}$, and a filter with the resistance $R_{\mathrm{f},i} \in \mathbb{R}_{>0}$, inductance $L_{\mathrm{f},i} \in \mathbb{R}_{>0}$ and capacitance $C_{\mathrm{f},i} \in \mathbb{R}_{>0}$. The buck converter is idealized by considering the widely used averaging model [MC76]. The dynamics for every bus with DGU $i \in \mathcal{B}_{\mathrm{DGU}}$ are described with the states $v_i \in \mathbb{R}_{\geq 0}$ and $i_{\mathrm{f},i} \in \mathbb{R}$, which describe the node voltage and filter current, by

$$C_{\mathrm{f},i}\dot{v}_i = i_{\mathrm{f},i} - i_{\mathrm{L},i}(v_i) - i_{\mathrm{ext},i} \tag{3.27a}$$

$$L_{\mathrm{f},i}\dot{i}_{\mathrm{f},i} = v_{\mathrm{t},i} - R_{\mathrm{f},i}i_{\mathrm{f},i} - v_i, \tag{3.27b}$$

where $i_{\mathrm{ext},i} \in \mathbb{R}$ is the cumulative current injected by interconnecting lines. The DGUs at the nodes are equipped with a passivity-based primary voltage controller as in [Nah+20], which regulates v_i to a reference voltage $v_{\mathrm{ref},i} \in \mathbb{R}_{\geq 0}$. Similar controllers, e.g., based on a port Hamiltonian system representation, have been presented in [Str+20; Str+21]. In this work, however, the controller in [Nah+20] is chosen because it is a full state-feedback (see (3.28)), and it is thus a more general approach compared to a port-Hamiltonian approach[34] and allows more degrees of freedom for the control design. Such a controller is often called grid-forming, since it tries to maintain a constant node voltage regardless the load or power system state. The controller adds a state $e_i \in \mathbb{R}$ to the system for obtaining an integral action, and employs a state feedback

$$v_{\mathrm{t},i} = \boldsymbol{k}_i^\top [v_i, i_{\mathrm{f},i}, e_i]^\top \tag{3.28}$$

with $\boldsymbol{k}_i \in \mathbb{R}^3$. The node dynamics with the passivity-based voltage controller are

$$C_{\mathrm{f},i}\dot{v}_i = i_{\mathrm{f},i} - i_{\mathrm{L},i}(v_i) - i_{\mathrm{ext},i} \tag{3.29a}$$

$$\dot{i}_{\mathrm{f},i} = \alpha_i v_i + \beta_i i_{\mathrm{f},i} + \gamma_i e_i \tag{3.29b}$$

$$\dot{e}_i = v_{\mathrm{ref},i} - v_i, \tag{3.29c}$$

where

$$\alpha_i = \frac{k_{1,i} - 1}{L_{\mathrm{f},i}},\ \beta_i = \frac{k_{2,i} - R_{\mathrm{f},i}}{L_{\mathrm{f},i}},\ \gamma_i = \frac{k_{3,i}}{L_{\mathrm{f},i}}. \tag{3.30}$$

[34] This is because not all controllers can be described as a port Hamiltonian system.

are controller parameters. In this work, a time-varying, nonlinear ZIP load is assumed, i.e.,

$$i_{\mathrm{L},i}(v_i) = Y_i(t)v_i + \frac{P_{\mathrm{L},i}(t)}{v_i} + I_i(t), \tag{3.31}$$

where $Y_i \in \mathbb{R}_{>0}$ is the load admittance, $P_{\mathrm{L},i} \in \mathbb{R}$ the power load, and $I_i \in \mathbb{R}$ the load current. Such a load modelling is standard in power system analysis [KM22]. Here, it is assumed that the load parameters Y_i, P_i and I_i are piecewise constant. In the following, an important result from [Nah+20] which will prove instrumental for the MPC stability analysis in Chapter 4 is presented. It states that choosing the control parameters according to [Nah+20, Th. 2], the node dynamics are EIP w.r.t. the input-output pair $(-i_{\mathrm{ext},i}, v_i)$. This allows to interconnect arbitrarily many nodes by (passive) lines while guaranteeing stability for a constant voltage references $v_{\mathrm{ref},i}$.

Proposition 3.5 (EIP properties of a DGU)
Let $[\bar{v}_i, \bar{i}_{\mathrm{f},i}, \bar{e}_i]$ be an equilibrium point of (3.29) *and define the error variables $\tilde{v}_i = v_i - \bar{v}_i$, $\tilde{i}_{\mathrm{f},i} = i_{\mathrm{f},i} - \bar{i}_{\mathrm{f},i}$ and $\tilde{e}_i = e_i - \bar{e}_i$. Let the constant power load P_i be zero. System* (3.29) *is EIP w.r.t. the input-output pair $(-\tilde{i}_{\mathrm{ext},i}, \tilde{v}_i)$ for any $v_{\mathrm{ref},i} > 0$ with the storage function $S_i : \mathbb{R}^3 \to \mathbb{R}_{\geq 0}$*

$$S_i(\tilde{v}_i, \tilde{i}_{\mathrm{f},i}, \tilde{e}_i) = \begin{bmatrix} \tilde{v}_i \\ \tilde{i}_{\mathrm{f},i} \\ \tilde{e}_i \end{bmatrix}^\top \begin{bmatrix} C_{\mathrm{f},i} & 0 & 0 \\ 0 & \frac{\beta_i}{\omega_i} & \frac{\gamma_i}{\omega_i} \\ 0 & \frac{\gamma_i}{\omega_i} & \frac{\alpha_i \gamma_i}{\omega_i} \end{bmatrix} \begin{bmatrix} \tilde{v}_i \\ \tilde{i}_{\mathrm{f},i} \\ \tilde{e}_i \end{bmatrix}, \tag{3.32}$$

with $S(0,0,0) = 0$, if $\omega_i < 0$ and the control parameters are chosen such that

$$k_{1,i} < 1 \tag{3.33}$$

$$k_{2,i} < R_{\mathrm{f},i} \tag{3.34}$$

$$0 < k_{3,i} < \frac{1}{L_{\mathrm{f},i}}(k_{1,i} - 1)(k_{2,i} - R_{\mathrm{f},i}). \tag{3.35}$$

Proof. The proof can be found in [Nah+20]. □

Remark 3.7. *It is further proven in [Nah+20], that a DGU is locally EIP for a nonzero power load P_i, provided that*

$$P_{\mathrm{L},i}(t) < Y_i(t)v_{\mathrm{ref},i} \tag{3.36}$$

holds. The DGU is then EIP in the subset of the state space

$$\mathcal{D}_i = \{v_i \geq \frac{P_{\mathrm{L},i}}{Y_i v_{\mathrm{ref},i}} - v_{\mathrm{ref},i}, i_{\mathrm{f},i} \in \mathbb{R}, e_i \in \mathbb{R}\}. \tag{3.37}$$

A positively invariant set for any constant $v_{\mathrm{ref},i}$ system (3.29) *is then the largest sublevel set of S_i which lies inside $\mathcal{D}_i$.*

Remark 3.8. *By observing the proof of Proposition 3.5 in [Nah+20], it can be concluded that system* (3.29) *is not only EIP but also OFEIP(ρ_i) w.r.t. the supply rate*

$$s(-i_{\mathrm{ext},i}, v_i) = -i_{\mathrm{ext},i}^\top v_i - \rho_i v_i^2, \tag{3.38}$$

with $0 < \rho_i \leq Y_i v_{\mathrm{ref},i} - P_{\mathrm{L},i}$. This plays a key role for the determination of asymptotic stability of networked grids in Chapter 4.

Remark 3.9. *Optionally, a node can contain only a load, without a DGU. Then, the system is again EIP if condition* (3.36) *is fulfilled. This is proven in the next section.*

3.4.2 Load Node

A load node is modeled as a DGU node without the filter and buck converter. The dynamics are governed by the nonlinear dynamic equation

$$C_{\mathrm{L},i}\dot{v}_i = -i_{\mathrm{L},i}(v_i) - i_{\mathrm{ext},i}, \tag{3.39}$$

where $i_{\mathrm{L},i}(v_i)$ is the load as in (3.31), and $C_{\mathrm{L},i} \in \mathbb{R}$ is capacitance of that node. This capacitance depends on the power line capacitance as explained in Section 3.4.3, and on any other element connected to that node. The following proposition establishes EIP properties of a load node.

Proposition 3.6 (EIP properties of load node)
Let $\bar{v}_i$, $\bar{i}_{\mathrm{ext}}$ be an equilibrium of (3.39)*. Then, system* (3.39) *is EIP w.r.t. the port $(\tilde{v}_i, -\tilde{i}_{\mathrm{ext}})$ and storage function $S_i(\tilde{v}_i) = \frac{C_{\mathrm{L},i}}{2}\tilde{v}_i^2$, if the load $i_{\mathrm{L},i}(v_i)$ is a monotone function.*

Proof. First, the shifted dynamics of system (3.39) are derived. For that, subtract an equilibrium of (3.39) from the dynamics (3.39) to obtain

$$C_{\mathrm{L},i}\dot{\tilde{v}}_i = -i_{\mathrm{L},i}(v_i) - i_{\mathrm{ext},i} + i_{\mathrm{L},i}(\bar{v}_i) + \bar{i}_{\mathrm{ext},i} \tag{3.40}$$

$$= -(i_{\mathrm{L},i}(v_i) - i_{\mathrm{L},i}(\bar{v}_i)) - \tilde{i}_{\mathrm{ext},i}. \tag{3.41}$$

The time derivative of the storage function is

$$\dot{S}_i = \tilde{v}_i(-(i_{\mathrm{L},i}(v_i) - i_{\mathrm{L},i}(\bar{v}_i)) - \tilde{i}_{\mathrm{ext},i}) \tag{3.42}$$

$$= -\tilde{v}_i(i_{\mathrm{L},i}(v_i) - i_{\mathrm{L},i}(\bar{v}_i)) - \tilde{v}_i\tilde{i}_{\mathrm{ext},i}. \tag{3.43}$$

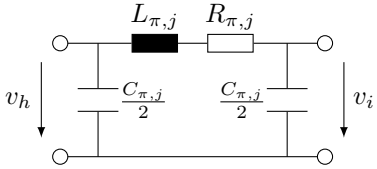

Figure 3.5: Graphical representation of a line in the pi equivalent circuit.

Inserting $v_i = \bar{v}_i + \tilde{v}_i$ in the first term in (3.43) yields $\tilde{v}_i(i_{\mathrm{L},i}(\bar{v}_i+\tilde{v}_i) - i_{\mathrm{L},i}(\bar{v}_i))$. If condition

$$\tilde{v}_i(i_{\mathrm{L},i}(\bar{v}_i + \tilde{v}_i) - i_{\mathrm{L},i}(\bar{v}_i)) \geq 0 \tag{3.44}$$

holds, then $\dot{S}_i \leq -\tilde{v}_i\tilde{i}_{\mathrm{ext},i}$ directly follows from (3.43), which implies EIP w.r.t. the port $(\tilde{v}_i, -\tilde{i}_{\mathrm{ext}})$. Furthermore, observe that (3.44) is a monotonicity condition (see [BC17, Def. 20.1] or [RW98, Def. 12.1]) for the nonlinear load function $i_{\mathrm{L},i}$, which is stated in the proposition. □

Remark 3.10. *Note that if the load $i_{\mathrm{L},i}(v_i)$ is a strictly monotone function of v_i, it follows directly from* (3.43) *that the node dynamics* (3.39) *are OFEIP(ρ) where ρ is the lower bound of the derivative of i_{L,v_i}.*

Remark 3.11. *For a ZIP load* (3.31)*, the monotonicity condition is* (3.36)*. Thus, the EIP conditions for a DGU or a load node are identical when ZIP loads are used.*

3.4.3 Power Line

The power lines are modeled with the π equivalent circuit [Mac+20], which is shown in Figure 3.5. This power line model is seen as adequate to analyze stability in power systems based on power electronics [KCRC24]. The model is composed of a series inductance $L_{\pi,j} \in \mathbb{R}_{>0}$ and resistance $R_{\pi,j} \in \mathbb{R}_{>0}$, and two parallel capacitances $\frac{C_{\pi,j}}{2} \in \mathbb{R}_{>0}$. Note that the line capacitance is connected in parallel to the bus capacitance of the buses to which the line connects. Hence, only one capacitor with a capacitance that equals to the sum of both can be considered. Furthermore, since the capacitance of typical filter capacitors [Tuc+16; Nah+20] are higher than line capacitances of medium voltage power lines [Rud+06] by several orders of magnitude, the line capacitances can be neglected if the line connects to a node with a DGU. The dynamics for line $j \in \mathcal{E}$ interconnecting nodes $k, l \in \mathcal{B}$ are thus described by a current $i_{\pi,j} \in \mathbb{R}$ with

$$L_{\pi,j}\dot{i}_{\pi,j} = -R_{\pi,j}i_{\pi,j} + v_{\Delta j}, \tag{3.45}$$

where $v_{\Delta j} = v_l - v_k$ is the input and v_k, v_l are the bus voltages and $k, l \in \mathcal{B}$. The next proposition serves as an important building block towards an overall Lyapunov function in Subsection 4.1.

Proposition 3.7 (power line EIP)
Let $\bar{i}_{\pi,j}, \bar{v}_{\Delta,j}$ *be an equilibrium point of* (3.45) *and define* $\tilde{i}_{\pi,j} = i_{\pi,j} - \bar{i}_{\pi,j}$, $\tilde{v}_{\Delta,j} = v_{\Delta j} - \bar{v}_{\Delta,j}$. *System* (3.45) *is strictly EIP w.r.t. the input-output pair* $(\tilde{i}_{\pi,j}, \tilde{v}_{\Delta,j})$ *with the storage function* $S_j : \mathbb{R} \to \mathbb{R}_{\geq 0}$

$$S_j(\tilde{i}_{\pi,j}) = \frac{1}{2} L_{\pi,j} \tilde{i}_{\pi,j}^2. \tag{3.46}$$

Proof. The proof is standard and follows directly from taking the derivative of the storage function and inserting the shifted dynamics (3.45). The derivative of the storage function is

$$\dot{S}_j = L_{\pi,j} \tilde{i}_{\pi,j} \dot{\tilde{i}}_{\pi,j}, \tag{3.47}$$

and inserting the shifted dynamics (3.45) yields

$$\dot{S}_j = L_{\pi,j} \tilde{i}_{\pi,j} \left(-\frac{R_{\pi,j}}{L_{\pi,j}} \tilde{i}_{\pi,j} + \frac{1}{L_{\pi,j}} \tilde{v}_{\Delta,j} \right) \tag{3.48}$$

$$= -R_{\pi,j} \tilde{i}_{\pi,j}^2 + \tilde{i}_{\pi,j} \tilde{v}_{\Delta,j}, \tag{3.49}$$

which proofs the strict EIP w.r.t. the input-output pair $(\tilde{i}_{\pi,j}, \tilde{v}_{\Delta,j})$ taking into account that the only state of the line dynamics (3.45) is the inductance current $i_{\pi,j}$. □

4 Model Predictive Control for Optimal Operation of Regulated Power Systems

In this chapter, the first optimization-based method of this dissertation tailored to future power systems is presented.[35] The method builds upon the classical MPC theory, extending this theory in order to allow the application of MPC to large-scale future power systems by exploiting passivity-based underlying controllers. The proposed methodology results in a regulated power system. This method corresponds to Contribution 1 in Figure 2.4.

The methodology presented in this chapter tackles the first requirement in distributed MPC (see Figure 3.3 in Section 3.2.3). In particular, a modular global Lyapunov function is designed in order to ensure stability without the necessity of exchanging further information. Hence, local conditions for the agents to construct a modular, global Lyapunov function are the main result of this chapter. The power system is then stable if every grid uses the proposed distributed MPC, without the necessity of sharing the individual system dynamics. The second requirement regarding a distributed optimization algorithm is addressed in Chapter 5. This is illustrated in Figure 4.1.

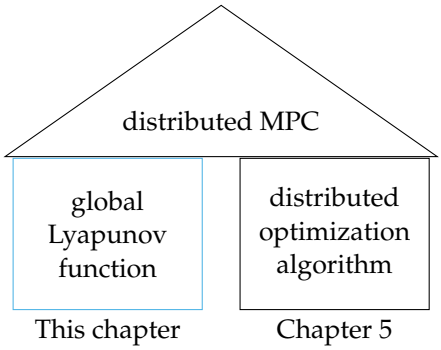

Figure 4.1: Organization of the presented method tackling the requirements for distributed MPC

In Section 4.1, the general setup and system model are presented. In Section 4.1.1, the network participants are described. In Section 4.1.2, the system model of a grid based on the basic components introduced in Section 3.4 is presented and its EIP properties are established. The result of this section is a nonlinear system describing the grid dynamics and its EIP properties w.r.t. an electric port.

[35] Preliminary results leading to the content of this chapter have been presented in the book chapter and [JS+25b] and in the conference proceedings [JS+23c; JSPH22].

In Section 4.2, a model reduction is presented. The model reduction neglects the fast line dynamics, obtaining then a reduced system suitable for the online optimization in MPC. Furthermore, the EIP of every grid established in the past section is exploited for deriving a separable[36] Lyapunov function. This is later used for the terminal cost and constraints in the MPC control design (see the first requirement in Figure 4.1).

In Section 4.3, two MPC controllers are derived, a setpoint-tracking and an economic MPC. A stability proof is given for the setpoint-tracking MPC. The economic MPC is verified in simulations. Further, it is highlighted that the stability conditions are local, i.e., only depend on variables of the individual grid, which is the main contribution of this chapter. However, it is also shown that for solving the MPC problem in a distributed manner, a distributed optimization algorithms is necessary (see the second requirement in Figure 4.1).

In Section 4.4, an illustrative example is given, where setpoint-tracking and economic MPC are compared. It is shown that economic MPC outperforms setpoint-tracking MPC. To conclude this chapter, a discussion of the proposed method, which results in a regulated power system, is provided.

4.1 Network Participants and Power System Model

In this subsection, the grid model employed in this chapter is presented. For that, the power system components presented in Section 3.4 are used. Before deriving the differential equations describing the system, the network participants and their interactions are introduced.

4.1.1 Network Participants

The approach proposed in this chapter corresponds to a fully technically regulated power system as in Term 2.1. Thus, there is no separation of roles between rational decision-makers pursuing own goals and system operators ensuring an efficient and stable operation. Consequently, there is only one type of agent, and these agents do not pursue own economic goals but carry out predefined computations to jointly achieve global optimality as well as stability.

The only agent considered in this approach is the grid operator. He is responsible for the DGUs $i \in \mathcal{B}_{\text{DGU}}^m$ in its respective grid $m \in \mathcal{M}$, where $\mathcal{M}$ is the set of grids. All the DGUs are controlled by the grid-forming controllers as presented in Section 3.4. The grid operator has full knowledge over its own grid, but no knowledge about any parameters of other grids. The stability conditions resulting from the method in this chapter are local conditions. The conditions hence depend, for every grid, only on

[36] See Section A.1 for a concise definition.

own parameters or variables. However, the method proposed in this chapter requires each grid operator to perform predefined computations and to periodically exchange information, in order to contribute towards solving the global optimization problem.

4.1.2 Power System Model

In this section, the differential equations describing a grid $m \in \mathcal{M}$ are derived. A grid comprises a set of nodes $\mathcal{B}$ of $n_{\mathcal{B}}^m = |\mathcal{B}^m|$ electrical buses connected via a set $\mathcal{E}^m$ of $n_{\mathcal{E}}^m = |\mathcal{E}^m|$ electrical lines. The set of nodes is divided into a set of nodes with a DGU $\mathcal{B}_{\text{DGU}}^m$ and nodes with only a load $\mathcal{B}_{\text{L}}^m$, i.e., $\mathcal{B}^m = \mathcal{B}_{\text{DGU}}^m \cup \mathcal{B}_{\text{L}}^m$. There are $n_{\text{DGU}}^m = |\mathcal{B}_{\text{DGU}}^m|$ nodes with a DGU, and $n_{\mathcal{B}}^m - n_{\text{DGU}}^m$ nodes with only a load. Since the model of a single grid is considered in the following, the grid index m is omitted until further notice.

A group of $n_{\mathcal{B}} = |\mathcal{B}|$ independent load and DGU buses is described by

$$\boldsymbol{C}_{\text{f}}\dot{\boldsymbol{v}} = \boldsymbol{I}_{\text{f}}\boldsymbol{i}_{\text{f}} - \boldsymbol{i}_{\text{L}}(\boldsymbol{v}) - \boldsymbol{i}_{\text{ext}} \tag{4.1a}$$

$$\dot{\boldsymbol{i}}_{\text{f}} = \boldsymbol{\alpha}\boldsymbol{I}_{\text{f}}^{\top}\boldsymbol{v} + \boldsymbol{\beta}\boldsymbol{i}_{\text{f}} + \boldsymbol{\gamma}\boldsymbol{e} \tag{4.1b}$$

$$\dot{\boldsymbol{e}} = \boldsymbol{v}_{\text{ref}} - \boldsymbol{v} \tag{4.1c}$$

where $\boldsymbol{\alpha} = \text{diag}\{\alpha_i\} \in \mathbb{R}^{n_{\text{DGU}} \times n_{\text{DGU}}}$, $\boldsymbol{\beta} = \text{diag}\{\beta_i\} \in \mathbb{R}^{n_{\text{DGU}} \times n_{\text{DGU}}}$ and $\boldsymbol{\gamma} = \text{diag}\{\gamma_i\} \in \mathbb{R}^{n_{\text{DGU}} \times n_{\text{DGU}}}$ contain the control parameters as in (3.30), $\boldsymbol{C}_{\text{f}} = \text{diag}\{C_{\text{f},i}\}$ are the bus capacitances, $\boldsymbol{i}_{\text{L}} = \text{col}\{i_{\text{L},i}\}$ are the stacked load currents, and $\boldsymbol{v} = \text{col}\{v_i\} \in \mathbb{R}^{n_{\mathcal{B}}}$, $\boldsymbol{i}_{\text{f}} = \text{col}\{i_{\text{f},i}\} \in \mathbb{R}^{n_{\text{DGU}}}$ and $\boldsymbol{e} = \text{col}\{e_i\} \in \mathbb{R}^{n_{\text{DGU}}}$ are the stacked states. The matrix $\boldsymbol{I}_{\text{f}} \in \mathbb{R}^{n_{\mathcal{B}} \times n_{\text{DGU}}}$ is a matrix composed of zeros and ones assigning the filter currents of the nodes with a DGU $i \in \mathcal{B}_{\text{DGU}}$ to the correct voltages.[37] The variable $\boldsymbol{v}_{\text{ref}} \in \mathbb{R}^{n_{\text{DGU}}}$ are the stacked inputs. A group of uncoupled $n_{\mathcal{E}} = |\mathcal{E}|$ power lines is described by the equations

$$\boldsymbol{L}_{\pi}\dot{\boldsymbol{i}}_{\pi} = -\boldsymbol{R}_{\pi}\boldsymbol{i}_{\pi} + \boldsymbol{v}_{\Delta}, \tag{4.2}$$

where $\boldsymbol{i}_{\text{f}} = \text{col}\{i_{\text{f},i}\} \in \mathbb{R}^{n_{\mathcal{E}}}$, $\boldsymbol{v}_{\Delta} = \text{col}\{v_{\Delta j}\} \in \mathbb{R}^{n_{\mathcal{E}}}$ are the stacked states and inputs, and $\boldsymbol{R}_{\pi} = \text{diag}\{R_{\pi,j}\} \in \mathbb{R}^{n_{\mathcal{E}} \times n_{\mathcal{E}}}$ and $\boldsymbol{L}_{\pi} = \text{diag}\{L_{\pi,j}\} \in \mathbb{R}^{n_{\mathcal{E}} \times n_{\mathcal{E}}}$ the parameters of each power line $j \in \mathcal{E}$. The interconnection of the buses $i \in \mathcal{B}$ and the power lines $j \in \mathcal{E}$ according to the connected graph[38] $\mathcal{G}(\mathcal{B}, \mathcal{E})$ is described by the incidence matrix $\boldsymbol{E} \in \mathbb{R}^{n_{\mathcal{B}} \times n_{\mathcal{E}}}$. In particular, the voltage drop over the power lines $\boldsymbol{v}_{\Delta} \in \mathbb{R}^{n_{\mathcal{E}}}$ can be described with the voltages of the buses they are connected to, i.e.,

$$\text{col}\{v_{\Delta j}\} = \boldsymbol{v}_{\Delta} = \boldsymbol{E}^{\top}\boldsymbol{v} = \boldsymbol{E}^{\top}\text{col}\{v_i\}. \tag{4.3}$$

The current drawn from bus $i \in \mathcal{B}$ is the sum of the currents through the lines connected to bus i, i.e.,

$$\text{col}\{-i_{\text{ext},i}\} = -\boldsymbol{i}_{\text{ext}} = -\boldsymbol{E}\boldsymbol{i}_{\pi} = -\boldsymbol{E}\text{col}\{i_{\pi,j}\}. \tag{4.4}$$

[37] In the case that all nodes have a DGU, i.e., $\mathcal{B}_{\text{DGU}} = \mathcal{B}$, $\boldsymbol{I}_{\text{f}}$ is the identity matrix.

[38] Note that the buses and power lines form a networked system as defined in Term 3.1.

Note, however, that in the incidence matrix $\boldsymbol{E}$, only the power lines interconnecting nodes *within* the grid are considered. To consider also an interconnection of a node with a node in another grid, an external port $(\boldsymbol{v}, -\boldsymbol{i}_{\text{int}})$ is defined, where $\boldsymbol{i}_{\text{int}} = \text{col}\{i_{\text{int},i}\} \in \mathbb{R}^{n_\mathcal{B}}$ is the current injected at buses $i \in \mathcal{B}$ by other grids. The port interfaces with the system through

$$-\boldsymbol{i}_{\text{ext}} = -\boldsymbol{E}\boldsymbol{i}_\pi - \boldsymbol{i}_{\text{int}}, \tag{4.5}$$

i.e., it adds up to the external currents $\boldsymbol{i}_{\text{ext}}$ coming from other nodes of the same grid. Having described the interconnection, the whole grid composed of $n_\mathcal{B} = |\mathcal{B}|$ nodes (4.1) interconnected by $n_\mathcal{E} = |\mathcal{E}|$ lines (4.2) via (4.3) and (4.5) obeys the dynamics

$$\boldsymbol{C}_{\text{f}}\dot{\boldsymbol{v}} = \boldsymbol{I}_{\text{f}}\boldsymbol{i}_{\text{f}} - \boldsymbol{i}_{\text{L}}(\boldsymbol{v}) - \boldsymbol{E}\boldsymbol{i}_\pi - \boldsymbol{i}_{\text{int}} \tag{4.6a}$$

$$\dot{\boldsymbol{i}}_{\text{f}} = \boldsymbol{\alpha}\boldsymbol{I}_{\text{f}}^\top \boldsymbol{v} + \boldsymbol{\beta}\boldsymbol{i}_{\text{f}} + \boldsymbol{\gamma}\boldsymbol{e} \tag{4.6b}$$

$$\dot{\boldsymbol{e}} = \boldsymbol{v}_{\text{ref}} - \boldsymbol{v} \tag{4.6c}$$

$$\boldsymbol{L}_\pi \dot{\boldsymbol{i}}_\pi = -\boldsymbol{R}_\pi \boldsymbol{i}_\pi + \boldsymbol{E}^T \boldsymbol{v}. \tag{4.6d}$$

The following result about the EIP of a grid system paves the way for proving stability of the closed-loop system with MPC.

Proposition 4.1 (EIP at grid level)
Consider a system of independent buses and lines as in (4.1) *and* (4.2) *interconnected through* (4.3) *and* (4.5) *as in* (4.6) *forming grid* $m \in \mathcal{M}$*. The grid* $m \in \mathcal{M}$ *is, for any* $\boldsymbol{v}_{\text{ref}} > 0$*, EIP w.r.t.* $(-\tilde{\boldsymbol{i}}_{\text{int}}, \tilde{\boldsymbol{v}})$ *with storage function*

$$S(\tilde{\boldsymbol{x}}) = \sum_{i \in \mathcal{B}^m} S_i(\tilde{v}_i, \tilde{i}_{\text{f},i}, \tilde{e}_i) + \sum_{j \in \mathcal{E}^m} S_j(\tilde{i}_{\pi,j}), \tag{4.7}$$

where $\tilde{\boldsymbol{x}} = \text{col}\{\tilde{v}_i, \tilde{i}_{\text{f},i}, \tilde{e}_i, \tilde{i}_{\pi,j}\} \in \mathbb{R}^{n_\mathcal{B}+2n_{DGU}+n_\mathcal{E}}$*. The storage functions* S_i *are the storage functions for the nodes as in Proposition 3.5 or 3.6, and* S_j *for the nodes as in Proposition 3.7.*

Proof. Note that $S(0) = 0$ follows directly from Propositions 3.5 and 3.7. System (4.1) is EIP w.r.t. the input-output pair $(-\tilde{\boldsymbol{i}}_{\text{ext}}, \tilde{\boldsymbol{v}})$ with the storage function $S_{\text{bus}} = \sum S_i(\tilde{v}_i, \tilde{i}_{\text{f},i}, \tilde{e}_i)$, $i \in \mathcal{B}$, which follows from Proposition 3.5 and 3.6, since the bus dynamics in (4.1) are independent. Applying the same reasoning, system (4.2) is strictly EIP w.r.t. $(\tilde{\boldsymbol{v}}_\Delta, \tilde{\boldsymbol{i}}_\pi)$ with storage function $S_{\text{lines}} = \sum S_j(\tilde{i}_{\pi,j})$, $j \in \mathcal{E}^m$, by Proposition 3.7. From (4.7), it holds that

$$\dot{S} = \sum_{i \in \mathcal{B}^m} \dot{S}_i(\tilde{v}_i, \tilde{i}_{\text{f},i}, \tilde{e}_i) + \sum_{j \in \mathcal{E}^m} \dot{S}_j(\tilde{i}_{\pi,j}) \tag{4.8a}$$

$$< -\tilde{\boldsymbol{i}}_{\text{ext}}^\top \tilde{\boldsymbol{v}} + \tilde{\boldsymbol{i}}_\pi^\top \tilde{\boldsymbol{v}}_\Delta \overset{(4.3),(4.5)}{=} -\tilde{\boldsymbol{i}}_{\text{int}}^\top \tilde{\boldsymbol{v}}. \tag{4.8b}$$

The inequality in (4.8b) follows from the EIP of (4.1) and the strict EIP of (4.2) as in Proposition 3.5 and Proposition 3.7. The last equality follows from the skew symmetric interconnection (4.3) and (4.5). Recall that the EIP results are valid on the same set $\mathcal{D}_i$ as in Proposition 3.5 (see Remark 3.7). □

Note that the EIP result holds for an arbitrary number of interconnected buses and lines, as long as the DGU controllers fulfill Proposition 3.5. Furthermore, if the constant power load $\boldsymbol{P}_{\mathrm{L}} = \mathrm{col}\{P_{\mathrm{L},i}\}$ of the grid $m \in \mathcal{M}$ is nonzero, Proposition 4.1 holds only locally on the set $\mathcal{D} = \bigcup_i \mathcal{D}_i$.

Remark 4.1. *Note that for a single grid without any external interconnection with another grid, i.e., $\boldsymbol{i}_{\mathrm{int}} = \mathbf{0}$, the system is asymptotically stable for any voltage reference $\boldsymbol{v}_{\mathrm{ref}} > 0$ and Proposition 4.1 readily provides a Lyapunov function which is independent of any topology, line or DGU parameters, as long as Proposition 3.5 holds.*

4.2 Model Reduction and Separable Lyapunov Function

Having presented the EIP properties of a single grid, a model reduction is presented in this subsection. The model reduction serves two purposes. First, it simplifies the MPC problem, which depends on the system dynamics. In particular, the model is simplified by reducing the order and neglecting the fastest dynamics, allowing thus larger discretization steps. Secondly, the model reduction allows the derivation of a separable Lyapunov function (see Section A.1) for networked grids later on.

The grid model in (4.6) contains fast dynamics, especially the power lines[39] in (4.6d). This requires small step sizes when describing these dynamics as a discrete-time system, which compromises the real time optimization of the MPC. Since the power line dynamics in (3.45) are a first order lag, the solution adopted here is to neglect the inductances in the lines, i.e., to use the quasi-stationary line approximation [NTG18; VSZ95]. Note that the resulting grid model is still EIP w.r.t $(-\boldsymbol{i}_{\mathrm{int}}, \boldsymbol{v})$ since Proposition 4.1 still applies to the reduced system due to the EIP properties of static power lines. This is formalized in the following proposition.

Proposition 4.2 (EIP static lines)
Consider static power lines with $L_{\pi,j} = 0$ described by the algebraic equation

$$i_{\pi}^{j} = \frac{1}{R_{\pi,j}} v_{\Delta,j}, \tag{4.9}$$

[39] The power line dynamics constitute a first order lag with a time constant of $T = \frac{L_{\pi,j}}{R_{\pi,j}}$, which takes values around 10^{-6} for typical medium voltage power lines [Tuc+16].

where i_π^j is the line current and $v_{\Delta,j}$ the voltage drop over the line. System (4.9) *is EIP w.r.t. the port $(i_\pi^j, v_{\Delta,j})$.*

Proof. For static power lines, i.e., if the inductance is neglected, system (4.9) is still strictly EIP w.r.t. $(\tilde{v}_{\Delta,j}, \tilde{i}_{\pi,j})$, since it represents an offset-free strictly increasing map from input to output [SP18]. □

With this approximation, the grid dynamics can be described with

$$\boldsymbol{C}_\mathrm{f}\dot{\boldsymbol{v}} = \boldsymbol{i}_\mathrm{f} - \boldsymbol{i}_\mathrm{L}(\boldsymbol{v}) - \boldsymbol{E}\boldsymbol{R}_\pi^{-1}\boldsymbol{E}^\top\boldsymbol{v} - \boldsymbol{i}_\mathrm{int} \tag{4.10a}$$

$$\dot{\boldsymbol{i}}_\mathrm{f} = \boldsymbol{\alpha}\boldsymbol{v} + \boldsymbol{\beta}\boldsymbol{i}_\mathrm{f} + \boldsymbol{\gamma}\boldsymbol{e} \tag{4.10b}$$

$$\dot{\boldsymbol{e}} = \boldsymbol{v}_\mathrm{ref} - \boldsymbol{v}. \tag{4.10c}$$

These equations capture the dynamics of the passivity-based controlled DGUs interconnected with lossy static lines. The EIP of (4.10) is stated in the next proposition.

Proposition 4.3 (EIP reduced system)
Consider a grid $m \in \mathcal{M}$ composed of buses and static lines interconnected through (4.3) *and* (4.5) *obtaining* (4.10). *The grid $m \in \mathcal{M}$ is, for any $\boldsymbol{v}_\mathrm{ref} > 0$, EIP w.r.t. $(-\tilde{\boldsymbol{i}}_\mathrm{int}, \tilde{\boldsymbol{v}})$ with storage function*

$$S(\tilde{\boldsymbol{x}}) = \sum_{i \in \mathcal{B}^m} S_i(\tilde{v}_i, \tilde{i}_{\mathrm{f},i}, \tilde{e}_i), \tag{4.11}$$

where $\tilde{\boldsymbol{x}} = \mathrm{col}\{\tilde{v}_i, \tilde{i}_{\mathrm{f},i}, \tilde{e}_i\} \in \mathbb{R}^{n_\mathcal{B}+2n_{DGU}}$ and S_i are the storage functions as in Proposition 3.5 and 3.6.

Proof. Note that the node systems are EIP as per Proposition 3.5 and 3.6 and the static lines as per Proposition 4.2. From Proposition 3.5 it also follows directly that $S(\mathbf{0}_{n_\mathcal{B}+2n_\mathrm{DGU}}) = 0$. Following the same reasoning as in the proof of Proposition 4.1, the EIP property is obtained. □

Again, for nonzero power loads, EIP holds locally on $\mathcal{D}$ as a consequence of Proposition 3.5. Note that the storage (and also Lyapunov) function (4.11) for the reduced system does not contain any states of the power lines as the storage function (4.7) did. This is an advantage in terms of the distributed MPC implementation (see first requirement in Figure 4.1). Using storage function (4.7), the states of power lines contribute to the global storage function. Then, when considering various grids interconnected

by power lines, the storage functions are coupled via these power line states. This prevents the construction of a storage function that is separable in the variables of the individual grids. With the model reduction, this is now possible. Storage functions that are separable in the variables of the individual grids are important, because the individual grids are the local computing agents in the distributed implementation presented in Chapter 7. This is further studied in the next subsection. Note that since various interconnected grids are considered from now on, the grid index $m \in \mathcal{M}$ is not omitted anymore.

4.2.1 Properties of Networked Grids

In this section, a set $\mathcal{M} = \{1, \dots, n_{\text{mg}}\}$ of networked grids are considered, each composed of DGUs and power lines. The n_{mg} grids are interconnected via a set $\mathcal{E}_{\text{int}} = \{1, \dots, n_{\mathcal{E},\text{int}}\}$ of power lines (4.9) as defined by graph $\mathcal{G}_{\text{int}}(\mathcal{B}_{\text{int}}, \mathcal{E}_{\text{int}})$. The set $\mathcal{B}_{\text{int}} = \bigcup_{m\in\mathcal{M}} \mathcal{B}^m$ contains all the buses in the networked system, i.e., $|\mathcal{B}_{\text{int}}| = \sum_{m\in\mathcal{M}} n_{\mathcal{B}}^m$, and $\mathcal{E}_{\text{int}} \subset \bigcup_{m,q\in\mathcal{M}} \mathcal{B}^m \times \mathcal{B}^q$, for $m \neq q$ is the set of lines interconnecting the different grids. The power system model is composed of the grids $m \in \mathcal{M}$ as in (4.10), written compactly as

$$\dot{\boldsymbol{x}}^m = \boldsymbol{f}^m(\boldsymbol{x}^m) + \boldsymbol{B}^m \boldsymbol{v}_{\text{ref}}^m + \boldsymbol{B}_{\text{int}}^m \boldsymbol{i}_{\text{int}}^m \tag{4.12a}$$

$$\boldsymbol{y}^m = \boldsymbol{v}^m = {\boldsymbol{B}_{\text{int}}^m}^\top \boldsymbol{x}^m \tag{4.12b}$$

where $\boldsymbol{i}_{\text{int}}^m \in \mathbb{R}^{n_{\mathcal{B}}}$ is the vector containing the line currents of the power lines interconnecting grid m with other grids as in (4.6) and $\boldsymbol{v} \in \mathbb{R}^{n_{\mathcal{B}}}$ the node voltages. System (4.12) is nonlinear in the state with $\boldsymbol{f}^m : \mathbb{R}^{n_{\mathcal{B}}^m + 2n_{\text{DGU}}^m} \to \mathbb{R}^{n_{\mathcal{B}}^m + 2n_{\text{DGU}}^m}$ when nonzero constant power loads are connected. The matrix

$$\boldsymbol{B}_{\text{int}}^m = \left(\boldsymbol{I}_{n_{\mathcal{B}}^m}, \boldsymbol{0}_{n_{\mathcal{B}}^m \times 2n_{\mathcal{B}}^m}\right)^\top \in \mathbb{R}^{n_{\mathcal{B}}^m + 2n_{\text{DGU}}^m \times n_{\mathcal{B}}} \tag{4.13}$$

in (4.12) assigns the line currents $\boldsymbol{i}_{\text{int}}^m$ to the voltage dynamics or extracts the voltages from the state $\boldsymbol{x}^m$.

The grids $m \in \mathcal{M}$ are interconnected via power lines $j \in \mathcal{E}_{\text{int}}$. Thus, we have

$$i_{\pi,\text{int},j} = \frac{1}{R_{\pi,j}} v_{\Delta,\text{int},j}, \tag{4.14}$$

where $i_{\pi,\text{int},j}$ is the line current and $v_{\Delta,\text{int},j}$ is the voltage drop over the line $j \in \mathcal{E}_{\text{int}}$, i.e., the voltage difference between the nodes of both grids interconnected by the power line $j \in \mathcal{E}_{\text{int}}$. Similar as in (4.3) and (4.4), the grids (4.12) and power lines (4.14) are interconnected using the incidence matrix $\boldsymbol{E}_{\text{int}} \in \mathbb{R}^{\sum n_{\mathcal{B}}^m \times n_{\mathcal{E},\text{int}}}$ of graph $\mathcal{G}_{\text{int}}$, i.e.,

$$\text{col}\{v_{\Delta,\text{int},j}\} = \boldsymbol{v}_{\Delta,\text{int}} = \boldsymbol{E}_{\text{int}}^\top \boldsymbol{v} = \boldsymbol{E}_{\text{int}}^\top \text{col}\{\boldsymbol{v}^m\} \tag{4.15}$$

and

$$-\text{col}\{\boldsymbol{i}_{\text{int}}^m\} = -\boldsymbol{i}_{\text{int}} = -\boldsymbol{E}_{\text{int}}\boldsymbol{i}_{\pi,\text{int}} = -\boldsymbol{E}_{\text{int}}\text{col}\{i_{\pi,\text{int},j}\}. \tag{4.16}$$

Similar as in Proposition 4.1 for a single grid composed of nodes interconnected by power lines, a Lyapunov function for the networked grids is proposed here. Furthermore, it is shown that the Lyapunov function is separable. This is essential for guaranteeing stability with local conditions (see Theorem 4.6).

Proposition 4.4 (Lyapunov function of networked grids)
Consider a set of networked grids (4.12) *interconnected with static power lines* (4.9) *according to* $\mathcal{G}_{\text{int}}(\mathcal{B}_{\text{int}}, \mathcal{E}_{\text{int}})$*, described by the incidence matrix* $\boldsymbol{E}_{\text{int}}$ *as in* (4.15) *and* (4.16)*. Given any* $\boldsymbol{v}_{\text{ref}} > \boldsymbol{0}$*, a Lyapunov function for the networked grid is given by*

$$V(\tilde{\boldsymbol{x}}) = \sum_{m\in\mathcal{M}} S^m(\tilde{\boldsymbol{x}}^m) \tag{4.17}$$

where $\tilde{\boldsymbol{x}} = \text{col}\{\tilde{\boldsymbol{x}}^m\} \in \mathbb{R}^{n_{\text{int}}}$ *and* $S^m(\tilde{\boldsymbol{x}}^m)$ *as in*[40] (4.11)*, with* n_{int} *the total number of states of the networked grids.*

Proof. Note that $V(\boldsymbol{0}) = 0$ follows directly from Proposition 4.3, and $V(\tilde{\boldsymbol{x}}) > 0$ for all $\tilde{\boldsymbol{x}} \neq \boldsymbol{0}$ since the storage function is quadratic. Define the variables $\boldsymbol{v} = \text{col}\{\boldsymbol{v}^m\}$ and $\boldsymbol{i}_{\text{int}} = \text{col}\{\boldsymbol{i}_{\text{int}}^m\}$ describing the group of n_{mg} grids as in (4.15) and (4.16). Using Proposition 4.3 and taking into account that the storage function of the individual grids in (4.12) are separable, the time derivative of the Lyapunov function (4.17) is

$$\dot{V} = \sum_{m\in\mathcal{M}} \dot{S}^m(\tilde{\boldsymbol{x}}^m) \leq -\sum_{m\in\mathcal{M}} \tilde{\boldsymbol{i}}_{\text{int}}^{m\top}\tilde{\boldsymbol{v}}^m = -\tilde{\boldsymbol{i}}_{\text{int}}^{\top}\tilde{\boldsymbol{v}}. \tag{4.18}$$

Considering the interconnection equations (4.15) and (4.16), (4.18) reads

$$\dot{V} \leq -\tilde{\boldsymbol{i}}_{\pi,\text{int}}^{\top}\boldsymbol{E}_{\text{int}}^{\top}\tilde{\boldsymbol{v}} = -\tilde{\boldsymbol{i}}_{\pi,\text{int}}^{\top}\tilde{\boldsymbol{v}}_{\Delta} \tag{4.19}$$

$$\overset{(4.14)}{=} -\tilde{\boldsymbol{i}}_{\pi,\text{int}}^{\top}\boldsymbol{R}_{\pi,\text{int}}^{-1}\tilde{\boldsymbol{i}}_{\pi,\text{int}} = -\tilde{\boldsymbol{v}}^{\top}\boldsymbol{E}_{\text{int}}\boldsymbol{R}_{\pi,\text{int}}^{-1}\boldsymbol{E}_{\text{int}}^{\top}\tilde{\boldsymbol{v}} \leq 0, \tag{4.20}$$

which implies stability of any equilibrium. In (4.19), Proposition 4.3 and the interconnection equations (4.15) and (4.16) were used. In the last equality, the line equation (4.14) along with the interconnection equation (4.15) were used, and $\boldsymbol{R}_{\pi,\text{int}} = \text{diag}\{R_{\pi,\text{int}}^j\}$ was defined. □

The Lyapunov function (4.17) holds locally in $\mathcal{D}$ when nonzero power loads are present. The whole power system model (i.e., the networked grids) is given by

[40] Remember that in (4.11), the index m was neglected, so S^m was S.

$$\boldsymbol{C}_\mathrm{f}\dot{\boldsymbol{v}} = \boldsymbol{i}_\mathrm{f} - \boldsymbol{i}_\mathrm{L}(\boldsymbol{v}) - \boldsymbol{E}\boldsymbol{R}_\pi^{-1}\boldsymbol{E}^\top\boldsymbol{v} - \boldsymbol{E}_\mathrm{int}\boldsymbol{R}_{\pi,\mathrm{int}}^{-1}\boldsymbol{E}_\mathrm{int}^\top\boldsymbol{v} \tag{4.21a}$$

$$\boldsymbol{L}_\mathrm{f}\dot{\boldsymbol{i}}_\mathrm{f} = \boldsymbol{\alpha}\boldsymbol{v} + \boldsymbol{\beta}\boldsymbol{i}_\mathrm{f} + \boldsymbol{\gamma}\boldsymbol{e} \tag{4.21b}$$

$$\dot{\boldsymbol{e}} = \boldsymbol{v}_\mathrm{ref} - \boldsymbol{v}, \tag{4.21c}$$

where $\boldsymbol{E} = \mathrm{blkdiag}\{\boldsymbol{E}^m\}$, $m \in \mathcal{M}$, is block diagonal and describes the static power lines inside a grid, and $\boldsymbol{E}_\mathrm{int}$ describes the lines between grids. All the states are network variables, i.e., $\boldsymbol{v} = \mathrm{col}\{\boldsymbol{v}^m\}$. By analyzing the set where the derivative of the Lyapunov function (4.18) is zero, the following proposition is stated.

Proposition 4.5 (asymptotic stability networked grids)
All equilibria of system (4.21) *induced by any* $\boldsymbol{v}_\mathrm{ref} > 0$ *are asymptotically stable.*

Proof. Consider the Lyapunov function (4.17). With Remark 3.8 and Remark 3.10, the derivative (4.18) becomes

$$\dot{V} \leq -\tilde{\boldsymbol{v}}^\top\boldsymbol{E}_\mathrm{int}\boldsymbol{R}_{\pi,\mathrm{int}}^{-1}\boldsymbol{E}_\mathrm{int}^\top\tilde{\boldsymbol{v}} - \rho\boldsymbol{v}^\top\boldsymbol{v}, \tag{4.22}$$

where $\boldsymbol{\rho} = \mathrm{diag}\{\rho_i\}$ is a positive definite matrix. The set

$$\mathcal{L} = \{\tilde{\boldsymbol{x}} \,|\, \dot{V} = 0\} = \{\tilde{\boldsymbol{x}} \,|\, \tilde{\boldsymbol{v}} = 0\} \tag{4.23}$$

reduces to $\tilde{\boldsymbol{x}} = 0$ after considering (4.21) as follows. With (4.21a) and $\tilde{\boldsymbol{v}} = 0$, $\tilde{\dot{\boldsymbol{i}}}_\mathrm{f} = 0$ is obtained, and with (4.21b), $\tilde{\boldsymbol{e}} = 0$ is obtained. This proves asymptotic stability for the origin for any equilibrium point. Furthermore, following Remark 3.7, a positively invariant set is given by the largest sublevel set of V in $\mathcal{D}$, i.e.,

$$\Omega = \{\boldsymbol{x} \in \mathcal{D} \,|\, V(\tilde{\boldsymbol{x}}) \leq c\}, \tag{4.24}$$

for a constant $c \in \mathbb{R}_{>0}$. □

Remark 4.2. *Note that the Lyapunov function (and the positively invariant set) of the networked grids* (4.17) *is separable among the grids, i.e., it is composed of the sum of independent functions of* $\boldsymbol{x}^m$*, or of the union of independent sets. This allows to ensure stability with independent conditions for all grids, since every grid can evaluate its terminal cost and terminal constraints without information of other grids states. Hence, this enables a distributed MPC implementation.*

Remark 4.3. *As can be seen in the system dynamics* (4.21a)*, the dynamics of the individual grids are coupled via the voltages with the symmetric but nondiagonal matrix* $\boldsymbol{E}_\mathrm{int}\boldsymbol{R}_{\pi,\mathrm{int}}^{-1}\boldsymbol{E}_\mathrm{int}^\top$.

4.3 Optimal Control of Networked Grids with MPC Strategies

In the previous sections, the models and system properties for the grids that are used for the MPC-based high level control have been derived. In this subsection, two controller designs for networked grids based on MPC strategies are presented.

The controller computes suitable voltage references (i.e., the input of the system) such that (i) a performance index is minimized, (ii) stability of the whole power system depends only on local conditions for each grid, allowing thus a plug-and-play operation. First, in Section 4.3.2, a classical, setpoint-tracking MPC is proposed, which requires the prior computation of optimal setpoints. A formal stability proof using the results of Proposition 4.4 and Proposition 4.5 is provided. Secondly, an economic MPC for the same problem is designed, which is shown to have superior performance[41] compared to the classical setpoint-tracking MPC. For the economic MPC, the closed-loop stability is studied with simulations in Section 4.4 and later in Chapter 7. Before designing the specific MPC strategies, the performance index and the setpoint computation for the setpoint-tracking MPC are introduced in Section 4.3.1.

4.3.1 Performance Index and Setpoint Computation

The setpoint-tracking MPC requires the a priori computation of setpoints (see Section 3.2). In the following, the computation of those setpoints is presented.

The setpoints are computed solving a general OPF problem as in

$$\mathrm{Opt}_{\mathrm{ss}}(t)^{42} := \begin{cases} \min_{\boldsymbol{p},\boldsymbol{v},\boldsymbol{x}} & J(\boldsymbol{p},\boldsymbol{v},\boldsymbol{x}) \\ \text{s. t.} & \boldsymbol{p} + \boldsymbol{P}_{\mathrm{L}} + \boldsymbol{Y}_{\mathrm{ad}}\, \boldsymbol{v} \circ \boldsymbol{v} = 0 \\ & \boldsymbol{v} \in \mathbb{V} \\ & \boldsymbol{p} \in \mathbb{P}, \end{cases} \tag{4.25}$$

where J is an objective function, $\boldsymbol{p} = \mathrm{col}\{p_i\} \in \mathbb{R}^{n_{\mathcal{B}}}$ is the power injection of a DGU to the bus and $\boldsymbol{P}_{\mathrm{L}} \in \mathbb{R}^{n_{\mathcal{B}}}$ are the constant power loads. The objective function may be designed, for example, to minimize the costs of power generation in the whole power system, to minimize power line losses, or to fulfill similar objectives. The constraints in (4.25) represent the power flow equations, described through the nodal admittance matrix $\boldsymbol{Y}_{\mathrm{ad}}$ [Mac+20] as well as the voltage $\mathbb{V} \subseteq \mathbb{R}^{n_{\mathcal{B}}}$ and power constraints $\mathbb{P} \subseteq \mathbb{R}^{n_{\mathcal{B}}}$, which may be different for each bus and DGU. Note that the matrix $\boldsymbol{Y}_{\mathrm{ad}}$ contains, apart from the line admittance, also the impedance loads in (3.31) in the shunt. With an estimation of the loads in the next time steps, this optimization problem is solved for some optimization horizon and $\boldsymbol{v}_{\mathrm{opt}}(t) = \arg\min \mathrm{Opt}_{\mathrm{ss}}(t)$ is obtained. Such an optimal

[41] With performance, it is meant the control performance, which is defined in Section 4.4.

[42] The name indicates that it is an optimization to find an appropriate steady state.

setpoint computation is typically performed every few minutes, when the estimated load changes. Since the time constants of the network are in the range of a few seconds and load estimation typically in the range of minutes, the voltage references are seen as piecewise constant for the grid.

Note that for computing the optimal setpoints in (4.25), information about all grids is necessary. This is due to the couplings introduced by the power flow equations in (4.25). However, for OPF problems, there exist many methods for obtaining a solution in a distributed manner, see the survey in [Mol+17].

4.3.2 MPC Design

In the following, two MPC strategies for the networked grids (4.21) are proposed. The Lyapunov function (4.17) is used to ensure stability. Furthermore, the necessary information exchange between grids arising from the optimization problem is studied. The MPC problem is defined as

$$\mathrm{MPC}(t) := \begin{cases} \min & \displaystyle\int_{\tau=t}^{T} l(\boldsymbol{x}(\tau), \boldsymbol{u}(\tau))\mathrm{d}\tau + V_T(\boldsymbol{x}(T)) \\ \text{s. t.} & \dot{\boldsymbol{x}} = \boldsymbol{f}(\boldsymbol{x}(t), \boldsymbol{u}(t)), \\ & \boldsymbol{x}(\tau) \in \mathbb{X} \\ & \boldsymbol{x}(T) \in \mathbb{X}_T \\ & \boldsymbol{u}(\tau) \in \mathbb{U} \\ & \tau \in [t, T]\,, \end{cases} \tag{4.26}$$

where $\boldsymbol{x} = \mathrm{col}\{\boldsymbol{x}^m\}$, $\boldsymbol{u} = \mathrm{col}\{\boldsymbol{u}^m\}$ and $\boldsymbol{u}^m = \boldsymbol{v}^m_{\mathrm{ref}}$. The input and state constraints are described by $\mathbb{X}$ and $\mathbb{U}$, and $\mathbb{X}_T$ are the terminal constraints. The system dynamics in (4.26) are the interconnected grids in (4.21). The stage cost $l(\boldsymbol{x}, \boldsymbol{u})$ in the objective function defines whether it is a setpoint-tracking or an economic MPC and is specified in the following.

Setpoint-tracking MPC with local stability conditions

The setpoint-tracking MPC employs an objective function for grid $m \in \mathcal{M}$ of the form

$$l^m(\boldsymbol{y}^m, \boldsymbol{u}^m) = \|\boldsymbol{y}^m - \boldsymbol{v}^m_{\mathrm{opt}}\|^2 + \|\boldsymbol{u}^m - \boldsymbol{v}^m_{\mathrm{opt}}\|^2_{\alpha \boldsymbol{I}}, \tag{4.27}$$

where $\boldsymbol{v}^m_{\mathrm{opt}}$ is a given voltage reference computed in order to minimize some performance index $J(\boldsymbol{x}, \boldsymbol{u})$ (see (4.25)). The performance index is application-specific and is described in more detail in the simulation results in Section 4.4 and Chapter 7. The parameter $\alpha \in \mathbb{R}_{>0}$ is a constant which determines how strongly the input is penalized w.r.t. the output. The global stage cost is defined as

$$l(\boldsymbol{y}, \boldsymbol{u}) = \sum_{m \in \mathcal{M}} l^m(\boldsymbol{y}^m, \boldsymbol{u}^m). \tag{4.28}$$

The following theorem ensures a stabilizing receding horizon operation of the setpoint-tracking MPC.

Theorem 4.6 (stability of the setpoint-tracking MPC)
Let an optimal voltage reference $\boldsymbol{v}_{\text{opt}}(t)$ be given (e.g., according to (4.25)*). Consider a setpoint-tracking MPC of the form* (4.26) *with an objective function as in* (4.27)*. Let Propositions 4.4 and 4.5 hold. For the terminal costs, use the Lyapunov function* (4.17) *from Proposition 4.4, and additionally the constraints from Proposition 4.5 as terminal constraints for the case of nonzero constant power loads. Then, the closed-loop system operating in a receding horizon is asymptotically stable.*

Proof. Since the terminal cost (4.17) is a Lyapunov function for all constant $\boldsymbol{v}_{\text{opt}}$ for all $\boldsymbol{x} \in \mathcal{D}$, condition A4 in [May+00, p. 797] is fulfilled. Condition A2 and A3 are fulfilled as per Proposition 4.5. Condition A1 is fulfilled because the constraints are closed. Thus, asymptotic stability follows directly from the classic setpoint-tracking MPC theory using the separable, positively invariant set Ω from Proposition 4.5 as terminal constraint, assuming that the system in (4.26) is stabilizable [May+00, p. 797]. When the power loads are zero, $\mathcal{D}$ corresponds to $\mathbb{R}^{n_{\text{int}}}$ and no terminal constraints in addition to the terminal costs (4.17) are necessary. □

Observe that due to the separable Lyapunov function, the stability condition of Theorem 4.6 decomposes in local conditions for each individual grid. This can be explained as follows: the objective function of the global setpoint-tracking MPC in (4.26)

$$\sum_{m\in\mathcal{M}} \left\{ \int_t^T l^m(\boldsymbol{y}^m, \boldsymbol{u}^m) \mathrm{d}\tau \right\} + V_T(\boldsymbol{x}(T)). \tag{4.29}$$

decomposes, using the Lyapunov function as in Theorem 4.6, in

$$\sum_{m\in\mathcal{M}} \left\{ \int_t^T l^m(\boldsymbol{y}^m, \boldsymbol{u}^m) \mathrm{d}\tau + S^m(\boldsymbol{x}^m) \right\}. \tag{4.30}$$

Note that such a decomposition does not hold in general. It requires having a Lyapunov function with a special (separable) structure, as in (4.17). In this method, the special structure is obtained exploiting passivity theory at grid level. As a consequence of such a structure, a change in the network in some grid $m \in \mathcal{M}$ is only reflected in the storage function S^m, which does only affect the objective function of grid m (see (4.30)). Due to the modular Lyapunov function network changes in the individual grids only affect the local stability conditions, which thus allows a plug-and-play operation without compromising stability provided that all grids fulfill the local conditions.

Despite the *local* stability conditions, problem (4.26) is a coupled, global optimization problem. Thus, a *distributed optimization* algorithm is necessary for solving it in a distributed manner (see requirements in Figure 4.1). Ideally, the algorithm should have plug-and-play capabilities to allow network changes. Furthermore, the agents should not be obliged to disclose their private objective function or constraints, since it may contain sensitive information. An appropriate algorithm is developed within this thesis and presented in Chapter 5. Then, combining the methods of this chapter and Chapter 5, all the requirements of distributed MPC are fulfilled (see Figure 4.1).

Economic MPC

For economic MPC, the performance index J of (4.25) used to compute the optimal setpoint for the stage cost is employed in the stage cost of the MPC, i.e.

$$l(\boldsymbol{x}, \boldsymbol{u}) = J(\boldsymbol{p}, \boldsymbol{v}, \boldsymbol{x}) + \|\boldsymbol{u}\|_{\beta I}^2, \tag{4.31}$$

where $\beta \in \mathbb{R}_{>0}$ is a small constant for regularization.

The traditional control structure of computing the optimal setpoint and controlling it by feedback setpoint-tracking MPC is therefore combined into a single feedback structure as described in Section 3.2. Thus, it is not necessary to compute or know the optimal setpoint in advance. It can therefore react immediately to load changes without having to compute new steady-state optimal setpoints, which is an advantage when dealing with volatile renewable energy resources. In the context of distributed control, omitting the prior setpoint computation is also an advantage, since for computing the optimal setpoint, information about all the systems is necessary. However, as the objective function does not have a minimum at the optimal setpoint to be stabilized,[43] the mature theory about classical setpoint-tracking MPC does not hold [MA17]. Nevertheless, an economic MPC is designed and benchmarked in this work because of the superior performance it achieves. Asymptotic stability is later assessed via simulations in Section 4.4 and Chapter 7.

Note that the formulation in (4.26) requires (independently of whether an economic or setpoint-tracking objective function is used) information about all grids for computing the solution, which is not desirable. The goal is to obtain an approach where every grid solves an individual optimization problem and coordination is achieved through communication. The objective function in (4.26) is separable (in both cases) and does not couple the individual grid dynamics. However, the system dynamics in (4.26), especially the last term in (4.21a), induces a coupling of the variables of individual grids. More precisely, the voltage of grid $m \in \mathcal{M}$ influences the dynamics of grid $l \in \mathcal{M}$ if they are interconnected with a power line. This couples the optimization problem and requires, similarly as outlined above for the setpoint-tracking MPC, information about

[43] Here, the deviations to a setpoint are not penalized, and the cost is not necessarily decreasing until the setpoint is reached [MA17].

all grids in order to compute the solution (see the second requirement in Figure 4.1). Thus, a distributed optimization algorithm is also necessary for the economic MPC. In the next chapter, a novel distributed optimization algorithm tailored to solving this global optimization problem in a distributed manner is derived. But first, in the next section, both MPC strategies are compared on a small example without using distributed computation.

4.4 Numerical Example

In this section, the setpoint-tracking and economic MPC are illustrated via simulations. The focus of this example is the comparison of the two proposed MPC strategies. In particular, it is shown that economic MPC achieves a better performance than setpoint-tracking MPC when disturbances occur. Since a suitable distributed optimization algorithm allowing a distributed computation of the MPC problem (4.26) has not been proposed yet (cf. Chapter 5), a single grid is considered in this illustrative example, since this is enough for comparing both MPC approaches. We refer to Chapter 7 for a scenario with three networked grids using distributed optimization.

The grid considered in this work is based on the CIGRE medium voltage benchmark system, since it represents the network topology of a typical distribution system, and it is aimed to serve as a benchmark system for voltage control studies [Rud+06], [Far+18, p. 42ff.]. It is composed of 11 nodes and 12 power lines and shows a meshed structure (see Figure 4.2). Since the benchmark system is conceived as an AC system, the system is adapted as in [Str24, Section 4.4]. The high voltage connection at Node 1 is eliminated, and a DGU and a ZIP load is added to each node. Typical DC system parameters are taken from [Str24, Section 4.4] and [Tuc+16] for the lines and DGU filters. The step size is chosen to be $h = 10\,\mathrm{ms}$ for both MPCs, since it is in the order of magnitude of the largest step size that lead to a stable discrete-time system using the forward Euler discretization method. The optimization horizon is set to $N = 300$, which corresponds to $3\,\mathrm{s}$ and covers the typical transients in converter-based grids. The problem is set up with CasADi in Matlab and the nonlinear programming solver ipopt[44] [WB06] is used. For the setpoint-tracking MPC, new optimal setpoints are computed every 30 seconds. The parameter α in (4.27) is set to $\alpha = 10^{-2}$ in order to achieve a better voltage tracking. The parameter β in (4.31) is also set to $\beta = 10^{-2}$ for regularization.

[44] Ipopt is an open source solver used in many (commercial) nonlinear optimization tools (GAMS, AMPL, CasADi, Yalmip, JuMP, Pyomo, Matlab, etc.) and is widely regarded as one of the best in its class.

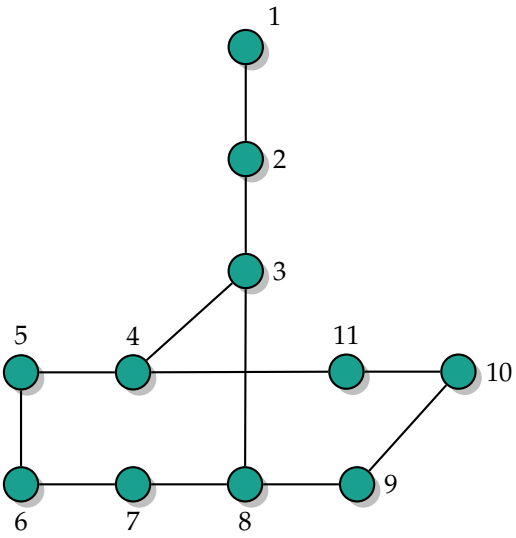

Figure 4.2: Structure of the CIGRE medium voltage benchmark system [Rud+06].

4.4.1 Performance Index for Setpoint Computation

First, the optimal setpoints for the setpoint-tracking MPC are to be computed. Exemplary, the power line losses in the networked grids are minimized.[45] Hence, the objective function in (4.25) is chosen to be

$$J(\boldsymbol{v}) = \boldsymbol{v}^\top \boldsymbol{E}\boldsymbol{R}_\pi^{-1}\boldsymbol{E}^\top \boldsymbol{v} + \boldsymbol{v}^\top \boldsymbol{E}_{\text{int}}\boldsymbol{R}_{\pi,\text{int}}^{-1}\boldsymbol{E}_{\text{int}}^\top \boldsymbol{v}, \tag{4.32}$$

where $\boldsymbol{R}_\pi^{-1}$ describes the line resistances of the lines strictly inside all grids $m \in \mathcal{M}$, and $\boldsymbol{R}_{\pi,\text{int}}^{-1}$ describes the resistances of the lines between the different grids, i.e., grids $k, i \in \mathcal{M}$, $i \neq k$ (see Sections 4.1 and 4.2.1). The matrices $\boldsymbol{E}$ and $\boldsymbol{E}_{\text{int}}$ are the corresponding incidence matrices describing the line interconnection topology (see Section 4.2.1).

4.4.2 Simulation Results

In the following, both MPC approaches are compared in the nominal case, i.e., when the load is known with no error. Afterwards, the case when load disturbances occur is considered. As disturbances, load noise, load steps and a line failure are considered. A quantitative comparison is provided in Table 4.1.

[45] Indeed, to best fulfill the Objective of the Thesis, minimizing the total cost of power injection is the best option. This is done in Chapter 7, where also a comparison with the other methods derived in this work is presented. To show one of the strengths of this method, i.e., that the optimization objective can simply be changed by computing different setpoints without compromising the stability result of Theorem 4.6, the power line losses are minimized in this illustrative example.

Scenario 1: Nominal Case

First, the nominal case is considered, where the load is assumed to be known with no error by the predictive controllers. The load during the simulation time is shown in Figure 4.3. At time $t = 30\,\mathrm{s}$, a load step occurs in all nodes. The load step time is chosen to be at the same time when new optimal setpoints are computed for the setpoint-tracking MPC, such that the MPC always receives the optimal setpoints. Note that in real applications, the optimal setpoints will likely not be computed at the same time as the load changes. The scenario presented here is hence the best case scenario for the setpoint-tracking MPC in order to allow a fair comparison with the economic MPC. The node voltages in the grid with the setpoint-tracking MPC and the economic MPC

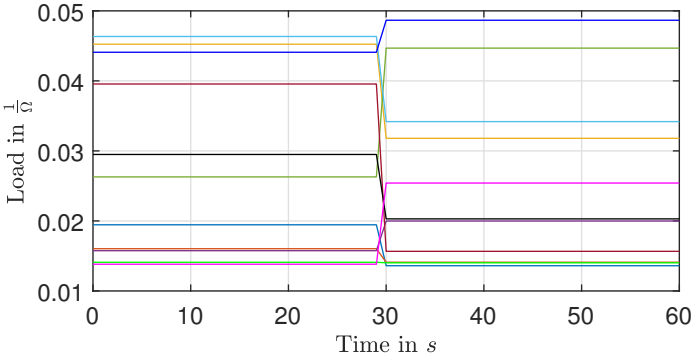

Figure 4.3: Load at Nodes 1 to 11 over the simulation time in the nominal case.

are shown in Figure 4.4. The dot-dashed lines are the optimal setpoints computed by the setpoint computation (4.25). Due to voltage, current or power flow constraints in (4.25), different voltage references that induce power flows through the lines are necessary. In the case of setpoint-tracking MPC, the node voltages follow the optimal setpoints (dot-dashed) accurately. Since the optimal setpoints of the voltages are computed with (4.25) and lead to minimal power line losses, the closed-loop behavior with the setpoint-tracking MPC is (only) steady-state optimal. Considering the system dynamics also during transients for the explicit task of minimizing losses instead of regulating a setpoint may improve performance. The economic MPC achieves the optimal steady-state voltages (dot-dashed) without requiring a priori voltage setpoints. The node voltages with the economic MPC are identical to the voltages with the setpoint-tracking MPC, except for the time around the load step.

The line losses resulting from the node voltages are computed for comparing the performance of setpoint-tracking and economic MPC. The economic MPC achieves $0.2\,\%$ less transmission losses than the setpoint-tracking MPC in the nominal case (viz. Table 4.1). This improvement is due to a better transient behavior during the load step at $t = 30\,\mathrm{s}$. In the case of the setpoint-tracking MPC, since the deviations are penalized, the node voltages follow the steps arising from the setpoint $\boldsymbol{v}_{\mathrm{opt}}(k)$

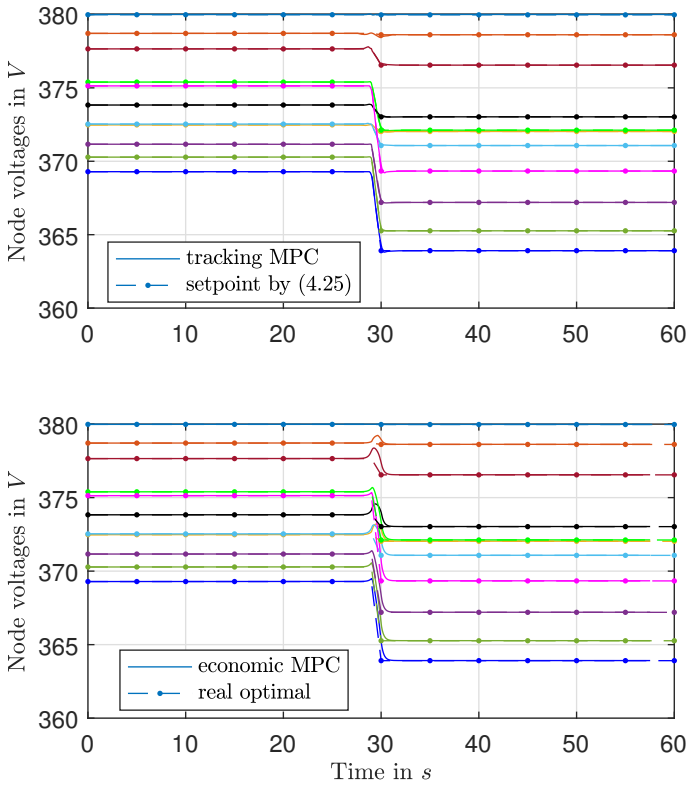

Figure 4.4: Grid bus voltages when using a setpoint-tracking MPC (above) and an economic MPC (below) in the nominal case.

which changes once at $t = 30\,\mathrm{s}$. This is, however, not optimal w.r.t. minimizing the losses. On the other hand, the economic MPC does not minimize the deviations to some setpoint, it chooses the input on the basis of minimizing the losses, also during transients. Thus, it achieves a better performance. This effect is assumed to gain importance when disturbances occur. Thus, in the next subsection, the performance of both MPC approaches will be compared for the case when disturbances in the load occur.

Scenario 2: Disturbances

In the following, load variations are considered in order to highlight the performance of economic MPC. Three types of disturbances are considered, 1) unknown load steps, 2) load noise and 3) a line failure. The unknown load steps and load noise are depicted in Figures 4.5 and 4.7, respectively. The unknown load steps occur in Nodes 2 and 6, while the load noise occurs only in Node 1. Since the predictive controllers need a prediction of the load over the optimization horizon, it is assumed that the actual

load is measured and considered to be constant over the optimization horizon of 3 s. The optimal setpoint computation in (4.25) is assumed to not have knowledge about these measurable disturbances, since it computed the optimal setpoints in advance. The voltage trajectories are reported in this section, while the performance comparison is made in Table 4.1.

Unknown load steps The node voltages in the grid equipped with both predictive controllers can be seen in Figure 4.6. The setpoint-tracking MPC still achieves an acceptable regulating behavior when the load step occurs, since it penalizes the deviations to that given setpoint. However, note that the optimal setpoint computed in advance is no longer optimal due to the load steps, which are not known in advance and not considered in (4.25). On the other hand, the node voltages set by the economic MPC differ with respect to the setpoints from (4.25) when the disturbances occur. Since the economic MPC does not minimize the deviations to a given setpoint and instead directly minimizes the losses, a new but optimal steady state arises.

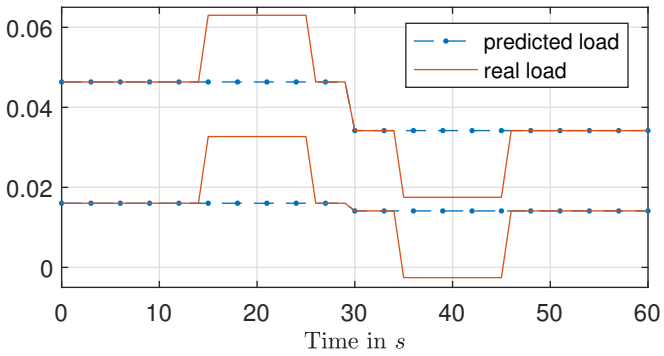

Figure 4.5: Predicted (dot-dashed) and real load in the case of unknown steps in Node 2 (above) and 6 (below).

Load noise The node voltages in the grid with both predictive controllers in the case of load noise (see Figure 4.7) are shown in Figure 4.8. All the node voltages set by the setpoint-tracking MPC show significant oscillations around the given optimal setpoints, even if the load noise is only in Node 1. In contrast, the node voltages produced by the economic MPC are smooth and slightly differ from the optimal steady-state voltages computed in advance, as expected.

Line failure In the scenario of a line failure, the line between Node 3 and 8 fails at time $t_{\text{fail}} = 20\,\text{s}$ and is unavailable thereafter. The line failure is assumed to be measurable and known by the predictive controllers, but not by the optimal setpoint computation in (4.25) which happens in advance. The node voltages in the grid with both predictive controllers in the case of a line fail can be seen in Figure 4.9. The setpoint-tracking MPC

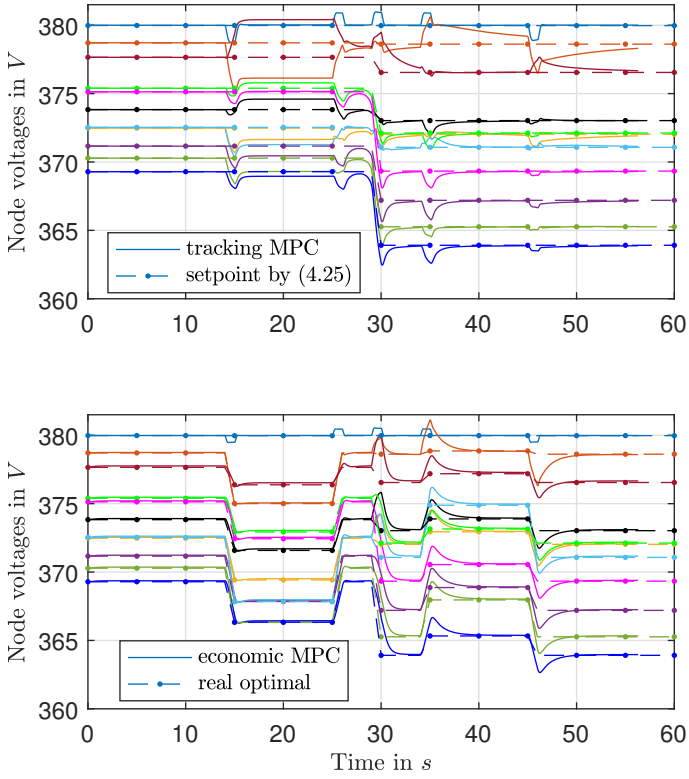

Figure 4.6: Grid bus voltages when using a setpoint-tracking MPC (above) and an economic MPC (below) under an unknown load step.

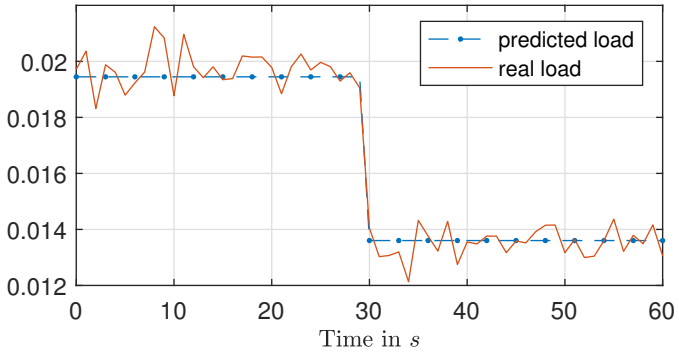

Figure 4.7: Predicted (dot-dashed) and real load in the case of load noise in Node 1.

minimizes the deviation to the provided setpoint (dot-dashed line), which is not optimal for the new grid topology. The voltages when using the economic MPC converge to a new steady state, which is optimal under the new grid configuration.

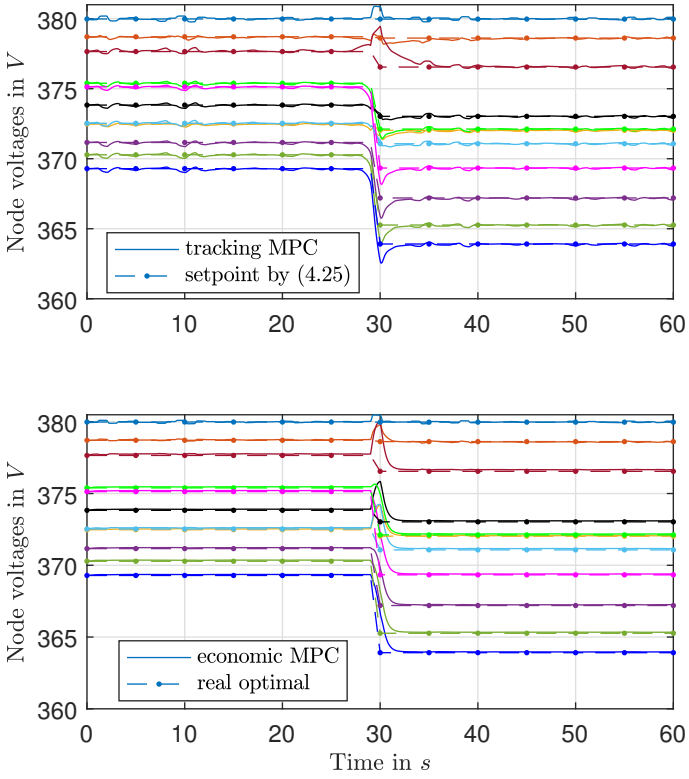

Figure 4.8: Grid bus voltages when using a setpoint-tracking MPC (above) and an economic MPC (below) under unknown load noise.

Performance comparison

The performance increase of the economic MPC with respect to the setpoint-tracking MPC is shown in Table 4.1. It shows the reduction of transmission losses for the described scenarios normalized to the transmission losses from the economic MPC. The economic MPC achieves a better performance in all cases. The increase in performance depends clearly on the severity of the disturbance. The small disturbance from the load noise shows a $2.6\,\%$ less transmission losses. For greater disturbances, the reduction increases to $9.3\,\%$ (load step), and $15.6\,\%$ (line failure). Thus, greater disturbances yield greater performance benefits from the economic MPC, since the optimal voltages differ more from the a priori calculated setpoints. Since the economic MPC does not need to compute any optimal setpoint in advance, it has a clear advantage also in terms of computation and enjoys a simpler feedback control structure naturally achieving the optimal setpoints as a result of the control action. Lastly, note that the setpoint-tracking MPC is operated in the best case scenario, since it receives the setpoints exactly when the load change occurs. If this is not the case, the performance increase of the economic

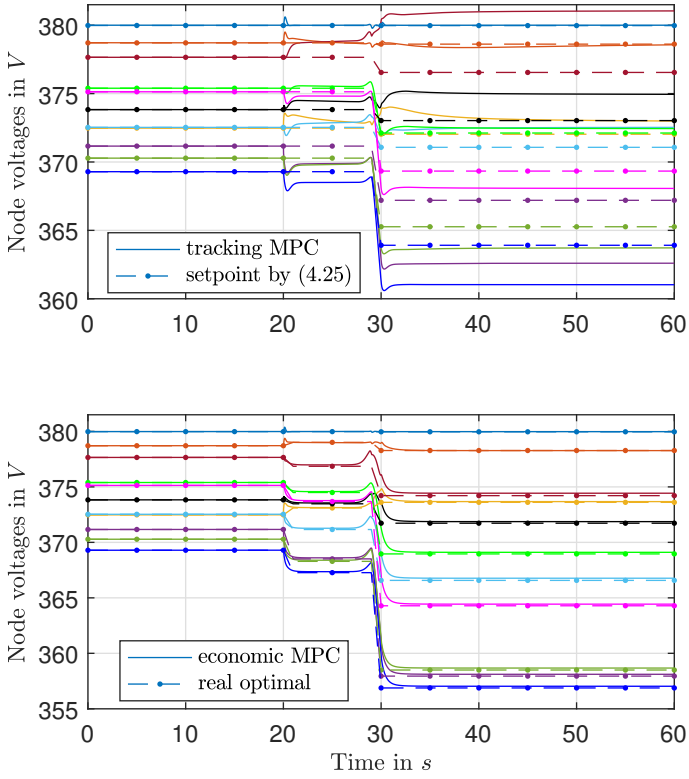

Figure 4.9: Grid bus voltages when using a setpoint-tracking MPC (above) and an economic MPC (below) under a line failure.

MPC is expected to be greater.

Table 4.1: Performance increase of economic MPC over setpoint-tracking MPC in different scenarios.

Scenario	Performance increase of economic MPC
Nominal	0.2 %
Unknown load steps	9.3 %
Unknown load noise	2.6 %
Line failure	15.6 %

4.5 Discussion and Outlook

The main contribution of this chapter is a setpoint-tracking MPC framework with local stability conditions. The MPC framework exploits EIP theory to obtain a separable

Lyapunov function, which yields the local stability conditions. These conditions are independent for each grid. As a result, each grid can independently assess its own stability requirements when network changes occur, without the need for coordination with other grids. This allows individual grids to disconnect from or reconnect to the network without jeopardizing overall system stability.

This local, independent stability conditions also allow a distributed implementation of the MPC framework without relying on information from (or communication with) other grids for achieving stability. However, recall that this distributed implementation has not been shown in this chapter, since the required distributed optimization algorithm is an original contribution of this dissertation and is presented in Chapter 5.

A further contribution is the design of an economic MPC framework, which does not necessitate any setpoints in advance and drives the system to an optimal steady state as a result of its control actions. It has been shown that it achieves superior performance while solving a comparable optimization problem from the point of view of complexity. However, the overall computation complexity of the economic MPC is less, due to the omission of the setpoint computation. The rigorous stability proof of the economic MPC is not addressed in this chapter and thus still remains an open challenge.

Both proposed approaches result in a framework for regulated power systems. This is due to various reasons. On the one hand, the objective function is a global objective function of all grids, for example to minimize the sum of all power line losses or power injection costs. Thus, the objective function is given by a superordinate entity or is agreed upon by the grids. A profit-driven agent, who would rather seek to minimize own costs, is not allowed to use another objective function while guaranteeing system stability. The fact that the objective function in (4.27) or (4.31) is a sum over all grids makes every single grid act network friendly, which may not be compatible with own interests of profit-driven agents.

The setpoint-tracking exhibits a control structure which is conceptually similar to the status quo in power systems (see Figure 2.1 and Section 2.1). The setpoint computation corresponds to the feedforward part (i.e., the energy market in current power systems), and the MPC corresponds to the feedback control (i.e., the balancing and balancing capacity market). For the MPC approach considered here, however, asymptotic stability has also been rigorously shown under varying network or load conditions. In contrast to that, in current power systems, only regulations concerning the amount of balancing capacity exist, which are based on probabilistic worst-case scenarios (see Section 2.1). On the other hand, the economic MPC breaks this conceptual control structure, since no feedforward term is necessary. Hence, as shown in Section 4.4, it can react better (i.e., in an optimal way) to uncertainty.

A challenging aspect of the proposed approaches are the computation requirements. The model was discretized with a sample time of $10\,\mathrm{ms}$, and thus the MPC problem has to be solved in, at most, $10\,\mathrm{ms}$. Conventional MPC controllers for power electronics already function with even higher sample rates [Gey+11], in the range of microseconds.

However, the MPC problem of a grid in this case comprises several nodes and devices and thus has a higher complexity. Consequently, powerful hardware is necessary. An alternative may be to explore multi-step MPC strategies. In such an approach, not only the next control action computed by the MPC is applied, but a number of next control actions. These approaches are active research topics in the literature [Bai+20; Bai+19; GP14].

4.6 Summary and Contributions

In this chapter, two MPC frameworks for optimization and control of future power systems have been presented. Exploiting EIP theory, the proposed methodology ensures stability using local conditions for the individual grids. This opens up the possibility of a distributed implementation, without necessitating information or communication with the other grids to ensure stability. Furthermore, these frameworks establish a technically regulated power system as in Term 2.1.

In Figure 4.10, a summary of the main results of this chapter and their relation to the contributions of this dissertation is shown. On the left, the main steps in the setpoint-tracking MPC operation are shown as presented in Figure 3.2. On the right, the main results of this chapter are shown. These are grouped together in contributions of the dissertation, and connected to the main steps in the MPC operation. For the first step, the setpoint computation, standard OPF algorithms from the literature (gray color) are used [Mol+17]. The setpoint-tracking MPC along with the stability conditions, the distributed optimization algorithm and the system model and analysis are original to this work. The setpoint-tracking MPC design provides local stability conditions for each grid (see Theorem 4.6). This corresponds to the first requirement in Figure 4.1. The distributed optimization algorithm necessary to solve the problem in a distributed manner is presented in the next chapter (green color) and corresponds to Contribution 2 of this dissertation. The main result regarding the grid properties is the EIP property at grid level. This is achieved using underlying passivity-based controllers to prove EIP properties at grid level. The storage function which certifies the EIP properties at grid level then serves as a pillar for the separable Lyapunov function of the power system, i.e., all networked grids. The setpoint-tracking MPC design, based on the proposed power system model and its EIP properties, along with the distributed optimization algorithm allowing a distributed computation, fulfills Contribution 1 of this work (red color).

A further contribution of this chapter is the comparison of economic and setpoint-tracking MPC. It has been shown that economic MPC outperforms setpoint-tracking MPC when disturbances occur. Furthermore, it has advantages for the distributed implementation, since an optimal steady state has not to be computed — or even known — in advance.

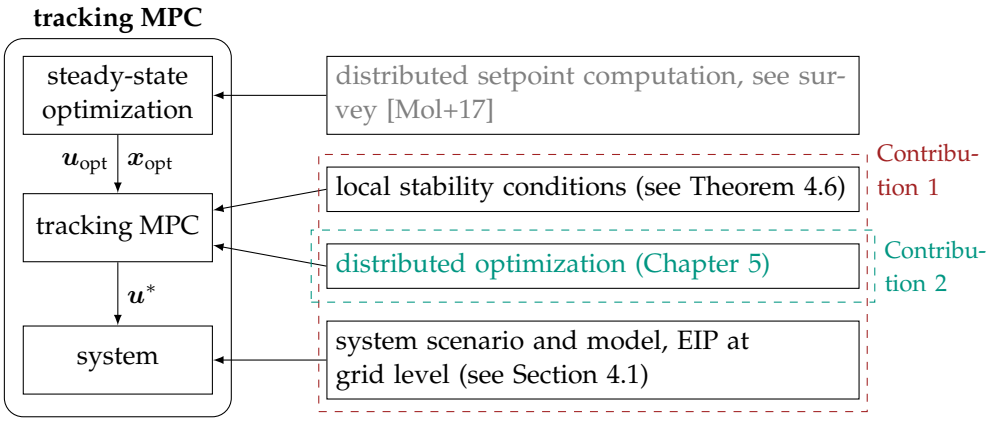

Figure 4.10: Overview and interrelation of the contributions presented in this chapter. Grey color represents methods taken from the literature, and in blue contributions of other chapters of this thesis.

5 Local Design Requirements for Global Optimality in Distributed Convex Optimization

In this chapter, a novel distributed optimization framework addressing Research Gaps 2 and 3 is presented.[46] The goal is that the agents compute the global optimizer[47] without disclosing their private objective function and constraints. In the existing work, specific algorithms are proposed, and optimality and convergence are proven provided that all agents follow the same algorithm. Thus, these are global conditions for optimality and convergence. In sharp contrast to that, in this dissertation, local design requirements for distributed optimization algorithms are derived.

The proposed distributed optimization can be utilized to solve the MPC problem of Chapter 4 in a distributed manner. It thus corresponds to requirement two in Figure 3.3. Every grid then corresponds to an agent in the distributed optimization framework. The technical aspects regarding the practical implementation of the distributed optimization algorithm introduced in this chapter for the MPC problem of Chapter 4 are presented in detail in Chapter 7. Note that the proposed distributed optimization algorithm is general and is not limited to power system applications.

The chapter is structured as follows. In Section 5.1, the mathematical problem formulation and main idea is introduced. In Section 5.2, the local design requirements for both the agent and controller dynamics are presented. Two types of requirements are proposed: requirements to obtain optimality in Section 5.2.1 and requirements to obtain convergence in Section 5.2.2. These design requirements are posed to the agent dynamics, controller dynamics and communication topology in order to achieve global optimality and convergence.[48]

In Section 5.3, specific agent and controller dynamics complying with those design requirements are given. These dynamics have different EIP properties, which are necessary to ensure convergence in different scenarios, i.e., when directed communication topologies are considered.

---

[46] Preliminary results leading to the content of this chapter have been presented in [JS+22] and have been submitted to a publication in a journal [JS+25a].

[47] In this chapter, *global* is used in the sense of networked systems, i.e., *global* means for the whole network. However, *global* optimizer should not be understood in the sense of global minima in nonconvex optimization.

[48] In this chapter, the word *convergence* is used as a synonym for asymptotic stability. This is done because *convergence* is typically used in the literature about distributed optimization, but it means asymptotic stability of the difference (or differential) equation of the optimization algorithm.

In Sections 5.4 and 5.5, less restrictive convergence results are proposed by imposing minor further restrictions on the agent dynamics. In Section 5.4, convergence is established under undirected topologies requiring only strict convexity of the sum of all objective functions. In Section 5.5, convergence is established under directed communication topologies.

An illustrative example of the proposed methodology is presented in Section 5.6. In Section 5.7, the proposed methods are discussed. Finally, in Section 5.8, the chapter is concluded with a summary of the contributions and an outlook.

Note that in this chapter, similar to Chapter 4, Lyapunov theory is used to ensure that a dynamic system converges to an equilibrium point. However, observe that the same methodology is used for two tasks of different nature: in Chapter 4, Lyapunov theory is used to ensure that a feedback control law, stemming from repeatedly solving an MPC problem and applying the optimizer every time, stabilizes an equilibrium point of the system when time passes. In contrast to that, in this chapter, Lyapunov theory is used to ensure convergence of an optimization algorithm, described as a continuous-time dynamic system. The stability property is then not in the time domain, but in the iterations of the optimization. Compared to Chapter 4, Lyapunov theory here ensures that the MPC optimization converges to the optimizer at *every individual* time step.

5.1 Problem Formulation and Main Idea

Consider a set of agents $\mathcal{A} = \{1, \dots, n_{\mathcal{A}}\}$, $n_{\mathcal{A}} \in \mathbb{N}$. Next, consider the network optimization problem

$$\min \sum_{i \in \mathcal{A}} f_i(\mathbf{y}) \tag{5.1a}$$

$$\text{s.t. } g_{il}(\mathbf{y}) \leq 0, \quad \forall l \in \mathcal{C}_{\text{in},i}, \forall i \in \mathcal{A} \tag{5.1b}$$

$$h_{ij}(\mathbf{y}) = 0, \quad \forall j \in \mathcal{C}_{\text{eq},i}, \forall i \in \mathcal{A} \tag{5.1c}$$

where $\mathbf{y} \in \mathbb{R}^n$. The objective function $f_i : \mathbb{R}^n \to \mathbb{R}$ and the constraints $g_{il} : \mathbb{R}^n \to \mathbb{R}$ and $h_{ij} : \mathbb{R}^n \to \mathbb{R}$ are private to agent $i \in \mathcal{A}$. The variable $\mathbf{y} \in \mathbb{R}^n$ is a global variable of the agents. The sets $\mathcal{C}_{\text{in},i} = \{1, \dots, n_{\text{IC},i}\}$ and $\mathcal{C}_{\text{eq},i} = \{1, \dots, n_{\text{EQ},i}\}$ are the sets of inequality and equality constraints of agent $i \in \mathcal{A}$. The functions $g_{il} : \mathbb{R}^n \to \mathbb{R}$ are assumed to be convex, the functions $h_{ij} : \mathbb{R}^n \to \mathbb{R}$ to be affine, i.e., $h_{ij}(\mathbf{y}) = \boldsymbol{a}_{ij}^\top \mathbf{y} + c_{ij}$. Further, it is assumed that (5.1) is strictly convex and Slater's condition holds, i.e., there exists an $\mathbf{y} \in \mathbb{R}^n$ where constraints (5.1c) hold and constraints (5.1b) are strictly feasible [BV04, p. 244]. Note that these are standard assumptions in convex optimization [Hat+18; LCF16; BV04].

In this work, the focus is on enabling agents to collaboratively solve the network-wide optimization problem (5.1) using only local information and communication with their

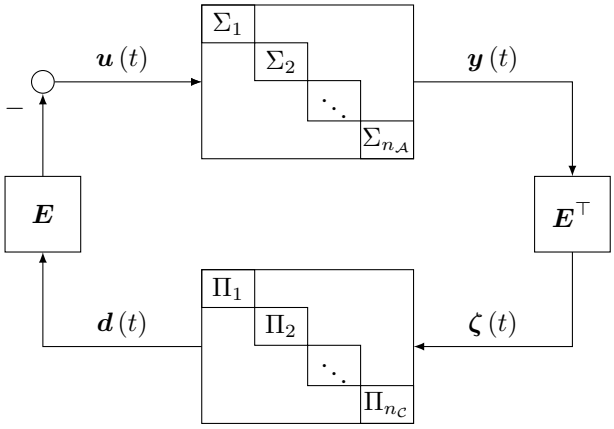

Figure 5.1: Block diagram of the proposed algorithm structure, composed of agent systems Σ_i and controller systems Π_k. The block diagonal structure of the nodes and edges systems indicates that the node (and edge) systems are not directly dynamically coupled, but only via the feedback.

neighbors. For that, each agent $i \in \mathcal{A}$ holds a local estimate $\boldsymbol{y}_i \in \mathbb{R}^n$ of the global optimizer $\mathbf{y}^* \in \mathbb{R}^n$. The agents can perform local computations based on their private objective functions and constraints, and communicate the local estimate $\boldsymbol{y}_i$ with the neighbors. The communication topology is described by an undirected graph $\mathcal{G}(\mathcal{A}, \mathcal{E})$, where nodes represent agents and an edge $o_k \in \mathcal{E} \subset \mathcal{A} \times \mathcal{A}$ between agent i and j means that the agents i and j can exchange their local estimations.

In this thesis, a novel class of algorithms that decompose into the form shown in Figure 5.1 is proposed. It consists of agent systems Σ_i, $i \in \mathcal{A}$ and controller systems Π_k, $k \in \mathcal{C}$, where $\mathcal{C} = \{1, \dots, n_\mathcal{C}\}$ is the set of controllers[49]. Each controller is associated with an edge of graph $\mathcal{G}$, i.e., with the communication between two agents, and thus $|\mathcal{C}| = |\mathcal{E}|$. The agent systems

$$\Sigma_i : \quad \begin{aligned} \dot{\boldsymbol{x}}_i &= \boldsymbol{\chi}_i(\boldsymbol{x}_i, \boldsymbol{u}_i) \\ \boldsymbol{y}_i &= \boldsymbol{\psi}_i(\boldsymbol{x}_i, \boldsymbol{u}_i), \end{aligned} \tag{5.2}$$

with $\boldsymbol{\chi}_i : \mathbb{R}^n \times \mathbb{R}^n \to \mathbb{R}^n$ and $\boldsymbol{\psi}_i : \mathbb{R}^n \times \mathbb{R}^n \to \mathbb{R}^n$, hold the state $\boldsymbol{x}_i \in \mathbb{R}^n$, which represents an intermediate value for the estimation $\boldsymbol{y}_i \in \mathbb{R}^n$ of the global optimizer $\mathbf{y}^* \in \mathbb{R}^n$. The input of the agent systems is $\boldsymbol{u}_i \in \mathbb{R}^n$, which should be chosen such that the output $\boldsymbol{y}_i \in \mathbb{R}^n$ of the agents converges to the global optimizer $\mathbf{y}^*$. The controller systems are described by

$$\Pi_k : \quad \begin{aligned} \dot{\boldsymbol{z}}_k &= \boldsymbol{\Phi}_k(\boldsymbol{z}_k, \boldsymbol{\zeta}_k) \\ \boldsymbol{d}_k &= \boldsymbol{\sigma}_k(\boldsymbol{z}_k, \boldsymbol{\zeta}_k), \end{aligned} \tag{5.3}$$

with $\boldsymbol{\Phi}_k : \mathbb{R}^n \times \mathbb{R}^n \to \mathbb{R}^n$, $\boldsymbol{\sigma}_k : \mathbb{R}^n \times \mathbb{R}^n \to \mathbb{R}^n$, state $\boldsymbol{z}_k \in \mathbb{R}^n$, input $\boldsymbol{\zeta}_k \in \mathbb{R}^n$, and output $\boldsymbol{d}_k \in \mathbb{R}^n$, which is fed back to the agent systems in order to find the global

[49] Note that the agents and controllers form a networked system as defined in Term 3.1.

optimizer $\mathbf{y}^*$. The agent and controller systems are interconnected by an incidence matrix $\boldsymbol{E} \in \mathbb{R}^{n_\mathcal{A} \times n_\mathcal{C}}$ lifted to the space $\mathbb{R}^n$ of the optimization variables as in

$$\boldsymbol{\zeta} = (\boldsymbol{E} \otimes \boldsymbol{I}_n)^\top \boldsymbol{y} \tag{5.4a}$$
$$\boldsymbol{u} = -(\boldsymbol{E} \otimes \boldsymbol{I}_n)\, \boldsymbol{d}, \tag{5.4b}$$

where $\boldsymbol{\zeta} \in \mathbb{R}^{n_\mathcal{C} \cdot n}$, $\boldsymbol{u} \in \mathbb{R}^{n_\mathcal{A} \cdot n}$, $\boldsymbol{d} \in \mathbb{R}^{n_\mathcal{A} \cdot n}$ and $\boldsymbol{y} \in \mathbb{R}^{n_\mathcal{A} \cdot n}$ are the stacked variables of the agents and controllers, e.g., $\boldsymbol{y} = \text{col}\{\boldsymbol{y}_i\}$, which are called network variables further on. Taking into account the definition of the incidence matrix $\boldsymbol{E}$, it becomes clear from (5.4a) that the inputs $\boldsymbol{\zeta}_k$ of the controller systems are the differences between the outputs $\boldsymbol{y}_i$ of different agents, i.e., the estimations $\boldsymbol{y}_i$ of different agents of the global optimizer $\mathbf{y}^*$.

With the partitioning of the algorithm into agent and controller systems, the question arises of where to physically implement the controller systems. In the next example, it is shown that this is a purely technical implementation issue which does not limit the findings of this chapter.

Example 5.1:
Consider a network of four agents interconnected as in Figure 5.2.

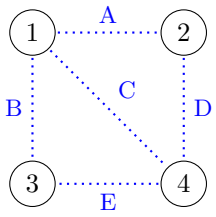

Figure 5.2: Exemplary network composed of four agents (nodes) and communication links in blue (edges).

The proposed method introduces five controllers A - E, one for each edge. The controller dynamics can be interpreted as independent entities with computation capabilities or, alternatively, as part of the same system implementing the agent dynamics, as shown in Figure 5.3. In the first case (see Figure 5.3a), the controllers are independent entities. In the second case, the agents implement the subsystems inside the dashed line in Figure 5.3b, composed of the agent dynamics (5.2) *and the controller dynamics* (5.3)*. Depending on the interpretation, the agents have to exchange different variables and different information flows occur. When the controllers are independent entities, the agents send their estimation $\boldsymbol{y}_i$ and receive the input $\boldsymbol{u}_i$. When the controllers are implemented together with the agent dynamics, the agents send either their estimation $\boldsymbol{y}_i$ or the controller output $\boldsymbol{d}_k$, depending on whether they have the controller or not (c.f. Figure 5.3b).*

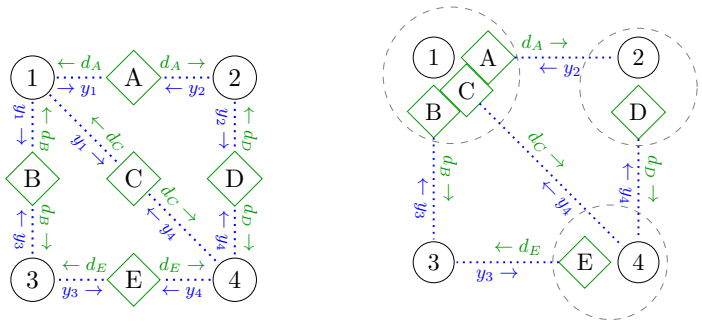

(a) Controllers as independent entities

(b) Controllers as part of the agents

Figure 5.3: Different technical realization of the controller systems.

The decision of considering the controllers as independent entities or not may depend on the application. When the agents are likely to leave or rejoin the network often and there exists an independent computing infrastructure, a configuration with controllers as independent entities may be favorable. Otherwise, a configuration with the controllers as part of the agents may be advantageous.

5.2 Local Design Requirements for Global Optimality and Convergence

In this section, local design requirements for the agent systems (5.2), the controller systems (5.3), and the communication structure (5.4) are derived such that the networked systems (see Figure 5.1) achieve global optimality and convergence. First, in Section 5.2.1, the design requirements for optimality are presented. Next, in Section 5.2.2, the design requirements for convergence are derived.

First, a definition which is paramount to deriving the local design requirements for the distributed optimization algorithms is introduced.

Definition 5.1 (system with integral action)
A state space system (3.7) *is called a system with integral action, if there exist no other input* $\bar{u}$ *leading to an equilibrium other than* $\bar{u} = \mathbf{0}$.

In the next subsection, Section 5.2.1, the design requirements for the agent systems Σ_i, the controller systems Π_k, and the communication topology are explored.

5.2.1 Design Requirements for Global Optimality

In this subsection, the design requirements for the agent systems (5.2), the controller systems (5.3), and the communication structure (5.4) are proposed such that the closed-loop, networked system in Figure 5.1 meets the network-wide optimality conditions (3.24) or (3.26) (see Section 3.3) at steady state.

Unconstrained Optimization

First, the local design requirements in the case of an unconstrained optimization problem, i.e., (5.1) without (5.1b)-(5.1c) are stated.

Theorem 5.1 (design requirements unconstrained optimization)
Consider systems (5.2) *and* (5.3) *interconnected by* (5.4). *Let the communication graph be connected. If the equilibria of the agent systems* (5.2) *fulfill*

$$\bar{\boldsymbol{u}}_i = \nabla f_i(\bar{\boldsymbol{y}}_i) \tag{5.5}$$

and the controllers (5.3) *are systems with integral action as in Definition 5.1, all equilibria* $(\bar{\boldsymbol{y}}, \bar{\boldsymbol{d}})$ *of the networked system are in the manifold given by* $\mathcal{M}_{eq} = \{(\bar{\boldsymbol{y}}, \bar{\boldsymbol{d}}) \in \mathbb{R}^{n_{\mathcal{A}} \cdot n} \times \mathbb{R}^{n_c \cdot n} \mid \bar{\boldsymbol{y}} = \mathbf{1}_{n_{\mathcal{A}}} \otimes \mathbf{y}^*\}$, *where* $\mathbf{y}^* \in \mathbb{R}^n$ *is the minimizer of the unconstrained problem* (5.1).

Proof. With Definition 5.1, it follows for the equilibria of the controller systems Π_k that $\bar{\boldsymbol{\zeta}}_k = \mathbf{0}$. Inserting it in (5.4a) yields

$$\mathbf{0} = (\boldsymbol{E} \otimes \boldsymbol{I}_n)^\top \bar{\boldsymbol{y}}, \tag{5.6}$$

which is fulfilled if and only if $\bar{\boldsymbol{y}}$ is contained in the kernel of $(\boldsymbol{E} \otimes \boldsymbol{I}_n)^\top$. Since the graph is connected, using Proposition B.1[50] from Appendix B.2, it follows from (5.6) that all agents are in consensus, i.e., $\bar{\boldsymbol{y}} = \mathbf{1}_{n_{\mathcal{A}}} \otimes \boldsymbol{\theta}$, where $\boldsymbol{\theta} \in \mathbb{R}^n$ is some constant vector. Left-multiplying (5.4b) with the matrix $(\mathbf{1}_{n_{\mathcal{A}}}^\top \otimes \boldsymbol{I}_n)$ and taking into account that $\mathbf{1}_{n_{\mathcal{A}}}^\top \boldsymbol{E} = \mathbf{0}$ and property P1 of the Kronecker product as in Appendix B.1, it follows

$$\begin{aligned}(\mathbf{1}_{n_{\mathcal{A}}}^\top \otimes \boldsymbol{I}_n)\bar{\boldsymbol{u}} &= -(\mathbf{1}_{n_{\mathcal{A}}}^\top \otimes \boldsymbol{I}_n)\,(\boldsymbol{E} \otimes \boldsymbol{I}_n)\,\bar{\boldsymbol{d}} \\ &= -(\mathbf{1}_{n_{\mathcal{A}}}^\top \boldsymbol{E} \otimes \boldsymbol{I}_n)\bar{\boldsymbol{d}} = \mathbf{0}.\end{aligned} \tag{5.7}$$

[50] Proposition B.1 is original from this work. However, it is presented in the appendix to improve the reading flow, since it is a purely mathematical proposition characterizing the kernel of a matrix multiplied with the unity matrix with a Kronecker product.

Note that the left-hand side of (5.7) can be rewritten as

$$(\mathbf{1}_n^\top \otimes \boldsymbol{I}_n)\bar{\boldsymbol{u}} = \sum_{i\in\mathcal{A}} \bar{\boldsymbol{u}}_i. \tag{5.8}$$

Inserting the design requirement (5.5) for the equilibrium of the agent systems into (5.8), the optimality condition (3.24) is obtained. Thus, together with the consensus established above, it holds that $\bar{\boldsymbol{y}}_i = \mathbf{y}^* \; \forall i \in \mathcal{A}$ in steady state. Since the controller outputs $\boldsymbol{d}_k$ remain unspecified, any value $\bar{\boldsymbol{d}} \in \mathbb{R}^{n\cdot n_c}$ may be an equilibrium. Thus, the equilibria are described by the manifold $\mathcal{M}_{\text{eq}}$ as stated in the theorem. □

Remark 5.1. *Note that $\mathcal{M}_{\text{eq}}$ is a positively invariant set w.r.t. the networked system composed of systems* (5.2) *and* (5.3) *interconnected by* (5.4).

Remark 5.2. *Note that the equilibria of systems* (5.2) *and* (5.3) *interconnected by* (5.4) *are not unique, since $\bar{\boldsymbol{z}}$ remains unspecified apart from $\bar{\boldsymbol{\zeta}}_k = \mathbf{0}$. Depending on the initial values of the states $\boldsymbol{z}_k$ and $\boldsymbol{x}_i$, different equilibria arise in closed-loop operation. However, for all equilibria it holds that $\bar{\boldsymbol{y}}_i = \mathbf{y}^*, \forall i \in \mathcal{A}$.*

Remark 5.3. *Even if not included in the definition of the manifold $\mathcal{M}_{\text{eq}}$, the equilibria for the controller inputs $\boldsymbol{\zeta}_k$ are also uniquely determined by* (5.5)*, viz. $\boldsymbol{\zeta}_k = \mathbf{0}$, as it becomes clear from the proof of Theorem 5.1.*

Constrained Optimization

In the following, the design requirements for the agent and controller systems in the case of a constrained optimization problem as in (5.1) are stated.

Theorem 5.2 (design requirements constrained optimization)
Consider systems (5.2) *and* (5.3) *interconnected by* (5.4)*. Let the communication graph be connected. Let $L_i : \mathbb{R}^n \to \mathbb{R}$ be the Lagrange function of agent $i \in \mathcal{A}$ as in* (3.25) *in Section 3.3. If the equilibria of the agent systems* (5.2) *fulfill*

$$\bar{\boldsymbol{u}}_i = \nabla_{\boldsymbol{y}_i} L_i(\bar{\boldsymbol{y}}_i, \bar{\boldsymbol{\lambda}}_i, \bar{\boldsymbol{\mu}}_i) \tag{5.9a}$$
$$g_{il}(\bar{\boldsymbol{y}}_i) \leq 0 \tag{5.9b}$$
$$h_{ij}(\bar{\boldsymbol{y}}_i) = 0 \tag{5.9c}$$
$$\bar{\lambda}^*_{il} \geq 0 \tag{5.9d}$$
$$\bar{\lambda}^*_{il} g_{il}(\bar{\boldsymbol{y}}) = 0, \tag{5.9e}$$

$\forall l \in \mathcal{C}_{\text{in},i}$ and $\forall j \in \mathcal{C}_{\text{eq},i}$, and the controllers (5.3) *are systems with integral action as in Definition 5.1, all equilibria $(\bar{\boldsymbol{y}}, \bar{\boldsymbol{d}})$ of the networked system are in the manifold*

given by $\mathcal{M}_{eq} = \{(\bar{\boldsymbol{y}}, \bar{\boldsymbol{d}}) \in \mathbb{R}^{n_{\mathcal{A}} \cdot n} \times \mathbb{R}^{n_{\mathcal{C}} \cdot n} \mid \bar{\boldsymbol{y}} = \mathbf{1}_{n_{\mathcal{A}}} \otimes \mathbf{y}^*\}$, *where* $\mathbf{y}^*$ *is the minimizer of the constrained problem* (5.1).

Proof. This proof largely follows the proof of Theorem 5.1 for the unconstrained case. Due to the interconnection (5.4), consensus on the outputs $\boldsymbol{y}_i$ of the agents is obtained using Proposition B.1 of Appendix B.2 and the integral action of the controller systems. Further, following the same procedure as in the proof of Theorem 5.1, (5.7) is obtained. Inserting condition (5.9a) on the left side and taking into account that all outputs $\bar{\boldsymbol{y}}_i$ are in consensus together with (5.9b)-(5.9e), the KKT optimality condition (3.26) are obtained. □

Due to the proposed algorithm structure in Figure 5.1, the classic optimality conditions (3.24) and (3.26) hold *per design* at steady state. Consequently, in contrast to the literature (see Research Gap 2 in Chapter 2), no global initialization or other conditions have to be imposed to achieve global optimality. This implies that agents with optimization dynamics complying with the requirements given in (5.5) or (5.9) may leave or rejoin the networked optimization, while the remaining agents in the network automatically have an equilibrium at the new global optimum $\mathbf{y}^*$ arising from the new network configuration.

Remark 5.4. *Note that in the proofs of Theorems 5.1 and 5.2, only the fact that the nullspace of the transposed communication incidence matrix* $\boldsymbol{E}^\top$ *is of dimension one and contains the vector* $\mathbf{1}_{n_{\mathcal{A}}}$ *is used to achieve consensus and global optimality. Thus, any matrix fulfilling this nullspace property can be used.*

Communication Topology

At this point, design requirements on the agent and controller dynamics have been posed such that all equilibria correspond to the global optimizer $\mathbf{y}^*$. In this subsection, the effects of different agent communication structures on global optimality are studied. First, the case where a controller is connected to more than two agents is studied. It is shown that such generalized communication structures exhibit a certain skew-symmetry property, and are thus amenable to common passivity theory. Afterwards, the proposed framework is extended to allow directed communication topologies, in which a controller does not have to send its state back to the agents from whom it received the estimations, but can instead send it to other agents in the network. Hence, such directed communication topologies are called non-symmetric communication structures from now on.

$$\boldsymbol{R} = \begin{bmatrix} 1 & 0 \\ -2 & 1 \\ 1 & -1 \end{bmatrix}$$

(a) Communication matrix

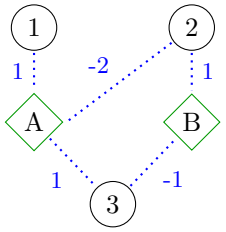

(b) Graph

Figure 5.4: Network composed of three agents and two controllers with a generalized symmetric communication structure.

Generalized Undirected Topology Consider the interconnection equations (5.4) in matrix form

$$\begin{bmatrix} -\boldsymbol{u} \\ \boldsymbol{\zeta} \end{bmatrix} = \begin{bmatrix} \mathbf{0} & \boldsymbol{E} \otimes \boldsymbol{I}_n \\ (\boldsymbol{E} \otimes \boldsymbol{I}_n)^\top & \mathbf{0} \end{bmatrix} \begin{bmatrix} \boldsymbol{y} \\ \boldsymbol{d} \end{bmatrix}. \tag{5.10}$$

Instead of considering the controller systems to be located on the edges of the communication graph between agents, the structure can be interpreted as a bipartite graph. The disjunct set of agent and controller systems are the nodes of the graph, and the communication between agents and controllers are the edges. The matrix in (5.10) can be interpreted as the weighted adjacency matrix[51] of the bipartite graph [BH12]. Observe that the adjacency matrix is symmetric, which implies a bidirectional or undirected communication topology. This symmetry property is instrumental in the derivation of the Lyapunov function in Section 5.4. However, the only property of the communication incidence matrix $\boldsymbol{E}^\top$ that is used in Theorems 5.1 and 5.2 is that $\boldsymbol{E}^\top$ has a nullspace of dimension one spanned by the $\mathbf{1}_{n_\mathcal{A}}$ vector, i.e.,

$$\ker\{\boldsymbol{E}^\top\} = \{\alpha \mathbf{1}_{n_\mathcal{A}} \mid \alpha \in \mathbb{R}\} \tag{5.11}$$

(recall Remark 5.4). The incidence matrices of connected graphs are, however, only a subset of the matrices with this nullspace property (5.11). Thus, any matrix $\boldsymbol{R} \in \mathbb{R}^{n_\mathcal{A} \times n_\mathcal{C}}$ with the nullspace property (5.11) can readily be used, and this is the only requirement for the communication structure. In particular, all the results of Theorems 5.1 and 5.2 hold for such an $\boldsymbol{R}$. Figure 5.4 shows the effect of generalized communication for the graph structure. Observe that a controller is connected to more than two nodes, instead of being associated with an edge between only two agents as before. With the generalized communication structure, the second equation in (5.10) computes a weighted average of the outputs $\boldsymbol{y}_i$. Such a communication matrix is called mixing matrix in [Shi+15]. The next proposition provides a relation between the number of agents and controllers necessary to obtain the nullspace property and thus globally optimal equilibria.

[51] A definition where the weights of the adjacency matrix can be negative is adopted here as in [CKG16; ZB15].

Proposition 5.3 (minimum number of controller systems)
The network has to contain at least $n_{\mathcal{A}} - 1$ controllers in order to fulfill the nullspace property.

Proof. The nullspace property states that the communication matrix $\boldsymbol{R}^\top \in \mathbb{R}^{n_{\mathcal{C}} \times n_{\mathcal{A}}}$ should have a nullspace of dimension one spanned by the vector $\mathbf{1}_{n_{\mathcal{A}}}$. Assume $n_{\mathcal{C}} < n_{\mathcal{A}} - 1$. Then, the rank of $\boldsymbol{R}^\top \in \mathbb{R}^{n_{\mathcal{C}} \times n_{\mathcal{A}}}$ is at most $n_{\mathcal{A}} - 2$, since it has at most $n_{\mathcal{A}} - 2$ rows. Due to the rank-nullity theorem [HJ12, p. 6], having $n_{\mathcal{A}}$ columns and a rank of $n_{\mathcal{A}} - 2$ implies that the kernel of $\boldsymbol{R}^\top$ must have dimension two, which violates the nullspace property. □

Directed Graphs and Non-Symmetric Communication Structure In the case of a directed communication structure, the information exchange is not necessarily bi-directional between agents and controllers. This is described by a non-symmetric communication structure, composed of two different matrices $\boldsymbol{R}_{\mathcal{A}}$ and $\boldsymbol{R}_{\mathcal{C}} \in \mathbb{R}^{n_{\mathcal{A}} \times n_{\mathcal{C}}}$ of identical size, i.e.,

$$\begin{bmatrix} -\boldsymbol{u} \\ \boldsymbol{\zeta} \end{bmatrix} = \begin{bmatrix} 0 & \boldsymbol{R}_{\mathcal{C}} \otimes \boldsymbol{I}_n \\ (\boldsymbol{R}_{\mathcal{A}} \otimes \boldsymbol{I}_n)^\top & 0 \end{bmatrix} \begin{bmatrix} \boldsymbol{y} \\ \boldsymbol{d} \end{bmatrix}. \tag{5.12}$$

The matrix $\boldsymbol{R}_{\mathcal{A}}$ describes the information flow from agents to controllers, $\boldsymbol{R}_{\mathcal{C}}$ from controllers to agents. An example is given in Figure 5.5. The directed communication from agents to controllers described by $\boldsymbol{R}_{\mathcal{A}}$ is displayed in blue, and the directed communication from controllers to agents $\boldsymbol{R}_{\mathcal{C}}$ in red. Observe that an agent may send its output $\boldsymbol{y}_i$ to a controller which does not send its integrator state back. As before, the only requirement for global optimality in Theorems 5.1 and 5.2 is that the communication matrices $\boldsymbol{R}_{\mathcal{A}}$ and $\boldsymbol{R}_{\mathcal{C}}$ have, individually, the stated nullspace property (5.11). Graphically, the nullspace property of $\boldsymbol{R}_{\mathcal{A}}$ means that the weights of incoming edges at any controller have to sum up to zero. Similarly, the nullspace property of $\boldsymbol{R}_{\mathcal{C}}$ means that the weights of the outgoing edges at the controller have to sum up to zero (see Figure 5.5).

The main issue with the directed communication topology is that it does not generally translate into a skew-symmetric interconnection. This is, however, crucial for a direct passivity-based stability analysis. The matrix in (5.12) describes a non-symmetric adjacency matrix of a bipartite graph. In order to cope with that, a greater excess of EIP on the agent dynamics will be necessary to ensure convergence, as is explained in Section 5.5 in detail.

Remark 5.5. *Note that in both undirected and directed communication structures, the nullspace property can be trivially fulfilled individually by the controllers and does not require any*

$$\boldsymbol{R}_{\mathcal{A}} = \begin{bmatrix} 1 & 0 \\ -2 & 1 \\ 1 & -1 \end{bmatrix}$$

$$\boldsymbol{R}_{\mathcal{C}} = \begin{bmatrix} 0 & 1 \\ 2 & 0 \\ -2 & -1 \end{bmatrix}$$

(a) Communication matrices

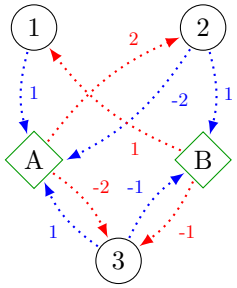

(b) Graph

Figure 5.5: Network composed of three agents and two controllers with a directed, non-symmetric communication structure.

global coordination. Provided that all agents send their output $\boldsymbol{y}_i$, each controller can assign individually a weight to each incoming (or, similarly, outgoing) edge such that the sum is zero.

In the next subsection, requirements for the agent and controller dynamics to converge to the global optimizers characterized in this subsection are derived.

5.2.2 Design Requirements for Convergence with Undirected Communication Topologies

The design requirements which are posed on the agent and controller systems to ensure convergence to the global optimizers characterized in Section 5.2.1 are, in a broad sense, EIP properties [SP18; AMP16]. Depending on the scenario, i.e., unconstrained or constrained optimization with undirected or directed communication topologies, different EIP properties are necessary. The following theorem provides local design requirements for achieving convergence in the case of undirected communication topologies.

Theorem 5.4 (design requirements for convergence)
Let the agents $i \in \mathcal{A}$ and controller systems $k \in \mathcal{C}$ fulfill the design requirements of Theorems 5.1 or 5.2 and Definition 5.1, respectively. Further, let the agents be interconnected by a communication structure (5.10) *fulfilling property* (5.11)*. In addition, let the agent systems $i \in \mathcal{A}$ be EIO and OFEIP(ρ_i) with $\rho_i > 0$ and positive definite storage function S_i, and the controller systems $k \in \mathcal{C}$ be EIO and EIP with positive definite storage function W_k. Then, all trajectories of the networked system converge to a point in the invariant equilibrium manifold $\mathcal{M}_{\text{eq}}$ as specified in Theorem 5.1 or 5.2, which implies that the estimation $\boldsymbol{y}_i$ of all agents converges to the global optimizer $\mathbf{y}^*$.*

Proof. Consider the network-wide Lyapunov function

$$V = \sum_{i \in \mathcal{A}} S_i + \sum_{k \in \mathcal{C}} W_k. \tag{5.13}$$

The time derivative, using the OFEIP(ρ_i) and EIP properties of the agent and controller systems, reads

$$\dot{V} \leq \sum_{i \in \mathcal{A}} \left(\tilde{\boldsymbol{u}}_i^\top \tilde{\boldsymbol{y}}_i - \rho_i \tilde{\boldsymbol{y}}_i^\top \tilde{\boldsymbol{y}}_i \right) + \sum_{k \in \mathcal{C}} \tilde{\boldsymbol{\zeta}}_k^\top \tilde{\boldsymbol{d}}_k. \tag{5.14}$$

Written in stacked network variables, (5.14) reads

$$\begin{aligned} \dot{V} &\leq \tilde{\boldsymbol{u}}^\top \tilde{\boldsymbol{y}} - \tilde{\boldsymbol{y}}^\top \left(\operatorname{diag}\{\rho_i\} \otimes \boldsymbol{I}_n \right) \tilde{\boldsymbol{y}} + \tilde{\boldsymbol{\zeta}}^\top \tilde{\boldsymbol{d}} \\ &= -\tilde{\boldsymbol{y}}^\top \boldsymbol{K} \tilde{\boldsymbol{y}}, \end{aligned} \tag{5.15}$$

where the last equality follows by inserting the interconnection topology (5.10) into the first and third term, and introducing $\boldsymbol{K} = \operatorname{diag}\{\rho_i\} \otimes \boldsymbol{I}_n$. The matrix $\boldsymbol{K}$ is positive definite, since $\rho_i > 0$. Hence, all trajectories converge to $\tilde{\boldsymbol{y}} = \mathbf{0}$, which corresponds to the manifold $\mathcal{M}_{\text{eq}}$, and $\boldsymbol{y}_i = \mathbf{y}^*$. Since all agents are in consensus, $\boldsymbol{\zeta}_k$ is zero and with EIO, all $\boldsymbol{z}_k$, $k \in \mathcal{C}$ and $\boldsymbol{x}_i$, $i \in \mathcal{A}$ are constant. □

Note that Theorem 5.4 covers both unconstrained and constrained optimization. The state-of-the-art algorithms for the constrained case in continuous time, however, comprise discontinuous agent dynamics [Hat+18; CMC16] or differential inclusions [LW15; ZYH17]. In this case, Theorem 5.4 can still be applied to such dynamics using generalized gradients and Lyapunov theory for discontinuous dynamic systems (e.g., [Cor08, Th. 1] or [BC06, Lemma 1]). To do so, the following additional assumption needs to hold (see Section 5.4.2 for details):

Table 5.1: Summary of the design requirement theorems.

	Global optimality	Convergence
unconstrained	Theorem 5.1	Theorem 5.4
constrained	Theorem 5.2	Theorem 5.4 (+ Assumption 5.1 for discontinuous agent dynamics)

Assumption 5.1 (existence of solutions)
Consider a discontinuous dynamic system composed of agents $i \in \mathcal{A}$ and controllers $k \in \mathcal{C}$ interconnected by a communication structure (5.10)*. For all admissible initial states, a solution of the discontinuous dynamic system exists.*

Remark 5.6. *Assumption 5.1 is stated as an additional requirement instead of merging it into Theorem 5.4, since technically, the agent dynamics must not necessarily have discontinuities in the constrained case. Continuous agent dynamics for a constrained, distributed optimization problem as in* (5.1) *may be conceivable, but, to the best of the authors' knowledge, have not been proposed yet.*

In addition, note that the global optimality design requirements in Theorems 5.1 and 5.2 are local properties for each agent and controller system. Also, OFEIP and EIP are per design local subsystem properties. Therefore, with the proposed framework, there is no need for all agents to follow a specific, given algorithm. Networks composed of agents with heterogeneous optimization dynamics converge to the global optimizer, provided that the local design requirements for global optimality and convergence given in Theorems 5.1, 5.2, and 5.4, as well as the nullspace requirement (5.11) for the communication structure are satisfied. This make the proposed distributed optimization framework easily scalable and enables agents to leave or (re)join the optimization without compromising global optimality and convergence. A summary of the original theorems regarding the design requirements for optimality and convergence is shown in Table 5.1.

Remark 5.7. *The requirement of OFEIP agent dynamics may be restrictive in some cases and can be relaxed for both the unconstrained and constrained problem with an undirected communication topology under minor additional information on the agent dynamics (see Section 5.4).*

After introducing the novel distributed optimization framework and deriving local requirements for the agent and controller subsystems, system dynamics for both subsystems satisfying these requirements are proposed in the next section.

5.3 Agent and Controller Dynamics

In this section, various agent and controller dynamics are proposed and their EIP properties are analyzed. In Section 5.3.1, different agent dynamics for unconstrained optimization are proposed. Different EIP properties can be derived depending on the convexity properties of the objective function or on the specific form of the dynamics. In Section 5.3.2, agent dynamics for constrained optimization are proposed and analyzed. Lastly, in Section 5.3.3, various controller dynamics are proposed and their EIP properties are analyzed.

5.3.1 Agent Dynamics for Unconstrained Optimization

First, the EIP properties of a simple gradient descent as agent dynamics are studied. This is the simplest form of agent dynamics. Although it does not consider any constraints, strong passivity properties can be derived without having to do conservative approximations.

Basic Gradient-based Agent Dynamics Consider the system dynamics for the agents

$$\Sigma_i: \quad \begin{aligned} \dot{\boldsymbol{x}}_i &= -\alpha_i \nabla f_i(\boldsymbol{x}_i) + \alpha_i \boldsymbol{u}_i \\ \boldsymbol{y}_i &= \boldsymbol{x}_i, \end{aligned} \tag{5.16}$$

where $\alpha_i > 0$ is a scalar design parameter and f_i the objective function of agent $i \in \mathcal{A}$ as described in (5.1). Condition (5.5) of Theorem 5.1 is trivially fulfilled. The EIP properties of (5.16) are studied in the next proposition.

Proposition 5.5 (OFEIP agent dynamics)
Consider the storage function $S_i(\tilde{\boldsymbol{x}}_i) = \frac{1}{2\alpha_i}\tilde{\boldsymbol{x}}_i^\top \tilde{\boldsymbol{x}}_i$. System (5.16) *is EIP, if f_i is convex, and OFEIP($M_{\text{conv},i}$), if f_i is $M_{\text{conv},i}$-strongly convex.*

Proof. Consider the time derivative of the storage function

$$\dot{S}_i = \frac{1}{\alpha_i}\tilde{\boldsymbol{x}}_i^\top \dot{\boldsymbol{x}}_i \tag{5.17}$$

$$= \frac{1}{\alpha_i}\tilde{\boldsymbol{x}}_i^\top (-\alpha_i \nabla f_i(\boldsymbol{x}_i) + \alpha_i \boldsymbol{u}_i). \tag{5.18}$$

Next, add $\tilde{\boldsymbol{x}}_i^\top (\nabla f_i(\bar{\boldsymbol{x}}_i) - \bar{\boldsymbol{u}}_i)$, which equals to zero for any equilibrium $\bar{\boldsymbol{x}}_i$, $\bar{\boldsymbol{u}}_i$, to (5.18) to obtain

$$\begin{aligned}\dot{S}_i &= \tilde{\boldsymbol{x}}_i^\top(-\nabla f_i(\boldsymbol{x}_i) + \boldsymbol{u}_i) - \tilde{\boldsymbol{x}}_i^\top(-\nabla f_i(\bar{\boldsymbol{x}}_i) + \bar{\boldsymbol{u}}_i) \\ &= \tilde{\boldsymbol{y}}_i^\top \tilde{\boldsymbol{u}}_i - \tilde{\boldsymbol{y}}_i^\top(\nabla f_i(\boldsymbol{y}_i) - \nabla f_i(\bar{\boldsymbol{y}}_i)).\end{aligned} \tag{5.19}$$

Taking into account the convexity condition for differentiable functions (3.20), it follows from (5.19) that $\dot{S}_i \leq \tilde{\boldsymbol{y}}_i^\top \tilde{\boldsymbol{u}}_i$, if f_i is convex, which shows EIP of (5.16). Furthermore, it follows from (5.19) that $\dot{S}_i \leq \tilde{\boldsymbol{y}}_i^\top \tilde{\boldsymbol{u}}_i - M_{\text{conv},i}\tilde{\boldsymbol{y}}_i^\top \tilde{\boldsymbol{y}}_i$ if $f_i : \mathbb{R}^n \to \mathbb{R}$ is $M_{\text{conv},i}$-strongly convex, which proves OFEIP($M_{\text{conv},i}$) of (5.16). □

Corollary 5.6 (EIP agent dynamics)
The system dynamics of the agents (5.16) *is also equilibrium-independent dissipative with a supply rate* $w(\tilde{\boldsymbol{u}}_i, \tilde{\boldsymbol{y}}_i) = \tilde{\boldsymbol{y}}_i^\top \tilde{\boldsymbol{u}}_i - \Psi_i(\tilde{\boldsymbol{y}}_i)$ *with* $\Psi_i(\tilde{\boldsymbol{y}}_i) = \tilde{\boldsymbol{y}}_i^\top(\nabla f_i(\boldsymbol{y}_i) - \nabla f_i(\bar{\boldsymbol{y}}_i))$*, as follows directly from* (5.19)*. Note that* $\Psi_i(\tilde{\boldsymbol{y}}_i) \geq 0$ *if the function* $f_i : \mathbb{R}^n \to \mathbb{R}$ *is convex, thus obtaining EIP as in Definition 3.3.*

Agent Dynamics with Feedthrough The agent dynamics (5.16) proposed above show an excess of output passivity OFEIP, but it does not have any excess of input passivity IFEIP. However, in some applications, an additional excess of IFEIP is necessary. For example, when using directed communication topologies, an excess of input passivity is necessary to ensure stability (c.f. Section 5.5). Therefore, consider the modified agent dynamics

$$\Sigma_i : \begin{aligned}\dot{\boldsymbol{x}}_i &= -\alpha_i \nabla f_i(\boldsymbol{x}_i + \gamma_i \boldsymbol{u}_i) + \alpha_i \boldsymbol{u}_i \\ \boldsymbol{y}_i &= \boldsymbol{x}_i + \gamma_i \boldsymbol{u}_i,\end{aligned} \tag{5.20}$$

with $\gamma_i \in \mathbb{R}_{\geq 0}$. Note that the dynamics (5.20) fulfill the equilibrium requirement of Theorem 5.1. These particular agent dynamics exhibits a direct feedthrough from input to output, which is expected to induce an excess of input-feedforward EIP [SJK12, p. 36]. This is formally proven in the next proposition.

Proposition 5.7 (IF-OFEIP agent dynamics)
Consider the storage function $S_i(\tilde{\boldsymbol{x}}_i) = \frac{1}{2\alpha_i}\tilde{\boldsymbol{x}}_i^\top \tilde{\boldsymbol{x}}_i$*. System* (5.20) *is IF-OFEIP*(ν_i, ρ_i) *w.r.t. the supply rate* $w(\tilde{\boldsymbol{u}}_i, \tilde{\boldsymbol{y}}_i) = \tilde{\boldsymbol{y}}_i^\top \tilde{\boldsymbol{u}}_i - \nu_i \tilde{\boldsymbol{u}}_i^\top \tilde{\boldsymbol{u}}_i - \rho_i \tilde{\boldsymbol{y}}_i^\top \tilde{\boldsymbol{y}}_i$*, with* $\nu_i = \frac{1}{2}\gamma_i$ *and* $\rho_i = M_{\text{conv},i} - \frac{1}{2}\gamma_i M_{\text{Lip},i}$*, if the objective function* $f_i : \mathbb{R}^n \to \mathbb{R}$ *is* $M_{\text{conv},i}$*-strongly convex and has* $M_{\text{Lip},i}$*-Lipschitz gradients.*

Proof. Consider the derivative of the storage function

$$\begin{aligned}\dot{S}_i &= \frac{1}{\alpha_i}\tilde{\boldsymbol{x}}_i^\top \dot{\boldsymbol{x}}_i \\ &= \frac{1}{\alpha_i}\tilde{\boldsymbol{x}}_i^\top \left(-\alpha_i \nabla f_i(\boldsymbol{x}_i + \gamma_i \boldsymbol{u}_i) + \alpha_i \boldsymbol{u}_i\right) \\ &= \tilde{\boldsymbol{x}}_i^\top \boldsymbol{u}_i - \tilde{\boldsymbol{x}}_i^\top \nabla f_i(\boldsymbol{x}_i + \gamma_i \boldsymbol{u}_i) \end{aligned} \tag{5.21}$$

Next, add $\tilde{\boldsymbol{x}}_i^\top \left(\nabla f_i(\bar{\boldsymbol{x}}_i + \gamma_i \bar{\boldsymbol{u}}_i) - \bar{\boldsymbol{u}}_i\right)$, which equals to zero, to (5.21) and obtain

$$\dot{S}_i = \tilde{\boldsymbol{x}}_i^\top \tilde{\boldsymbol{u}}_i - \tilde{\boldsymbol{x}}_i^\top \left(\nabla f_i(\boldsymbol{x}_i + \gamma_i \boldsymbol{u}_i) - \nabla f_i(\bar{\boldsymbol{x}}_i + \gamma_i \bar{\boldsymbol{u}}_i)\right). \tag{5.22}$$

Substituting $\boldsymbol{y}_i = \boldsymbol{x}_i + \gamma_i \boldsymbol{u}_i$ and $\tilde{\boldsymbol{x}}_i = \tilde{\boldsymbol{y}}_i - \gamma_i \tilde{\boldsymbol{u}}_i$ in (5.22) and defining for convenience $\tilde{f}_i(\boldsymbol{y}_i, \bar{\boldsymbol{y}}_i) := f_i(\boldsymbol{y}_i) - f_i(\bar{\boldsymbol{y}}_i)$ yields

$$\begin{aligned}\dot{S}_i &= \left(\tilde{\boldsymbol{y}}_i - \gamma_i \tilde{\boldsymbol{u}}_i\right)^\top \tilde{\boldsymbol{u}}_i - \left(\tilde{\boldsymbol{y}}_i - \gamma_i \tilde{\boldsymbol{u}}_i\right)^\top \nabla \tilde{f}_i(\boldsymbol{y}_i, \bar{\boldsymbol{y}}_i) \\ &= \tilde{\boldsymbol{y}}_i^\top \tilde{\boldsymbol{u}}_i - \gamma_i \tilde{\boldsymbol{u}}_i^\top \tilde{\boldsymbol{u}}_i - \tilde{\boldsymbol{y}}_i^\top \nabla \tilde{f}_i(\boldsymbol{y}_i, \bar{\boldsymbol{y}}_i) + \gamma_i \tilde{\boldsymbol{u}}_i^\top \nabla \tilde{f}_i(\boldsymbol{y}_i, \bar{\boldsymbol{y}}_i). \end{aligned} \tag{5.23}$$

In the following, an upper bound for the third and fourth term in (5.23) is derived, since they are not in a form amenable to the quadratic supply rate provided in the statement of the proposition. Taking into account the strong convexity condition (3.20), it holds for the third term that

$$-\tilde{\boldsymbol{y}}_i^\top \nabla \tilde{f}_i(\boldsymbol{y}_i, \bar{\boldsymbol{y}}_i) \leq -M_{\text{conv},i} \tilde{\boldsymbol{y}}_i^\top \tilde{\boldsymbol{y}}_i. \tag{5.24}$$

For an upper bound for the fourth term, first consider that the shifted dynamics $\dot{\tilde{\boldsymbol{x}}}_i = -\alpha_i \nabla \tilde{f}_i(\boldsymbol{y}_i, \bar{\boldsymbol{y}}_i) + \alpha_i \tilde{\boldsymbol{u}}_i$ and note that

$$\begin{aligned}\frac{1}{\alpha_i^2}\dot{\tilde{\boldsymbol{x}}}_i^\top \dot{\tilde{\boldsymbol{x}}}_i &= \left(\tilde{\boldsymbol{u}}_i - \nabla \tilde{f}_i(\boldsymbol{y}_i, \bar{\boldsymbol{y}}_i)\right)^\top \left(\tilde{\boldsymbol{u}}_i - \nabla \tilde{f}_i(\boldsymbol{y}_i, \bar{\boldsymbol{y}}_i)\right) \\ &= \tilde{\boldsymbol{u}}_i^\top \tilde{\boldsymbol{u}}_i + \nabla \tilde{f}_i(\boldsymbol{y}_i, \bar{\boldsymbol{y}}_i)^\top \nabla \tilde{f}_i(\boldsymbol{y}_i, \bar{\boldsymbol{y}}_i) - 2\tilde{\boldsymbol{u}}_i^\top \nabla \tilde{f}_i(\boldsymbol{y}_i, \bar{\boldsymbol{y}}_i) \geq 0 \end{aligned} \tag{5.25}$$

always holds. Furthermore, bringing the third term of (5.25) into the right-hand side and taking into account the $M_{\text{Lip},i}$-Lipschitz property (3.22) of ∇f_i, (5.25) reads

$$\begin{aligned}\tilde{\boldsymbol{u}}_i^\top \nabla \tilde{f}_i(\boldsymbol{y}_i, \bar{\boldsymbol{y}}_i) &\leq \frac{1}{2}\tilde{\boldsymbol{u}}_i^\top \tilde{\boldsymbol{u}}_i + \frac{1}{2}\nabla \tilde{f}_i(\boldsymbol{y}_i, \bar{\boldsymbol{y}}_i)^\top \nabla \tilde{f}_i(\boldsymbol{y}_i, \bar{\boldsymbol{y}}_i) \\ &\leq \frac{1}{2}\tilde{\boldsymbol{u}}_i^\top \tilde{\boldsymbol{u}}_i + \frac{1}{2} M_{\text{Lip},i} \tilde{\boldsymbol{y}}_i^\top \tilde{\boldsymbol{y}}_i. \end{aligned} \tag{5.26}$$

Substituting (5.24) and (5.26) in the third and fourth term, respectively, in the derivative of the storage function (5.23), it results

$$\dot{S}_i \leq \tilde{\boldsymbol{y}}_i^\top \tilde{\boldsymbol{u}}_i - \frac{1}{2}\gamma_i \tilde{\boldsymbol{u}}_i^\top \tilde{\boldsymbol{u}}_i - \left(M_{\text{conv},i} - \frac{1}{2}\gamma_i M_{\text{Lip},i}\right) \tilde{\boldsymbol{y}}_i^\top \tilde{\boldsymbol{y}}_i, \tag{5.27}$$

which concludes the proof. □

In the last proposition, it is shown that the agent dynamics (5.20) are IF-OFEIP(ν_i, ρ_i) with indices $\nu_i = \frac{1}{2}\gamma_i$ and $\rho_i = M_{\text{conv},i} - \frac{1}{2}\gamma_i M_{\text{Lip},i}$. Note that by choosing $\gamma_i = 0$, the result of Proposition 5.5 are recovered as expected. As known from the literature, the OFEIP and IFEIP indices cannot be chosen independently of each other. An increase of the OFEIP index implies a decrease of the IFEIP index and vice versa [SP18], which also applies to (5.27). However, even if typically the Lipschitz index is greater than the strong convexity parameter, i.e., $M_{\text{Lip},i} \geq M_{\text{conv},i}$, by choosing γ_i small enough, it is always possible to obtain IF-OFEIP(ν_i, ρ_i) for system (5.20) with an excess of input and output passivity, i.e., $\nu_i, \rho_i > 0$. The largest bound for γ_i can be computed by imposing that $\rho_i > 0$ and solving for γ_i, i.e., $\gamma_i < \frac{2M_{\text{conv},i}}{M_{\text{Lip},i}} \leq 2$. Thus, the upper bounds on the indices are $\rho_i = M_{\text{conv},i}$ (when $\gamma_i = 0$) and $\nu_i = 1$ (when $\gamma_i = 2$).

Agent Dynamics with Quadratic Objective Functions When agents use quadratic objective functions, Proposition 5.7 can be improved to remove the need for strong convexity. In Proposition 5.7, strong convexity is required because, without $M_{\text{conv},i} > 0$, the output passivity index ρ_i cannot be greater or equal to zero. However, for quadratic objective functions, fewer conservative approximations are necessary, resulting in tighter bounds for both the OFEIP and IFEIP indices.

Corollary 5.8 (agent dynamics with quadratic objective function)
Assume an agent $i \in \mathcal{A}$ has a convex quadratic objective function of the form $f_i(\boldsymbol{x}_i) = \frac{1}{2}\boldsymbol{x}_i^\top \boldsymbol{Q}_i \boldsymbol{x}_i + \boldsymbol{q}_i^\top \boldsymbol{x}_i + c_i$, with $\boldsymbol{Q}_i \in \mathbb{R}^{n\times n}$ positive semidefinite, $\boldsymbol{q}_i \in \mathbb{R}^n$ and $c_i \in \mathbb{R}$. Consider the storage function $S_i(\tilde{\boldsymbol{x}}_i) = \frac{1}{2\alpha_i}\tilde{\boldsymbol{x}}_i^\top \boldsymbol{G}_i \tilde{\boldsymbol{x}}_i$ with $\boldsymbol{G}_i = (\boldsymbol{I}_n + \gamma_i \boldsymbol{Q}_i)^{-1}$ positive definite for $\gamma_i \geq 0$. System (5.20) is IF-OFEIP(ν_i, ρ_i) with $\rho_i = \text{eigmin}\{\boldsymbol{G}_i \boldsymbol{Q}_i\}$ and $\nu_i = \text{eigmin}\{\gamma_i \boldsymbol{G}_i\}$.

Proof. With (5.20), the time derivative of the storage function S_i is given by

$$\begin{aligned}\dot{S}_i &= \frac{1}{\alpha_i}\tilde{\boldsymbol{x}}_i^\top \boldsymbol{G}_i \dot{\boldsymbol{x}}_i \\ &= \frac{1}{\alpha_i}\tilde{\boldsymbol{x}}_i^\top \boldsymbol{G}_i \left(-\alpha_i \boldsymbol{Q}_i(\boldsymbol{x}_i + \gamma_i \boldsymbol{u}_i) - \alpha_i \boldsymbol{q}_i + \alpha_i \boldsymbol{u}_i\right) \\ &= \tilde{\boldsymbol{x}}_i^\top \boldsymbol{G}_i \left(-\boldsymbol{Q}_i(\boldsymbol{x}_i + \gamma_i \boldsymbol{u}_i) - \boldsymbol{q}_i + \boldsymbol{u}_i\right). \end{aligned} \tag{5.28}$$

Adding $\tilde{\boldsymbol{x}}_i^\top \boldsymbol{G}_i \left(\boldsymbol{Q}_i(\bar{\boldsymbol{x}}_i + \gamma_i \bar{\boldsymbol{u}}_i) + \boldsymbol{q}_i - \bar{\boldsymbol{u}}_i\right)$, which equals to zero, to (5.28), it results

$$\begin{aligned}\dot{S}_i &= \tilde{\boldsymbol{x}}_i^\top \boldsymbol{G}_i \left(-\boldsymbol{Q}_i(\tilde{\boldsymbol{x}}_i + \gamma_i \tilde{\boldsymbol{u}}_i) + \tilde{\boldsymbol{u}}_i\right) \\ &= \tilde{\boldsymbol{x}}_i^\top \boldsymbol{G}_i (\boldsymbol{I}_n - \gamma_i \boldsymbol{Q}_i)\tilde{\boldsymbol{u}}_i - \tilde{\boldsymbol{x}}_i^\top \boldsymbol{G}_i \boldsymbol{Q}_i \tilde{\boldsymbol{x}}_i. \end{aligned} \tag{5.29}$$

Substituting $\tilde{\boldsymbol{x}}_i = \tilde{\boldsymbol{y}}_i - \gamma_i \tilde{\boldsymbol{u}}_i$ in (5.29) and expanding all the products yields

$$\begin{aligned}
\dot{S}_i &= \tilde{\boldsymbol{y}}_i^\top (\boldsymbol{G}_i - \gamma_i \boldsymbol{G}_i \boldsymbol{Q}_i) \tilde{\boldsymbol{u}}_i - (\tilde{\boldsymbol{y}}_i - \gamma_i \tilde{\boldsymbol{u}}_i)^\top \boldsymbol{G}_i \boldsymbol{Q}_i (\tilde{\boldsymbol{y}}_i - \gamma_i \tilde{\boldsymbol{u}}_i) - \gamma_i \tilde{\boldsymbol{u}}_i^\top \boldsymbol{G}_i (\boldsymbol{I}_n - \gamma_i \boldsymbol{Q}_i) \tilde{\boldsymbol{u}}_i \\
&= \tilde{\boldsymbol{y}}_i^\top (\boldsymbol{G}_i - \gamma_i \boldsymbol{G}_i \boldsymbol{Q}_i) \tilde{\boldsymbol{u}}_i + \gamma_i \tilde{\boldsymbol{y}}_i^\top \boldsymbol{Q}_i \boldsymbol{G}_i \tilde{\boldsymbol{u}}_i + \gamma_i \tilde{\boldsymbol{y}}_i^\top \boldsymbol{G}_i \boldsymbol{Q}_i \tilde{\boldsymbol{u}}_i \\
&\quad - \tilde{\boldsymbol{y}}_i^\top \boldsymbol{G}_i \boldsymbol{Q}_i \tilde{\boldsymbol{y}}_i - \gamma_i^2 \tilde{\boldsymbol{u}}_i^\top \boldsymbol{G}_i \boldsymbol{Q}_i \tilde{\boldsymbol{u}}_i - \gamma_i \tilde{\boldsymbol{u}}_i^\top \boldsymbol{G}_i (\boldsymbol{I}_n - \gamma_i \boldsymbol{Q}_i) \tilde{\boldsymbol{u}}_i \\
&= \tilde{\boldsymbol{y}}_i^\top (\boldsymbol{I}_n + \gamma_i \boldsymbol{Q}_i) \boldsymbol{G}_i \tilde{\boldsymbol{u}}_i - \tilde{\boldsymbol{y}}_i^\top \boldsymbol{G}_i \boldsymbol{Q}_i \tilde{\boldsymbol{y}}_i - \gamma_i \tilde{\boldsymbol{u}}_i^\top \boldsymbol{G}_i \tilde{\boldsymbol{u}}_i \\
&= \tilde{\boldsymbol{y}}_i^\top \tilde{\boldsymbol{u}}_i - \tilde{\boldsymbol{y}}_i^\top \boldsymbol{G}_i \boldsymbol{Q}_i \tilde{\boldsymbol{y}}_i - \gamma_i \tilde{\boldsymbol{u}}_i^\top \boldsymbol{G}_i \tilde{\boldsymbol{u}}_i. \qquad (5.30)
\end{aligned}$$

Note that $\boldsymbol{G}_i \boldsymbol{Q}_i$ in (5.30) is positive semidefinite, which is proven in Proposition B.2 in the Appendix Section B.2. Thus, from (5.30) follows the supply rate stated in the corollary. □

With the last corollary, it is shown that the agent dynamics (5.20) have an IFEIP index greater than zero even without having a strongly convex objective function. Inspecting the OFEIP and IFEIP indices as a function of γ_i, it results

$$\nu_i(\gamma_i) = \text{eigmin}\{\gamma_i \left(\boldsymbol{I}_n + \gamma_i \boldsymbol{Q}_i\right)^{-1}\} \qquad (5.31)$$

$$\rho_i(\gamma_i) = \text{eigmin}\{\left(\boldsymbol{I}_n + \gamma_i \boldsymbol{Q}_i\right)^{-1} \boldsymbol{Q}_i\}. \qquad (5.32)$$

Due to the positive definiteness of $\left(\boldsymbol{I}_n + \gamma_i \boldsymbol{Q}_i\right)^{-1}$, it directly follows that $\nu_i(\gamma_i) \geq 0$ and equality holds only when $\gamma_i = 0$. Furthermore, $\rho_i(\gamma_i) \geq 0$, and $\rho_i(\gamma_i) = 0$ for all γ_i if $\boldsymbol{Q}_i$ does not have full rank, which is the case for convex (i.e. not strongly convex) objective functions. For a strongly convex objective function, $\boldsymbol{Q}_i^{-1}$ exists and thus $\rho_i(\gamma_i) = \text{eigmin}\{\left(\boldsymbol{Q}_i^{-1} + \gamma_i \boldsymbol{I}_n\right)^{-1}\}$. For $\gamma_i \to 0$, it results $\nu_i(\gamma_i) \to 0$ and $\rho_i(\gamma_i) \to \text{eigmin}\{\boldsymbol{Q}_i\}$. For $\gamma_i \to \infty$, it results $\nu_i(\gamma_i) \to \frac{1}{\text{eigmax}\{\boldsymbol{Q}_i\}}$ and $\rho_i(\gamma_i) \to 0$ from simple limit calculations as proven in Proposition B.3 in Appendix B. Thus, compared to Proposition 5.7, in Corollary 5.8 the upper bound $\gamma_i \leq 2$ is dropped and a wider range of possible OFEIP and IFEIP index values are obtained. Furthermore, when the objective function is only convex, the OFEIP index is zero instead of negative.

All in all, in this subsection, various agent dynamics for unconstrained optimization fulfilling the local design requirements of Section 5.2 have been proposed. The basic agent dynamics (5.16) are OFEIP($M_{\text{conv},i}$) if the objective function f_i is $M_{\text{conv},i}$-strongly convex. Adding a feedthrough in (5.20) introduces an excess of input passivity, obtaining then IF-OFEIPagent dynamics if f_i is strongly convex and the gradient is Lipschitz. Finally, it has been shown that choosing a quadratic objective function, sharper bounds on an excess of input and output EIP are obtained.

5.3.2 Agent Dynamics for Constrained Optimization

For considering constraints in the distributed optimization framework, the approached developed in this dissertation is inspired by the approach in [Hat+18]. It uses a gradient

descent and projected dual ascent studied in detail in [CMC16]. The method implicitly constraints the Lagrange multipliers λ_{il} to the positive real numbers. Consider the agent system dynamics

$$\Sigma_i : \begin{cases} \dot{\boldsymbol{x}}_i &= -\alpha_i \nabla_{\boldsymbol{x}_i} L_i(\boldsymbol{x}_i, \boldsymbol{\lambda}_i, \boldsymbol{\mu}_i) + \alpha_i \boldsymbol{u}_i \\ \dot{\lambda}_{il} &= \begin{cases} 0 & \text{if } \lambda_{il} = 0 \text{ and } g_{il}(\boldsymbol{x}_i) < 0 \quad \text{(mode 1)} \\ g_{il}(\boldsymbol{x}_i) & \text{otherwise} \quad \text{(mode 2)} \end{cases} \\ \dot{\mu}_{ij} &= h_{ij}(\boldsymbol{x}_i) \\ \boldsymbol{y}_i &= \boldsymbol{x}_i, \end{cases} \tag{5.33}$$

with $\alpha_i > 0$ and the Lagrange function L_i as in (3.25). The variables $\boldsymbol{\lambda}_i = \text{col}\{\lambda_{il}\}$ and $\boldsymbol{\mu}_i = \text{col}\{\mu_{ij}\}$ are defined as in Section 3.3. Note that system (5.33) has discontinuous dynamics and the solutions are understood in the Carathéodory[52] sense [Cor08]. The time derivative of a storage function $S_i(\boldsymbol{x}_i, \boldsymbol{\lambda}_i, \boldsymbol{\mu}_i)$ may thus not exist everywhere. Therefore, the nonpathological derivative of [BC06, Definition 4] is used, which for a function $V(\boldsymbol{x})$ is defined as $\dot{\overline{V}} = \nabla_{\boldsymbol{x}} V^\top \dot{\boldsymbol{x}}$ in the case that V is continuously differentiable. Before analyzing the EIP properties, the properties of a steady state of (5.33) are studied in order to show that it complies with the design requirements for global optimality (5.9).

Proposition 5.9 (local design requirements fulfilled)
Consider system (5.33). *Any equilibrium point* $(\bar{\boldsymbol{x}}_i, \bar{\boldsymbol{\lambda}}_i, \bar{\boldsymbol{\mu}}_i)$ *fulfills the design requirements* (5.9). *Further, it holds that* $\lambda(t) \geq 0 \; \forall t \geq 0$ *if* $\lambda(0) \geq 0$.

Proof. Equations (5.9a), (5.9c) are trivially fulfilled in the equilibria of (5.33). Furthermore, the multiplier λ_{il} is always greater or equal than zero, which can be seen by inspecting the derivative of λ_{il} in (5.33). When the multiplier is zero, the derivative $\dot{\lambda}_{il}$ is either positive or zero, in the case $g_{il}(\bar{\boldsymbol{x}}_i) < 0$. Thus, for any steady state, $\bar{\lambda}_{il} \geq 0$ must hold, which is (5.9d). Condition (5.9b) also follows from the previous argumentation, since $g_{il}(\boldsymbol{x}_i) > 0$ implies λ_{il} is not in an equilibrium. Thus, in all equilibria, it holds either that $\bar{\lambda}_{il} = 0$ and $g_{il}(\bar{\boldsymbol{x}}_i) \leq 0$, or $\bar{\lambda}_{il} \geq 0$ and $g_{il}(\bar{\boldsymbol{x}}_i) = 0$ per design of the algorithm (5.33), which corresponds to (5.9e). □

After showing that all equilibria of the proposed agent dynamics for constrained optimization (5.33) fulfill the global optimality design requirements (5.9), their EIP properties are investigated next.

Proposition 5.10 (EIP properties of constrained agent dynamics)

[52] The notion of solutions for discontinuous dynamic systems is introduced in Section B.3.

Consider the storage function $S_i(\tilde{\boldsymbol{x}}_i, \tilde{\boldsymbol{\lambda}}_i, \tilde{\boldsymbol{\mu}}_i) = \frac{1}{2\alpha_i}\tilde{\boldsymbol{x}}_i^\top \tilde{\boldsymbol{x}}_i + \frac{1}{2}\tilde{\boldsymbol{\lambda}}_i^\top \tilde{\boldsymbol{\lambda}}_i + \frac{1}{2}\tilde{\boldsymbol{\mu}}_i^\top \tilde{\boldsymbol{\mu}}_i$*, with* $\boldsymbol{\lambda}_i = \mathrm{col}\{\lambda_{il}\}$ *and* $\boldsymbol{\mu}_i = \mathrm{col}\{\mu_{ij}\}$*. System* (5.33) *is EIP if the objective function* f_i *is convex, and OFEIP(*$M_{\mathrm{conv},i}$*) if* f_i *is* $M_{\mathrm{conv},i}$*-strongly convex, provided that the constraints* g_{il} *and* h_{ij} *are convex and affine, respectively.*

Proof. The nonpathological derivative of S_i along (5.33) is

$$\dot{\bar{S}}_i = \frac{1}{\alpha_i}\tilde{\boldsymbol{x}}_i^\top \dot{\boldsymbol{x}}_i + \tilde{\boldsymbol{\lambda}}_i^\top \dot{\boldsymbol{\lambda}}_i + \tilde{\boldsymbol{\mu}}_i^\top \dot{\boldsymbol{\mu}}_i. \tag{5.34}$$

Next, inserting $\dot{\boldsymbol{x}}_i$ from (5.33) in (5.34) yields

$$\dot{\bar{S}}_i = \frac{1}{\alpha_i}\tilde{\boldsymbol{x}}_i^\top \big(-\alpha_i \nabla_{\boldsymbol{x}_i} L_i(\boldsymbol{x}_i, \boldsymbol{\lambda}_i) + \alpha_i \boldsymbol{u}_i \big) + \tilde{\boldsymbol{\lambda}}_i^\top \dot{\boldsymbol{\lambda}}_i + \tilde{\boldsymbol{\mu}}_i^\top \dot{\boldsymbol{\mu}}_i. \tag{5.35}$$

Adding $\nabla_{x_i} L_i(\bar{\boldsymbol{x}}_i, \bar{\boldsymbol{\lambda}}_i, \bar{\boldsymbol{\mu}}_i) - \bar{\boldsymbol{u}}_i$, which equals to zero, to (5.35), it results

$$\dot{\bar{S}}_i = \tilde{\boldsymbol{x}}_i^\top \big(-\nabla_{\boldsymbol{x}_i} \tilde{L}_i(\boldsymbol{x}_i, \boldsymbol{\lambda}_i, \boldsymbol{\mu}_i) + \tilde{\boldsymbol{u}}_i \big) + \tilde{\boldsymbol{\lambda}}_i^\top \dot{\boldsymbol{\lambda}}_i + \tilde{\boldsymbol{\mu}}_i^\top \dot{\boldsymbol{\mu}}_i. \tag{5.36}$$

Substituting the Lagrange function and expanding $\tilde{\boldsymbol{x}}_i$ yields

$$\begin{aligned}\dot{\bar{S}}_i = \tilde{\boldsymbol{x}}_i^\top \tilde{\boldsymbol{u}}_i &- \underbrace{\tilde{\boldsymbol{x}}_i^\top \nabla \tilde{f}_i(\boldsymbol{x}_i, \bar{\boldsymbol{x}}_i)}_{\mathrm{(A)}} - \underbrace{\tilde{\boldsymbol{x}}_i^\top \left(\nabla \boldsymbol{g}_i(\boldsymbol{x}_i)^\top \boldsymbol{\lambda}_i - \nabla \boldsymbol{g}_i(\bar{\boldsymbol{x}}_i)^\top \bar{\boldsymbol{\lambda}}_i \right)}_{\mathrm{(B)}} \\ &- \underbrace{\tilde{\boldsymbol{x}}_i^\top \left(\nabla \boldsymbol{h}_i(\boldsymbol{x}_i)^\top \boldsymbol{\mu}_i - \nabla \boldsymbol{h}_i(\bar{\boldsymbol{x}}_i)^\top \bar{\boldsymbol{\mu}}_i \right)}_{\mathrm{(C)}} + \underbrace{\tilde{\boldsymbol{\lambda}}_i^\top \dot{\boldsymbol{\lambda}}_i}_{\mathrm{(D)}} + \underbrace{\tilde{\boldsymbol{\mu}}_i^\top \dot{\boldsymbol{\mu}}_i}_{\mathrm{(E)}},\end{aligned} \tag{5.37}$$

where $\boldsymbol{g}_i : \mathbb{R}^n \to \mathbb{R}^{n_{\mathrm{IC},i}}$ are the stacked functions g_{il}, i.e., $\boldsymbol{g}_i = \mathrm{col}\{g_{il}\}$. The function $\boldsymbol{h}_i : \mathbb{R}^n \to \mathbb{R}^{n_{\mathrm{EQ},i}}$ is defined analogously. Subsequently, it is shown that $-\mathrm{B} + \mathrm{D} \leq 0$ and $-\mathrm{C} + \mathrm{E} = 0$. Hence, $\dot{\bar{S}} \leq \tilde{\boldsymbol{x}}_i^\top \tilde{\boldsymbol{u}}_i - \mathrm{A}$ follows from (5.37), which is identical to (5.19) in Proposition 5.5 and thus the EIP and OFEIP($M_{\mathrm{conv},i}$) properties follow with the same argumentation.

First, it is shown that $-\mathrm{C} + \mathrm{E} = 0$. Inserting $\dot{\boldsymbol{\mu}}_i$ from (5.33) into term E and taking into account that in any equilibrium $\bar{\boldsymbol{x}}_i$, $\boldsymbol{h}_i(\bar{\boldsymbol{x}}_i) = 0$ holds, it results

$$\begin{aligned}\tilde{\boldsymbol{\mu}}_i^\top \boldsymbol{h}_i(\boldsymbol{x}_i) &= \tilde{\boldsymbol{\mu}}_i^\top \boldsymbol{h}_i(\boldsymbol{x}_i) - \tilde{\boldsymbol{\mu}}_i^\top \boldsymbol{h}_i(\bar{\boldsymbol{x}}_i) = \tilde{\boldsymbol{\mu}}_i^\top \tilde{\boldsymbol{h}}_i(\boldsymbol{x}_i, \bar{\boldsymbol{x}}_i) \\ &= \tilde{\boldsymbol{\mu}}_i^\top \boldsymbol{A}_i \tilde{\boldsymbol{x}}_i.\end{aligned} \tag{5.38}$$

Taking into account that $\nabla \boldsymbol{h}_i(\boldsymbol{x}_i) = \boldsymbol{A}_i^\top$, $\boldsymbol{A}_i = \mathrm{col}\{\boldsymbol{a}_{ij}^\top\}$ (as introduced in (5.1)), the term C is identical to (5.38), thus proving

$$-\mathrm{C} + \mathrm{E} = 0. \tag{5.39}$$

W.r.t. term D, both modes are analyzed, i.e., when $\boldsymbol{\lambda}_i = \mathbf{0}$ (mode 1) and $\boldsymbol{g}_i(\boldsymbol{x}_i) < \mathbf{0}$ or when $\boldsymbol{\lambda}_i > \mathbf{0}$ (mode 2), where all operations apply component-wise. In mode 1, $\boldsymbol{\lambda}_i = \mathbf{0}$ holds and the term D becomes

$$\tilde{\boldsymbol{\lambda}}_i^\top \dot{\boldsymbol{\lambda}}_i = 0 = \boldsymbol{\lambda}_i^\top \boldsymbol{g}_i(\boldsymbol{x}_i). \tag{5.40}$$

Adding $-\bar{\boldsymbol{\lambda}}_i^\top \boldsymbol{g}_i(\boldsymbol{x}_i) + \bar{\boldsymbol{\lambda}}_i^\top \boldsymbol{g}_i(\boldsymbol{x}_i)$, which equals to zero, yields

$$\tilde{\boldsymbol{\lambda}}_i^\top \dot{\boldsymbol{\lambda}}_i = \tilde{\boldsymbol{\lambda}}_i^\top \boldsymbol{g}_i(\boldsymbol{x}_i) + \bar{\boldsymbol{\lambda}}_i^\top \boldsymbol{g}_i(\boldsymbol{x}_i) \leq \tilde{\boldsymbol{\lambda}}_i^\top \boldsymbol{g}_i(\boldsymbol{x}_i), \tag{5.41}$$

since $\bar{\boldsymbol{\lambda}}_i \geq 0$ and $\boldsymbol{g}_i(\boldsymbol{x}_i) < 0$, and thus $\bar{\boldsymbol{\lambda}}_i^\top \boldsymbol{g}_i(\boldsymbol{x}_i) \leq 0$. In mode 2, it holds that

$$\tilde{\boldsymbol{\lambda}}_i^\top \dot{\boldsymbol{\lambda}}_i = \tilde{\boldsymbol{\lambda}}_i^\top \boldsymbol{g}_i(\boldsymbol{x}_i), \tag{5.42}$$

and thus it can be concluded that

$$\tilde{\boldsymbol{\lambda}}_i^\top \dot{\boldsymbol{\lambda}}_i \leq \tilde{\boldsymbol{\lambda}}_i^\top \boldsymbol{g}_i(\boldsymbol{x}_i) \tag{5.43}$$

always holds, regardless of the actual mode. Furthermore, adding $-\tilde{\boldsymbol{\lambda}}_i^\top \boldsymbol{g}_i(\bar{\boldsymbol{x}}_i) + \tilde{\boldsymbol{\lambda}}_i^\top \boldsymbol{g}_i(\bar{\boldsymbol{x}}_i)$ to (5.43) yields

$$\tilde{\boldsymbol{\lambda}}_i^\top \dot{\boldsymbol{\lambda}}_i \leq \tilde{\boldsymbol{\lambda}}_i^\top \tilde{\boldsymbol{g}}_i(\boldsymbol{x}_i, \bar{\boldsymbol{x}}_i) + \tilde{\boldsymbol{\lambda}}_i^\top \boldsymbol{g}_i(\bar{\boldsymbol{x}}_i). \tag{5.44}$$

Note that $\tilde{\boldsymbol{\lambda}}_i \boldsymbol{g}_i(\bar{\boldsymbol{x}}_i) = \left(\boldsymbol{\lambda}_i - \bar{\boldsymbol{\lambda}}_i\right) \boldsymbol{g}_i(\bar{\boldsymbol{x}}_i) \leq 0$, since $-\bar{\boldsymbol{\lambda}}_i \boldsymbol{g}_i(\bar{\boldsymbol{x}}_i) = 0$ and $\boldsymbol{\lambda}_i \boldsymbol{g}_i(\bar{\boldsymbol{x}}_i) \leq 0$ (c.f. Proposition 5.9), and thus (5.44) reads

$$\tilde{\boldsymbol{\lambda}}_i^\top \dot{\boldsymbol{\lambda}}_i \leq \left(\boldsymbol{\lambda}_i - \bar{\boldsymbol{\lambda}}_i\right)^\top \tilde{\boldsymbol{g}}_i(\boldsymbol{x}_i, \bar{\boldsymbol{x}}_i). \tag{5.45}$$

Taking into account the fact that the functions $\boldsymbol{g}_i$ are convex and using (3.21), (5.45) can be overestimated by

$$\tilde{\boldsymbol{\lambda}}_i^\top \dot{\boldsymbol{\lambda}}_i \leq \boldsymbol{\lambda}_i^\top \nabla \boldsymbol{g}_i(\boldsymbol{x}_i)^\top \tilde{\boldsymbol{x}}_i - \bar{\boldsymbol{\lambda}}_i^\top \nabla \boldsymbol{g}_i(\bar{\boldsymbol{x}}_i)^\top \tilde{\boldsymbol{x}}_i,$$

and factorizing $\tilde{\boldsymbol{x}}_i$ yields

$$\tilde{\boldsymbol{\lambda}}_i^\top \dot{\boldsymbol{\lambda}}_i \leq \tilde{\boldsymbol{x}}_i^\top \left(\nabla \boldsymbol{g}_i(\boldsymbol{x}_i) \boldsymbol{\lambda}_i - \nabla \boldsymbol{g}_i(\bar{\boldsymbol{x}}_i) \bar{\boldsymbol{\lambda}}_i\right). \tag{5.46}$$

Define the right-hand side of (5.46) as term $\tilde{\mathrm{D}}$, which is equal to term $-\mathrm{B}$. Note that $\mathrm{D} \leq \tilde{\mathrm{D}}$ and thus

$$-\mathrm{B} + \mathrm{D} \leq -\mathrm{B} + \tilde{\mathrm{D}} = 0. \tag{5.47}$$

With (5.39) and (5.47), it has been shown for (5.37) that

$$\dot{\bar{S}}_i \leq \tilde{\boldsymbol{y}}_i^\top \tilde{\boldsymbol{u}}_i - \tilde{\boldsymbol{y}}_i^\top \nabla \tilde{f}_i(\boldsymbol{y}_i, \bar{\boldsymbol{y}}_i),$$

holds, which completes the proof. □

Having specified agent dynamics for different optimization cases and investigating their EIP properties, the dynamics for the controller systems are considered next.

5.3.3 Controller Dynamics

For the controller systems, consider the integrator with feedthrough

$$\Pi_k : \begin{aligned} \dot{\boldsymbol{z}}_k &= \beta_k \boldsymbol{\zeta}_k \\ \boldsymbol{d}_k &= \boldsymbol{z}_k + \beta_k \boldsymbol{\zeta}_k. \end{aligned} \tag{5.48}$$

The controller dynamics (5.48) with $\beta_k \in \mathbb{R}_{>0}$ are chosen in that form since they then are a system with integral action as in Definition 5.1, and thus $\bar{\boldsymbol{\zeta}}_k = \mathbf{0}$, as required for an optimal steady state by Theorem 5.1 and 5.2. In addition, (5.48) is EIO. In the next proposition, the EIP properties of (5.48) are established.

Proposition 5.11 (EIP properties of controller systems)
Consider the storage function $W_k(\tilde{\boldsymbol{z}}_k) = \frac{1}{2\beta_k} \tilde{\boldsymbol{z}}_k^\top \tilde{\boldsymbol{z}}_k$. *System* (5.48) *is IFEIP(β_k) for any* $\beta_k > 0$.

Proof. Consider the time derivative of the storage function W_k and insert the system dynamics of (5.48) to obtain

$$\dot{W}_k = \frac{1}{\beta_k} \tilde{\boldsymbol{z}}_k^\top \dot{\boldsymbol{z}}_k \tag{5.49}$$

$$= \frac{1}{\beta_k} \tilde{\boldsymbol{z}}_k^\top \beta_k \boldsymbol{\zeta}_k. \tag{5.50}$$

Next, subtracting the equilibrium $0 = \tilde{\boldsymbol{z}}_k^\top \bar{\boldsymbol{\zeta}}_k$ on the right-hand side yields

$$\begin{aligned} \dot{W}_k &= \tilde{\boldsymbol{z}}_k^\top \boldsymbol{\zeta}_k - \tilde{\boldsymbol{z}}_k^\top \bar{\boldsymbol{\zeta}}_k \\ &= \tilde{\boldsymbol{z}}_k^\top \tilde{\boldsymbol{\zeta}}_k \\ &= \tilde{\boldsymbol{d}}_k^\top \tilde{\boldsymbol{\zeta}}_k - \beta_k \tilde{\boldsymbol{\zeta}}_k^\top \tilde{\boldsymbol{\zeta}}_k, \end{aligned} \tag{5.51}$$

where the output equation of the system dynamics (5.48) is used in the last equation. Note that (5.51) verifies the IFEIP(β_k) property with $\beta_k > 0$. □

Remark 5.8. *If the feedthrough in the output equation of* (5.48) *is eliminated,* (5.48) *is merely EIP instead of IFEIP(β_k), which directly follows from the proof of Proposition 5.11.*

Remark 5.9. *Note that the controller dynamics* (5.48) *are a special case of the agent dynamics* (5.20) *with* $\gamma_i = \alpha_i = \beta_k$ *and the objective function* $f_i = 0$. *However, Proposition 5.11 is stated here because it allows to state less conservative results compared to Proposition 5.7, since there several over- and underestimations of the (nonlinear) objective function using the Lipschitz constant and the strong convexity index were required.*

In this section, different agent and controller dynamics have been proposed and their EIP properties have been analyzed. The proposed agent dynamics exhibit OFEIP and IFEIP properties and are capable of handling private, convex constraints. Furthermore, it has been shown that the design requirements of Theorems 5.1 and 5.2 are fulfilled with the proposed systems, thus ensuring globally optimal equilibria. In the next sections, milder conditions for convergence to these equilibria using a similar reasoning as in Theorem 5.4 are developed.

5.4 Convergence for Undirected Communication Topologies

In this section, the convergence of the closed-loop system in Figure 5.1 is analyzed for both unconstrained and constrained optimization with undirected communication topologies. It is shown that Theorem 5.4 can be applied with the dynamics proposed in Section 5.3. Furthermore, it is demonstrated that less restrictive convergence requirements can be obtained when the admissible agent and controller dynamics are narrowed to the ones proposed in Section 5.3.

The case of unconstrained optimization is covered in Section 5.4.1, and constrained optimization in Section 5.4.2.

5.4.1 Unconstrained Optimization

In Section 5.3, it has been shown that the agent dynamics (5.16), (5.20), and (5.33) are OFEIP with an excess of passivity if the objective function of the agent is strongly convex (see Propositions 5.5, 5.7 and 5.10).[53] In this case, with any of the controller systems proposed in Section 5.3, convergence to the global optimizer directly follows from Theorem 5.4. In some applications, however, the agents may only have convex objective functions, thus having EIP but no OFEIP dynamics according to Propositions 5.5, 5.7 and 5.10. In the following theorem, it is shown that for the unconstrained problem and an undirected communication topology, the proposed agent and controller dynamics from Section 5.3 achieve still achieve convergence requiring only convex (and not *strongly* convex) objective functions, provided that the sum of all objective functions is strictly convex.

Theorem 5.12 (convergence without strong convexity)
Let the agents $i \in \mathcal{A}$ and controller systems $k \in \mathcal{C}$ obey the dynamics (5.16)

[53] Note that the assumption of strongly convex functions is widely adopted in the literature (see, e.g., [LCH20; LSL20; KCM15]).

and (5.48)*, respectively, and let Propositions 5.5 and 5.11 hold. Further, let the agents be interconnected by a symmetric communication topology* (5.10) *fulfilling property* (5.11)*. Then, all trajectories converge to an equilibrium point in the invariant manifold $\mathcal{M}_{\text{eq}}$ as specified in Theorem 5.1, if the objective functions of the agents $f_i : \mathbb{R}^n \to \mathbb{R}$ are convex and the sum of all objective functions is strictly convex.*

Proof. Consider the network-wide Lyapunov function (5.13) and the time derivative

$$\dot{V} \leq \sum_{i\in\mathcal{A}} \left(\tilde{\boldsymbol{u}}_i^\top \tilde{\boldsymbol{y}}_i - \Psi_i(\tilde{\boldsymbol{y}}_i) \right) + \sum_{k\in\mathcal{C}} \left(\tilde{\boldsymbol{\zeta}}_k^\top \tilde{\boldsymbol{d}}_k - \nu_k \boldsymbol{\zeta}_k^\top \boldsymbol{\zeta}_k \right), \tag{5.52}$$

where Corollary 5.6 is used for the derivative of the agent systems. In network variables, (5.52) reads

$$\begin{aligned} \dot{V} &\leq \tilde{\boldsymbol{u}}^\top \tilde{\boldsymbol{y}} - \sum_{i\in\mathcal{A}} \Psi_i(\tilde{\boldsymbol{y}}_i) + \tilde{\boldsymbol{\zeta}}^\top \tilde{\boldsymbol{d}} - \tilde{\boldsymbol{\zeta}}^\top \left(\operatorname{diag}\{\nu_k\} \otimes \boldsymbol{I}_n \right) \tilde{\boldsymbol{\zeta}} \\ &= -\sum_{i\in\mathcal{A}} \Psi_i(\tilde{\boldsymbol{y}}_i) - \tilde{\boldsymbol{y}}^\top \boldsymbol{K} \tilde{\boldsymbol{y}}, \end{aligned} \tag{5.53}$$

where the last equality follows by inserting the interconnection topology (5.4) into the first, third and fourth term, and introducing $\boldsymbol{K} = (\boldsymbol{E} \otimes \boldsymbol{I}_n) \left(\operatorname{diag}\{\nu_k\} \otimes \boldsymbol{I}_n \right) (\boldsymbol{E} \otimes \boldsymbol{I}_n)^\top$. The first term in (5.53) is positive semidefinite, since every $\Psi_i(\tilde{\boldsymbol{y}}_i)$ is nonnegative when $f_i : \mathbb{R}^n \to \mathbb{R}$ is convex, see Corollary 5.6. Furthermore, the first term in (5.53) is positive definite when all $\tilde{\boldsymbol{y}}_i$, $i \in \mathcal{A}$ are in consensus. To show that, assume that the agents are in consensus, i.e., $\tilde{\boldsymbol{y}}_i = \tilde{\boldsymbol{y}}_\text{c} \forall i \in \mathcal{A}$, and since $\mathbf{y}^*$ is unique due to strict convexity of the sum of all f_i, it holds that

$$\sum_{i\in\mathcal{A}} \Psi_i(\tilde{\boldsymbol{y}}_i) = \tilde{\boldsymbol{y}}_\text{c}^\top \Big(\sum_{i\in\mathcal{A}} \nabla f_i(\boldsymbol{y}_\text{c}) - \sum_{i\in\mathcal{A}} \nabla f_i(\bar{\boldsymbol{y}}_\text{c}) \Big),$$

which is positive for all $\boldsymbol{y}_\text{c}$ other than $\mathbf{y}^*$, if the sum of all objective functions is strictly convex (see condition (3.20)), as required in the theorem. The second term $\tilde{\boldsymbol{y}}^\top \boldsymbol{K} \tilde{\boldsymbol{y}}$ in (5.53) is nonnegative, and positive whenever $\tilde{\boldsymbol{y}}_i$ are not in consensus. This is because the matrix $\boldsymbol{K}$ is positive semidefinite, and $\tilde{\boldsymbol{y}}^\top \boldsymbol{K} \tilde{\boldsymbol{y}} = 0$ is equivalent to $(\boldsymbol{E} \otimes \boldsymbol{I}_n)^\top \tilde{\boldsymbol{y}} = \mathbf{0}$ [HJ12, Observation 7.1.6]. With Proposition B.1, it holds that $\tilde{\boldsymbol{y}}^\top \boldsymbol{K} \tilde{\boldsymbol{y}} = 0$ if and only if $\tilde{\boldsymbol{y}}_i$, $i \in \mathcal{A}$ are in consensus. Thus, (5.53) is nonpositive, being zero only if the agents are at the optimizer and at consensus, i.e., $\boldsymbol{y}_i = \mathbf{y}^*$, $i \in \mathcal{A}$, which also is the definition of the manifold $\mathcal{M}_{\text{eq}}$ in Theorem 5.1. Thus, it can be concluded that the output $\boldsymbol{y}_i$ of all agents converge to an equilibrium in $\mathcal{M}_{\text{eq}}$. Furthermore, with the EIO of the Σ_i systems, the states $\boldsymbol{x}_i$ are also constant. Since in the equilibrium manifold $\mathcal{M}_{\text{eq}}$ the outputs of the agents $\boldsymbol{y}_i$ are in consensus, it holds with (5.4a) and Proposition B.1 in the Appendix B.2 that $\boldsymbol{\zeta}_k = \mathbf{0}$, and thus also $\dot{\boldsymbol{z}}_k = \mathbf{0}$, which means that all $\bar{\boldsymbol{z}}_k$, and thus $\bar{\boldsymbol{d}}_k$, are constant. □

5.4.2 Constrained Optimization

In this subsection, the convergence behavior for constrained optimization using the discontinuous agent dynamics (5.33) with undirected communication structures is investigated. In this case, Theorem 5.4 is only applicable under Assumption 5.1. Thus, the closed-loop networked system (see Figure 5.1) is analyzed to ensure that appropriate solutions exists, i.e., that Assumption 5.1 holds. Afterwards, similar steps as in Theorem 5.12 are followed for the unconstrained case to show via Lyapunov theory that the convergence of all solutions to the global optimizer $\mathbf{y}^*$ requires only the sum of all objective functions to be strictly convex.

The closed-loop system is composed of agent systems (5.33) and controller systems (5.48) interconnected by a generalized communication structure (5.10), i.e.,

$$\dot{\boldsymbol{x}} = -\boldsymbol{\alpha}_\circ \nabla_{\boldsymbol{x}} \boldsymbol{L}(\boldsymbol{x}, \boldsymbol{\lambda}, \boldsymbol{\mu}) - \boldsymbol{\alpha}_\circ (\boldsymbol{R} \otimes \boldsymbol{I}_n) \boldsymbol{d} \tag{5.54a}$$

$$\dot{\boldsymbol{\lambda}} = \begin{cases} \boldsymbol{0} & \text{if } \boldsymbol{\lambda} = \boldsymbol{0} \text{ and } \boldsymbol{g}(\boldsymbol{x}) < \boldsymbol{0} \\ \boldsymbol{g}(\boldsymbol{x}) & \text{otherwise} \end{cases} \tag{5.54b}$$

$$\dot{\boldsymbol{\mu}} = \boldsymbol{h}(\boldsymbol{x}) \tag{5.54c}$$

$$\dot{\boldsymbol{z}} = \boldsymbol{\beta}_\circ (\boldsymbol{R} \otimes \boldsymbol{I}_n)^\top \boldsymbol{y}, \tag{5.54d}$$

with the outputs $\boldsymbol{y} = \boldsymbol{x}$ and $\boldsymbol{d} = \boldsymbol{z} + \boldsymbol{\beta}_\circ (\boldsymbol{R} \otimes \boldsymbol{I}_n)^\top \boldsymbol{y}$. The variables $\boldsymbol{x}$, $\boldsymbol{\lambda}$, $\boldsymbol{\mu}$, $\boldsymbol{z}$, and functions $\boldsymbol{L} : \mathbb{R}^{n_{\mathcal{A}} \cdot n} \times \mathbb{R}^{n_{\text{EQ}}} \times \mathbb{R}^{n_{\text{IC}}} \to \mathbb{R}^{n_{\mathcal{A}} \cdot n}$, $\boldsymbol{g} : \mathbb{R}^{n_{\mathcal{A}} \cdot n} \to \mathbb{R}^{n_{\text{IC}}}$, $\boldsymbol{h} : \mathbb{R}^{n_{\mathcal{A}} \cdot n} \to \mathbb{R}^{n_{\text{EQ}}}$ are network variables and functions, respectively, i.e., $\boldsymbol{x} = \text{col}\{\boldsymbol{x}_i\} \in \mathbb{R}^{n_{\mathcal{A}} \cdot n}$ and $\boldsymbol{L} = \text{col}\{L_i\}$, $i \in \mathcal{A}$. The variables $\boldsymbol{\alpha}_\circ$ and $\boldsymbol{\beta}_\circ$ are diagonal matrices, i.e., $\boldsymbol{\alpha}_\circ = \boldsymbol{\alpha} \otimes \boldsymbol{I}_n$ and $\boldsymbol{\alpha} = \text{diag}\{\alpha_i\}$.[54] In (5.54b), the operations apply component-wise. Note that the closed-loop system is a dynamic system with discontinuous right-hand side due to (5.54b). For such systems, the existence of a solution is not ensured by classical theorems, since the vector field is not locally Lipschitz. Instead, the existence of solutions has to be studied for each specific system before the properties of their solutions are analyzed [Cor08]. In the following, existence, uniqueness and continuity w.r.t. initial states of the solution of (5.54) is proven. For that, similar arguments as in [CMC16] are followed leveraging the theory of projected dynamic systems, which are a special type of dynamic systems with discontinuous right-hand side. For projected dynamic systems, there exist useful results about the existence of solutions, see Appendix B.4. The following proposition shows that the closed-loop system (5.54) can be cast as such a projected dynamic system.

Proposition 5.13 (equivalence with projected dynamic system)
The discontinuous system (5.54) *can be written as a projected dynamic system.*

[54] Note that the notation with the circle as a subscript has been introduced in Section 1.2 and is used in the rest of this chapter without further explanation.

Proof. The proof consists of finding a continuous vector field and a closed convex set $\mathcal{K}$ such that the projected dynamic system defined thereby is equal to system (5.54). Consider the vector field

$$\boldsymbol{\phi}(\boldsymbol{x}, \boldsymbol{\lambda}, \boldsymbol{\mu}, \boldsymbol{z}) = \begin{bmatrix} -\boldsymbol{\alpha}_\circ \nabla_{\boldsymbol{x}} L - \boldsymbol{\alpha}_\circ (\boldsymbol{R} \otimes \boldsymbol{I}_n) \boldsymbol{z} \\ \boldsymbol{g}(\boldsymbol{x}) \\ \boldsymbol{h}(\boldsymbol{x}) \\ \boldsymbol{\beta}_\circ (\boldsymbol{R} \otimes \boldsymbol{I}_n)^\top \boldsymbol{x} \end{bmatrix}, \tag{5.55}$$

which is a version of (5.54) without the discontinuity at $\boldsymbol{\lambda} = \mathbf{0}$, and the closed and convex set $\mathcal{K} = \mathbb{R}^{n_{\mathcal{A}} \cdot n} \times \mathbb{R}^{n_{\text{IC}}}_{\geq 0} \times \mathbb{R}^{n_{\text{EQ}}} \times \mathbb{R}^{n_{\mathcal{C}} \cdot n}$. Observe that the set $\mathcal{K}$ excludes negative Lagrange multipliers $\boldsymbol{\lambda}$, understood to be component-wise. Next, consider the projected dynamic system

$$\begin{bmatrix} \dot{\boldsymbol{x}}^\diamond \\ \dot{\boldsymbol{\lambda}}^\diamond \\ \dot{\boldsymbol{\mu}}^\diamond \\ \dot{\boldsymbol{z}}^\diamond \end{bmatrix} = \boldsymbol{\Gamma}_{\mathcal{K}}(\boldsymbol{\phi}((\boldsymbol{x}^\diamond, \boldsymbol{\lambda}^\diamond, \boldsymbol{\mu}^\diamond, \boldsymbol{z}^\diamond)), (\boldsymbol{x}^\diamond, \boldsymbol{\lambda}^\diamond, \boldsymbol{\mu}^\diamond, \boldsymbol{z}^\diamond)). \tag{5.56}$$

The notation with a diamond in the superscript is chosen for the projected dynamic system in order to distinguish it from the discontinuous dynamic system (5.54). Note that as per Proposition B.4, Case (i), in the interior of $\mathcal{K}$, i.e., when $\boldsymbol{\lambda}^\diamond > 0$, the projection is not active and (5.56) is identical to (5.54), i.e., $\dot{\boldsymbol{\lambda}}^\diamond = \boldsymbol{g}(\boldsymbol{x}^\diamond)$. Thus, (5.56) has to be investigated only at the boundary of $\mathcal{K}$ by comparing it with (5.54). Note that the boundary of $\mathcal{K}$ is also where the discontinuity in (5.54) is. On the boundary of $\mathcal{K}$, some Lagrange multipliers are zero, i.e., $\lambda_q^\diamond = \mathbf{0}$, with $q \in \mathcal{I}$, where $\mathcal{I} \subseteq \mathcal{C}_{\text{in}}$ is the set of multipliers that are zero. For these multipliers on the boundary of $\mathcal{K}$, either $g_q(\boldsymbol{x}^\diamond) \geq 0$ or $g_q(\boldsymbol{x}^\diamond) < 0$ holds. In case of $g_q(\boldsymbol{x}^\diamond) \geq 0$, note that the vector field points inwards into $\mathcal{K}$ and thus the projection is not active. In this case, (5.54) has no discontinuity, and thus it holds $\dot{\lambda}_q^\diamond = g_q(\boldsymbol{x}^\diamond)$ in (5.56) and $\dot{\lambda}_q = g_q(\boldsymbol{x})$ in (5.54), which is equal in both systems. When $g_q(\boldsymbol{x}^\diamond) < 0$, the vector field points outwards perpendicular to the boundary of $\mathcal{K}$, and due to Remark B.1, in such a case the vector projection onto $\mathcal{K}$ is zero, i.e., $\dot{\lambda}_q^\diamond = 0$. For (5.54), in case that $g_q(\boldsymbol{x}) < 0$, it holds that $\dot{\lambda}_q = \mathbf{0}$, which is again identical to the projected system. This completes the proof. □

With Proposition 5.13, Proposition B.5 in Appendix B.4, and by assuming that all functions f_i, g_{il} and h_{ij} are Lipschitz, it can be concluded that the closed-loop system (5.54) has a unique continuous solution which is continuous w.r.t. the initial state. Consequently, the stability properties of the system trajectories can now be studied. For that, Lyapunov theory for systems with discontinuous right-hand side is used, in particular the invariance principle for Carathéodory systems proposed in [BC06].

Theorem 5.14 (convergence constrained optimization)

Let the agents and controller systems obey the dynamics (5.33) *and* (5.48)*, respectively, let Propositions 5.10 and 5.11 hold, and let the systems be interconnected by* (5.4)*. Then, the equilibrium $\bar{\boldsymbol{y}}_i = \mathbf{y}^*$, $i \in \mathcal{A}$ is globally asymptotically stable, if the sum of all objective functions $f_i : \mathbb{R}^n \to \mathbb{R}$, $i \in \mathcal{A}$ is strictly convex, f_i and g_i are Lipschitz, and $\lambda_{il}(0) \geq 0$.*

Proof. Consider the Lyapunov function (5.13) and its time derivative

$$\dot{\bar{V}} = \sum_{i \in \mathcal{A}} \dot{\bar{S}}_i + \sum_{k \in \mathcal{C}} \dot{W}_k \tag{5.57}$$

which holds for almost every $t \in [0, \infty)$, [BC06]. Note that the agent dynamics (5.33) are dissipative w.r.t. the same supply rate as the agent dynamics (5.16) as per Proposition 5.10. Thus, with identical arguments as in the derivation of the inequality (5.53), it holds for (5.57)

$$\dot{\bar{V}} = \sum_{i \in \mathcal{A}} \dot{\bar{S}}_i + \sum_{k \in \mathcal{C}} \dot{W}_k \leq - \sum_{i \in \mathcal{A}} \Psi_i(\tilde{\boldsymbol{y}}_i) - \tilde{\boldsymbol{y}}^\top \boldsymbol{K} \tilde{\boldsymbol{y}}, \tag{5.58}$$

where $\boldsymbol{K} = (\boldsymbol{E} \otimes \boldsymbol{I}_n) \left(\operatorname{diag}\{\nu_k\} \otimes \boldsymbol{I}_n\right) (\boldsymbol{E} \otimes \boldsymbol{I}_n)^\top$. With the invariance principle in [BC06, Proposition 3], all trajectories converge to the largest invariant set in the set $\{(\boldsymbol{x}, \boldsymbol{\lambda}, \boldsymbol{\mu}, \boldsymbol{z}) \in \mathbb{R}^{n_{\mathcal{A}} \cdot n \times n_{\mathcal{C}} \cdot n \times n_{\text{EQ}} \times n_{\text{IC}}} \mid \dot{\bar{V}} = 0\}$. With the same reasoning as in Theorem 5.12, it can be concluded that all trajectories are bounded and converge to $\mathcal{M}_{\text{eq}}$. Since the sum of all objective functions is strictly convex, the minimizer is unique [BV04] and thus $\boldsymbol{\lambda} = \boldsymbol{\lambda}^*$ and $\boldsymbol{\mu} = \boldsymbol{\mu}^*$ at steady state. Since all $\tilde{\boldsymbol{y}}_i$ are in consensus, the states $\boldsymbol{z}$ and outputs $\boldsymbol{d}$ are constant. □

Note that inequality (5.58) is fulfilled when using any agent dynamics (5.16), (5.20) and (5.33), since they have structurally identical EIP properties. Thus, convergence is ensured even when agents use different system dynamics (5.16), (5.20) or (5.33) with convex functions, or other dynamics as long as these dynamics are OFEIP(ρ_i) and the design requirements from Theorem 5.1 or 5.2 hold.

5.5 Convergence for Directed Communication Topologies

In this section, the unconstrained problem in which agents and controllers are connected via a directed communication structure is considered. First, it is shown that such a directed communication structure hampers obtaining convergence results as in the previous sections. Afterwards, convergence results are derived that require, in contrast

to the case of undirected communication, verifying a global linear matrix inequality to ensure convergence.

Consider a set $\mathcal{A}$ of agents Σ_i, $i \in \mathcal{A}$ and a set $\mathcal{C}$ of controllers Π_k, $k \in \mathcal{C}$. Assume the agent dynamics are OFEIP(ρ_i) and the controller dynamics IFEIP(ν_k). Consider a Lyapunov function (5.13) as in Theorem 5.12. Using the OFEIP(ρ_i) and IFEIP(ν_k) properties, the time derivative of the Lyapunov function in network variables is

$$\dot{V} \leq \tilde{\boldsymbol{u}}^\top \tilde{\boldsymbol{y}} - \tilde{\boldsymbol{y}}^\top (\boldsymbol{\rho}_{\mathcal{A}} \otimes \boldsymbol{I}_n) \tilde{\boldsymbol{y}} + \tilde{\boldsymbol{\zeta}}^\top \tilde{\boldsymbol{d}} - \tilde{\boldsymbol{\zeta}}^\top (\boldsymbol{\nu}_{\mathcal{C}} \otimes \boldsymbol{I}_n) \tilde{\boldsymbol{\zeta}}, \tag{5.59}$$

with $\boldsymbol{\rho}_{\mathcal{A}} = \operatorname{diag}\{\rho_i\}$ and $\boldsymbol{\nu}_{\mathcal{C}} = \operatorname{diag}\{\nu_k\}$. Inserting the directed interconnection structure (5.12) into (5.59) yields

$$\dot{V} \leq -\frac{1}{2} \begin{bmatrix} \tilde{\boldsymbol{y}} \\ \tilde{\boldsymbol{d}} \end{bmatrix}^\top \begin{bmatrix} 2\boldsymbol{K} & (\boldsymbol{R}_{\mathcal{C}} - \boldsymbol{R}_{\mathcal{A}}) \\ (\boldsymbol{R}_{\mathcal{C}} - \boldsymbol{R}_{\mathcal{A}})^\top & \boldsymbol{0} \end{bmatrix} \otimes \boldsymbol{I}_n \begin{bmatrix} \tilde{\boldsymbol{y}} \\ \tilde{\boldsymbol{d}} \end{bmatrix}, \tag{5.60}$$

with $\boldsymbol{K} = \boldsymbol{\rho}_{\mathcal{A}} + \boldsymbol{R}_{\mathcal{A}} \boldsymbol{\nu}_{\mathcal{C}} \boldsymbol{R}_{\mathcal{A}}^\top$. Note that the matrix in (5.60) is indefinite if $\boldsymbol{R}_{\mathcal{A}} \neq \boldsymbol{R}_{\mathcal{C}}$ since it is a so-called saddle-point matrix [BGL05], and thus fails to prove asymptotic stability.[55] To provide remedy, the zero block in the bottom right of the matrix in (5.60) needs to be replaced by at least a positive semidefinite matrix in order to achieve positive semidefiniteness. This can be accomplished either by requiring the agent dynamics to possess, in addition to the OFEIP(ρ_i) property, an IFEIP(ν_i) property, or by requiring the controller dynamics to be OFEIP(ρ_k) as well as IFEIP(ν_k). Then, the matrix becomes

$$\begin{bmatrix} 2\boldsymbol{K} & (\boldsymbol{R}_{\mathcal{C}} - \boldsymbol{R}_{\mathcal{A}}) \\ (\boldsymbol{R}_{\mathcal{C}} - \boldsymbol{R}_{\mathcal{A}})^\top & 2\boldsymbol{L} \end{bmatrix}, \tag{5.61}$$

with $\boldsymbol{L} = \boldsymbol{\rho}_{\mathcal{C}} + \boldsymbol{R}_{\mathcal{C}}^\top \boldsymbol{\nu}_{\mathcal{A}} \boldsymbol{R}_{\mathcal{C}}$ and $\boldsymbol{\rho}_{\mathcal{C}}$, $\boldsymbol{\nu}_{\mathcal{A}}$ analogously to $\boldsymbol{\rho}_{\mathcal{A}}$ in (5.60). Since an OFEIP(ρ_k) property for the controller systems would prevent the systems having integral action as in Definition 5.1, which is instrumental for achieving global optimality, the only option is to require the agent dynamics to be IFEIP(ν_i). In (5.20), a system which is IF-OFEIP(ν_i, ρ_i) is proposed. This system is used in the next theorem to establish convergence to the global optimizer. Consider a group of agents (5.20) and controllers (5.48) without feedthrough as in Remark 5.8 interconnected by a directed, non-symmetric communication structure (5.12)

$$\dot{\boldsymbol{x}} = -\boldsymbol{\alpha}_\circ \nabla f(\boldsymbol{x} + \boldsymbol{\gamma}_\circ \boldsymbol{u}) - \boldsymbol{\alpha}_\circ (\boldsymbol{R}_{\mathcal{C}} \otimes \boldsymbol{I}_n) \boldsymbol{d} \tag{5.62a}$$

$$\dot{\boldsymbol{z}} = \boldsymbol{\beta}_\circ (\boldsymbol{R}_{\mathcal{A}} \otimes \boldsymbol{I}_n)^\top \boldsymbol{y}, \tag{5.62b}$$

with $\boldsymbol{y} = \boldsymbol{x} + \boldsymbol{\gamma}\boldsymbol{u}$, $\boldsymbol{\gamma} = \operatorname{diag}\{\gamma_i\}$, $\boldsymbol{d} = \boldsymbol{z}$ and $\boldsymbol{u} = -(\boldsymbol{R}_{\mathcal{C}} \otimes \boldsymbol{I}_n) \boldsymbol{d}$, and $\boldsymbol{\alpha}_\circ, \boldsymbol{\beta}_\circ$ as in (5.54).

Theorem 5.15 (convergence with directed communication topology)

[55] Note that the Kronecker product with $\boldsymbol{I}_n$ does not alter the definiteness of the matrix.

Consider the closed-loop system (5.62)*. Let the dynamics of the agents $i \in \mathcal{A}$ and controllers $k \in \mathcal{C}$ fulfill Propositions 5.7 and 5.11, respectively. Assume that the matrices $\boldsymbol{R}_\mathcal{A}$ and $\boldsymbol{R}_\mathcal{C}$ of the non-symmetric communication structure* (5.12) *fulfill property* (5.11)*. Then, the equilibrium $\bar{\boldsymbol{y}}_i = \mathbf{y}^*$, $i \in \mathcal{A}$ is a globally asymptotically stable equilibrium point of the closed-loop system* (5.62)*, if the singular matrix*

$$\begin{bmatrix} 2\boldsymbol{K} & (\boldsymbol{R}_\mathcal{C} - \boldsymbol{R}_\mathcal{A}) \\ (\boldsymbol{R}_\mathcal{C} - \boldsymbol{R}_\mathcal{A})^\top & 2\boldsymbol{L} \end{bmatrix}, \tag{5.63}$$

with $\boldsymbol{K} = \boldsymbol{\rho}_\mathcal{A}$ and $\boldsymbol{L} = \boldsymbol{R}_\mathcal{C}^\top \nu_\mathcal{A} \boldsymbol{R}_\mathcal{C}$, is positive semidefinite and the matrix $\boldsymbol{\beta}\boldsymbol{R}_\mathcal{A}^\top \boldsymbol{K}^{-1} \tilde{\boldsymbol{R}}$, with $\tilde{\boldsymbol{R}} = \boldsymbol{R}_\mathcal{C} - \boldsymbol{R}_\mathcal{A}$ and $\boldsymbol{\beta} = \operatorname{diag}\{\beta_k\}$, has eigenvalues which are either zero or have a positive real part.

Proof. Since the agent dynamics (5.20) are IF-OFEIP(ν_i, ρ_i) as in Proposition 5.7 and the controller dynamics (5.48) are EIP, the derivative of the Lyapunov function (5.13) is

$$\dot{V} \leq -\frac{1}{2} \begin{bmatrix} \tilde{\boldsymbol{y}} \\ \tilde{\boldsymbol{d}} \end{bmatrix}^\top \begin{bmatrix} 2\boldsymbol{K} & \boldsymbol{R}_\mathcal{C} - \boldsymbol{R}_\mathcal{A} \\ (\boldsymbol{R}_\mathcal{C} - \boldsymbol{R}_\mathcal{A})^\top & 2\boldsymbol{L} \end{bmatrix} \otimes \boldsymbol{I}_n \begin{bmatrix} \tilde{\boldsymbol{y}} \\ \tilde{\boldsymbol{d}} \end{bmatrix}, \tag{5.64}$$

with $\boldsymbol{K}$ and $\boldsymbol{L}$ as stated in the theorem. Since it is required by the theorem that the matrix in (5.64) is positive semidefinite, $\dot{V} \leq 0$ holds and boundedness of the trajectories is guaranteed. For proving that all trajectories converge to the set $\mathcal{M}_\text{eq}$, Lasalle's Invariance Principle is invoked. The proof consists of showing that the trajectory converges to a point, i.e., there are no persistent oscillations. Since all equilibria are in the set $\mathcal{M}_\text{eq}$ as per Theorem (5.1), it suffices to show that the convergence is to a point.

Denote $\boldsymbol{v}^\top = (\tilde{\boldsymbol{y}}^\top, \tilde{\boldsymbol{d}}^\top)$ and $\boldsymbol{U}$ the matrix in (5.64). Note that a vector $\boldsymbol{v} \in \mathbb{R}^{(n_\mathcal{A}+n_\mathcal{C})n}$ corresponds to the set $\mathcal{L} = \{(\boldsymbol{x}, \boldsymbol{z}) \in \mathbb{R}^{(n_\mathcal{A}+n_\mathcal{C})n} \mid \dot{V} = 0\}$ if and only if $\boldsymbol{v}^\top \boldsymbol{U} \boldsymbol{v} = 0$ holds. To inspect which vectors $\boldsymbol{v}$ belong to the set $\mathcal{L}$, consider first

$$\frac{1}{2}\boldsymbol{v}^\top \boldsymbol{U} \boldsymbol{v} = \tilde{\boldsymbol{y}}^\top \boldsymbol{K}_\circ \tilde{\boldsymbol{y}} + \tilde{\boldsymbol{y}}^\top \left((\boldsymbol{R}_\mathcal{C} - \boldsymbol{R}_\mathcal{A}) \otimes \boldsymbol{I}_n\right) \tilde{\boldsymbol{d}} + \tilde{\boldsymbol{d}}^\top \boldsymbol{L}_\circ \tilde{\boldsymbol{d}}, \tag{5.65}$$

where $\boldsymbol{K}_\circ = \boldsymbol{K} \otimes \boldsymbol{I}_n$ and $\boldsymbol{L}_\circ = \boldsymbol{L} \otimes \boldsymbol{I}_n$ for convenience. With [HJ12, Observation 7.1.6], it holds that $\boldsymbol{v}^\top \boldsymbol{U} \boldsymbol{v} = 0$ if and only if $\boldsymbol{U}\boldsymbol{v} = \mathbf{0}$. The first equation in $\boldsymbol{U}\boldsymbol{v} = \mathbf{0}$, i.e,

$$\boldsymbol{K}_\circ \tilde{\boldsymbol{y}} + \left((\boldsymbol{R}_\mathcal{C} - \boldsymbol{R}_\mathcal{A}) \otimes \boldsymbol{I}_n\right) \tilde{\boldsymbol{d}} = \mathbf{0}, \tag{5.66}$$

relates the output of agents and controllers in the set $\mathcal{L}$. Solving (5.66) w.r.t. $\tilde{\boldsymbol{y}}$ and inserting it in the system dynamics (5.62b) of the controllers, it results

$$\dot{\tilde{\boldsymbol{d}}} = \dot{\tilde{\boldsymbol{z}}} = -\boldsymbol{\beta} \left(\boldsymbol{R}_\mathcal{A}^\top \otimes \boldsymbol{I}_n\right) \boldsymbol{K}_\circ^{-1} \left((\boldsymbol{R}_\mathcal{C} - \boldsymbol{R}_\mathcal{A}) \otimes \boldsymbol{I}_n\right) \tilde{\boldsymbol{d}}, \tag{5.67}$$

which describes the dynamics in $\mathcal{L}$. Thus, it suffices to show that the output $\boldsymbol{d}$ and state $\boldsymbol{z}$ in (5.67) converge to a steady state. Note that the system matrix in (5.67) does not have full rank and thus cannot be Hurwitz. However, if the matrix in (5.67) has only eigenvalues at the origin or with a positive real part, all trajectories $\boldsymbol{d}(t)$ converge to a steady state[56]. Thus, the input of the agent systems (5.20) is constant, and the system reaches a steady state. The condition stated in the theorem that $\beta \boldsymbol{R}_{\mathcal{A}}^{\top} \boldsymbol{K}^{-1} \tilde{\boldsymbol{R}}$ has only eigenvalues at the origin or with a positive real part implies that the matrix in (5.67) has also only eigenvalues at the origin or with a positive real part, since they are related by the Kronecker product with the unity matrix. Since the conditions of Theorem 5.1 are fulfilled, all equilibria correspond to the global minimizer $\bar{\boldsymbol{y}}_i = \mathbf{y}^*$, which concludes the proof. □

Remark 5.10. *For undirected communication, $\boldsymbol{R}_{\mathcal{A}} = \boldsymbol{R}_{\mathcal{C}}$ holds, so $\tilde{\boldsymbol{R}} = \mathbf{0}$ and $\dot{\tilde{\boldsymbol{d}}} = \mathbf{0}$. Therefore, the eigenvalue condition in Theorem 5.15 is always satisfied, and we obtain exactly the results for undirected topolgies of Theorem 5.12 in that special case.*

With the following corollary, the second condition in Theorem 5.15 can be dropped when a certain number of controllers are used.

Corollary 5.16 (less restrictive convergence with directed communication)
Consider the setup of Theorem 5.15. Then, the equilibrium $\bar{\boldsymbol{y}}_i = \mathbf{y}^*$, $i \in \mathcal{A}$ is a globally exponentially stable equilibrium point of the closed-loop system if exactly $n_{\mathcal{C}} = n_{\mathcal{A}} - 1$ controllers are used and the matrix

$$\begin{bmatrix} 2\boldsymbol{K} & \boldsymbol{R}_{\mathcal{C}} - \boldsymbol{R}_{\mathcal{A}} \\ (\boldsymbol{R}_{\mathcal{C}} - \boldsymbol{R}_{\mathcal{A}})^{\top} & 2\boldsymbol{L} \end{bmatrix}, \tag{5.68}$$

with $\boldsymbol{K}$ and $\boldsymbol{L}$ as in (5.63) *is positive definite.*

Proof. Consider the same Lyapunov function as in Theorem 5.15. Note that the matrices $\boldsymbol{K}$ and $\boldsymbol{L}$ in (5.59) are, in general, positive definite and positive semidefinite, respectively. If $n_{\mathcal{C}} = n_{\mathcal{A}} - 1$, matrix $\boldsymbol{L} = \boldsymbol{R}_{\mathcal{C}}^{\top} \boldsymbol{\nu}_{\mathcal{C}} \boldsymbol{R}_{\mathcal{C}}$ is positive definite since $\boldsymbol{R}_{\mathcal{C}}$ has full column rank. Thus, depending on the communication topology, the matrix (5.68) may be positive definite, which is set as a condition in the corollary. □

[56] This follows from linear systems theory: the solution of the state space differential equation is a linear combination of exponential functions with exponents given by the eigenvalues. Persistent oscillations can only occur if there are purely imaginary eigenvalues, which is excluded by the stated condition of having eigenvalues at zero or with a negative real part.

Note that both results for directed communication structures require, in contrast to the case with undirected topologies, to check global LMIs of the size $n_{\mathcal{A}} + n_{\mathcal{C}}$, i.e., the added number of agents and controllers. While such a check is numerically cheap and feasible for small networks, it becomes costly for larger networks with many participants. Thus, undirected communication topologies seem preferable for large-scale networks.

5.6 Numerical Examples

In this section, we give numerical examples to illustrate some of the theoretical results obtained throughout the chapter. We highlight that the agents may use different optimization algorithms and may leave/(re)join the optimization without compromising global optimality and convergence nor requiring a global initialization. First, we demonstrate these features by means of an illustrative example comprising also constrained optimization. Afterwards, we provide a comparison with prevalent algorithms from the literature to show the advantages of the proposed framework.

5.6.1 Illustrative Example with Constrained Optimization

Consider 100 agents with scalar objective functions $f_i : \mathbb{R} \to \mathbb{R}$ and constraints randomly generated out of the three possible objective function models

$$\text{Model 1:} \quad f_i(\mathbf{y}) = a_i \mathbf{y}^2 + b_i \mathbf{y} \tag{5.69}$$

$$\text{Model 2:} \quad \begin{aligned} &f_i(\mathbf{y}) = a_i \mathbf{y}^2 + b_i \mathbf{y} \\ &\text{s.t. } \mathbf{y} \leq 0.5 \end{aligned} \tag{5.70}$$

$$\text{Model 3:} \quad f_i(\mathbf{y}) = e^{\mathbf{y}+b_i} + e^{-(\mathbf{y}+b_i)} \ . \tag{5.71}$$

The parameters $a_i \in [0, 2]$ and $b_i \in [-2, 2]$ are randomly generated with uniform distributions. Note that the objective function Models 1 and 2 have an optimizer at $\mathbf{y}^* = -\frac{b_i}{2a_i}$, and Model 3 at $\mathbf{y}^* = -b_i$. Since all b_i are uniformly distributed with a mean at zero, it is to be expected that the $n_{\mathcal{A}}$ agents have an optimizer near to zero.

Further, each agent has a controller (5.48) with $\beta_k = 35$. The agents use heterogeneous dynamics, i.e., (5.16) or (5.20), randomly, for the unconstrained Models 1 and 3. Dynamics (5.33) are used for all agents having Model 2. The parameters of the agent dynamics are set to $\alpha_i = 1$ and $\gamma_i = 1$. For the generalized communication structure (5.10), a randomly generated matrix $\boldsymbol{R} \in \mathbb{R}^{100\times 100}$ fulfilling property (5.11) is generated. The probability of an agent $i \in \mathcal{A}$ to exchange information with agent $j \in \mathcal{A}$ is 10%, such that every agent is on average connected to 10 other agents. At time $t = 100\,\mathrm{s}$, the group of 100 agents is separated into two groups of 50 agents, which form two independent groups. The groups are chosen such that the 50 agents with the greatest b_i, roughly speaking with $b_i \in [0, 2]$, are in a group. Since Models 1 and 2 have on average in this

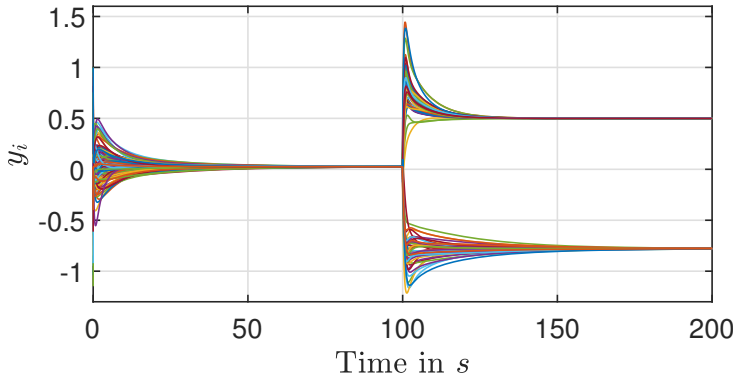

Figure 5.6: Estimations of the global optimizer of all agents.

group an optimizer at $\mathbf{y}^* = -0.5$ and Model 3 at $\mathbf{y}^* = -1$, an optimizer at around -0.75 for this group is expected. Conversely, the 50 agents with the smallest b_i, roughly speaking with $b_i \in [-2, 0]$, are in the second group. Analogously, for this group, an optimizer at 0.75 is expected, which is restricted to 0.5 due to the constraint of Model 2. Then, two connected groups of agents remain in individual distributed optimizations. The probability to be connected with another agent remains 10%, such that every agent is on average connected to 5 agents of its group.

In Figure 5.6, the local estimations of the agents are shown. Until time $t = 100\,\mathrm{s}$, all agents are connected and the global minimizer $\mathbf{y}^* = 0.0258$ is found cooperatively. At time $t = 100\,\mathrm{s}$, the group splits in two (in real applications this could be due to network failure of critical links, or due to agents disconnecting). However, the two groups find cooperatively their respective global minima of $\mathbf{y}_1^* = 0.5$ and $\mathbf{y}_2^* = -0.7789$.

5.6.2 Comparison with State of the Art

In this section, the proposed framework is compared with the most prevalent distributed optimization algorithms, i.e. EXTRA [Shi+15, Algorithm 1], DIGing [NOS17, Algorithm 1], and distributed PI [KCM15, (4)][57]. In this example, the same scenario as in the previous example is implemented but without the constraint in Model 2, since EXTRA, DIGing and distributed PI are not designed for handling constraints. All algorithms use the same initial estimation $x(0)$. As in the previous example, the 100 agents split up in two groups of 50 agents at time $t = 100$ s (or iteration $k = 250$ for the discrete time algorithms).

Note that the algorithms from the literature require a global initialization. In contrast, the framework proposed in this work does not require any global initialization at any

[57] Note that all these algorithms have a similar computational complexity. The algorithms comprise sums, multiplications and gradient function evaluations.

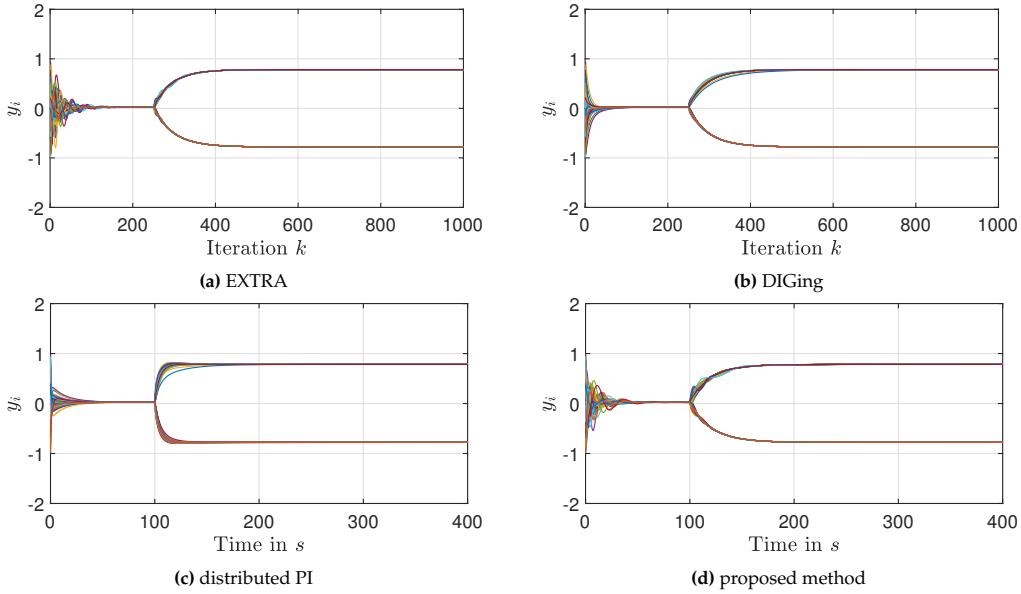

(a) EXTRA **(b)** DIGing

(c) distributed PI **(d)** proposed method

Figure 5.7: Evolution of all agents' optimizer estimates during distributed optimization. DIGing, EXTRA and dPI are (re-)initialized at the beginning and after the split.

time. The advantage of not requiring a global initialization is showcased in the following. In order to illustrate the effects of this initialization requirement, the distributed optimization is performed with each algorithm in two ways: (1) the algorithms are executed as described in the respective papers without any special routine during the agent split at $t = 100$ s (or iteration $k = 250$); and (2) performing again, in a synchronous manner, the respective global initialization right after the agents split into two groups. The results of this distributed optimization for each algorithm can be seen in Figures 5.7-5.9.

First, the mode of execution (2) is considered. Figure 5.7 shows the evolution of the estimations of all agents for each algorithm. Until $t = 100$ s (or $k = 250$ for the discrete-time algorithms), the agents form a group and all algorithms converge to the global optimizer, $y^* = 0.0258$. At $t = 100$ s (or $k = 250$), the agents split in two groups and each group converges to its respective optimizer at $y_1^* = 0.7825$ and $y_2^* = -0.7789$. It can be observed that the dynamics of each algorithm are different despite converging to the same optimizer. It is important to note that the step sizes have not been tuned for achieving best performance, but for achieving a similar convergence rate to improve comparability. The average distance to the optimizer of all agents can be seen in Figure 5.8 for EXTRA, DIGing, distributed PI and the proposed method. It can be seen that all four algorithms are able to reduce the distance to the optimizer when all agents form a group (blue line, until $t = 100$ s or $k = 250$) and also after the agents split up in two groups (orange and yellow). This is because the initialization is performed right

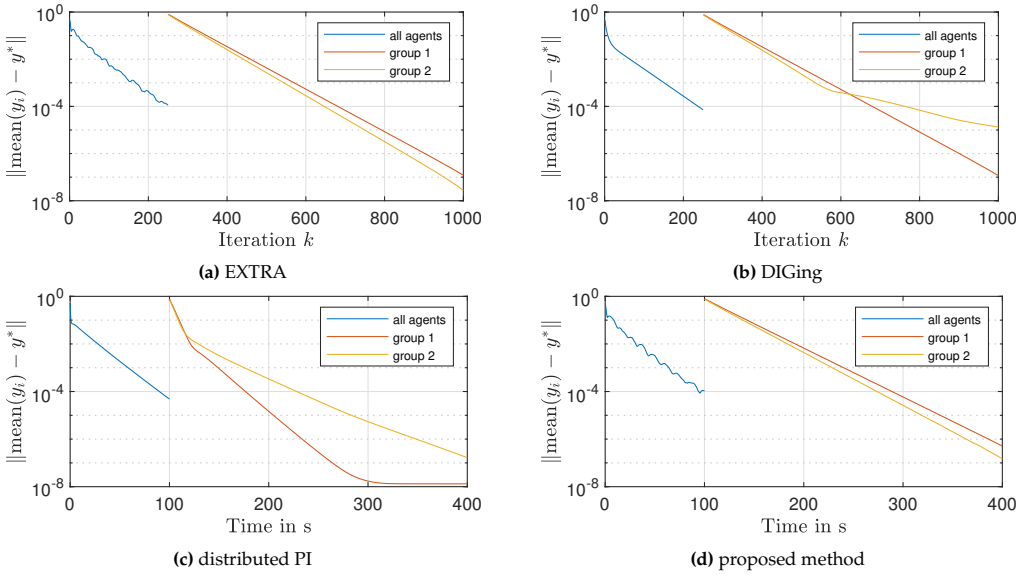

(a) EXTRA **(b)** DIGing

(c) distributed PI **(d)** proposed method

Figure 5.8: Average distance to the optimizer of all agents' estimates during distributed optimization. DIGing, EXTRA and dPI are (re-)initialized at the beginning and after the split.

after the split in all algorithms as described for mode of execution (2) (except for the proposed method, which does not require any initialization).

Now, the mode of execution (1) is studied, i.e. the algorithms are executed as described in the respective papers without any special routine during the agent split at $t = 100$ s (or $k = 250$). In Figure 5.9, the average distance to the optimizer of all agents is shown for the mode of execution (1). It can be seen that all existing algorithms (EXTRA, DIGing, dPI) fail to converge to the optimizer after the agents split due to the need of a global initialization. Thus, as shown in Figure 5.8, the EXTRA, DIGing and distributed PI only converge if they are reinitialized whenever a change in the network occurs. In the proposed method, convergence to the optimizer is given *per design*. In terms of functionality, this is the main difference between the proposed method and the literature. This is an advantage when considering scenarios where the number of agents is not constant, i.e. where agents may join or leave the distributed optimization.

5.7 Discussion and Outlook

The main contribution of this chapter are local design requirements for distributed optimization algorithms. All existing methods assume that all agents use a specific algorithm and thus rely on a centralized convergence and optimality analysis. The method proposed here opens up the possibility to use heterogeneous algorithms for

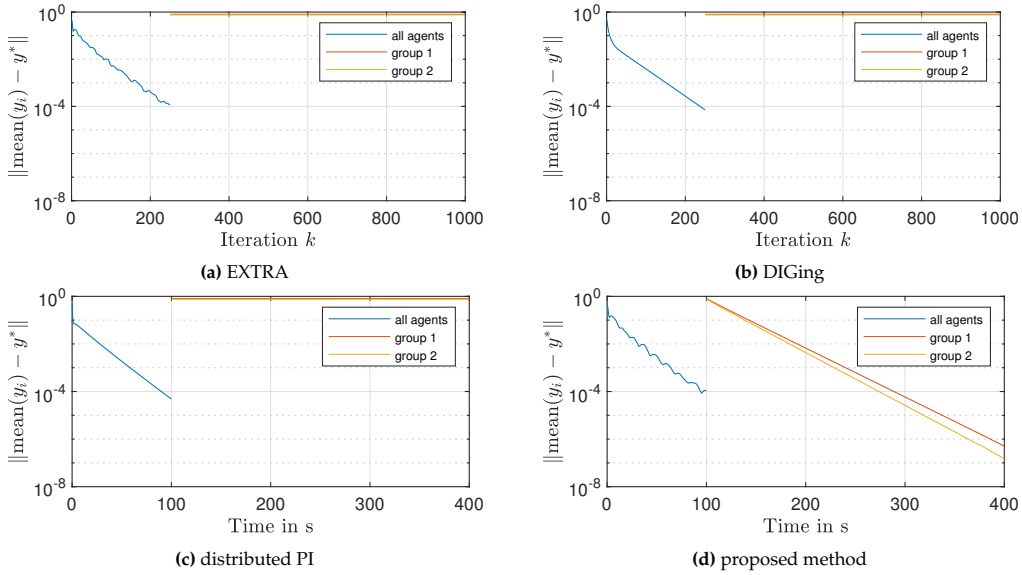

(a) EXTRA **(b)** DIGing

(c) distributed PI **(d)** proposed method

Figure 5.9: Average distance to the optimizer of all agents' estimates during distributed optimization. DIGing, EXTRA and dPI are (re-)initialized only at the beginning ($k = 0$ or $t = 0$) and not after the split.

each agent within a distributed optimization. In addition, individual agents may leave or (re)join the distributed optimization and the communication topology may change almost arbitrarily.[58] The local design requirements are derived by exploiting the classic control structure of passivity-based control as seen in Figure 5.1, yielding a distributed optimization framework without requiring any global coordination or initialization. The proposed optimization structure first introduces controller systems in distributed optimization, that are responsible for achieving consensus among the agents by penalizing the consensus error with a PI-like structure. However, the controller systems raise the question of where such controller systems should be physically implemented. It has been shown in Example 5.1, that the controller systems may be physically implemented as part of the agent systems, or alternatively as independent entities with computation capabilities, leading both possibilities to (mathematically speaking) identical algorithms. For the practical implementation, protocols regarding where and by whom controller systems are created and physically implemented are necessary. These practical implementation aspects lay outside of the scope of this thesis and were not considered in this work.

Still regarding the controller systems, it is important to note that only an integrator with feedthrough (PI controllers) is considered in this chapter. However, the only local design requirement posed on the controller systems is that they are systems with integral action

[58] It is assumed that the communication topology is always described by a connected graph. If the graph is not connected for some time period, it results automatically in individual distributed optimizations corresponding to the connected subgraphs during that time period, as presented in the numerical example.

as in Definition 5.1. Thus, a nonlinear function weighting the consensus error[59] can be readily considered and analyzed via Proposition 5.11. With a nonlinear weighting, large consensus errors can be penalized[60] more than small errors. This may lead to higher performance, i.e., faster convergence, if properly designed. Even an adaptive consensus error weighting is possible and complies with Proposition 5.11 whenever $\beta_k(t) > 0$.

Furthermore, the proposed distributed optimization framework is formulated in continuous time, exploiting the large body of passivity theory which is traditionally formulated in continuous time. Despite the strong theoretical results in the continuous-time setting, for a practical implementation, a discrete-time version is necessary. In this work, forward Euler and Runge-Kutta methods have been used for solving the differential equations (via SIMULINK). Apart from simply discretizing the continuous-time system with well-known methods, the distributed optimization framework may be entirely formulated in discrete time using the corresponding discrete-time passivity theory [SP18]. This may open up a whole new dimension for the agent dynamics, which may profit from widely used algorithmic refinements such as the proximal operator [PB14]. By using the proximal operator, it is expected that OFEIP discrete-time agent dynamics are be obtained even without strong convexity.

Convergence and optimality are also ensured when using directed communication topologies within the distributed optimization framework. In this case, however, the feasibility of a network-wide LMI of the order $n_{\mathcal{A}} + n_{\mathcal{C}}$ has to be checked. This is because the structure of the closed-loop system does not correspond to a pure skew-symmetric interconnection anymore, and passivity theory is not readily applicable. A possibility to avoid the feasibility check of a network-wide LMI in the proof of convergence may be to use non-separable Lyapunov functions along with complex variable transformations as it is done for a particular algorithm in [KCM15].

Finally, the flexibility introduced with the local design requirements implies that, if satisfied, the agents can use heterogeneous agent dynamics. Thus, it is possible to include other popular optimization algorithms, i.e., heavy ball [Pol64] or Nesterov acceleration [Nes18]. For that, the analysis of their EIP properties is necessary. This docks on recent pioneering work [Les22; Zhe+24], which studies the EIP properties of such algorithms for achieving robustly, with minimal information about the objective function, the fastest convergence rate in central optimization.

5.8 Summary and Contributions

In this chapter, a novel passivity-based perspective for distributed optimization algorithms composed of agent and controller systems has been presented. Local design

[59] The nonlinear function must be strictly monotone and pass through the origin.

[60] With *penalized* it is meant that the PI controller gives a larger output and the integrator grows faster, leading to a faster response from the agents.

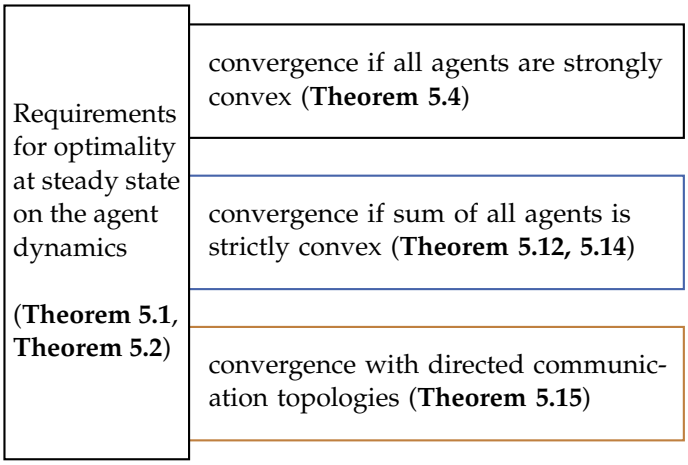

Figure 5.10: Summary and interrelation of the main theorems presented in this chapter. Blue color indicates that minor information on the agent dynamics has to be known, and brown color that the feasibility of a network-wide LMI has to be checked.

requirements for the agent and controller systems ensuring convergence to the global optimizer are derived. Therefore, in contrast to the literature, the focus is not on deriving a specific algorithm which all agents have to follow, but on deriving the conditions the agents have to fulfill to achieve global optimality and convergence. In particular, the approach works without any global initialization and by exchanging only a single variable, in contrast to existing methods (see Research Gap 2 in Section 2.4). As a consequence, the agents may leave and rejoin the distributed optimization without compromising global optimality and convergence. Hence, the approach is especially suited for flexible multi-agent systems, where the network size and participants may vary. An example of such a use case are power systems, where a DGU or market participant may leave the networked optimization due to a lack of available power or other, economic reasons.

With this chapter, Research Gaps 2 and 3 are addressed and a method fulfilling Contribution 2 is proposed. In Figure 5.10, the interrelation of the main theorems proven in this chapter is shown. Theorems 5.1 and 5.2 set the basis for the distributed optimization framework by introducing the local design requirements ensuring global optimality at steady state in both the unconstrained and constrained case. Assuming that every agent fulfills the design requirements, the remaining theorems ensure convergence when different convexity conditions on the objective function of the agents or the communication topologies are posed. Blue color indicates that minor information on the agent dynamics has to be known, and brown color indicates that the feasibility of a network-wide LMI has to be checked.

This distributed optimization framework can be readily utilized for solving the distributed MPC presented in Chapter 4, by incorporating the grid dynamics as a private constraint for agent $i \in \mathcal{A}$. With the proposed distributed optimization framework,

the individual grids may disconnect from the rest of the grid and reconnect without compromising the solution of the distributed optimization — and without the other agents even noticing.

6 Economic Ports for Optimal Operation of Liberalized Power Systems

In this chapter, a framework for the optimal operation of power systems compatible with a liberalized power system as defined in Term 2.2 is presented.[61] The method proposed in this chapter is an alternative to the method of Chapter 4 for achieving optimality and stability, but considering a liberalized power system. In sharp contrast to Chapter 4, there is no superior authority that dictates which computations have to be performed.

The framework proposed in this chapter addresses Research Gaps 4, 5 and 6. To tackle these gaps, a novel price-forming mechanism and the concept of economic ports are introduced, specifically designed for future power systems dominated by power electronics.

The chapter is organized as follows. In Section 6.1, the system dynamics and the network participants are presented. The system dynamics are based, analogously to Chapter 4, on the power system components introduced in Section 3.4. However, in this chapter, different control paradigms, which represent different agents or network participants, are considered for the DGUs. The grid-forming DGUs which stabilize the system belong to the system operator. The grid-following DGUs, which inject a specified amount of active power irrespectively of the grid state, belong to the flexible prosumers which are rational, profit-driven agents.

In Section 6.2, the participants along with their goals are modelled mathematically through the perspective of a liberalized power system. As mentioned before, two fundamental types of network participants are distinguished: system operators and prosumers. The prosumers can be further categorized in flexible and inflexible prosumers.

In Section 6.3, the controllers for each participant are derived. The controllers are designed such that the goals of the network participants, modelled in the previous section, are fulfilled at steady state. The profit-driven prosumers implement a controller aimed at minimizing their own cost. The system operator implements a price-forming mechanism linked to the stabilizing grid-forming DGU. The price-forming mechanism can be interpreted as connecting the control effort necessary to stabilize the grid to the price.

Sections 6.4 and 6.5 consider a single grid. In Section 6.4, a grid and its interconnection ports are defined mathematically. Two types of ports are distinguished, electric and

[61] Preliminary results leading to the content of this chapter have been presented in the conference papers [JS+23a; JSDH23; JSH23].

novel economic ports. In Section 6.5, the stability of a single grid is studied by means of Lyapunov theory.

In Section 6.6, the interconnection of several grids forming a power system is studied. The stability properties of networked grids are analyzed using the EIP properties of the individual grids characterized in Section 6.6.1. In Sections 6.6.2 and 6.6.3, the electric and economic interconnection of grids is proposed and their stability and optimality properties are studied. In particular, it is shown that all equilibria arising in the proposed framework correspond to a uniform marginal pricing (UMP) as resulting from the merit order principle in current energy markets (see Section 2.1).

Finally, the chapter is concluded with a discussion and a summary in Sections 6.8 and 6.9.

6.1 Network Participants and Power System Model

In this section, the whole power system model and the network participants are introduced. A main difference with respect to the power system model in Chapter 4 is that also grid-following DGUs are considered in this framework, which belong to the price takers that do not exist as such in the regulated framework in Chapter 4.

6.1.1 State-Space Grid Model

A set of grids $m \in \mathcal{M} = \{1, \dots, n_{\mathrm{mg}}\}$ is considered, where each grid consists of a set $\mathcal{B}^m$ containing $n_{\mathcal{B}}^m = |\mathcal{B}^m|$ electrical buses or nodes, interconnected by a set $\mathcal{E}^m$ of $n_{\mathcal{E}}^m = |\mathcal{E}^m|$ electrical lines. By assigning an arbitrary direction to the positive line current on each power line, the topology of each grid can be represented as a directed graph $\mathcal{G}^m(\mathcal{B}^m, \mathcal{E}^m)$, where $\mathcal{B}^m$ denotes the nodes and $\mathcal{E}^m$ the edges. A subset of nodes, i.e., $\mathcal{B}_{\mathrm{L}}^m \subseteq \mathcal{B}^m$, are equipped only with a nonlinear load, while other nodes, i.e., $\mathcal{B}_{\mathrm{DGU}}^m \subseteq \mathcal{B}^m$, also include a DGU. The sets $\mathcal{B}_{\mathrm{L}}^m$ and $\mathcal{B}_{\mathrm{DGU}}^m$ together comprise all nodes in the grid, i.e., $\mathcal{B}_{\mathrm{L}}^m \cup \mathcal{B}_{\mathrm{DGU}}^m = \mathcal{B}^m$. The nodes $i \in \mathcal{B}_{\mathrm{DGU}}^m$ are equipped with a DGU and its voltage v_i can be directly controlled.

In the following, the model of a single grid is considered. Thus, the grid index m is omitted until further notice.

Grid-forming and grid-following control of DGU

The dynamics for every bus $i \in \mathcal{B}_{\text{DGU}}$ are derived in detail in Section 3.4 (see Figure 3.4). The dynamics are governed by the differential equations

$$C_{\text{f},i}\dot{v}_i = i_{\text{f},i} - i_{\text{L},i}(v_i) - i_{\text{ext},i} \tag{6.1a}$$

$$L_{\text{f},i}\dot{i}_{\text{f},i} = v_{\text{t},i} - R_{\text{f},i}i_{\text{f},i} - v_i, \tag{6.1b}$$

where $i_{\text{ext},i}$ is the cumulative current injected by interconnecting lines. The load $i_{\text{L},i}$ is modelled as a nonlinear, static ZIP load as introduced in (3.31).

The DGU described above is normally equipped with a grid-forming or a grid-following controller [Roc+12]. Grid-forming controllers inject the necessary current $i_{\text{f},i}$ (and thus indirectly the necessary power) in order to regulate the node voltage v_i to a desired voltage reference $v_{\text{ref},i}$, and stabilize thus the grid voltages regardless of the load disturbance or volatile power injections. Grid-following controllers set the converter voltage $v_{\text{t},i}$ such that a given power reference $p_{\text{ref},i}$ (indirectly the filter current $i_{\text{f},i}$) is injected, without considering the resulting node voltage level v_i. Grid-forming DGUs are used to achieve robust voltage stability and grid-following DGUs to inject a certain amount of power irrespective of grid stability, e.g., for achieving optimal dispatch. In this chapter, it is assumed there is exactly one grid-forming DGU in every grid, and an arbitrary number of grid-following DGUs. The first DGU $1 \in \mathcal{B}_{\text{DGU}}$ is defined, without loss of generalization, as the grid-forming DGU, while $i \in \mathcal{B}_{\text{DGU}} \setminus \{1\}$ are grid-following DGUs.

The grid-forming controller is taken from [Nah+20] and is designed by introducing an error state (6.2b) and a state feedback as

$$v_{\text{t},1} = k_{\alpha,1}v_1 + k_{\beta,1}i_{\text{f},1} + k_{\gamma,1}e_1 \tag{6.2a}$$

$$\dot{e}_1 = v_{\text{ref},1} - v_1, \tag{6.2b}$$

where $k_{\alpha,1} \in \mathbb{R}$, $k_{\beta,1} \in \mathbb{R}$ and $k_{\gamma,1} \in \mathbb{R}$ are the controller parameters. The grid-following controller is designed as

$$v_{\text{t},i} = k_{\alpha,i}v_i + k_{\beta,i}i_{\text{f},i} + k_{\gamma,i}e_i \tag{6.3a}$$

$$\dot{e}_i = p_{\text{ref},i} - v_i i_{\text{f},i}, \tag{6.3b}$$

for all $i \in \mathcal{B}_{\text{dgu}} \setminus \{1\}$, using the injected power error (6.3b) instead. Note that the grid-following DGU introduces a nonlinearity when computing the injected power $v_i i_{\text{f},i}$ in (6.3b). Applying either (6.2) or (6.3) to the DGU (6.1) thus yields

$$C_{\text{f},i}\dot{v}_i = i_{\text{f},i} - i_{\text{L},i}(v_i) - i_{\text{ext},i} \tag{6.4a}$$

$$\dot{i}_{\text{f},i} = \alpha_i v_i + \beta_i i_{\text{f},i} + \gamma_i e_i \tag{6.4b}$$

$$\text{(6.2b) or (6.3b)}, \tag{6.4c}$$

depending if it is a grid-forming or grid-following DGU, with the variables $\alpha_i = \frac{k_{\alpha,i}-1}{L_{\text{f},i}}$, $\beta_i = \frac{k_{\beta,i}-R_{\text{f},i}}{L_{\text{f},i}}$ and $\gamma_i = \frac{k_{\gamma,i}}{L_{\text{f},i}}$ containing the controller parameters. A schematic representation of both control schemes is shown in Figure 6.1.

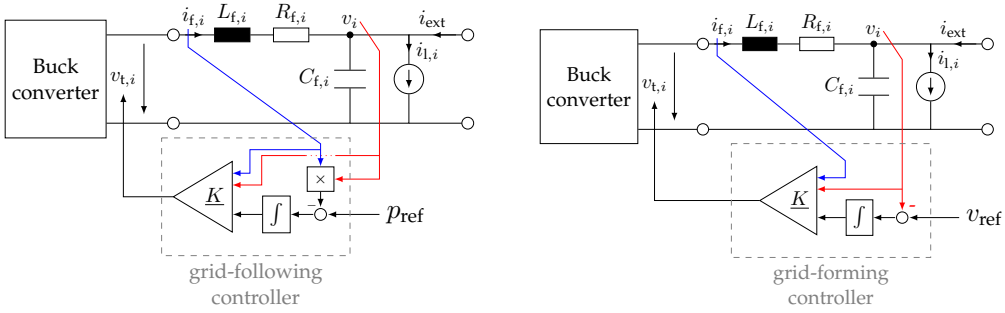

(a) Control scheme of a grid-following DGU.

(b) Control scheme of a grid-forming DGU.

Figure 6.1: Grid-following and grid-forming DGUs with their control schemes ($\underline{K} = [k_{\alpha,i}, k_{\beta,i}, k_{\gamma,i}]$).

Grid Model

The whole grid is then composed of $n_{\mathcal{B}}$ electrical buses with $n_{\text{DGU}} = |\mathcal{B}_{\text{DGU}}| > 1$ DGUs[62]. With respect to the n_{DGU} DGUs, recall that there is one grid-forming DGU which stabilizes the grid voltages and $n_{\text{DGU}} - 1$ grid-following DGUs that may inject power according to their availability or preferences. The grid model reads

$$\boldsymbol{C}_{\text{f}}\dot{\boldsymbol{v}} = \boldsymbol{I}_{\text{f}}\boldsymbol{i}_{\text{f}} - \boldsymbol{i}_{\text{L}}(\boldsymbol{v}) - \boldsymbol{E}\boldsymbol{i}_{\pi} \tag{6.5a}$$

$$\dot{\boldsymbol{i}}_{\text{f}} = \boldsymbol{\alpha}\boldsymbol{I}_{\text{f}}^{\top}\boldsymbol{v} + \boldsymbol{\beta}\boldsymbol{i}_{\text{f}} + \boldsymbol{\gamma}\boldsymbol{e} \tag{6.5b}$$

$$\dot{\boldsymbol{e}} = \boldsymbol{I}_{v}\boldsymbol{I}_{\text{f}}^{\top}\boldsymbol{v} + \boldsymbol{I}_{p}\,\text{diag}\{\boldsymbol{I}_{\text{f}}^{\top}\boldsymbol{v}\}\boldsymbol{i}_{\text{f}} + \begin{bmatrix} v_{\text{ref},1} \\ \boldsymbol{p}_{\text{ref}} \end{bmatrix} \tag{6.5c}$$

$$\boldsymbol{L}_{\pi}\dot{\boldsymbol{i}}_{\pi} = -\boldsymbol{R}_{\pi}\boldsymbol{i}_{\pi} + \boldsymbol{E}^{T}\boldsymbol{v}, \tag{6.5d}$$

where $\boldsymbol{\alpha} = \text{diag}\{\alpha_i\}$, $\boldsymbol{\beta} = \text{diag}\{\beta_i\}$ and $\boldsymbol{\gamma} = \text{diag}\{\gamma_i\}$ contain the control parameters; $\boldsymbol{C}_{\text{f}} = \text{diag}\{C_{\text{f},i}\}$, $\boldsymbol{R}_{\text{f}} = \text{diag}\{R_{\text{f},i}\}$, $\boldsymbol{L}_{\text{f}} = \text{diag}\{L_{\text{f},i}\}$, $\boldsymbol{i}_{\text{L}} = \text{diag}\{i_{\text{L},i}\}$, $\boldsymbol{R}_{\pi} = \text{diag}\{R_{\pi,j}\}$ and $\boldsymbol{L}_{\pi} = \text{diag}\{L_{\pi,j}\}$ are the filter, load and line parameters; and $\boldsymbol{v} = \text{col}\{v_i\} \in \mathbb{R}^{n_{\mathcal{B}}}$, $\boldsymbol{i}_{\text{f}} = \text{col}\{i_{\text{f},i}\} \in \mathbb{R}^{n_{\text{DGU}}}$, $\boldsymbol{e} = \text{col}\{e_i\} \in \mathbb{R}^{n_{\text{DGU}}}$ and $\boldsymbol{i}_{\pi} = \text{col}\{i_{\pi,j}\} \in \mathbb{R}^{n_{\mathcal{E}}}$ are the stacked states of the DGUs $i \in \mathcal{B}$ and power lines $j \in \mathcal{E}$. The voltage and power references $v_{\text{ref}} \in \mathbb{R}_{>0}$ and $\boldsymbol{p}_{\text{ref}} \in \mathbb{R}^{n_{\text{DGU}}-1}$ are inputs, where n_{DGU} defines the number of inputs of the grid. The matrix $\boldsymbol{I}_{\text{f}} \in \mathbb{R}^{n_{\mathcal{B}} \times n_{\text{DGU}}}$ is a permutation matrix assigning the filter currents of n_{DGU} DGUs to the correct $n_{\mathcal{B}} \geq n_{\text{DGU}}$ nodes.[63] The matrices $\boldsymbol{I}_{v} = \text{diag}\{1, 0, \ldots, 0\} \in \mathbb{R}^{n_{\text{DGU}} \times n_{\text{DGU}}}$ and $\boldsymbol{I}_{p} = \text{diag}\{0, 1, \ldots, 1\} \in \mathbb{R}^{n_{\text{DGU}} \times n_{\text{DGU}}}$ are diagonal matrices such that the correct error signals are induced for the integrator states[64] as in (6.2b) and (6.3b). Note that in (6.5a) and (6.5d) it has been taken into account that the voltage drop over the power lines $\boldsymbol{v}_{\Delta} \in \mathbb{R}^{n_{\mathcal{E}}}$ can be expressed as $\boldsymbol{v}_{\Delta} = \boldsymbol{E}^{\top}\boldsymbol{v}$ and the current drawn from

[62] Note that the buses and power lines form a networked system as defined in Term 3.1.

[63] If all nodes have a DGU, the vectors $\boldsymbol{v}$ and $\boldsymbol{i}_{\text{f}}$ have the same dimension and the matrix $\boldsymbol{I}_{\text{f}}$ is the unity matrix (and is thus not necessary and can be left out.)

[64] See Remark 6.1 for more details.

the buses by the power lines as $\boldsymbol{i}_{\text{ext}} = \boldsymbol{E}\boldsymbol{i}_{\pi}$, where $\boldsymbol{E}$ is the incidence matrix of $\mathcal{G}$ (see Section 4.1.2).

Remark 6.1. *The matrices $\boldsymbol{I}_v = \text{diag}\{1, 0, \dots, 0\} \in \mathbb{R}^{n_{DGU} \times n_{DGU}}$ and $\boldsymbol{I}_p = \text{diag}\{0, 1, \dots, 1\} \in \mathbb{R}^{n_{DGU} \times n_{DGU}}$ have this form assuming the Node 1 contains the grid-forming DGU. Then, in* (6.5c)*, the first error state integrates the voltage error and the remaining states the power error. Further, it always holds that $\boldsymbol{I}_v + \boldsymbol{I}_p = \boldsymbol{I}_{n_{DGU}}$, since all DGUs are either grid-forming or grid-following.*

A schematic representation of the grid model can be seen in Figure 6.2. The system inputs are the power references of the grid-following DGUs $\boldsymbol{p}_{\text{ref}}$, and the scalar output is the current $i_{\text{f},1}$ of the grid-forming DGU. The voltage reference $v_{\text{ref},1}$ for the grid-forming DGU is seen as an internal variable instead of as an input, because it is not supposed to be controlled in closed-loop. Note that the current of the grid-forming DGU contains information about the effort necessary to maintain stability in the grid. This is formalized in the next proposition. This aspect is exploited later by the system operator (see Section 6.2.3 and 6.3.2) for defining a novel, control-inspired price-forming mechanism.

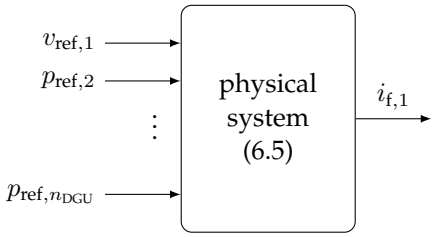

Figure 6.2: Schematic representation of a grid with inputs, outputs and the voltage reference for the grid-forming DGU.

Proposition 6.1 (grid-forming DGU as power balance indicator)
Let $v_{\text{ref}} \in \mathbb{R}_{>0}$. Let the sum of the power usage and losses in a grid as in (6.5)*, which includes all the loads and transmission losses, be denoted by $p_{\text{L},\Sigma}$. Then, at steady state, it holds $i_{\text{f},1} = 0$ if and only if*

$$\sum_{i=2}^{n_{DGU}} p_{\text{ref},i} = p_{\text{L},\Sigma}. \tag{6.6}$$

Proof. In any steady state with $v_{\text{ref}} \in \mathbb{R}_{>0}$ and $\boldsymbol{p}_{\text{ref}} \in \mathbb{R}^{n_{\text{DGU}}-1}$, it holds from (6.5) that

$$\mathbf{0} = \boldsymbol{I}_{\text{f}}\boldsymbol{i}_{\text{f}} - \boldsymbol{i}_{\text{L}}(\boldsymbol{v}) - \boldsymbol{E}\boldsymbol{i}_{\pi} \tag{6.7a}$$

$$\mathbf{0} = \boldsymbol{\alpha}\boldsymbol{I}_{\text{f}}^{\top}\boldsymbol{v} + \boldsymbol{\beta}\boldsymbol{i}_{\text{f}} + \boldsymbol{\gamma}\boldsymbol{e} \tag{6.7b}$$

$$0 = v_{\text{ref}} - v_1 \tag{6.7c}$$

$$\mathbf{0} = \boldsymbol{p}_{\text{ref}} - \boldsymbol{I}_p \operatorname{diag}\{\boldsymbol{I}_{\text{f}}^{\top}\boldsymbol{v}\}\boldsymbol{i}_{\text{f}} \tag{6.7d}$$

$$\mathbf{0} = \boldsymbol{E}^{\top}\boldsymbol{v} - \boldsymbol{R}_{\pi}\boldsymbol{i}_{\pi}. \tag{6.7e}$$

Rearranging (6.7e) to $\boldsymbol{i}_{\pi} = \boldsymbol{R}_{\pi}^{-1}\boldsymbol{E}^{\top}\boldsymbol{v}$ and inserting it in (6.7a), it results

$$\mathbf{0} = \boldsymbol{I}_{\text{f}}\boldsymbol{i}_{\text{f}} - \boldsymbol{i}_{\text{L}}(\boldsymbol{v}) - \boldsymbol{E}\boldsymbol{R}_{\pi}^{-1}\boldsymbol{E}^{\top}\boldsymbol{v}. \tag{6.8}$$

Multiplying (6.8) with $\boldsymbol{v}^{\top}$ from the left yields

$$0 = \boldsymbol{v}^{\top}\boldsymbol{I}_{\text{f}}\boldsymbol{i}_{\text{f}} \underbrace{-\boldsymbol{v}^{\top}\boldsymbol{i}_{\text{L}}(\boldsymbol{v}) - \boldsymbol{v}^{\top}\boldsymbol{E}\boldsymbol{R}_{\pi}^{-1}\boldsymbol{E}^{\top}\boldsymbol{v}}_{-p_{\text{L},\Sigma}}. \tag{6.9}$$

Note that the last two terms in (6.9), denoted as $p_{\text{L},\Sigma}$, describe the sum of all loads and the power line losses. The first term of $p_{\text{L},\Sigma}$ corresponds to the power of the ZIP loads, and the second are the losses over the lossy power lines. With that, (6.9) simplifies to

$$\boldsymbol{v}^{\top}\boldsymbol{I}_{\text{f}}\boldsymbol{i}_{\text{f}} = p_{\text{L},\Sigma}. \tag{6.10}$$

Now, sum over all equations (6.7d) to obtain

$$\boldsymbol{v}^{\top}\boldsymbol{I}_{\text{f}}\boldsymbol{I}_p\boldsymbol{i}_{\text{f}} = \sum_{i=2}^{n_{\text{DGU}}} p_{\text{ref},i}, \tag{6.11}$$

and note that, due to Remark 6.1, it holds that

$$\boldsymbol{v}^{\top}\boldsymbol{I}_{\text{f}}\boldsymbol{i}_{\text{f}} = \boldsymbol{v}^{\top}\boldsymbol{I}_{\text{f}}\boldsymbol{I}_p\boldsymbol{i}_{\text{f}} + \boldsymbol{v}^{\top}\boldsymbol{I}_{\text{f}}\boldsymbol{I}_v\boldsymbol{i}_{\text{f}}. \tag{6.12}$$

Insert equations (6.11) and (6.12) into the left-hand side of (6.10) to obtain

$$\sum_{i=2}^{n_{\text{DGU}}} p_{\text{ref},i} + \boldsymbol{v}^{\top}\boldsymbol{I}_{\text{f}}\boldsymbol{I}_v\boldsymbol{i}_{\text{f}} = p_{\text{L},\Sigma}. \tag{6.13}$$

Then, taking into account that $v_1 = v_{\text{ref}} > 0$, it follows from $i_{\text{f},1} = 0$ that (6.13) is equivalent to (6.6), since $i_{\text{f},1} = 0$ leads to $\boldsymbol{v}^{\top}\boldsymbol{I}_{\text{f}}\boldsymbol{I}_v\boldsymbol{i}_{\text{f}} = v_1 i_{\text{f},1} = 0$. □

The last proposition relates a particular steady state of the grid to the power balance equation (6.6). Concretely, it proves that whenever the grid-forming DGU does not need to inject or withdraw power in order to stabilize the system, the whole power usage $p_{\text{L},\Sigma}$ is being met entirely by the grid-following DGUs $i \in \mathcal{B}_{\text{DGU}} \setminus \{1\}$. This is a crucial result for the development of the novel price-forming mechanism, which is designed to exploit this connection in the next sections.

6.1.2 Network Participants and their Roles

After modelling the grid, the different network participants and their roles are outlined. The network participants and their proposed roles are inspired by the functioning of current, unbundled power systems. Thus, two sides coexist in the power system design: the regulated sector responsible for the stable operation, and the liberalized, competitive sector. In the following, the roles of a system operator, inflexible prosumers and flexible prosumers are introduced.

The **system operator** is responsible for ensuring that the system is stable. The task of a system operator in the proposed framework is thus comparable to the tasks of a system operator in current power systems as outlined in Section 2.1.2. However, the means how the system operator achieves that task are very different in the proposed framework. Here, a price generated by a suitable price-forming mechanism reflecting, in real time, the current state of the grid is to be used in order to be compatible for volatile power systems with a large share of renewable generation. For designing the price-forming mechanism, the system operator may use any measurement available taken from its own grid. As in the current power systems, the system operator does not have natural competition (i.e., no other system operator can offer their service in the same grid) and needs to receive a compensation for ensuring system stability.

The **prosumers** are divided into two disjunct sets: the set flexible prosumers $\mathcal{F}$ and the set of inflexible prosumers $\mathcal{U}$. Inflexible prosumers may represent uncontrollable power generation or loads that do not change according to the price. On the other hand, flexible prosumers represent controllable generators, that can inject power according to the current price, and flexible loads responding to the price of electric power.

6.2 Mathematical Modelling of Network Participants

In this subsection, the different network participants are mathematically modelled. It is distinguished between flexible and inflexible prosumers, and the system operator in Sections 6.2.1, 6.2.2 and 6.2.3. In particular, their respective goals are modelled with an objective function as an optimization problem, capturing the rational profit-driven behavior of the different participants.

6.2.1 Flexible Prosumers

In the proposed framework, flexible prosumers $i \in \mathcal{F}$ correspond physically to the grid-following DGUs, thus $\mathcal{F} = \mathcal{B}_{\text{DGU}} \setminus \{1\}$. They can freely choose their injected (or consumed) power and are interfaced to the grid via power electronics as modelled in Section 3.4. The next assumption characterizes the behavior of prosumers in this chapter.

Assumption 6.1 (rational decision makers)
Prosumers $i \in \mathcal{F}$ are rational decision makers driven to maximize their own benefit. They do not provide ancillary services and act irrespectively of the system stability.

Since prosumers are assumed to be rational decision makers, the power reference $p_{\text{ref},i}$ is chosen to maximize their own profit. First, DGUs injecting power, i.e., operating as a source, are considered.

The cost of prosumer $i \in \mathcal{F}$ is modelled as an objective function $f_{\text{flx},i} : \mathbb{R} \to \mathbb{R}$

$$f_{\text{flx},i}(p_{\text{ref},i}), \tag{6.14}$$

and it is assumed to contain all the costs, in particular also the indirect or external costs such as the cost arising from the greenhouse gas emission allowance trading scheme [Cou03]. These external costs can typically be described by an additional affine term in the costs (6.14), which may have slope zero or near to zero for DGUs based on renewable energy sources [Koe22]. On a mathematical level, the next assumption is introduced, which is a common assumption both in convex optimization theory (see Chapter 5) and in power systems (see Remark 6.2).

Assumption 6.2 (strong convexity of costs)
The functions $f_{\text{flx},i}$ are strongly convex and their gradients are Lipschitz for all $i \in \mathcal{F}$.

Remark 6.2. *Assumption 6.2 is mild and standard in power systems literature concerning traditional, thermal generation [Ber09; ZP15; ZDMK12]. However, recent research also justifies strongly convex costs for power electronics-based generation due to increased wear-out at high active power setpoints. It has been empirically shown that wear-out and aging effects are proportional to the power routed through the converters due to increased thermal [Pey+19] and electrical stress on the transistors, causing, e.g., the hazardous gate oxide [Hos+24].*

The profit $J_{\text{flx},i}$ of the prosumers $i \in \mathcal{F}$ reads then

$$J_{\text{flx},i} = -f_{\text{flx},i}(p_{\text{ref},i}) + \lambda p_{\text{ref},i}, \tag{6.15}$$

where $\lambda \in \mathbb{R}$ is a given price for remuneration of the power injection. The first term of (6.15) describes the total (direct and indirect) cost of the power generation. The second term describes the revenue the individual rational prosumers receives due to the power injected to the grid. The rational prosumers thus want to maximize the profit, i.e., choose a power injection $p_{\text{ref},i}$ in order to solve the optimization problem

$$\max_{p_{\text{ref},i}} J_{\text{flx},i}(p_{\text{ref},i}). \tag{6.16}$$

Remark 6.3. *Note that* (6.16) *automatically includes the case of producers and consumers. A consumer does not have costs* $f_{\text{flx},i}(p_{\text{ref},i})$*, but have concave utility functions* $U_{\text{flx},i}(p_{\text{ref},i})$ *such that Assumption 6.2 holds for* $-U_{\text{flx},i}$*. Thus, to maximize its utility, a consumer solves the optimization problem*

$$\max_{p_{\text{ref},i}} \{U_{\text{flx},i}(p_{\text{ref},i}) + \lambda p_{\text{ref},i}\}, \tag{6.17}$$

which is structurally identical to (6.16)*. Thus, it suffices to use the objective function* (6.15) *to model prosumers in both operating regions, power injection and power consumption. When* $p_{\text{ref},i} < 0$*,* $-f_{\text{flx},i}$ *is considered to be a utility instead of a cost function. Thus, a unified consideration of flexible producers and consumers is possible.*

The unifying consideration in Remark 6.3 allows DGUs capable of operating in both regimes, as a producer or consumer (e.g., a battery), to describe their operation in both regimes with the profit maximization introduced above.

6.2.2 Inflexible Prosumers

Inflexible loads and producers $i \in \mathcal{U}$ are described with the physical ZIP loads introduced in (3.31) in Section 3.4, thus $\mathcal{U} = \mathcal{B}_{\text{L}}$. Inflexible producers are associated with a negative constant power in the ZIP load. This is because inflexible producers are typically weather dependent renewable energy sources, which inject the specific amount of power they are currently transforming from, e.g., wind or solar power. These renewable energy sources thus behave like a constant power source. Since there are no inflexible produces in power systems typically modelled as a negative constant resistance or negative constant current, the inflexible producers are restricted to the constant power loads.

Inflexible loads for $i \in \mathcal{U}$ are considered as in Section 3.4, with $Y_i(t) > 0$, $P_{\text{L},i}(t) > 0$ and $I_i(t) > 0$. Depending on the concrete values of the ZIP load parameters, the static function

$$i_{\text{L},i}(v_i) = Y_i(t)v_i + \frac{P_{\text{L},i}(t)}{v_i} + I_i(t), \tag{6.18}$$

is strictly monotone (i.e., EIP, see [Kha02]) or not. Note that in the proposed analysis, it is not necessary that every load is EIP by itself. Instead, the EIP properties of the whole grid are studied in Section 6.5 and 6.6, such that EIP and non-EIP subsystems may compensate each other. A structured study when such compensations occur in DC grids with identical models can be found in [Mal+24a]. However, in this chapter, the focus lies on deriving EIP properties for the grid defining suitable ports by implicitly profiting from these compensation mechanisms as outlined in Section 6.5.

Analogously to the revenue of the flexible prosumers in (6.15), the inflexible prosumers $i \in \mathcal{U}$ have to remunerate the consumed power according to

$$J_{\text{up},i} = \lambda p_{\text{L},i}, \tag{6.19}$$

where $p_{\mathrm{L},i} = i_{\mathrm{L},i} v_i$ is the power consumed (or generated) by the inflexible load (or producer). Inflexible producers have a negative load current $i_{\mathrm{L},i}$ and thus a negative remuneration, meaning that they receive a monetary compensation. As can be observed in (6.19), the prosumers cannot react to a changing price or to other system variables or states, since they do not have any controllable system variable.

6.2.3 System Operator

The exclusive responsibility of the system operator is to maintain the system stability while inducing an economically efficient operation. By exclusive, it is meant that there is no other entity in the grid sharing the same responsibility.

The system operator is not a profit-driven agent.[65] Thus, it operates one grid-forming DGU and, in particular, no other grid-following DGU to comply with the unbundling principle in liberalized power systems as outlined in Section 2.1. For achieving the goal of enabling a stable and economically efficient operation in the whole grid, in the proposed framework, the system operator makes use of the grid-forming DGU, which is present in every grid.

A basic requirement for an economic efficient operation is that the sum of all positive and negative cashflows of the network participants sum up to zero, in order to avoid any inefficient accumulation of wealth. Thus, the main task of the system operator is to make sure that

$$\lambda \sum_{i=2}^{n_{\mathrm{DGU}}} p_{\mathrm{ref},i} - \lambda p_{\mathrm{L},\Sigma} = 0 \tag{6.20}$$

holds. The first term is the revenue of the flexible producers, whereas the second term describes the cost of inflexible loads and other losses. For achieving this, the system operator can freely choose a price, i.e., by designing a suitable price-forming mechanism such that (6.20) is fulfilled.

From (6.20), assuming that in general $\lambda \neq 0$, it can be observed that a necessary condition to fulfill the equation is that there is power balance, i.e.

$$\sum_{i=2}^{n_{\mathrm{DGU}}} p_{\mathrm{ref},i} - p_{\mathrm{L},\Sigma} = 0. \tag{6.21}$$

This is comparable to the traditional role of the system operator, who maintains power balance by managing primary, secondary, and tertiary control as described in Section 2.1. In contrast, the approach presented here enables the system operator to achieve

[65] The remuneration of the system operator could be oriented on the remuneration of a distribution system operator in current power systems. Its task is to make sure that the system works and the electrical energy is available to the customers.

power balance by dynamically adjusting the price in real time, rather than coordinating different control layers.

It is well established in power systems that a stable steady state can only be achieved when power balance is maintained; ensuring this balance is the primary objective of control systems in power networks [GECC18]. Therefore, the system operator's goal in (6.20) inherently promotes stable operation. The fact that this approach also guarantees economic efficiency will be demonstrated later, in Proposition 6.3 and Proposition 6.8.

In the next section, suitable controllers for the flexible prosumers and the system operators, e.g., the price-forming mechanism, are provided.

6.3 Controller Design for Network Participants

In this subsection, controllers are derived taking into account the models of the network participants from Section 6.2. In particular, the controllers are designed such that the respective network participants can fulfill, using their controllable variables, their goals as modelled mathematically in the previous section. These controllers form together with the grid dynamics (6.5) the closed-loop system for a single grid, which is formally analyzed in the next sections using EIP and Lyapunov theory.

6.3.1 Flexible Prosumers

The flexible prosumers $i \in \mathcal{F}$ are rational decision makers and are thus interested in controlling its power generation in order to maximize their profit as in (6.16). First, a crucial assumption for the functioning of the power system is introduced.

Assumption 6.3 (market dominance)
No flexible prosumer $i \in \mathcal{F}$ in charge of a DGU is large enough to exercise market dominance. In particular, the price is independent of the generation of every DGU, mathematically speaking, $\frac{\partial \lambda}{\partial p_{\mathrm{ref},i}} \approx 0$.

Assumption 6.3 is a standard assumption in microeconomic theory describing market equilibria [MCWG+95; Koe22]. This assumption is satisfied if there is a high amount of flexible prosumers, together with the assumption that no one is large enough to influence sufficiently the market solution.

With Assumption 6.3, the gradient of the objective function (6.15) of the flexible prosumers $i \in \mathcal{F}$ is

$$\nabla J_{\text{flx},i}(p_{\text{ref},i}) = -\nabla f_{\text{flx},i}(p_{\text{ref},i}) + \lambda. \tag{6.22}$$

The optimal power injection $p^*_{\text{ref},i}$ can be computed with a continuous-time gradient ascent to maximize (6.16), e.g.,

$$\dot{p}_{\text{ref},i} = \tau\Big(-\nabla f_{\text{flx},i}(p_{\text{ref},i}) + \lambda\Big), \tag{6.23}$$

where $\tau \in \mathbb{R}_{>0}$ is a tuning parameter. The multiplier λ can be interpreted as an exogenous input to the gradient ascent in (6.23), and the injected power $p_{\text{ref},i}$ adapts via gradient ascent to this exogenous input. Alternatively, since $f_{\text{flx},i}$ is strongly convex as per Assumption 6.2 and thus $\nabla f_{\text{flx},i}$ strictly monotone, for a given price λ, the optimal power injection $p^*_{\text{ref},i}$ can be uniquely determined by solving the equation

$$-\nabla f_{\text{flx},i}(p^*_{\text{ref},i}) + \lambda = 0. \tag{6.24}$$

6.3.2 System Operator

In order to achieve the primary goal of the system operator in (6.20), the price-forming mechanism

$$\dot{\lambda} = \kappa\Big(p_{\text{L},\Sigma} - \sum_{i=2}^{n_{\text{DGU}}} p_{\text{ref},i}\Big), \tag{6.25}$$

with $\kappa \in \mathbb{R}_{>0}$, is proposed. The price λ varies according to the unmet power balance (6.21), which is identified as a necessary condition for the primary goal in Section 6.2.3. When the total power usage $p_{\text{L},\Sigma}$ is greater than the total generation of the grid-following DGUs the price increases in order to incentivize more power generation by the grid-following DGUs, which are rational, price-driven decision makers. Conversely, if there is too much power injection, the price decreases.

The price-forming mechanism (6.25) can also be interpreted as the result of applying a primal-dual optimization [Arr+58; LY16] algorithm to an optimal dispatch problem. In particular, (6.25) represents the dual ascent of the dual variables in the optimization problem

$$\min\ J(p_{\text{ref},i}) \tag{6.26a}$$

$$\text{s.t.}\ \ p_{\text{L},\Sigma} - \sum_{i=2}^{n_{\text{DGU}}} p_{\text{ref},i} = 0. \tag{6.26b}$$

This directly follows since a primal-dual algorithm for (6.26) is given by

$$\dot{p}_{\mathrm{ref},i} = -\tau\left(\nabla J(p_{\mathrm{ref},i}) + \lambda\right) \tag{6.27a}$$

$$\dot{\lambda} = \kappa\left(p_{\mathrm{L},\Sigma} - \sum_{i=2}^{n_{\mathrm{DGU}}} p_{\mathrm{ref},i}\right), \tag{6.27b}$$

which converges to the global optimizer if the objective function is strictly convex.[66] The variable λ corresponds here to the Lagrange multiplier. Thus, the price-forming mechanism corresponds to the dual ascent in (6.27). The concise interrelation of the proposed framework with global optimality is analyzed later in Proposition 6.7 and Proposition 6.8.

The price-forming mechanism (6.25) requires that the system operator measures the total power usage $p_{\mathrm{L},\Sigma}$ in the system and the sum of all generations $p_{\mathrm{ref},i}$. The total power usage $p_{\mathrm{L},\Sigma}$ includes all ZIP loads and all losses over the power lines or filter resistances within the own grid. To measure all these variables would be costly, and the price-forming mechanism would be prone to error whenever a single measurement device fails. In order to simplify and yet retain the essence of the price-forming mechanism, Proposition 6.1 proven in Section 6.1 is applied, and the equivalent price-forming mechanism

$$\dot{\lambda} = \kappa i_{\mathrm{f},1} \tag{6.28}$$

is obtained. As per Proposition 6.1, the price-forming mechanism (6.28) steers the system to exactly the same steady state as mechanism (6.25); the price dynamics differ only during transients. Thus, for computing the price with price-forming mechanism (6.28), the system operator simply needs to measure the current of the stabilizing, grid-forming DGU for which it is responsible. The current of the grid-forming DGU acts thus as a proxy for the system stability and the power balance. When the grid-forming DGU needs great effort (viz., current) for stabilizing the system, the price increases and incentivizes the rational, price-driven decision makers to generate more power. Similarly, a negative current indicates a great stabilizing effort due to an excess of power injection in the grid, and the price decreases. Furthermore, the price-forming mechanism (6.28) considerably simplifies the relation of the price with the system variables, which is crucial for the EIP analysis in the next section, considering that the price will form one of the interconnection ports of the grid.

In this section, controllers have been proposed such that the network participants with degrees of freedom, i.e., the flexible prosumers and the system operator, control their variables such that *their own* objectives are fulfilled. The flexible prosumers seek to maximize their profit irrespective of system stability. The system operates aim to induce a stable and economically efficient operation irrespective of the economic profit of

[66] This only applies to the continuous-time formulation; in a discrete-time formulation an appropriate step size has to be chosen.

the remaining agents. In the next section, the interconnection ports of the resulting grid composed of the physical system as well as the controllers are defined, and the stability properties are studied.

6.4 Definition of Interconnection Ports of a Grid

This section provides a formal mathematical definition of the interconnection ports for a grid. Before presenting the precise mathematical definition, some background and context regarding the role and significance of these ports is discussed.

The resulting physical system equipped with the controllers derived in Section 6.2 is depicted in Figure 6.3. The physical system is composed of the lossy, dynamic power lines, grid-forming and grid-following DGUs, and the loads. The system operator, which operates the grid-forming DGU, measures the filter current and determines in real-time the price following the price-forming mechanism (6.28). This price is defined as the output of the physical system and is called the local price $\lambda_{\text{loc}} \in \mathbb{R}$ in the rest of the chapter. Conversely, the flexible prosumers determine the power injection of their respective grid-following DGUs using the price as an input, which may be, but is not necessarily, the local price λ_{loc}. Thus, the price for the flexible prosumers is defined as an input, and is called an external price $\lambda_{\text{ext}} \in \mathbb{R}$ in the rest of this chapter. The local price λ_{loc} and external price λ_{ext} together form the economic port $(\lambda_{\text{ext}}, \lambda_{\text{loc}})$. This port is later used for an economic cooperation of different grids, without needing to share any other information such as costs of power generation or physical system parameters.

Moreover, the grids can also be electrically interconnected with other grids via power lines. For that, the electric port as shown in Figure 6.3 is defined. The definition of such an electric voltage-current port is common in passivity-based approaches for power systems [Str+21; Nah+20; Mal+23]. However, up to now, such an electric port has been defined at node level in order to build a grid out of passive nodes. Here, we use an electric port at grid level for interconnecting with other grids. Such an electric port at grid level as here first proposed allows to study the EIP properties of the entire grid system w.r.t. this port. This allows the compensation of EIP and non-EIP subsystem, such as loads, implicitly in the grid. In the next subsection, both ports are defined mathematically.

Mathematical Definition of the Interconnection Ports

Consider the dynamic system formed by the physical system (6.5), the controllers of flexible prosumers (6.23) and the system operator (6.28). The nonlinear system dynamics neglecting the electric and economic ports can be written as

$$\dot{\boldsymbol{x}} = \boldsymbol{A}(\boldsymbol{x})\boldsymbol{x} \tag{6.29}$$

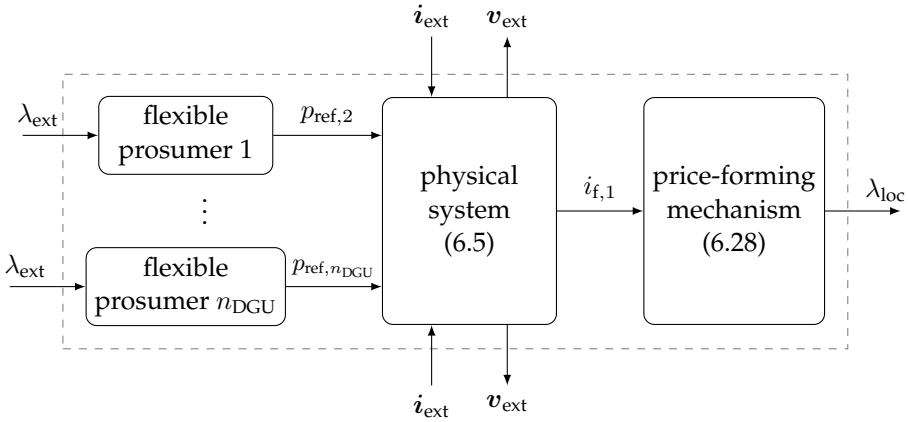

Figure 6.3: Definition of the grid composed of the physical system (6.5) with inflexible prosumers (6.18), flexible prosumers (6.23) and system operator (6.28), including the economic and electric ports.

where

$$A(\boldsymbol{x}) = \begin{bmatrix} -\boldsymbol{C}_{\text{f}}^{-1}\text{diag}\{\frac{i_{\text{L},i}(v_i)}{v_i}\} & \boldsymbol{C}_{\text{f}}^{-1}\boldsymbol{I}_{\text{f}} & \boldsymbol{0} & -\boldsymbol{C}_{\text{f}}^{-1}\boldsymbol{E} & \boldsymbol{0} & \boldsymbol{0} \\ \alpha\boldsymbol{I}_{\text{f}}^{\top} & \boldsymbol{\beta} & \boldsymbol{\gamma} & \boldsymbol{0} & \boldsymbol{0} & \boldsymbol{0} \\ -\boldsymbol{I}_v\boldsymbol{I}_{\text{f}}^{\top} & -\boldsymbol{I}_p\,\text{diag}\{\boldsymbol{I}_{\text{f}}^{\top}\boldsymbol{v}\} & \boldsymbol{0} & \boldsymbol{0} & \tilde{\boldsymbol{I}}_p & \boldsymbol{0} \\ \boldsymbol{L}_{\pi}^{-1}\boldsymbol{E} & \boldsymbol{0} & \boldsymbol{0} & -\boldsymbol{L}_{\pi}^{-1}\boldsymbol{R}_{\pi} & \boldsymbol{0} & \boldsymbol{0} \\ \boldsymbol{0} & \boldsymbol{0} & \boldsymbol{0} & \boldsymbol{0} & -\text{diag}\{\tau_i\frac{\nabla f_{\text{flx},i}}{p_{\text{ref},i}}\} & \boldsymbol{0} \\ \boldsymbol{0} & -\kappa\boldsymbol{1}_{n_{\text{DGU}}}^{\top}\boldsymbol{I}_v & \boldsymbol{0} & \boldsymbol{0} & \boldsymbol{0} & \boldsymbol{0} \end{bmatrix} \tag{6.30}$$

and with the state

$$\boldsymbol{x} = \begin{bmatrix} \boldsymbol{v}^{\top} & \boldsymbol{i}_{\text{f}}^{\top} & \boldsymbol{e}^{\top} & \boldsymbol{i}_{\pi}^{\top} & \boldsymbol{p}_{\text{ref}}^{\top} & \lambda_{\text{loc}} \end{bmatrix}^{\top} \in \mathbb{R}^n, \tag{6.31}$$

with $n = n_{\mathcal{B}} + 3n_{\text{DGU}} + n_{\mathcal{E}}$. All matrices and parameters are as defined in Section 6.1.1, and $\tilde{\boldsymbol{I}}_p$ is the matrix $\boldsymbol{I}_p$ but without the zero row and column. The nonlinear system (6.29) can be represented as a matrix vector product, which enables the analysis of EIP properties via LMIs in the next sections. First, the electric port for the autonomous grid system (6.29) is defined.

Definition 6.1 (electric ports)
Let $i_{\text{ext},i} \in \mathbb{R}$ be an external current injected at a node $i \in \mathcal{B}$ and $v_i \in \mathbb{R}$ the voltage at that node for grid $m \in \mathcal{M}$. The input-output pair $(-i_{\text{ext},i}, v_i)$ is called an electric port[67] for that grid.

The electric port is interfaced with system (6.29) through the vectors $\boldsymbol{b}_{\text{ext}} = \mathbb{1}^i_{n^m} \in \mathbb{R}^n$ and $\boldsymbol{c}_{\text{ext}} = \boldsymbol{b}^{m\top}_{\text{ext}}$, where $\mathbb{1}^i_n \in \mathbb{R}^{n_\mathcal{B}}$ has a 1 at the i-th element and zero elsewhere,[68] since an external current drawn to a node $i \in \mathcal{B}$ acts on the voltage dynamics (6.1a) or (3.39) of node $i \in \mathcal{B}$. Note that a grid may contain an arbitrary number $n_{\text{ext}} \in \mathbb{N}$ of electric ports at any node $i \in \mathcal{B}$, yielding the matrices

$$\boldsymbol{B}_{\text{ext}} = \begin{bmatrix} \boldsymbol{b}_{\text{ext},1} & \dots & \boldsymbol{b}_{\text{ext},n_{\text{ext}}} \end{bmatrix} \in \mathbb{R}^{n \times n_{\text{ext}}} \tag{6.32}$$

and $\boldsymbol{C}_{\text{ext}} = \boldsymbol{B}^{m\top}_{\text{ext}}$. Also, note that the current in the electric port is defined as negative because it enters negative into the voltage dynamics (6.1a) or (3.39).

The electric port defined here aligns with the concept of ports in port-Hamiltonian system theory and Dirac structures, where the product of port variables yields power, representing the energy exchanged with the system. In contrast, the economic port defined next provides an interface for economic interconnection between grids, but does not use traditional physical effort-flow pairs (such as voltage-current or pressure-flow). Instead, it is formulated as an input-output pair of prices, which flexible prosumers use to determine and optimize their power injection. Although the economic port differs in nature from physical ports such as the electric port, its analysis follows the same methodological approach, which is the reason why it is also called a port. The properties of both ports are studied using EIP theory, and stability is established via a skew-symmetric interconnection structure. The formal definition of the economic port is given below.

Definition 6.2 (economic ports)
Let $\lambda_{\text{ext}} \in \mathbb{R}$ denote an external electric power price and $\lambda_{\text{loc}} \in \mathbb{R}$ the local price for a certain grid. The input-output pair $(\lambda_{\text{ext}}, \lambda_{\text{loc}})$ is called the economic port for grid $m \in \mathcal{M}$.

The input and output vectors $\boldsymbol{b}_{\text{econ}} \in \mathbb{R}^n$ and $\boldsymbol{c}_{\text{econ}} \in \mathbb{R}^n$ have to be defined such that they properly interface with the system dynamics. The output is the local price arising from the price-forming mechanism of the system operator, and thus $\boldsymbol{c}_{\text{econ}} = \text{col}\{0_{n_\mathcal{B}+2n_{\text{DGU}}+n_\mathcal{E}-1}, 1\}$, since the local price is defined as the last state in (6.31) in system (6.29). The input matrix has to be defined such that the external price λ_{ext} is

[67] Note that electric ports have been used in the literature for interconnecting DGUs and lines *within* a grid, as pointed out before. Definition 6.1 can hence be understood as leveraging these ports *between* grids in order to study the EIP properties of grids instead of individual nodes.

[68] This notation is introduced in Section 1.2.

routed to the flexible prosumers, i.e., $\boldsymbol{b}_{\text{econ}} = \text{col}\{0_{n_{\mathcal{B}}+2n_{\text{DGU}}+n_{\mathcal{E}}+1}, \mathbf{1}_{n_{\text{DGU}}-1}, 0\}$, since the states corresponding to the power generation are the second last vector of states in (6.31). Note that there is exactly one economic port in each grid. The local price can be seen as metric for the control effort to stabilize the grid, and the external price as a signal for the power injection of prosumers.

Remark 6.4. *An alternative approach to defining the economic ports is to include a direct feedthrough from the input price. Specifically, the output can be expressed as*

$$\hat{\lambda}_{\text{loc}} = \lambda_{\text{loc}} + \iota\lambda_{\text{ext}}, \tag{6.33}$$

where $\iota \in \mathbb{R}$ is a weighting parameter. This formulation introduces an additional degree of freedom, which may improve the EIP properties of the economic ports by leveraging the direct feedthrough of the external price on the local price.[69]

6.5 Analysis of a Single Grid

In this section, a scenario with a single grid is considered. Such an operation occurs whenever a grid disconnects from the other grids and operates in an islanded mode. This may happen due to communication failures or due to the choice of a system operator to not exchange power with other grids.

In an islanded mode, the grid has no electric ports, i.e., $n_{\text{ext}} = 0$. Furthermore, the economic port is closed with the simple feedback $u_{\text{econ}} = y_{\text{econ}}$, i.e., $\lambda_{\text{ext}} = \lambda_{\text{loc}}$. This means that the flexible prosumers act on the price directly as it comes out of the price-forming mechanism.

In the following subsection, the stability of a single, islanded grid as described above is analyzed using Lyapunov theory. Additionally, the steady states that arise in an islanded grid are examined to assess their optimality.[70] Since only one grid is considered, the superscript $m = 1$ is further omitted for the remainder of this section.

Stability of a Single Grid in Closed-Loop

Consider the grid system (6.29) equipped with economic ports, but without electric ports, i.e.,

$$\dot{\boldsymbol{x}} = \boldsymbol{A}(\boldsymbol{x})\boldsymbol{x} + \boldsymbol{b}_{\text{econ}}\lambda_{\text{ext}} \tag{6.34}$$

$$y_{\text{econ}} = \lambda_{\text{loc}} = \boldsymbol{c}_{\text{econ}}^{\top}\boldsymbol{x}. \tag{6.35}$$

[69] It is well known that a direct feedthrough improves the EIP properties of a system, more specifically the IFEIP index [SJK12, p. 36].

[70] Stability and optimality are thus two separate questions: stability answers if the system converges to a steady state, and optimality evaluates the quality of the steady states reached by the system.

Let the economic port be self-closed, i.e., $y_{\text{econ}} = u_{\text{econ}}$ or $\lambda_{\text{ext}} = \lambda_{\text{loc}}$, as shown in Figure 6.4.

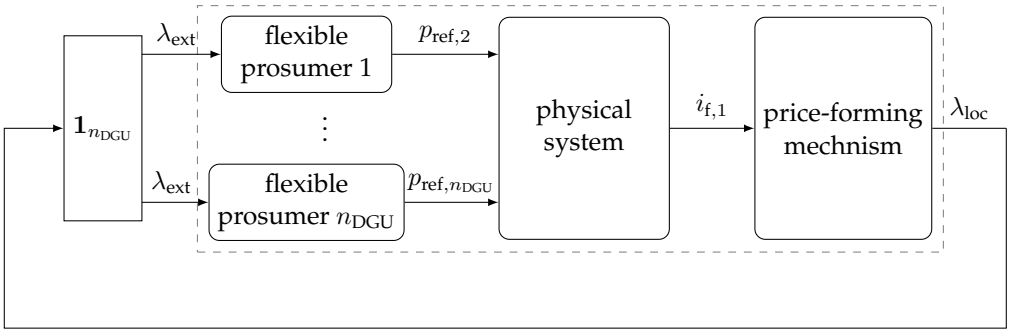

Figure 6.4: A single grid in islanded mode with self-closed economic ports and no electric ports.

Let $\bar{\boldsymbol{x}}$ denote a steady state arising from the closed-loop system with a constant v_{ref} for the grid-forming DGU. Next, shift system (6.34) to obtain

$$\dot{\tilde{\boldsymbol{x}}} = \boldsymbol{A}_{\text{s}}(\tilde{\boldsymbol{x}}, \bar{\boldsymbol{x}})\tilde{\boldsymbol{x}}, \tag{6.36}$$

where

$$\boldsymbol{A}_{\text{s}}(\tilde{\boldsymbol{x}}, \bar{\boldsymbol{x}}) = \begin{bmatrix} -\boldsymbol{C}_{\text{f}}^{-1}\text{diag}\{\tilde{i}_{\text{L},i}\} & \boldsymbol{C}_{\text{f}}^{-1}\boldsymbol{I}_{\text{f}} & 0 & -\boldsymbol{C}_{\text{f}}^{-1}\boldsymbol{E} & 0 & 0 \\ \alpha\boldsymbol{I}_{\text{f}}^{\top} & \boldsymbol{\beta} & \boldsymbol{\gamma} & 0 & 0 & 0 \\ -\boldsymbol{I}_v\boldsymbol{I}_{\text{f}}^{\top} - \boldsymbol{I}_p\text{diag}\{\bar{i}_{\text{f},i}\} & -\boldsymbol{I}_p\,\text{diag}\{\boldsymbol{I}_{\text{f}}^{\top}\boldsymbol{v}\} & 0 & 0 & \tilde{\boldsymbol{I}}_p & 0 \\ \boldsymbol{L}_{\pi}^{-1}\boldsymbol{E} & 0 & 0 & -\boldsymbol{L}_{\pi}^{-1}\boldsymbol{R}_{\pi} & 0 & 0 \\ 0 & 0 & 0 & 0 & -\text{diag}\{\tau_i\nabla\tilde{f}_{\text{flx},i}\} & \text{diag}\{\tau_i\} \\ 0 & -\kappa\mathbf{1}_{n_{\text{DGU}}}^{\top}\boldsymbol{I}_v & 0 & 0 & 0 & 0 \end{bmatrix}, \tag{6.37}$$

with

$$\tilde{i}_{\text{L},i} = \frac{i_{\text{L},i}(\bar{v}_i + \tilde{v}_i) - i_{\text{L},i}(\bar{v}_i)}{\tilde{v}_i} \tag{6.38}$$

and

$$\nabla\tilde{f}_{\text{flx},i} = \frac{\nabla f_{\text{flx},i}(\bar{p}_{\text{ref},i} + \tilde{p}_{\text{ref},i}) - \nabla f_{\text{flx},i}(\bar{p}_{\text{ref},i})}{\tilde{p}_{\text{ref},i}}. \tag{6.39}$$

Remark 6.5. *Note that the term $\tilde{i}_{\text{L},i}$ as in* (6.38)*, which appears in the voltage dynamics, represents the derivative of the nonlinear load map $i_{\text{L},i} : \mathbb{R} \to \mathbb{R}$ from* (3.31)*. Furthermore, it is well known that monotonicity properties of static maps are tightly connected to its EIP properties [SP18]. The load $i_{\text{L},i}$ is EIP if and only if it is monotone, i.e.,* (6.38) *is always greater or equal than zero. Observe also that the same argumentation holds for the objective function $\nabla\tilde{f}_i$ in the dynamics of $p_{\text{ref},i}$.*

Before stating the main stability theorem, the feasible set of the grid states is defined, which is used later in the stability analysis.

Definition 6.3 (feasible subspace)
The feasible subspace of the state space $\mathbb{X} \subset \mathbb{R}^n$ for safe operation is defined as

$$\mathbb{X} = \mathbb{V} \times \mathbb{I} \times \mathbb{R}^{2n_{DGU}+n_{\mathcal{E}}}, \tag{6.40}$$

where $\mathbb{V} = [\boldsymbol{v}_{\min}, \boldsymbol{v}_{\max}] \subset \mathbb{R}^{n_{\mathcal{B}}}$ and $\mathbb{I} = [\boldsymbol{i}_{f,\min}, \boldsymbol{i}_{f,\max}] \subset \mathbb{R}^{n_{DGU}}$ are polytopic sets describing maximum and minimum feasible node voltages and filter currents.

Further, define the sets of feasible steady states of voltages $\bar{\mathbb{V}}$ and filter currents $\bar{\mathbb{I}}$, and the load derivative bounds $\mathbb{L} = [\tilde{\boldsymbol{i}}_{\mathrm{L,min}}, \tilde{\boldsymbol{i}}_{\mathrm{L,max}}] \subset \mathbb{R}^{n_{\mathcal{B}}}$. In the following, a condition to assess stability of the closed-loop system by solving a semi-definite program is presented.

Theorem 6.2 (stability of the islanded grid)
Any equilibrium point of the grid system (6.36) *$\bar{\boldsymbol{x}}$ with $\bar{\boldsymbol{v}} \in \bar{\mathbb{V}}$ and $\bar{\boldsymbol{i}}_f \in \bar{\mathbb{I}}$ is asymptotically stable if there exists a symmetric $\boldsymbol{S} \in \mathbb{R}^{n \times n}$ such that*

$$\boldsymbol{S} > 0 \tag{6.41}$$

$$\boldsymbol{A}_s(\tilde{\boldsymbol{x}}, \bar{\boldsymbol{x}})^\top \boldsymbol{S} + \boldsymbol{S}\boldsymbol{A}_s(\tilde{\boldsymbol{x}}, \bar{\boldsymbol{x}}) < 0, \tag{6.42}$$

hold for all steady states $\bar{\boldsymbol{v}} \in \bar{\mathbb{V}}$, $\bar{\boldsymbol{i}}_f \in \bar{\mathbb{I}}$ and $\tilde{\boldsymbol{i}}_{\mathrm{L}} \in \mathbb{L}$, and for the subset of the state space $\tilde{\boldsymbol{v}} \in \tilde{\mathbb{V}}$, $\tilde{\boldsymbol{i}}_f \in \tilde{\mathbb{I}}$, where $\tilde{\mathbb{V}} = [\tilde{v}_{\min}, \tilde{v}_{\max}] \subset \mathbb{R}^{n_{\mathcal{B}}}$ and $\tilde{\mathbb{I}} = [\tilde{i}_{f,\min}, \tilde{i}_{f,\max}] \subset \mathbb{R}^{n_{DGU}}$ are sets describing the maximal deviation of node voltages and filter currents.

Proof. Denote $\tilde{\mathbb{X}} = \tilde{\mathbb{V}} \times \tilde{\mathbb{I}} \times \mathbb{R}^{2n_{\mathrm{DGU}}+n_{\mathcal{E}}}$. Consider the Lyapunov function $V : \tilde{\mathbb{X}} \to \mathbb{R}$ with $V(\tilde{\boldsymbol{x}}) = \tilde{\boldsymbol{x}}^\top \boldsymbol{S}\tilde{\boldsymbol{x}}$. With (6.41), the positive definiteness $V > 0$ in $\tilde{\mathbb{X}} - \{0\}$ is ensured, as well as $V(0) = 0$. The time derivative of the Lyapunov function is $\dot{V} = \tilde{\boldsymbol{x}}^\top \big(\boldsymbol{A}(\cdot)^\top \boldsymbol{S} + \boldsymbol{S}\boldsymbol{A}(\cdot)\big)\tilde{\boldsymbol{x}}$. The linear matrix inequality (6.42) ensures that the time derivative of the Lyapunov function is negative in $\tilde{\mathbb{X}} - \{0\}$ for any possible steady state $\bar{\boldsymbol{v}} \in \bar{\mathbb{V}}$, $\bar{\boldsymbol{i}}_{\mathrm{f}} \in \bar{\mathbb{I}}$. Thus, there exists a Lyapunov function fulfilling the conditions in [Kha02, Theorem 4.1] for all possible steady states, which implies asymptotically stability for any steady state contained in the feasible set. Likewise, the conditions (6.41) and (6.42) on the Lyapunov function hold for all loads within the derivative bounds $\mathbb{L}$, which makes it robust against load changes. □

Remark 6.6. *Computing a matrix $\boldsymbol{S}$ that fulfills* (6.41) *and* (6.42) *$\forall \tilde{\boldsymbol{x}} \in \tilde{\mathbb{X}}$, $\forall \bar{\boldsymbol{x}} \in \bar{\mathbb{X}}$ and $\forall \boldsymbol{i}_{\mathrm{L}} \in \mathbb{L}$ is a semi-definite program if the sets $\tilde{\mathbb{X}}, \bar{\mathbb{X}}$ and $\mathbb{L}$ are convex polytopes (see Section A.1).*

Then, matrix $\boldsymbol{S}$ has to satisfy (6.41) *and* (6.42) *for all the vertices of the convex hull of* $\tilde{\mathbb{X}}, \bar{\mathbb{X}}$, $\mathbb{L}$ *[Boy+94, Ch. 5.1].*

The next proposition characterizes the properties of equilibria of the islanded grid (6.36).

Proposition 6.3 (properties of equilibria in islanded mode)
Let $p_{\mathrm{L},\Sigma}$ be the total power usage of the islanded grid (6.36)*. All equilibria $\bar{\boldsymbol{x}}$ of the islanded grid are such that $p_{\mathrm{ref},i}$, $i \in \mathcal{F}$ fulfill*

$$\min_{p_{\mathrm{ref},i}} \sum_{i\in\mathcal{F}} f_{\mathrm{flx},i}(p_{\mathrm{ref},i}) \qquad \forall i \in \mathcal{F} \tag{6.43a}$$

$$\text{s.t.} \sum_{i\in\mathcal{F}} p_{\mathrm{ref},i} + p_{\mathrm{L},\Sigma} = 0. \tag{6.43b}$$

Proof. The proof consists in showing that all equilibria fulfill the KKT conditions of (6.43). The KKT conditions of (6.43) are

$$0 = -\nabla f_{\mathrm{flx},i} + \lambda_{\mathrm{M}}, \quad \forall i \in \mathcal{F} \tag{6.44a}$$

$$0 = \sum_{i\in\mathcal{F}} p_{\mathrm{ref},i} + p_{\mathrm{L},\Sigma}. \tag{6.44b}$$

The gradient descent of the power injection (6.23) automatically fulfills (6.44a) if the Lagrange multiplier λ_{M} corresponds to the external price λ_{ext}. The external and local prices are equal, $\lambda_{\mathrm{loc}} = \lambda_{\mathrm{ext}}$, since the economic port is self-closed. Thus, the dynamics of the price λ_{loc} of the grid evolves according to (6.28) (or, equivalently, as per Proposition 6.1, to (6.25)), which induces exactly the same steady state as the dual ascent of the constraint (6.44b). Consequently, all equilibria also fulfill (6.43). □

This means that the equilibria of an islanded grid are such that (i) the total usage of power $p_{\mathrm{L},\Sigma}$ is equal to the total power injection of the flexible proseumers, and (ii) the power injection of each flexible prosumer is such that it minimizer the sum of the cost functions of all flexible prosumers. This is a direct consequence of the price-forming mechanism, which is designed to achieve optimal dispatch in the grid and to ensure that the total power usage is equal to the total power injection.

6.6 Analysis of the Interconnection of Grids

After analyzing the stability properties of feasible equilibria of an islanded grid, the stability properties of a set of networked grids are studied in this section. For that,

passivity theory is leveraged to derive local conditions on the respective grids. Firstly, in Section 6.6.1, the EIP properties of a single grid are studied. In Section 6.6.2, stability of an electric interconnection of grids is studied. Lastly, in Section 6.6.3, an interconnection scheme for the economic ports leading to UMP is proposed and the stability of the electrically an economically networked grids are studied. Since various different grids are considered, the superscript m is recovered.

6.6.1 EIP Properties of a Grid

Consider the grid system $m \in \mathcal{M}$ with electric and economic ports described by

$$\dot{\boldsymbol{x}}^m = \boldsymbol{A}^m(\boldsymbol{x})\boldsymbol{x} + \boldsymbol{b}^m_{\text{econ}}\lambda^m_{\text{ext}} - \boldsymbol{B}^m_{\text{ext}}\boldsymbol{i}^m_{\text{ext}} \tag{6.45}$$

$$y^m_{\text{econ}} = \lambda^m_{\text{loc}} = \boldsymbol{c}^{m\top}_{\text{econ}}\boldsymbol{x}^m \tag{6.46}$$

$$\boldsymbol{y}^m_{\text{ext}} = \boldsymbol{v}^m_{\text{ext}} = \boldsymbol{C}^m_{\text{ext}}\boldsymbol{x}^m, \tag{6.47}$$

where $\boldsymbol{A}^m$ is the system matrix in (6.30), $\boldsymbol{B}^m_{\text{ext}}$ and $\boldsymbol{C}^m_{\text{ext}}$ are as in Definition 6.1, and $\boldsymbol{b}^m_{\text{econ}}$ and $\boldsymbol{c}^m_{\text{econ}}$ are as in Definition 6.2. The electric port $(-\boldsymbol{i}^m_{\text{ext}}, \boldsymbol{v}^m_{\text{ext}})$ is also denoted as $(\boldsymbol{u}^m_{\text{ext}}, \boldsymbol{y}^m_{\text{ext}})$, and the economic port $(\lambda^m_{\text{ext}}, \lambda^m_{\text{loc}})$ as $(u^m_{\text{econ}}, y^m_{\text{econ}})$. Note that the current $\boldsymbol{i}^m_{\text{ext}}$ enters negatively into the dynamics, as remarked in Definition 6.1. Shift the system to a feasible steady state $(\bar{\boldsymbol{x}}^m, \bar{\boldsymbol{u}}^m)$ to obtain

$$\dot{\tilde{\boldsymbol{x}}}^m = \boldsymbol{A}^m_{\text{s}}(\bar{\boldsymbol{x}}, \tilde{\boldsymbol{x}})\tilde{\boldsymbol{x}} + \boldsymbol{b}^m_{\text{econ}}\tilde{\lambda}^m_{\text{ext}} - \boldsymbol{B}^m_{\text{ext}}\tilde{\boldsymbol{i}}^m_{\text{ext}} \tag{6.48}$$

$$\tilde{y}^m_{\text{econ}} = \tilde{\lambda}^m_{\text{loc}} = \boldsymbol{c}^{m\top}_{\text{econ}}\tilde{\boldsymbol{x}}^m \tag{6.49}$$

$$\tilde{\boldsymbol{y}}^m_{\text{ext}} = \tilde{\boldsymbol{v}}^m_{\text{ext}} = \boldsymbol{C}^m_{\text{ext}}\tilde{\boldsymbol{x}}^m, \tag{6.50}$$

where $\boldsymbol{A}_{\text{s}}$ is the matrix in (6.37).

First, the EIP properties for the electric port are analyzed, assuming that each grid self-closes its economic port and thus there is no economic cooperation between grids.

Proposition 6.4 (EIP properties of electric port)
Let a grid self-close its economic port with $u^m_{\text{econ}} = \lambda^m_{\text{ext}} = y^m_{\text{econ}} = \lambda^m_{\text{loc}}$, i.e., without interconnecting economically with other grids. System (6.45) *is strictly EIP w.r.t. the electric port $(\tilde{\boldsymbol{v}}^m_{\text{ext}}, -\tilde{\boldsymbol{i}}^m_{\text{ext}})$ and the positive definite function $\Psi^m(\tilde{\boldsymbol{x}}^m) = \varrho^m_{\text{ext}}\tilde{\boldsymbol{x}}^{m\top}\tilde{\boldsymbol{x}}^m$ if a there exists a symmetric $\boldsymbol{S} \in \mathbb{R}^{n^m \times n^m}$ and a scalar ϱ^m_{ext} solving*

$$\boldsymbol{S} > 0 \tag{6.51a}$$

$$\begin{bmatrix} \boldsymbol{A}^m_s(\tilde{\boldsymbol{x}}^m, \bar{\boldsymbol{x}}^m)^\top \boldsymbol{S} + \boldsymbol{S}\boldsymbol{A}^m_s(\tilde{\boldsymbol{x}}^m, \bar{\boldsymbol{x}}^m) + \varrho^m_{\text{ext}}\boldsymbol{I}_{n^m} & \boldsymbol{S}\boldsymbol{B}^m_{\text{ext}} - \boldsymbol{C}^{m\top}_{\text{ext}} \\ \boldsymbol{B}^{m\top}_{\text{ext}}\boldsymbol{S} - \boldsymbol{C}^m_{\text{ext}} & \boldsymbol{0}_{n_{\text{ext}} \times n_{\text{ext}}} \end{bmatrix} \leq 0 \tag{6.51b}$$

$$\varrho^m_{\text{ext}} > 0 \tag{6.51c}$$

for all $\bar{\boldsymbol{x}}^m \in \bar{\mathbb{X}}$, $\tilde{\boldsymbol{x}}^m \in \tilde{\mathbb{X}}$ and $\tilde{\boldsymbol{i}}_{\mathrm{L}}^m \in \mathbb{L}$, with $\bar{\mathbb{X}}$, $\tilde{\mathbb{X}}$ and $\mathbb{L}$ defined as in Definition 6.3.

Proof. Consider the storage function $S(\tilde{\boldsymbol{x}}^m) = \tilde{\boldsymbol{x}}^{m\top} \boldsymbol{S} \tilde{\boldsymbol{x}}^m$ with $\boldsymbol{S} > 0$. The EIP condition $\dot{S} \leq \tilde{\boldsymbol{v}}_{\mathrm{ext}}^{m\top} (-\tilde{\boldsymbol{i}}_{\mathrm{ext}}^m) - \varrho_{\mathrm{ext}}^m \tilde{\boldsymbol{x}}^{m\top} \tilde{\boldsymbol{x}}^m = \tilde{\boldsymbol{x}}^{m\top} \boldsymbol{C}_{\mathrm{ext}}^\top \boldsymbol{B}_{\mathrm{ext}}^m \boldsymbol{u}_{\mathrm{ext}}^m - \varrho_{\mathrm{ext}}^m \tilde{\boldsymbol{x}}^{m\top} \tilde{\boldsymbol{x}}^m$ leads to the coupled LMIs (6.51) for the system with self-closed economic port, i.e., $\lambda_{\mathrm{ext}}^m = y_{\mathrm{econ}}^m$, by following the same steps as in Proposition 3.2. □

Remark 6.7. *LMI* (6.51) *is easy to solve numerically and solutions appear to exist with a wide range of voltage, currents and loads. This seems plausible since it is similar to the approaches in [Str+21; Nah+20], where similar EIP results are shown analytically with a similar system. The main difference, however, is that in the proposed approach, a price-forming mechanism and grid-following controllers are included, and that the EIP property is at grid level instead of node level.*

Proposition 6.4 ensures EIP w.r.t. the electric port and may serve for assessing stability of a scenario where different grids are interconnected via electric ports. Since an economic port is not considered, the electric power prices in the grids are independent, yielding optimal operation in each grid but suboptimal operation of the networked grids. This is shown later in a mathematically precise way in Proposition 6.7 in Section 6.6.2.

In order to interconnect the grids via the economic port and achieve an economic cooperation, the EIP properties of both port types are simultaneously studied.

Proposition 6.5 (EIP properties of electric and economic ports)
System (6.45) *is SIOEIP with indices ν_{econ}^m and ρ_{econ}^m and the positive definite function $\Psi^m(\tilde{\boldsymbol{x}}^m) = \varrho_{\mathrm{ext}}^m \tilde{\boldsymbol{x}}^{m\top} \tilde{\boldsymbol{x}}^m$ w.r.t. the electric $(\tilde{\boldsymbol{v}}_{\mathrm{ext}}^m, -\tilde{\boldsymbol{i}}_{\mathrm{ext}}^m)$ and economic ports $(\tilde{\lambda}_{\mathrm{ext}}^m, \tilde{\lambda}_{\mathrm{loc}}^m)$ if there exists a symmetric matrix $\boldsymbol{S} \in \mathbb{R}^{n^m \times n^m}$, and indices $\nu_{\mathrm{econ}}^m \in \mathbb{R}$, $\rho_{\mathrm{econ}}^m \in \mathbb{R}$ and $\varrho_{\mathrm{ext}}^m \in \mathbb{R}_{>0}$ such that*

$$\boldsymbol{S} > 0 \tag{6.52a}$$

$$\begin{bmatrix} \boldsymbol{X}(\tilde{\boldsymbol{x}}^m, \bar{\boldsymbol{x}}^m, \rho_{\mathrm{econ}}^m, \varrho_{\mathrm{ext}}^m) & \boldsymbol{S}\boldsymbol{B}_{\mathrm{ext}}^m - \boldsymbol{C}_{\mathrm{ext}}^{m\top} & \boldsymbol{S}\boldsymbol{b}_{\mathrm{econ}}^m - \boldsymbol{c}_{\mathrm{econ}}^{m\top} \\ \boldsymbol{B}_{\mathrm{ext}}^{m\top}\boldsymbol{S} - \boldsymbol{C}_{\mathrm{ext}}^m & \boldsymbol{0}_{n_{\mathrm{ext}}^m \times n_{\mathrm{ext}}^m} & \boldsymbol{0}_{n_{\mathrm{ext}}^m \times 1} \\ \boldsymbol{b}_{\mathrm{econ}}^{m\top}\boldsymbol{S} - \boldsymbol{c}_{\mathrm{econ}}^m & \boldsymbol{0}_{1 \times n_{\mathrm{ext}}^m} & \nu_{\mathrm{econ}}^m \end{bmatrix} \leq 0 \tag{6.52b}$$

$$\varrho_{\mathrm{ext}}^m > 0 \tag{6.52c}$$

holds for all $\bar{\boldsymbol{x}}^m \in \bar{\mathbb{X}}$, $\tilde{\boldsymbol{x}}^m \in \tilde{\mathbb{X}}$ and $\tilde{\boldsymbol{i}}_{\mathrm{L}}^m \in \mathbb{L}$, where

$$\boldsymbol{X}(\tilde{\boldsymbol{x}}^m, \bar{\boldsymbol{x}}^m, \rho_{\mathrm{econ}}^m, \varrho_{\mathrm{ext}}^m) = \boldsymbol{A}_{\mathrm{s}}^m(\tilde{\boldsymbol{x}}^m, \bar{\boldsymbol{x}}^m)^\top \boldsymbol{S} + \boldsymbol{S}\boldsymbol{A}_{\mathrm{s}}^m(\tilde{\boldsymbol{x}}^m, \bar{\boldsymbol{x}}^m) + \rho_{\mathrm{econ}}^m \boldsymbol{c}_{\mathrm{econ}}^{m\top} \boldsymbol{c}_{\mathrm{econ}}^m + \varrho_{\mathrm{ext}}^m \boldsymbol{I}. \tag{6.53}$$

Proof. Consider the storage function $S(\tilde{\boldsymbol{x}}^m) = \tilde{\boldsymbol{x}}^{m\top}\boldsymbol{S}\tilde{\boldsymbol{x}}^m$ with $\boldsymbol{S} > 0$. The EIP condition $\dot{S} \leq \boldsymbol{v}_{\text{ext}}^{m\top}(-\boldsymbol{i}_{\text{ext}}^m) + \tilde{\lambda}_{\text{loc}}^m\tilde{\lambda}_{\text{ext}}^m - \nu_{\text{econ}}^m(\tilde{\lambda}_{\text{ext}}^m)^2 - \rho_{\text{econ}}^m(\tilde{\lambda}_{\text{loc}}^m)^2 - \varrho_{\text{ext}}^m\tilde{\boldsymbol{x}}^{m\top}\tilde{\boldsymbol{x}}^m$ leads to (6.52b) when using (6.45) in the derivative of the storage function following the same steps as in Proposition 3.2. The indices ν_{econ}^m and ρ_{econ}^m indicate the excess or lack of passivity [SJK12, Ch. 2.2.2]. □

Remark 6.8. *Depending on the loads, parameters, topology or the DGUs of a grid, and due to $\boldsymbol{b}_{\text{econ}} \neq \boldsymbol{c}_{\text{econ}}^\top$, the indices ν_{econ}^m and ρ_{econ}^m may be negative, indicating a lack of passivity of the economic port. This may hamper to prove stability. Thus the lack of passivity needs to be compensated by a feedback structure as proposed in Section 6.6.3 or by using the alternative definition of economic ports as in Remark 6.4.*

In this subsection, the EIP properties of the interconnection ports in several scenarios have been studied. Next, an interconnection scheme for the electric and economic ports of networked grids ensuring global economic optimality and asymptotic stability is proposed.

6.6.2 Electric Interconnection of Grids

To highlight the effects of non-cooperation of the grids, first only electrically interconnected grids are considered. Each grid uses its own local price, i.e., $\lambda_{\text{ext}}^m = \lambda_{\text{loc}}^m$. In Section 6.6.3, an economic coordination scheme is proposed that yields UMP for the whole power system.

Consider a set $\mathcal{M}$ of independent grids with self-closed economic ports, each having n_{ext}^m electric ports. Define the network variables $\boldsymbol{x} = \text{col}\{\boldsymbol{x}^m\} \in \mathbb{R}^n$, $\boldsymbol{u} = \text{col}\{\boldsymbol{u}^m\} \in \mathbb{R}^{n_{\text{ext}}}$ and $\boldsymbol{y} = \text{col}\{\boldsymbol{y}^m\} \in \mathbb{R}^{n_{\text{ext}}}$, where $n = \sum_{m\in\mathcal{M}} n^m$ and $n_{\text{ext}} = \sum_{m\in\mathcal{M}} n_{\text{ext}}^m$ are the total number of states and electric ports in the set of grids $m \in \mathcal{M}$. Then, the set $\mathcal{M}$ of independent grids can be described by

$$\dot{\boldsymbol{x}} = \boldsymbol{A}(\boldsymbol{x})\boldsymbol{x} + \boldsymbol{B}_{\text{ext}}\boldsymbol{i}_{\text{ext}} \tag{6.54a}$$

$$\boldsymbol{y}_{\text{ext}} = \boldsymbol{v}_{\text{ext}} = \boldsymbol{C}_{\text{ext}}\boldsymbol{x}, \tag{6.54b}$$

with $\boldsymbol{A}(\boldsymbol{x}) = \text{diag}\{\boldsymbol{A}^m(\boldsymbol{x}^m)\} \in \mathbb{R}^{n\times n}$, $\boldsymbol{B}_{\text{ext}} = \text{diag}\{\boldsymbol{B}_{\text{ext}}^m\} \in \mathbb{R}^{n\times n_{\text{ext}}}$ and $\boldsymbol{C}_{\text{ext}} = \text{diag}\{\boldsymbol{C}_{\text{ext}}^m\} \in \mathbb{R}^{n_{\text{ext}}\times n}$. Note that system (6.54) may be shifted to a feasible steady state as done for a single grid in (6.37). Further, consider a set $\mathcal{E}_{\text{int}}$ of $n_{\mathcal{E},\text{int}} = |\mathcal{E}_{\text{int}}|$ lossy power lines[71]

$$\boldsymbol{L}_{\pi,\text{int}}\,\dot{\boldsymbol{i}}_{\pi,\text{int}} = -\boldsymbol{R}_{\pi,\text{int}}\,\boldsymbol{i}_{\pi,\text{int}} + \boldsymbol{v}_\Delta, \tag{6.55}$$

[71] Note that in Section 4.2.1, the grids are also interconnected via lossy power lines, and the skew-symmetric interconnection is exploited. This skew-symmetric interconnection is exploited here again.

where $\boldsymbol{i}_{\pi,\text{int}} = \text{col}\{i_{\pi,\text{int},j}\} \in \mathbb{R}^{n_{\mathcal{E},\text{int}}}$, $\boldsymbol{v}_\Delta = \text{col}\{v_{\Delta j}\} \in \mathbb{R}^{n_{\mathcal{E},\text{int}}}$ are the stacked states and inputs, and $\boldsymbol{R}_{\pi,\text{int}} = \text{diag}\{R_{\pi,\text{int},j}\} \in \mathbb{R}^{n_{\mathcal{E},\text{int}} \times n_{\mathcal{E},\text{int}}}$ and $\boldsymbol{L}_{\pi,\text{int}} = \text{diag}\{L_{\pi,\text{int},j}\} \in \mathbb{R}^{n_{\mathcal{E},\text{int}} \times n_{\mathcal{E},\text{int}}}$ the parameters of the power lines $j \in \mathcal{E}_{\text{int}}$. The grids (6.54) and the power lines (6.55) are interconnected according to the graph $\mathcal{G}_{\text{int}}$. The nodes represent a grid[72] $m \in \mathcal{M}$, respectively, and the edges represent power lines. Thus, the voltage drop over the power lines reads

$$\boldsymbol{v}_\Delta = \boldsymbol{E}_{\text{int}}^\top \boldsymbol{v}_{\text{ext}}, \tag{6.56}$$

where $\boldsymbol{E}_{\text{int}} \in \mathbb{R}^{n_{\text{ext}} \times n_{\mathcal{E},\text{int}}}$ is the incidence matrix of graph $\mathcal{G}_{\text{int}}$ and $\boldsymbol{v}_{\text{ext}} = \text{col}\{\boldsymbol{v}_{\text{ext}}^m\} \in \mathbb{R}^{n_{\text{ext}}}$ the voltages of the electric ports. The power line currents are associated with the grids with

$$-\boldsymbol{i}_{\text{ext}} = -\boldsymbol{E}_{\text{int}} \boldsymbol{i}_{\pi,\text{int}}. \tag{6.57}$$

In the following, the stability results of the grids interconnected via electric power lines are presented.

Theorem 6.6 (stability of electrically networked grids)
Let the group of independent grids $m \in \mathcal{M}$ in (6.54) *be interconnected via* (6.56) *and* (6.57) *with the power line dynamics* (6.55)*. Further, let all grids $m \in \mathcal{M}$ fulfill Proposition 6.4. Then, any feasible steady state of the networked grids is asymptotically stable.*

Proof. Consider the Lyapunov function for any feasible steady state $(\bar{\boldsymbol{x}}, \bar{\boldsymbol{i}}_{\pi,\text{int}})$

$$V(\tilde{\boldsymbol{x}}, \tilde{\boldsymbol{i}}_{\pi,\text{int}}) = \tilde{\boldsymbol{x}}^\top \boldsymbol{S} \tilde{\boldsymbol{x}} + \tilde{\boldsymbol{i}}_{\pi,\text{int}}^\top \boldsymbol{L}_{\pi,\text{int}} \tilde{\boldsymbol{i}}_{\pi,\text{int}} \tag{6.58}$$

where $\boldsymbol{S} = \text{diag}\{\boldsymbol{S}^m\}$ is composed of the matrices computed in Proposition 6.4 for each grid $m \in \mathcal{M}$. The derivative of (6.58) along the shifted dynamics of (6.54) and (6.55) reads

$$\begin{aligned}
\dot{V} &= \tilde{\boldsymbol{x}}^\top \boldsymbol{S} \dot{\tilde{\boldsymbol{x}}} + \dot{\tilde{\boldsymbol{x}}}^\top \boldsymbol{S} \tilde{\boldsymbol{x}} + \dot{\tilde{\boldsymbol{i}}}_{\pi,\text{int}}^\top \boldsymbol{L}_{\pi,\text{int}} \dot{\tilde{\boldsymbol{i}}}_{\pi,\text{int}} + \dot{\tilde{\boldsymbol{i}}}_{\pi,\text{int}}^\top \boldsymbol{L}_{\pi,\text{int}} \tilde{\boldsymbol{i}}_{\pi,\text{int}} \\
&= \tilde{\boldsymbol{x}}^\top \Big(\boldsymbol{A}_{\text{s}}(\tilde{\boldsymbol{x}}, \bar{\boldsymbol{x}})^\top \boldsymbol{S} + \boldsymbol{S} \boldsymbol{A}_{\text{s}}(\tilde{\boldsymbol{x}}, \bar{\boldsymbol{x}}) \Big) \tilde{\boldsymbol{x}} - 2 \tilde{\boldsymbol{x}}^\top \boldsymbol{S} \boldsymbol{B}_{\text{ext}} \tilde{\boldsymbol{i}}_{\text{ext}} - 2 \tilde{\boldsymbol{i}}_{\pi,\text{int}}^\top \boldsymbol{R}_{\pi,\text{int}} \tilde{\boldsymbol{i}}_{\pi,\text{int}} + 2 \tilde{\boldsymbol{v}}_\Delta^\top \tilde{\boldsymbol{i}}_{\pi,\text{int}},
\end{aligned} \tag{6.59}$$

where $\boldsymbol{A}_{\text{s}}(\tilde{\boldsymbol{x}}, \bar{\boldsymbol{x}}) = \text{diag}\{\boldsymbol{A}_{\text{s}}^m(\tilde{\boldsymbol{x}}^m, \bar{\boldsymbol{x}}^m)\}$ is the shifted system matrix as in (6.37). Note that the LMI (6.51b) in Proposition 6.4 implies[73] $\boldsymbol{A}_{\text{s}}(\tilde{\boldsymbol{x}}, \bar{\boldsymbol{x}})^\top \boldsymbol{S} + \boldsymbol{S} \boldsymbol{A}_{\text{s}}(\tilde{\boldsymbol{x}}, \bar{\boldsymbol{x}}) + \varrho^{\min} \tilde{\boldsymbol{x}}^\top \tilde{\boldsymbol{x}} \leq 0$

[72] More precisely, the nodes are not the grids but the n_{ext} electric ports of the grids where the lines are connected. This ensures a correct mathematical representation of the interconnection via the incidence matrix $\boldsymbol{E}_{\text{int}} \in \mathbb{R}^{n_{\text{ext}} \times n_{\mathcal{E},\text{int}}}$ which is compatible with the electric ports of the grids in (6.54).

[73] Take into account that LMI (6.51b) is for a single grid m, and here it is considered the aggregated grids.

with $\varrho^{\min} = \min_m \varrho^m \in \mathbb{R}_{>0}$ and $\boldsymbol{S}\boldsymbol{B}_{\text{ext}} = \boldsymbol{C}_{\text{ext}}$ (see Proposition C.1 in Section C.1). Substituting $\boldsymbol{S}\boldsymbol{B}_{\text{ext}} = \boldsymbol{C}_{\text{ext}}$ and (6.57) into the second term, and (6.56) into the fourth, it yields

$$\begin{aligned}\dot{V} = \tilde{\boldsymbol{x}}^\top \Big(\boldsymbol{A}_{\text{s}}(\tilde{\boldsymbol{x}}, \bar{\boldsymbol{x}})^\top \boldsymbol{S} + \boldsymbol{S}\boldsymbol{A}_{\text{s}}(\tilde{\boldsymbol{x}}, \bar{\boldsymbol{x}}) \Big) \tilde{\boldsymbol{x}} - 2\tilde{\boldsymbol{x}}^\top \boldsymbol{C}_{\text{ext}} \boldsymbol{E}_{\text{int}} \tilde{\boldsymbol{i}}_{\pi,\text{int}} \\ - 2\tilde{\boldsymbol{i}}_{\pi,\text{int}}^\top \boldsymbol{R}_{\pi,\text{int}} \tilde{\boldsymbol{i}}_{\pi,\text{int}} + 2\tilde{\boldsymbol{v}}_{\text{ext}} \boldsymbol{E}_{\text{int}} \tilde{\boldsymbol{i}}_{\pi,\text{int}}. \end{aligned} \tag{6.60}$$

Recall that $\tilde{\boldsymbol{y}}_{\text{ext}} = \tilde{\boldsymbol{v}}_{\text{ext}} = \boldsymbol{C}_{\text{ext}} \tilde{\boldsymbol{x}}$ and insert it in the second term of (6.60) to obtain

$$\dot{V} = \tilde{\boldsymbol{x}}^\top \Big(\boldsymbol{A}_{\text{s}}(\tilde{\boldsymbol{x}}, \bar{\boldsymbol{x}})^\top \boldsymbol{S} + \boldsymbol{S}\boldsymbol{A}_{\text{s}}(\tilde{\boldsymbol{x}}, \bar{\boldsymbol{x}}) \Big) \tilde{\boldsymbol{x}} - 2\boldsymbol{v}_{\text{ext}} \boldsymbol{E}_{\text{int}} \tilde{\boldsymbol{i}}_{\pi,\text{int}} \tag{6.61}$$

$$- 2\tilde{\boldsymbol{i}}_{\pi,\text{int}}^\top \boldsymbol{R}_{\pi,\text{int}} \tilde{\boldsymbol{i}}_{\pi,\text{int}} + 2\tilde{\boldsymbol{v}}_{\text{ext}} \boldsymbol{E}_{\text{int}} \tilde{\boldsymbol{i}}_{\pi,\text{int}} \tag{6.62}$$

$$\leq \tilde{\boldsymbol{x}}^\top \Big(\boldsymbol{A}_{\text{s}}(\tilde{\boldsymbol{x}}, \bar{\boldsymbol{x}})^\top \boldsymbol{S} + \boldsymbol{S}\boldsymbol{A}_{\text{s}}(\tilde{\boldsymbol{x}}, \bar{\boldsymbol{x}}) \Big) \tilde{\boldsymbol{x}} - 2\tilde{\boldsymbol{i}}_{\pi,\text{int}}^\top \boldsymbol{R}_{\pi,\text{int}} \tilde{\boldsymbol{i}}_{\pi,\text{int}}, \tag{6.63}$$

where the last inequality arises cancelling out the second and fourth term. Taking into account the LMI (6.51b) and that $\boldsymbol{R}_{\pi,\text{int}}$ is positive definite, it follows that $\dot{V} < 0$ for all $\tilde{\boldsymbol{x}}, \tilde{\boldsymbol{i}}_{\pi,\text{int}}$ other than zero. With classic Lyapunov theory [Kha02, Ch. 4], asymptotic stability of any feasible equilibrium $\bar{\boldsymbol{x}}$ follows. □

Remark 6.9. *Theorem 6.6 can also be proven using the classical passivity theory [Kha02, Th. 6.3], since the interconnection between the independent grids and independent lines can be seen as a skew-symmetric interconnection (see Figure 6.5). Note that this is exactly the same interconnection structure as exploited in Chapter 5 for the novel distributed optimization framework, with the grids corresponding to the node systems Σ and the lines corresponding to the edge systems Π. One of the main differences is that the edge systems, here the power lines, are not systems with integral action as in Definition 5.1, but rather have first order lag dynamics. As a consequence, the voltages of the electric ports are not in consensus as it is the case with the estimations of the global optimizer of different agents in Chapter 5.*

With Theorem 6.6, it is proven that any feasible steady state is asymptotically stable, and that the convergence is to a point. In the next proposition, the properties of the equilibria of the electrically networked grids are studied. In particular, it is shown that, within each grid, the DGUs are operated economically optimal. However, the lack of cooperation due to not using the economic ports yields a globally suboptimal operation of the electrically networked grids.

Before introducing the proposition, some important variables are defined. The total power usage of all grids $m \in \mathcal{M}$ is denoted as $p_{\text{L},\Sigma} = \sum_{m\in\mathcal{M}} p_{\text{L},\Sigma}^m$, where $p_{\text{L},\Sigma}^m$ is the power usage of grid $m \in \mathcal{M}$ as introduced in Section 6.5. Further, denote $\hat{p}_{\text{L},\Sigma}^m$ as the power injected by grid $m \in \mathcal{M}$, which does not necessarily coincide with the power usage in that particular grid $m \in \mathcal{M}$. For having power balance, it needs to hold that

$$\sum_{m\in\mathcal{M}} \hat{p}_{\text{L},\Sigma}^m = p_{\text{L},\Sigma}. \tag{6.64}$$

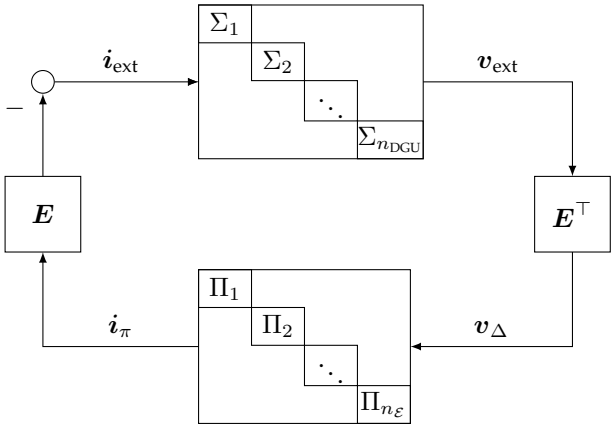

Figure 6.5: Feedback structure representing the interconnection between independent grid systems Σ and power lines Π. The block diagonal structure indicates that the node (and edge) systems are not directly dynamically coupled.

Now, the proposition is presented. An extensive interpretation of the results is provided afterwards.

Proposition 6.7 (properties of equilibria of electrically networked grids)
Consider the group of networked grids interconnected via lossy power lines as in Theorem 6.6, and let the grids fulfill Proposition 6.4. Assign the transmission losses of the power lines arbitrarily to grids $m \in \mathcal{M}$. Further, as introduced above, let $\hat{p}^m_{\text{L},\Sigma}$ be the power that grid $m \in \mathcal{M}$ is injecting, which does not necessarily correspond to its power usage $p^m_{\text{L},\Sigma}$. Then, at steady state, the power injections $\bar{p}^m_{\text{ref},i}$ of each DGU $i \in \mathcal{F}^m$ in grid $m \in \mathcal{M}$ are also the solution to the optimization problem

$$\min_{p^m_{\text{ref},i}} \sum_{i \in \mathcal{F}^m} f^m_{\text{flx},i}(p^m_{\text{ref},i}) \quad \forall i \in \mathcal{F}^m, \forall m \in \mathcal{M} \tag{6.65a}$$

$$\text{s.t.} \sum_{i \in \mathcal{F}^m} p^m_{\text{ref},i} + \hat{p}^m_{\text{L},\Sigma} = 0 \quad \forall m \in \mathcal{M}. \tag{6.65b}$$

Furthermore, at steady state, the global power balance equation

$$\sum_{m \in \mathcal{M}} \hat{p}^m_{\text{L},\Sigma} = \sum_{m \in \mathcal{M}} p^m_{\text{L},\Sigma} \tag{6.66}$$

is always fulfilled.

Proof. The Lagrange function for optimization problem (6.65) in each grid $m \in \mathcal{M}$ is given by

$$L^m_{\text{ext}} = \sum_{i \in \mathcal{F}^m} f^m_{\text{flx},i}(p^m_{\text{ref},i}) + \lambda^m_{\text{M}} \Bigg(\sum_{i \in \mathcal{F}^m} p^m_{\text{ref},i} + \hat{p}^m_{\text{L},\Sigma} \Bigg), \tag{6.67}$$

where $\lambda^m_{\text{M}} \in \mathbb{R}$ is the Lagrange multiplier corresponding to the power balance constraint (6.65b) of each grid $m \in \mathcal{M}$. Then, the KKT conditions of (6.65) are

$$0 = -\nabla f^m_{\text{flx},i} + \lambda^m_{\text{M}}, \quad \forall i \in \mathcal{F}^m, \forall m \in \mathcal{M} \tag{6.68a}$$

$$0 = \sum_{i \in \mathcal{F}^m} p^m_{\text{ref},i} + \hat{p}^m_{\text{L},\Sigma}, \quad \forall m \in \mathcal{M} \tag{6.68b}$$

The proof consists in showing that every equilibrium of the electrically networked grids $m \in \mathcal{M}$ fulfills (6.68), which corresponds to the optimization problems (6.65) for each $m \in \mathcal{M}$, and that (6.66) is automatically fulfilled at any steady state. The gradient descent dynamics of the power injection (6.23) automatically fulfills (6.68a) if the Lagrange multiplier λ^m_{M} corresponds to the external price λ^m_{ext}. The external and local prices are equal, $\lambda^m_{\text{loc}} = \lambda^m_{\text{ext}}$, since the economic ports are self-closed. The dynamics of the price λ^m_{loc} of every grid evolve according to (6.28) (or, equivalently, as per Proposition 6.1, to (6.25)). Observing the price dynamics (6.25), it becomes clear that at steady state, the constraint (6.68b) is fulfilled, since the error of constraint (6.68b) changes the local price λ^m_{loc}. Consequently, the local prices λ^m_{loc} correspond, at steady state, exactly to the Lagrange multipliers λ^m_{M}. Furthermore, at steady state, all prices λ^m_{loc}, $m \in \mathcal{M}$ are constant. This implies, due to the integral action in (6.28), that no grid-forming DGU has to provide control effort to stabilize the system, which occurs when power balance is met as per Proposition 6.1. Thus, (6.66) is automatically fulfilled at steady state. □

Note that the equilibria of electrically networked grids are characterized by n_{mg} individual optimization problems (6.65) over each individual grid $m \in \mathcal{M}$ coupled implicitly via the global power balance equation (6.66) that holds at any steady state. There exist an infinite number of solutions to this coupled optimization problem, since the constants $\hat{p}^m_{\text{L},\Sigma} \in \mathbb{R}$ in constraints (6.65b) are not further specified and do not need to meet further criteria other than the global power balance (6.66). This results in no coordination of the power injection *between* grids, since any power injection configuration ensuring power balance is a valid optimizer. However, *within* each grid $m \in \mathcal{M}$, the power injections $p^m_{\text{ref},i}$ are coordinated and each DGU $i \in \mathcal{B}^m_{\text{DGU}}$ injects power $p_{\text{ref},i}$ at marginal cost, since all the DGUs within a grid $m \in \mathcal{M}$ receive the same price λ_{M} as is seen in (6.68a).

The power sharing arising between grids is not controllable and depends on the dynamics of each grid and the initial values. In particular, it depends on the time constant κ^m in the price-forming mechanism of each grid. A grid having an aggressive price-forming mechanism, i.e., $\kappa^m \gg 1$, is prone to reach steady states with a very low price (thus injecting less power and contributing only to a small share of the total power usage of

all grids, i.e., $\hat{p}^m_{\mathrm{L},\Sigma} \ll p_{\mathrm{L},\Sigma}$) or very large prices (thus contributing to a large share of the total power usage, possibly more than the load within the grid itself, i.e., $\hat{p}^m_{\mathrm{L},\Sigma} \gg p^m_{\mathrm{L},\Sigma}$).

The following academic example illustrates the operating principle of two electrically interconnected grids.

Example 6.1:

Consider two grids electrically interconnected via electric ports over two power lines as in Figure 6.6. Nodes with grid-forming DGU are represented as a red square, nodes with grid-following DGU as a green circle, and load nodes in gray. Recall that a load can also be present in a node with a grid-forming or grid-following DGU. Grid 1 consists of eight nodes, from which three contain grid-following DGUs (nodes 1, 2 and 3) and one a grid-forming DGU (node 4), representing the system operator and implementing the price-forming mechanism for stabilizing the system. Grid 2 consists of four nodes, including two grid-following (nodes 1 and 4) and one grid-forming DGU (node 3). Table 6.1 shows the variation of the loads in both grids over time. The cost of the power injection is set to $f^m_{\mathrm{flx},i}(p^m_{\mathrm{ref},i}) = q^m_i (p^m_{\mathrm{ref},i})^2$*, and the parameter* q^m_i *is given in Table 6.2 for all DGUs.*

Table 6.1: Total grid load.

	$0\,\mathrm{s} - 20\,\mathrm{s}$	$20\,\mathrm{s} - 40\,\mathrm{s}$	$40\,\mathrm{s} - 60\,\mathrm{s}$
Grid 1	$16\,\mathrm{kW}$	$20.4\,\mathrm{kW}$	$9.5\,\mathrm{kW}$
Grid 2	$8\,\mathrm{kW}$	$8\,\mathrm{kW}$	$11\,\mathrm{kW}$
Sum	$24\,\mathrm{kW}$	$28.4\,\mathrm{kW}$	$20.5\,\mathrm{kW}$

Table 6.2: Parameter q^m_i of quadratic cost of power injection of the DGUs in both grids. The DGUs are numerated as number of the node.

	DGU 1	*DGU 2*	*DGU 3*	*DGU 4*
Grid 1	*1.2*	*1.3*	*1.4*	-
Grid 2	*1.4*	-	-	*1.5*

The power injection of the grid-following DGUs and the price in both grids are shown in Figures 6.7 and 6.8, respectively. When the load step at $t_1 = 20\,\mathrm{s}$ *occurs, the DGUs in Grid 1 increase their power injection, while the DGUs in Grid 2 decrease their power injection, even if the sum of the loads increases and the load in Grid 2 remains constant (see Table 6.1). At* $t_2 = 40\,\mathrm{s}$*, the power injection in Grid 1 decreases and increases in Grid 2, following the trend of their own load (see Table 6.1). The power injections follow proportionally the price in Figure 6.8. It can be clearly observed that the resulting price (and thus the power injections) do not follow any specific coordination such as power sharing, but result from the system dynamics, especially from the grid-forming DGUs.*

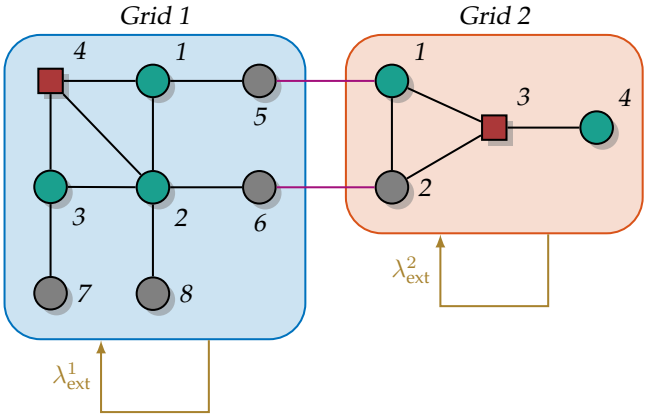

Figure 6.6: Schematic representation of the two electrically (purple) interconnected grids and self-closed economic ports (brown). The grid-following DGUs are represented as green circles, and the grid-forming DGUs as red squares.

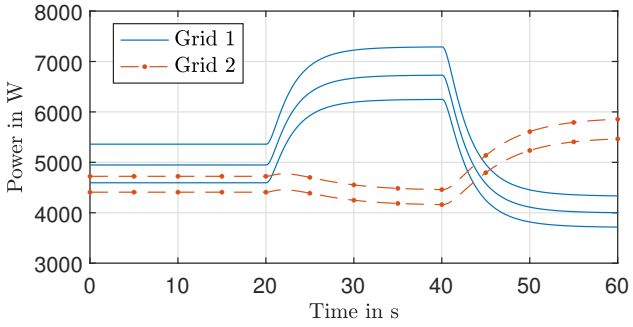

Figure 6.7: Power generation of the DGUs of both grids over the simulation time.

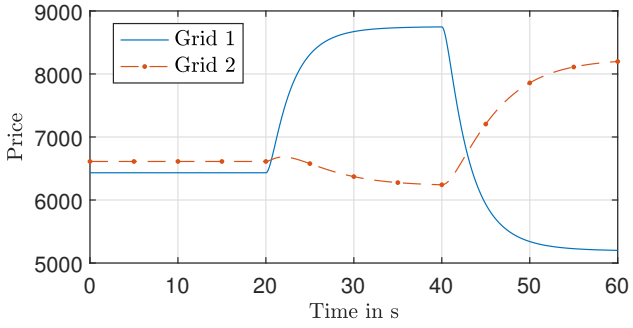

Figure 6.8: Local price of both grids over the simulation time.

In this subsection, the asymptotic stability of electrically networked grids has been shown. Furthermore, it has been shown that the prices arising in each grid in closed-

loop operation are not controllable, which results in a changing, non-assignable power-sharing configuration. In order to achieve a power-sharing configuration corresponding to the minimal cost in the power system (i.e., all networked grids), economic ports as per Definition 6.2 are used. Next, an interconnection scheme for economic ports is proposed.

6.6.3 Economic Interconnection of Grids

In this section, the stability properties of electrically *and* economically networked grids are analyzed. For that, the EIP properties of a single grid as established in Proposition 6.5 are exploited. Moreover, an interconnection scheme for the economic ports yielding UMP is proposed.

Consider a set $\mathcal{M}$ of $n_{\text{mg}} = |\mathcal{M}|$ grids with electric and economic ports as in (6.45). Defining network variables analogously to (6.54), the set $\mathcal{M}$ of grids is described by

$$\dot{\boldsymbol{x}} = \boldsymbol{A}(\boldsymbol{x})\boldsymbol{x} + \boldsymbol{B}_{\text{econ}}\boldsymbol{u}_{\text{econ}} + \boldsymbol{B}_{\text{ext}}\boldsymbol{i}_{\text{ext}} \tag{6.69a}$$

$$\boldsymbol{y}_{\text{econ}} = \boldsymbol{\lambda}_{\text{loc}} = \boldsymbol{C}_{\text{econ}}\boldsymbol{x} \tag{6.69b}$$

$$\boldsymbol{y}_{\text{ext}} = \boldsymbol{v}_{\text{ext}} = \boldsymbol{C}_{\text{ext}}\boldsymbol{x}, \tag{6.69c}$$

with $\boldsymbol{y}_{\text{ext}}, \boldsymbol{i}_{\text{ext}} \in \mathbb{R}^{n_{\text{ext}}}$ and $\boldsymbol{y}_{\text{econ}} = \text{col}\{y^m_{\text{econ}}\} = \text{col}\{\lambda^m_{\text{loc}}\} \in \mathbb{R}^{n_{\text{mg}}}$, $\boldsymbol{u}_{\text{econ}} = \text{col}\{u^m_{\text{econ}}\} = \text{col}\{\lambda^m_{\text{ext}}\} \in \mathbb{R}^{n_{\text{mg}}}$, since each grid $m \in \mathcal{M}$ has exactly one economic port. Further, consider a set $\mathcal{E}_{\text{int}}$ of lossy power lines

$$\boldsymbol{L}_{\pi,\text{int}}\,\dot{\boldsymbol{i}}_{\pi,\text{int}} = -\boldsymbol{R}_{\pi,\text{int}}\,\boldsymbol{i}_{\pi,\text{int}} + \boldsymbol{v}_{\Delta}, \tag{6.70}$$

interconnected with (6.69) via the electric ports with (6.56) and (6.57). Note that, in contrast to Section 6.6.2, the economic ports remain open and can be used to design an economic cooperation. An interconnection scheme achieving such an economic cooperation by inducing a UMP in the whole power system is proposed in the following.

Interconnection Scheme for Economic Ports

The grids are interconnected economically via the economic ports according to the graph $\mathcal{G}_{\text{econ}}(\mathcal{M}, \mathcal{E}_{\text{econ}})$. The set $\mathcal{E}_{\text{econ}}$ contains the edges, where $(i, j) \in \mathcal{E}_{\text{econ}}$ means that the grids i and $j \in \mathcal{M}$ exchange their local prices. The graph $\mathcal{G}_{\text{econ}}$ is assumed to be undirected, i.e $(i, j) \in \mathcal{E}_{\text{econ}}$ implies $(j, i) \in \mathcal{E}_{\text{econ}}$. Before designing the interconnection scheme, a globally optimal steady state for economically networked grids is characterized. The following proposition represents the counterpart of Proposition 6.7 but with an economic cooperation of the grids $m \in \mathcal{M}$ realized through the economic port (i.e., the local and external prices).

Proposition 6.8 (global optimal dispatch with UMP)
Consider a group of electrically networked grids $m \in \mathcal{M}$. Further, let the external electric power prices $\lambda^m_{\text{ext}} \in \mathbb{R}$ be equal for all grids $m \in \mathcal{M}$, i.e.,

$$\lambda^m_{\text{ext}} = \bar{\lambda}, \qquad \forall m \in \mathcal{M} \tag{6.71}$$

with a constant $\bar{\lambda} \in \mathbb{R}_{>0}$. Then, at steady state, the power injections $\bar{p}^m_{\text{ref},i}$ of the all networked grids fulfill the global optimal dispatch problem

$$\min_{p^m_{\text{ref},i}} \sum_{m\in\mathcal{M}} \sum_{i\in\mathcal{F}^m} f^m_{\text{flx},i} \tag{6.72a}$$

$$\text{s.t.} \sum_{m\in\mathcal{M}} \sum_{i\in\mathcal{F}^m} p^m_{\text{ref},i} + \sum_{m\in\mathcal{M}} p^m_{\text{L},\Sigma} = 0 \tag{6.72b}$$

where $\sum_{m\in\mathcal{M}} p^m_{\text{L},\Sigma}$ is the total power usage over all grids.

Proof. The proof consists in relating the optimization problems (6.65) in Proposition 6.7 with (6.72) by taking into account condition (6.71). First, problem (6.65) is recalled and the implication of condition (6.71), i.e., that the external prices are all equal and constant, is explored.

Consider the sum of the Lagrange functions (6.67) of problem (6.65) of all grids $m \in \mathcal{M}$

$$L_{\text{econ}} = \sum_{m\in\mathcal{M}} L^m_{\text{ext}} \tag{6.73}$$

$$= \sum_{m\in\mathcal{M}} \left\{ \sum_{i\in\mathcal{F}^m} f^m_{\text{flx},i} + \lambda^m_{\text{M}} \left(\sum_{i\in\mathcal{F}^m} p^m_{\text{ref},i} + \hat{p}^m_{\text{L},\Sigma} \right) \right\} \tag{6.74}$$

$$= \sum_{m\in\mathcal{M}} \sum_{i\in\mathcal{F}^m} f^m_{\text{flx},i} + \sum_{m\in\mathcal{M}} \lambda^m_{\text{M}} \left(\sum_{i\in\mathcal{F}^m} p^m_{\text{ref},i} + \hat{p}^m_{\text{L},\Sigma} \right). \tag{6.75}$$

Observe that with condition (6.71), the function (6.73) reads

$$L_{\text{econ}} = \sum_{m\in\mathcal{M}} \sum_{i\in\mathcal{F}^m} f^m_{\text{flx},i} + \bar{\lambda} \left(\sum_{m\in\mathcal{M}} \sum_{i\in\mathcal{F}^m} p^m_{\text{ref},i} + \sum_{m\in\mathcal{M}} \hat{p}^m_{\text{L},\Sigma} \right). \tag{6.76}$$

Taking into account that at steady state, (6.66) holds, the function L_{econ} reads

$$L_{\text{econ}} = \sum_{m\in\mathcal{M}} \sum_{i\in\mathcal{F}^m} f^m_{\text{flx},i} + \bar{\lambda} \left(\sum_{m\in\mathcal{M}} \sum_{i\in\mathcal{F}^m} p^m_{\text{ref},i} + \sum_{m\in\mathcal{M}} p^m_{\text{L},\Sigma} \right). \tag{6.77}$$

Note that (6.77) is in one to one correspondence with the Lagrange function of (6.72). Thus, imposing a common price in the grid-specific individual optimization problems (6.65) leads to global optimal dispatch (6.72). Mathematically speaking, imposing equal Lagrange multipliers leads to an aggregation of the respective constraints. □

It directly follows from Proposition 6.8 that it suffices to give a uniform price over the whole power system in addition to stabilizing the system in order to achieve global optimal dispatch. The question is how to compute the uniform price $\bar{\lambda}$ that stabilizes the system. In power systems nowadays, this stabilizing uniform price is computed in the market via a merit order mechanism which ensures that generation meets demand. The approach presented in the following proposes to compute the stabilizing price directly in the feedback via a distributed averaging algorithm. This allows to achieve the uniform price $\bar{\lambda}$ in a distributed manner, without the need for a central entity. Furthermore, it is more suited for power systems with a large share of volatile renewable generation, since the price is computed in feedback and taking into account the current state of the grid, rather than being computed in advance and being fixed for a certain time period (cf. Section 2.1.2).

To achieve $\lambda_{\text{ext}}^m = \bar{\lambda}$ for all $m \in \mathcal{M}$ at steady state as in Proposition 6.8, a distributed averaging algorithm is proposed. In such algorithms, the grids perform a distributed dynamic averaging of the local prices $y_{\text{econ}}^m = \lambda_{\text{loc}}^m$, i.e., the outputs of the economic port. The output $\boldsymbol{y}_{\text{DA}}$ of the distributed dynamic averaging is used as the external price λ_{ext}^m, i.e., the input of the economic port. The main requirement for achieving consensus is that the communication graph $\mathcal{G}_{\text{econ}}$ is connected. Such a distributed dynamic averaging reads

$$\mathcal{S}_{\text{DA}}: \quad \begin{aligned} \dot{\boldsymbol{x}}_{\text{DA}} &= \boldsymbol{f}_{\text{DA}}(\boldsymbol{x}_{\text{DA}}, \boldsymbol{u}_{\text{DA}}) \\ \boldsymbol{y}_{\text{DA}} &= \boldsymbol{C}_{\text{DA}} \boldsymbol{x}_{\text{DA}}, \end{aligned} \tag{6.78}$$

and it is interconnected with the economic ports of the grids with

$$\boldsymbol{u}_{\text{DA}} = -\boldsymbol{y}_{\text{econ}} = -\boldsymbol{\lambda}_{\text{loc}} \tag{6.79a}$$

$$\boldsymbol{u}_{\text{econ}} = \boldsymbol{y}_{\text{DA}} = \boldsymbol{\lambda}_{\text{ext}}, \tag{6.79b}$$

with $\boldsymbol{u}_{\text{DA}}, \boldsymbol{y}_{\text{DA}} \in \mathbb{R}^{n_{\text{mg}}}$ and $\boldsymbol{y}_{\text{econ}}, \boldsymbol{u}_{\text{econ}} \in \mathbb{R}^{n_{\text{mg}}}$. The output of the economic port in (6.79a) is negative in order to achieve a skew-symmetric interconnection (6.79) between the grids and the distributed averaging as required by the EIP stability analysis. This negative sign will be taken into account in the design of the distributed averaging in the following.

One of the main properties of such a distributed averaging is that, at steady state, each output in the output vector $\boldsymbol{y}_{\text{DA}}$ is the average of the inputs if a connected communication graph is used. Thus, with the interconnection (6.79), the external prices λ_{ext}^m (which are the inputs of the economic port $u_{\text{econ}}^m = \lambda_{\text{ext}}^m$) of all n_{mg} grids taking part in the distributed dynamic averaging are equal, i.e., $\lambda_{\text{ext}}^m = \frac{1}{n_{\text{mg}}} \sum_{m=1}^{n_{\text{mg}}} \lambda_{\text{loc}}^m$, and Proposition 6.8 is fulfilled. In addition, the averaging is performed in a distributed manner, using only neighbor-to-neighbor communication according to the graph $\mathcal{G}_{\text{econ}}$. There exist many dynamic consensus algorithms, see [Kia+19] for a survey. In this chapter, a dynamic consensus algorithm that has an excess of EIP is needed to compensate a potential lack of EIP of the economic port (characterized in Proposition 6.5 via ν_{econ}^m and ρ_{econ}^m).

The next assumption is necessary to ensure that the steady state aimed by the distributed averaging exists.

Assumption 6.4 (existence of suitable equilibria)
Consider a set of grids $\mathcal{M}$ interconnected with lossy power lines. Then, there exists a price $\bar{\lambda}$ such that, if all grids use this price, i.e., $\lambda_{\text{ext}}^m = \bar{\lambda}$, an equilibrium $\bar{\boldsymbol{x}}^*$ exists, with $\boldsymbol{x}$ as in (6.31).

A constant price corresponds to a constant power injection. The existence of an equilibrium implies the existence of a voltage configuration such that the power injection serves the loads and power balance is achieved. This is also described by the power flow equations. Thus, the assumption is equivalent to assuming that there exists at least one solution to the power flow equations with a given power injection configuration. In general, little can be proven about the solutions of power flow equations, and the assumption of existence of solutions is typically made [SP17]. If such an equilibrium exists, it is optimal as per Proposition 6.8.

Choice and Analysis of a Distributed Averaging Algorithm

Distributed averaging algorithms have been widely studied in control theory and related fields of research. There exist plenty of different algorithms with different stability or accuracy properties, both in continuous and discrete time [Kia+19]. In this chapter, the linear distributed averaging system

$$\dot{\boldsymbol{x}}_{\text{DA}} = \boldsymbol{A}_{\text{DA}}\boldsymbol{x}_{\text{DA}} + \boldsymbol{B}_{\text{DA}}\boldsymbol{u}_{\text{DA}} \tag{6.80a}$$
$$\boldsymbol{y}_{\text{DA}} = \boldsymbol{C}_{\text{DA}}\boldsymbol{x}_{\text{DA}} + \boldsymbol{D}_{\text{DA}}\boldsymbol{u}_{\text{DA}} \tag{6.80b}$$

with

$$\begin{aligned} \boldsymbol{A}_{\text{DA}} &= -\boldsymbol{L}\boldsymbol{L} \in \mathbb{R}^{n_{\text{mg}}\times n_{\text{mg}}} & \boldsymbol{B}_{\text{DA}} &= -\boldsymbol{L} \in \mathbb{R}^{n_{\text{mg}}\times n_{\text{mg}}} \\ \boldsymbol{C}_{\text{DA}} &= -\boldsymbol{L} \in \mathbb{R}^{n_{\text{mg}}\times n_{\text{mg}}} & \boldsymbol{D}_{\text{DA}} &= -\boldsymbol{I} \in \mathbb{R}^{n_{\text{mg}}\times n_{\text{mg}}} \end{aligned} \tag{6.81}$$

from [Kia+19, Eq. (36)] is used[74] due to the favorable EIP properties arising from the feedthrough and the fact that $\boldsymbol{C}_{\text{DA}}^\top = \boldsymbol{B}_{\text{DA}} \in \mathbb{R}^{n_{\text{mg}}\times n_{\text{mg}}}$. The matrix $\boldsymbol{L} \in \mathbb{R}^{n_{\text{mg}}\times n_{\text{mg}}}$ is the Laplacian of the graph $\mathcal{G}_{\text{econ}}$. The Laplacian $\boldsymbol{L}$ is symmetric because $\mathcal{G}_{\text{econ}}$ is undirected. Next, a condition for quantifying these favorable properties is derived. The quantification of the EIP properties is essential for the upcoming stability analysis.

[74] Observe that the input matrix $\boldsymbol{B}_{\text{DA}}$ has been changed from $\boldsymbol{L}$ in [Kia+19, Eq. (36)] to $-\boldsymbol{L}$ since the inputs are the negative local prices due to the skey-symmetric feedback interconnection (6.79) required for the EIP analysis. Thus, to obtain the average of the positive prices, the input matrix is multiplied by minus one.

Proposition 6.9 (EIP properties of distributed averaging)
Consider a distributed averaging system (6.80) *over a connected and undirected graph $\mathcal{G}_{\text{econ}}$. Then, the system is IF-OFEIP with indices ρ_{DA}, $\nu_{\text{DA}} \in \mathbb{R}$ and storage function $S_{\text{DA}}(\tilde{\boldsymbol{x}}_{\text{DA}}) = \frac{1}{2}\tilde{\boldsymbol{x}}_{\text{DA}}^\top \boldsymbol{S}\tilde{\boldsymbol{x}}_{\text{DA}}$ if the LMI*

$$\begin{bmatrix} \boldsymbol{A}_{\text{DA}}^\top \boldsymbol{S} + \boldsymbol{S}\boldsymbol{A}_{\text{DA}} + \rho_{\text{DA}}\boldsymbol{C}_{\text{DA}}^\top \boldsymbol{C}_{\text{DA}} & \boldsymbol{S}\boldsymbol{B}_{\text{DA}} - \frac{1}{2}\boldsymbol{C}_{\text{DA}}^\top + \rho_{\text{DA}}\boldsymbol{C}_{\text{DA}}^\top \boldsymbol{D}_{\text{DA}} \\ \boldsymbol{B}_{\text{DA}}^\top \boldsymbol{S} - \frac{1}{2}\boldsymbol{C}_{\text{DA}} + \rho_{\text{DA}}\boldsymbol{D}_{\text{DA}}^\top \boldsymbol{C}_{\text{DA}} & \nu_{\text{DA}}\boldsymbol{I} + \rho_{\text{DA}}\boldsymbol{D}_{\text{DA}}^\top \boldsymbol{D}_{\text{DA}} - \frac{1}{2}(\boldsymbol{D}_{\text{DA}} + \boldsymbol{D}_{\text{DA}}^\top) \end{bmatrix} \leq \boldsymbol{0} \tag{6.82}$$

holds.

Proof. The objective of the proof is to verify that $\dot{S}_{\text{DA}} \leq w(\tilde{\boldsymbol{y}}_{\text{DA}}, \tilde{\boldsymbol{u}}_{\text{DA}})$, where w is the IF-OFEIP($\rho_{\text{DA}}, \nu_{\text{DA}}$) supply rate as in Definition 3.3. First, the derivative of the storage function is computed, and then it is compared with the supply rate.

The derivative of the storage function S_{DA} along (6.80) reads[75]

$$\dot{S}_{\text{DA}} = \frac{1}{2}\dot{\tilde{\boldsymbol{x}}}_{\text{DA}}^\top \boldsymbol{S}\tilde{\boldsymbol{x}}_{\text{DA}} + \frac{1}{2}\tilde{\boldsymbol{x}}_{\text{DA}}^\top \boldsymbol{S}\dot{\tilde{\boldsymbol{x}}}_{\text{DA}} \tag{6.83}$$

$$= \frac{1}{2}(\boldsymbol{A}_{\text{DA}}\tilde{\boldsymbol{x}}_{\text{DA}} + \boldsymbol{B}_{\text{DA}}\tilde{\boldsymbol{u}}_{\text{DA}})^\top \boldsymbol{S}\tilde{\boldsymbol{x}}_{\text{DA}} + \frac{1}{2}\tilde{\boldsymbol{x}}_{\text{DA}}^\top \boldsymbol{S}(\boldsymbol{A}_{\text{DA}}\tilde{\boldsymbol{x}}_{\text{DA}} + \boldsymbol{B}_{\text{DA}}\tilde{\boldsymbol{u}}_{\text{DA}}). \tag{6.84}$$

Writing derivative (6.84) as a vector matrix multiplication, it reads

$$\dot{S}_{\text{DA}} = \begin{bmatrix} \tilde{\boldsymbol{x}}_{\text{DA}} \\ \tilde{\boldsymbol{u}}_{\text{DA}} \end{bmatrix}^\top \begin{bmatrix} \boldsymbol{A}_{\text{DA}}^\top \boldsymbol{S} + \boldsymbol{S}\boldsymbol{A}_{\text{DA}} & \boldsymbol{S}\boldsymbol{B}_{\text{DA}} \\ \boldsymbol{B}_{\text{DA}}^\top \boldsymbol{S} & \boldsymbol{0} \end{bmatrix} \begin{bmatrix} \tilde{\boldsymbol{x}}_{\text{DA}} \\ \tilde{\boldsymbol{u}}_{\text{DA}} \end{bmatrix}. \tag{6.85}$$

Now, consider the IF-OFEIP($\rho_{\text{DA}}, \nu_{\text{DA}}$) supply rate

$$w(\tilde{\boldsymbol{y}}_{\text{DA}}, \tilde{\boldsymbol{u}}_{\text{DA}}) = \tilde{\boldsymbol{y}}_{\text{DA}}^\top \tilde{\boldsymbol{u}}_{\text{DA}} - \rho_{\text{DA}}\tilde{\boldsymbol{y}}_{\text{DA}}^\top \tilde{\boldsymbol{y}}_{\text{DA}} - \nu_{\text{DA}}\tilde{\boldsymbol{u}}_{\text{DA}}^\top \tilde{\boldsymbol{u}}_{\text{DA}}. \tag{6.86}$$

Inserting $\tilde{\boldsymbol{y}}_{\text{DA}} = \boldsymbol{C}_{\text{DA}}\tilde{\boldsymbol{x}}_{\text{DA}} + \boldsymbol{D}_{\text{DA}}\tilde{\boldsymbol{u}}_{\text{DA}}$ in the first and second term of the supply rate (6.86) yields

$$\begin{aligned} w(\tilde{\boldsymbol{y}}_{\text{DA}}, \tilde{\boldsymbol{u}}_{\text{DA}}) = {} & (\boldsymbol{C}_{\text{DA}}\tilde{\boldsymbol{x}}_{\text{DA}} + \boldsymbol{D}_{\text{DA}}\tilde{\boldsymbol{u}}_{\text{DA}})^\top \tilde{\boldsymbol{u}}_{\text{DA}} \\ & - \rho_{\text{DA}}(\boldsymbol{C}_{\text{DA}}\tilde{\boldsymbol{x}}_{\text{DA}} + \boldsymbol{D}_{\text{DA}}\tilde{\boldsymbol{u}}_{\text{DA}})^\top (\boldsymbol{C}_{\text{DA}}\tilde{\boldsymbol{x}}_{\text{DA}} + \boldsymbol{D}_{\text{DA}}\tilde{\boldsymbol{u}}_{\text{DA}}) - \nu_{\text{DA}}\tilde{\boldsymbol{u}}_{\text{DA}}^\top \tilde{\boldsymbol{u}}_{\text{DA}}, \end{aligned} \tag{6.87}$$

[75] Since system (6.80) is linear, the shifted error dynamics w.r.t. any equilibrium $(\bar{\boldsymbol{x}}_{\text{DA}}, \bar{\boldsymbol{u}}_{\text{DA}})$ is identical to the unshifted dynamics (6.80).

and in matrix vector notation it reads

$$w(\tilde{\boldsymbol{y}}_{\mathrm{DA}}, \tilde{\boldsymbol{u}}_{\mathrm{DA}}) = \begin{bmatrix} \tilde{\boldsymbol{x}}_{\mathrm{DA}} \\ \tilde{\boldsymbol{u}}_{\mathrm{DA}} \end{bmatrix}^\top \begin{bmatrix} -\rho_{\mathrm{DA}} \boldsymbol{C}_{\mathrm{DA}}^\top \boldsymbol{C}_{\mathrm{DA}} & \frac{1}{2}\boldsymbol{C}_{\mathrm{DA}}^\top - \rho_{\mathrm{DA}} \boldsymbol{C}_{\mathrm{DA}}^\top \boldsymbol{D}_{\mathrm{DA}} \\ \frac{1}{2}\boldsymbol{C}_{\mathrm{DA}} - \rho_{\mathrm{DA}} \boldsymbol{D}_{\mathrm{DA}}^\top \boldsymbol{C}_{\mathrm{DA}} & -\nu_{\mathrm{DA}} \boldsymbol{I} - \rho_{\mathrm{DA}} \boldsymbol{D}_{\mathrm{DA}}^\top \boldsymbol{D}_{\mathrm{DA}} + \frac{1}{2}(\boldsymbol{D}_{\mathrm{DA}}^\top + \boldsymbol{D}_{\mathrm{DA}}) \end{bmatrix} \begin{bmatrix} \tilde{\boldsymbol{x}}_{\mathrm{DA}} \\ \tilde{\boldsymbol{u}}_{\mathrm{DA}} \end{bmatrix}. \tag{6.88}$$

Subtracting (6.88) from (6.85) to obtain $\dot{S}_{\mathrm{DA}} - w(\tilde{\boldsymbol{y}}_{\mathrm{DA}}, \tilde{\boldsymbol{u}}_{\mathrm{DA}}) \leq 0$, the EIP condition (6.82) in form of an LMI is obtained, which completes the proof. □

In the last proposition, a method for quantifying the EIP properties of the distributed averaging algorithm (6.80) have been derived. Notably, system (6.80) is chosen because it shows an excess of input and output EIP due to the feedthrough. Observe that other popular distributed averaging algorithms, such as the PI-DDA or P-DDA [FYL06; Kia+19], either do not provide an excess EIP properties due to a lack of feedthrough or do not achieve exact consensus at steady state. The distributed averaging algorithm chosen here with an excess of EIP is necessary for the interconnection with economic ports, since the indices ρ_{econ} and ν_{econ} may be negative and show a lack of passivity (see Remark 6.8), which needs to be compensated by the distributed averaging system.

In this section, a suitable distributed averaging algorithm has been chosen and a method for quantitatively characterizing its EIP properties have been derived. The EIP properties are used in the next section for proving asymptotic stability of feasible equilibria of the electrically and economically networked grids.

Stability Analysis for the Electrically and Economically Networked Grids

In the next theorem, one of the main results of this chapter is presented. It characterizes the stability of electrically and economically networked grids, i.e., grids with electric and economic ports as in Definitions 6.1 and 6.2 interconnected as in Sections 6.6.2 and 6.6.3. Such an interconnected system is shown in Figure 6.9. It is composed of the independent grid systems Σ (middle) in feedback with the power lines Π (bottom) and the distributed averaging $\mathcal{S}_{\mathrm{DA}}$ (top).

After the formal proof, an interpretation of the result and an illustrative example are provided.

Theorem 6.10 (asymptotic stability with electric and economic ports)
Consider a group of independent grids $m \in \mathcal{M}$ in (6.69) *fulfilling the conditions of Proposition 6.5, a group of independent power lines* (6.70) *fulfilling the conditions of Proposition 3.7, and the distributed averaging system* (6.80) *fulfilling the conditions of Proposition 6.9. Let the grids and power lines be interconnected via*

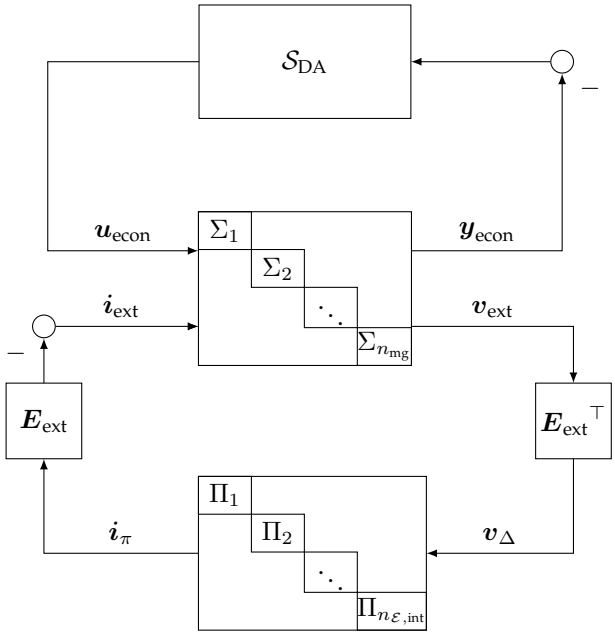

Figure 6.9: Feedback structure representing the interconnection between independent grid systems Σ, power lines Π and the distributed averaging $\mathcal{S}_{\mathrm{DA}}$.

electric ports through the interconnection structure (6.56) *and* (6.57)*. Further, let the grids* (6.69) *be interconnected via economic ports with the distributed averaging system* (6.80) *with the interconnection structure* (6.79)*. Then, all trajectories of the power system are bounded and converge to a point in the equilibrium manifold* $\mathcal{M}_{\mathrm{eq}} = \{(\bar{\boldsymbol{x}}, \bar{\boldsymbol{x}}_{\mathrm{DA}}, \bar{\boldsymbol{i}}_{\pi}) \mid \bar{\boldsymbol{x}} = \bar{\boldsymbol{x}}^*\}$ *with* $\bar{\boldsymbol{x}}^*$ *characterized in Assumption 6.4, if*

$$\rho_{\mathrm{econ}}^{\min} + \nu_{\mathrm{DA}} \geq 0 \tag{6.89}$$

$$\nu_{\mathrm{econ}}^{\min} + \rho_{\mathrm{DA}} > 0 \tag{6.90}$$

hold, where $\rho_{\mathrm{econ}}^{\min} = \min_m \rho_{\mathrm{econ}}^m \in \mathbb{R}$, $\nu_{\mathrm{econ}}^{\min} = \min_m \nu_{\mathrm{econ}}^m \in \mathbb{R}$, $\varrho_{\mathrm{ext}}^{\min} = \min_m \varrho_{\mathrm{ext}}^m \in \mathbb{R}_{>0}$ *and* $\rho_{\mathrm{DA}}, \nu_{\mathrm{DA}}$ *are the EIP properties derived in Proposition 6.5 and Proposition 6.9, respectively.*

Proof. Consider the Lyapunov function candidate

$$V(\tilde{\boldsymbol{x}}, \tilde{\boldsymbol{x}}_{\mathrm{DA}}, \tilde{\boldsymbol{i}}_{\pi,\mathrm{int}}) = \sum_{m \in \mathcal{M}} V^m(\tilde{\boldsymbol{x}}^m) + S_{\mathrm{DA}}(\tilde{\boldsymbol{x}}_{\mathrm{DA}}) + \tilde{\boldsymbol{i}}_{\pi,\mathrm{int}}^{\top} \boldsymbol{R}_{\pi,\mathrm{int}} \tilde{\boldsymbol{i}}_{\pi,\mathrm{int}}. \tag{6.91}$$

The derivative of (6.91) reads, using network variables as defined in (6.69)

$$\dot{V} \leq \tilde{\boldsymbol{y}}_{\text{econ}}^{\top}\tilde{\boldsymbol{u}}_{\text{econ}} - \rho_{\text{econ}}^{\min}\tilde{\boldsymbol{y}}_{\text{econ}}^{\top}\tilde{\boldsymbol{y}}_{\text{econ}} - \nu_{\text{econ}}^{\min}\tilde{\boldsymbol{u}}_{\text{econ}}^{\top}\tilde{\boldsymbol{u}}_{\text{econ}} + \tilde{\boldsymbol{y}}_{\text{ext}}^{\top}\tilde{\boldsymbol{u}}_{\text{ext}} - \varrho_{\text{ext}}^{\min}\tilde{\boldsymbol{x}}^{\top}\tilde{\boldsymbol{x}} \tag{6.92a}$$

$$+ \tilde{\boldsymbol{y}}_{\text{DA}}^{\top}\tilde{\boldsymbol{u}}_{\text{DA}} - \rho_{\text{DA}}\tilde{\boldsymbol{y}}_{\text{DA}}^{\top}\tilde{\boldsymbol{y}}_{\text{DA}} - \nu_{\text{DA}}\tilde{\boldsymbol{u}}_{\text{DA}}^{\top}\tilde{\boldsymbol{u}}_{\text{DA}} \tag{6.92b}$$

$$+ \tilde{\boldsymbol{i}}_{\pi,\text{int}}^{\top}\tilde{\boldsymbol{v}}_{\Delta} - \rho_{\pi}\tilde{\boldsymbol{i}}_{\pi,\text{int}}^{\top}\tilde{\boldsymbol{i}}_{\pi,\text{int}} \tag{6.92c}$$

by taking into account the EIP properties from the grids as in Proposition 6.5 in (6.92a), the EIP properties of the distributed averaging system (6.80) in (6.92b) and the EIP properties of the power lines as in Proposition 3.7 in (6.92c). Note that $\rho_{\pi} = \min\{\boldsymbol{R}_{\pi,\text{int}}\}$ is the smallest resistance of the power lines interconnecting the grids (see Proposition 3.7). Inserting the interconnection equation of the distributed averaging with the economic ports (6.79) into (6.92), the variables $\boldsymbol{u}_{\text{econ}}$ and $\boldsymbol{u}_{\text{DA}}$ are eliminated to obtain

$$\dot{V} \leq \tilde{\boldsymbol{y}}_{\text{econ}}^{\top}\tilde{\boldsymbol{y}}_{\text{DA}} - (\rho_{\text{econ}}^{\min} + \nu_{\text{DA}})\tilde{\boldsymbol{y}}_{\text{econ}}^{\top}\tilde{\boldsymbol{y}}_{\text{econ}} + \tilde{\boldsymbol{y}}_{\text{ext}}^{\top}\tilde{\boldsymbol{u}}_{\text{ext}} - \varrho_{\text{ext}}^{\min}\tilde{\boldsymbol{x}}^{\top}\tilde{\boldsymbol{x}} \tag{6.93a}$$

$$- \tilde{\boldsymbol{y}}_{\text{DA}}^{\top}\tilde{\boldsymbol{y}}_{\text{econ}} - (\rho_{\text{DA}} + \nu_{\text{econ}}^{\min})\tilde{\boldsymbol{y}}_{\text{DA}}^{\top}\tilde{\boldsymbol{y}}_{\text{DA}} \tag{6.93b}$$

$$+ \tilde{\boldsymbol{i}}_{\pi,\text{int}}^{\top}\tilde{\boldsymbol{v}}_{\Delta} - \rho_{\pi}\tilde{\boldsymbol{i}}_{\pi,\text{int}}^{\top}\tilde{\boldsymbol{i}}_{\pi,\text{int}}. \tag{6.93c}$$

Observe that the first term in (6.93a) and the first term in (6.93b) add up to zero. Furthermore, inserting the electric interconnection equations (6.56) and (6.57) into the third term of (6.93a) and into the first term of (6.93c), both terms add up to zero and it follows that

$$\dot{V} \leq -(\rho_{\text{econ}}^{\min} + \nu_{\text{DA}})\tilde{\boldsymbol{y}}_{\text{econ}}^{\top}\tilde{\boldsymbol{y}}_{\text{econ}} - \varrho_{\text{ext}}^{\min}\tilde{\boldsymbol{x}}^{\top}\tilde{\boldsymbol{x}} \tag{6.94a}$$

$$- (\rho_{\text{DA}} + \nu_{\text{econ}}^{\min})\tilde{\boldsymbol{y}}_{\text{DA}}^{\top}\tilde{\boldsymbol{y}}_{\text{DA}} \tag{6.94b}$$

$$- \rho_{\pi}\tilde{\boldsymbol{i}}_{\pi,\text{int}}^{\top}\tilde{\boldsymbol{i}}_{\pi,\text{int}}. \tag{6.94c}$$

With $\rho_{\text{econ}}^{\min} + \nu_{\text{DA}} \geq 0$ and $\nu_{\text{econ}}^{\min} + \rho_{\text{DA}} > 0$ it follows

$$\dot{V} \leq -\varrho_{\text{ext}}^{\min}\tilde{\boldsymbol{x}}^{\top}\tilde{\boldsymbol{x}} - (\rho_{\text{DA}} + \nu_{\text{econ}}^{\min})\tilde{\boldsymbol{y}}_{\text{DA}}^{\top}\tilde{\boldsymbol{y}}_{\text{DA}} - \rho_{\pi}\tilde{\boldsymbol{i}}_{\pi,\text{int}}^{\top}\tilde{\boldsymbol{i}}_{\pi,\text{int}} \leq 0. \tag{6.95}$$

From (6.95), it follows that all trajectories of the networked system are bounded. Furthermore, due to Lasalle's Invariance Theorem, all trajectories converge to the largest invariant set in $\mathcal{L} = \{(\boldsymbol{x}, \boldsymbol{x}_{\text{DA}}, \boldsymbol{i}_{\pi}) \mid \dot{V} = 0\}$, i.e., $\mathcal{L} = \{(\boldsymbol{x}, \boldsymbol{x}_{\text{DA}}, \boldsymbol{i}_{\pi}) \mid \tilde{\boldsymbol{x}} = \boldsymbol{0}, \tilde{\boldsymbol{y}}_{\text{DA}} = \boldsymbol{0}, \tilde{\boldsymbol{i}}_{\pi,\text{int}} = \boldsymbol{0}\}$. Observe that $\mathcal{L}$ is already contained in the equilibrium manifold $\mathcal{M}_{\text{eq}}$ stated in the proposition. Thus, it only remains to show that convergence is to a point. For that, the dynamics of the networked system inside the set $\mathcal{L}$ are studied. Note that in $\mathcal{L}$, the grid states $\tilde{\boldsymbol{x}}$ and $\tilde{\boldsymbol{i}}_{\pi,\text{int}}$ are already at equilibrium. Furthermore, it holds that $\tilde{\boldsymbol{y}}_{\text{DA}} = \boldsymbol{0}$, which, taking into account the output equation (6.80b) of the distributed averaging, induces the relation

$$\boldsymbol{0} = -\boldsymbol{L}\tilde{\boldsymbol{x}}_{\text{DA}} - \tilde{\boldsymbol{u}}_{\text{DA}}. \tag{6.96}$$

between $\tilde{\boldsymbol{x}}_{\text{DA}}$ and $\tilde{\boldsymbol{u}}_{\text{DA}}$. Inserting (6.96) into the distributed averaging dynamics (6.80a) yields

$$\dot{\tilde{\boldsymbol{x}}}_{\text{DA}} = -2\boldsymbol{L}\boldsymbol{L}\tilde{\boldsymbol{x}}_{\text{DA}}. \tag{6.97}$$

Since the matrix $\boldsymbol{LL}$ in (6.97) is symmetric and positive semidefinite (i.e., the eigenvalues have a nonnegative real part), the system (6.97) is stable in the sense of Lyapunov. Due to symmetry, the eigenvalues of $\boldsymbol{LL}$ are real, and thus all the trajectories $\tilde{\boldsymbol{x}}_{\mathrm{DA}}(t)$ converge to a point.[76] □

Remark 6.10. *The last part of the proof where it is shown that the convergence is to a point, could be circumvented by imposing EIO to all three subsystems, the grids, the power lines, and the distributed averaging algorithm. For the grids and power lines it can be easily shown that they are EIO. But it can also be proven that, in general, distributed averaging algorithms are not EIO. This is because the input and output matrices are typically weighted Laplacian matrices [Kia+19], which makes the system not fully controllable and observable, since the Laplacian matrices do not have full rank [BH12, Ch. 1.3.7]. This can, however, be circumvented by dividing the distributed averaging algorithm into a controllable and observable part, which is EIO, and an uncontrollable and unobservable part depending on the initial states. This elegant path is chosen in [Mal25] for proving stability with a distributed averaging in feedback. Here, the path exploiting Lasalle's Invariance Theorem is chosen instead in order to not depend on state transformations, which do not work for more performant, nonlinear distributed averaging algorithms [Kia+19].*

It is noteworthy that the stability and optimality results in Theorem 6.10 require only the communication of their local prices with other grids. In particular, no *information* about the loads, grid parameters or costs functions of the DGUs have to be disclosed to or exchanged with other grids *at any time*. The stability analysis is completely based on local EIP properties of the grids, the distributed averaging system and the power lines. The following example illustrates the presented results. In particular, it is shown that the economic interconnection scheme leads to UMP.

6.7 Numerical Example

Consider the same scenario as in Example 6.1, but using the economic ports with the interconnection scheme (6.80) proposed and analyzed in Section 6.6.3. A schematic representation of both grids with economic ports is shown in Figure 6.10.

[76] For undamped oscillations to occur, complex eigenvalues are necessary.

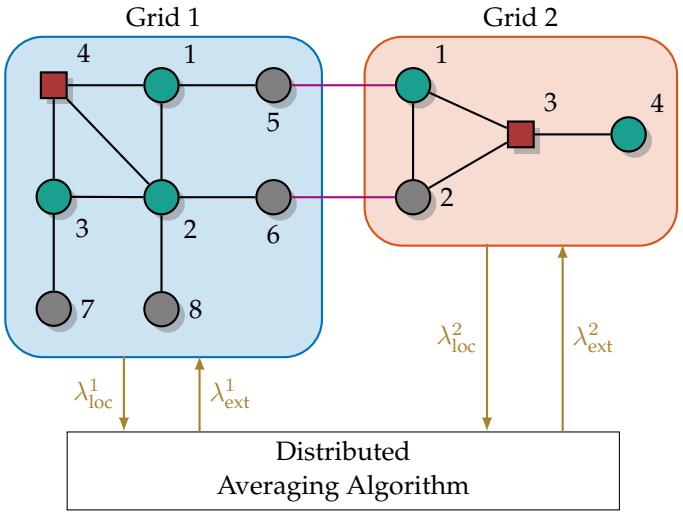

Figure 6.10: Schematic representation of the two electrically (purple) and economically (brown) interconnected grids via a distributed averaging algorithm. The grid-following DGUs are represented as green circles, and the grid-forming DGUs as red squares.

The power injection of the grid-forming DGUs and the price in both grids are shown in Figures 6.11 and 6.12, respectively. When a load step occurs, the prices in both grids vary. However, after a transient period, the prices in both grids become equal. This is due to the distributed averaging algorithm (6.80) interconnecting the grids via the economic port, which achieves a price consensus at steady state. The power injections of the grid-following DGUs in Figure 6.11 adjusts automatically according to the price in the grids. Note that the DGUs of Grid 2 inject less power than the DGUs in Grid 1, since they have greater injected power costs (see Table 6.2). DGUs with the same cost function (e.g., DGU 3 in Grid 1 and DGU 4 in Grid 2, see Table 6.2) inject the same amount of power in steady state despite being in different grids with different loads. Since at steady state a price consensus of both grids is achieved, it results, as per Proposition 6.8, global optimal dispatch. Note that global optimal dispatch is achieved solely by an exchange of the local prices in a distributed manner via the economic ports, without requiring further communication.

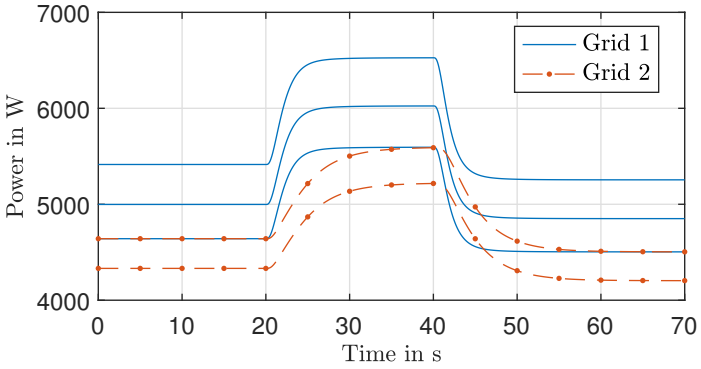

Figure 6.11: Power generation of the DGUs of both grids over the simulation time using economic ports and distributed averaging.

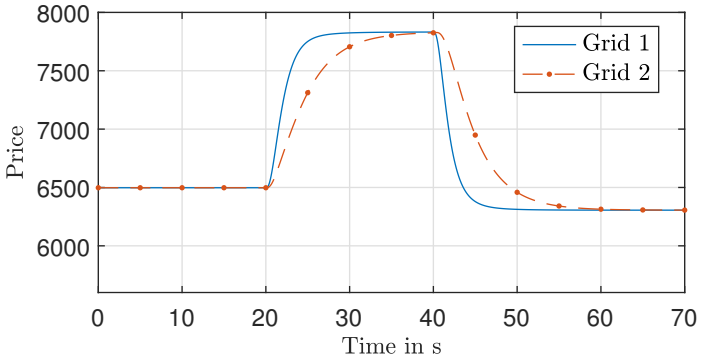

Figure 6.12: Local price of both grids over the simulation time using economic ports and distributed averaging.

6.8 Discussion and Outlook

The main contribution of this chapter is a control framework compatible with liberalized power systems as in Term 2.2. The proposed method complies with the unbundling in current power systems due to the following reasons. Firstly, the flexible prosumers are rational market participants and do not share any information. Secondly, the roles of power system operation and energy trading are performed by different, independent entities. This is achieved by designing a novel price-forming mechanism. This price signal features two main advantages. On the one hand, it provides enough information to the prosumers such that they can inject the amount of power to maximize their profit. On the other hand, the price signal induces asymptotic stability and convergence to an equilibrium where global optimal dispatch as in Proposition 6.8 holds. This novel price-forming mechanism also allows measuring just one variable to determine the unmet power balance and thus the price. In contrast, the existing approaches reviewed

in Section 2.5 need to measure all voltages and compute the losses for determining the price evolution. In the proposed approach, the control effort of the grid-forming DGU is used as a proxy signal for the unmet power balance and thus for determining the price.

In this chapter, the roles traditionally fulfilled by the market mechanism in power systems are partially assumed by the distributed averaging system and the system operators. The system operators determine a price, while the distributed averaging system establishes a UMP that each grid uses for the cost of power generation. Although UMP offers advantages such as social fairness, it does not account for transmission line constraints and necessitates a redispatch mechanism as implemented in Germany [Bun24b]. This limitation can be addressed by introducing weighting factors for the averaged prices λ_{ext} in order to achieve location-dependent prices [Koe22].

One of the main novelties of the proposed method is that the stability analysis in Theorem 6.10 requires only local conditions at grid level. This is a direct consequence of the introduction of the economic ports, which allow an economic cooperation and at the same time an EIP of an individual grid. Comparable approaches reviewed in Section 2.5 necessitate the EIP properties of the aggregated grids, including the interconnecting power lines, the objective functions or the communication matrices, which are not separable in individual grids, as shown graphically in Figure 2.3. All in all, the local conditions on all subsystems allow a plug-and-play operation of grids without compromising on stability or optimality. Note, however, that if a grid disconnects only economically and remains electrically interconnected, the results of grids interconnected via electric ports (see Theorem 6.6) still apply. Then, as per Proposition 6.7, a steady state arises that is locally (for each grid individually) optimal but globally suboptimal.

Another key element to underline in the proposed framework is the clear separation of roles between the system operator and prosumers. This role separation is reflected in the control paradigms of the power electronics corresponding to the different agents, i.e., grid-forming for the system operators and grid-following for the prosumers. The existing methods use controllers for power electronics of prosumers mimicking the linear droop-relation of synchronous generators. Thus, prosumers automatically are grid-forming entities and provide ancillary services, such as voltage regulation. In the proposed approach, the system operator is actually the only grid-forming entity, deciding on an adequate voltage level via $v_{\text{ref},i}$, yielding a clear separation of the roles.

An appropriate and fair remuneration scheme for all network participants is essential for practical operation. As it requires comprehensive legal and economic considerations, it lays outside the technical scope of this thesis. Apart from the payments of the flexible or inflexible prosumers, taken into account with (6.15) and (6.19), a scheme where the system operators are remunerated for stabilization and price-forming services they provide is necessary. These types of fixed costs for the regulated part of the power system have to be transferred adequately to the flexible and inflexible prosumers. Such a remuneration scheme has, however, not been proposed yet in the literature.

Another interesting extension would be the design of such a control framework for AC systems. First attempts show promising results, see [Dik23; JSDH23]. In [JSDH23], we have shown that, from a practical perspective, the same framework works when considering AC systems and linking the price-forming mechanism with the active power injection of the grid-forming DGU. This confirms that the extension of control approaches from DC to balanced, three-phase AC systems modelled in the dq (rotating) frame works well in practice, as is also observed in the literature in Section 2.6. However, the theoretical stability analysis was not studied and is left to future work.

As a matter of interest, a link between the proposed method and the distributed optimization in Chapter 5 is drawn. In both chapters, the subsystems are designed such that all equilibria automatically comply with optimality requirements. In the case of the distributed optimization, the edge systems are systems with integral action as in Definition 5.1, forcing the agents to reach consensus and optimality. Similarly, in this chapter, the novel price-forming mechanism is a system with integral action and ensures that, at steady state, power balance holds along with global optimal dispatch (due to the distributed averaging inducing UMP). Hence, both approaches are designed in such a way that all possible equilibria fulfill the given optimality requirements using integral action. Also, in both methods these equilibrium properties hold independently of the interconnection topology or the number of systems that are interconnected. This enables the possibility of a plug-and-play operation in both methods.

Finally, it has to be highlighted that the proposed control theory-inspired price-forming mechanism, using the control effort of a grid-forming DGU to determine the price, may be conceptually used in any domain of multi-energy systems. In heating networks, the control effort to stabilize the temperature of the medium in the pipes may be used as a price-forming mechanism. In gas networks, an analogy would be to use the control effort to stabilize the pressure. Such price-forming mechanisms may help to control and optimize meshed networks with numerous connections at all distribution levels, when those energy markets cannot be treated independently anymore.

6.9 Summary and Contributions

In this chapter, a liberalized framework for optimal operation of networked grids has been proposed. For that, the concept of electric ports at grid level and economic ports has been introduced. With EIP theory, asymptotic stability in the case of an interconnection with electric ports has been shown. Furthermore, an additional economic interconnection leading to UMP has been proposed, and it has been shown that an equilibrium manifold describing global optimal dispatch is asymptotically attractive. Two examples have been presented in order to showcase the proposed method. A more representative example as well as a more detailed analysis and comparison with the other methods proposed in this thesis is presented in Chapter 7.

With this chapter, Research Gaps 4, 6 and 5 are addressed. The proposed method fulfills Contributions 3 and 4. In Table 6.3, the propositions, theorems and corollaries proposed in this work are summarized and their interrelation is shown graphically. The statements are categorized depending on the scenario they address, i.e., a single islanded grid, electrically interconnected or electrically and economically interconnected grids. Furthermore, the statements are categorized w.r.t. their content — if they establish EIP properties, stability properties of suitable equilibria or optimality properties of equilibria.

Table 6.3: Summary and interrelation of the propositions and theorems.

	islanded	**electrically interconnected**	**electrically & economically interconnected**
EIP **properties**	-	Proposition 6.4	Proposition 6.5, Proposition 6.9
stability properties	Theorem 6.2	Theorem 6.6,	Theorem 6.10
optimality of equilibria	Proposition 6.3	Proposition 6.7	Proposition 6.8

7 Simulation Results: Comparison of the Proposed Methods

In this chapter, simulation results for the regulated and liberalized power system control frameworks, proposed in Chapter 4 and Chapter 6, are presented and compared. The goal is to illustrate the advantages and disadvantages of both approaches. Special attention is paid to comparing the performance, the information exchange and the computational complexity in order to assess the technical viability of each method.

First, in Section 7.1, the simulation scenario is presented. In particular, the system topology and the objective functions of the prosumers are stated. In Section 7.2, the simulation results for the regulated power system control framework proposed in Chapter 4, using the distributed optimization proposed algorithm in Chapter 5, are presented. Details about the implementation using the distributed optimization algorithm presented in Chapter 5 are given. Afterwards, in Section 7.3, the simulation results for the method compatible with liberalized power systems proposed in Chapter 6 are shown. Lastly, in Section 7.4, both results are compared in terms of performance, information exchange, and computational complexity.

7.1 Simulation Scenario

The simulation scenario considered in the rest of this chapter is composed of three networked grids forming a power system as in Figure 7.1. The first grid, in blue, comprises five nodes and six power lines. The second grid, in orange, is composed of four nodes and three lines, and the third grid, in yellow, of six nodes and five power lines. Grid 1 has a meshed topology, while Grids 2 and 3 have radial topologies. The grids are interconnected via three power lines, in purple, and create thus a meshed topology in the power system. Each grid $m \in \{1, 2, 3\}$ has two DGUs injecting power, depicted in green. The power injection of the DGUs has a quadratic[77] cost $f^m_{\text{flx},i}(p^m_{\text{ref},i})$ (see (6.14)), with $m \in \{1, 2, 3\}$ the grid index and $i = \{1, 2\}$ the DGU index, as in

$$f^m_{\text{flx},1}(p^m_{\text{ref},1}) = \left(p^m_{\text{ref},1}\right)^2, \quad k = \{1, 2, 3\}, \tag{7.1a}$$

$$f^m_{\text{flx},2}(p^m_{\text{ref},2}) = 2\left(p^m_{\text{ref},2}\right)^2, \quad k = \{1, 2, 3\}. \tag{7.1b}$$

[77] Quadratic cost functions are used for simplicity, without loss of generality.

Hence, the cost of the DGUs $i = \{1, 2\}$ of all three grids $m \in \{1, 2, 3\}$ are identical. All grids $m \in \{1, 2, 3\}$ have a DGU with cost $f^m_{\text{flx},1}$, and another one with double the cost, i.e., $f^m_{\text{flx},2} = 2f^m_{\text{flx},1}$. This is chosen in order to easily compare the power injection of different grids. Due to the cost of power injection, it is expected that, in each grid, the expensive DGU injects half the power that the cheap DGU injects. The cheap and expensive DGU should, respectively, inject a similar amount of power in each grid, since they have identical costs of generation. The system parameters are shown in Table D.1 in Section D.1. The simulation time is $80\,\text{s}$. At time steps $t_1 = 20\,\text{s}$, $t_2 = 40\,\text{s}$ and $t_3 = 60\,\text{s}$, the load changes as summarized in Figure 7.2. At time step t_1, the loads in Grid 3 increase by $3\,\text{kW}$ (see Figure 7.2). At time step t_2, the loads in Grid 3 further increase by $900\,\text{W}$ and, at the same time, decrease by $450\,\text{W}$ in both Grid 1 and 2, such that the total load in the system remains constant but shifts between grids. In time step t_3, the load in Grids 1 and 2 decreases such that the total load is equal to the total load in the first time period 0 - 20 s (see Figure 7.2 (bottom)). However, even though the total load in the time periods 1 and 4 (and also 2 and 3) is equal, the load is distributed differently among the grids in each of the time periods. It can be further observed that the load differences between the grids increase over time, i.e., the load shifts from Grids 1 and 2 to Grid 3.

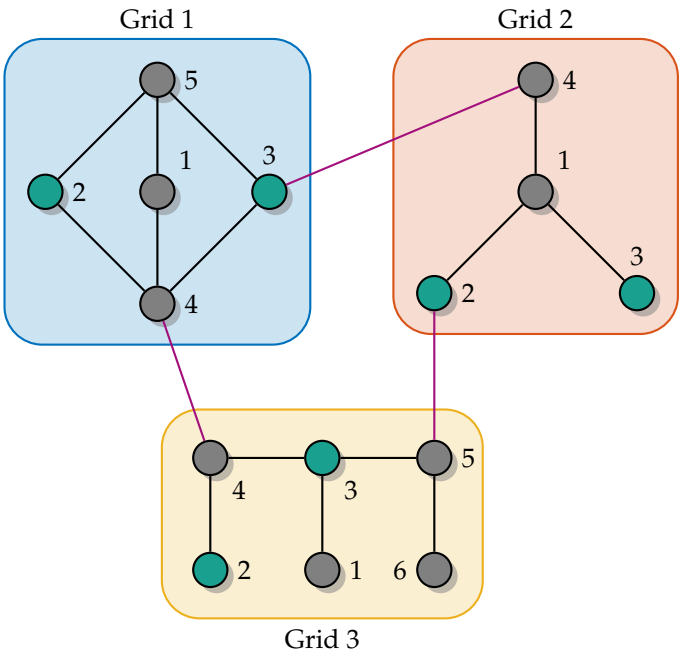

Figure 7.1: Simulation scenario of the power system comprising three grids. Gray nodes indicate there is only a load, green nodes have additionally a DGU.

Furthermore, as can be seen in Table D.1, apart from the total load, the load characterist-

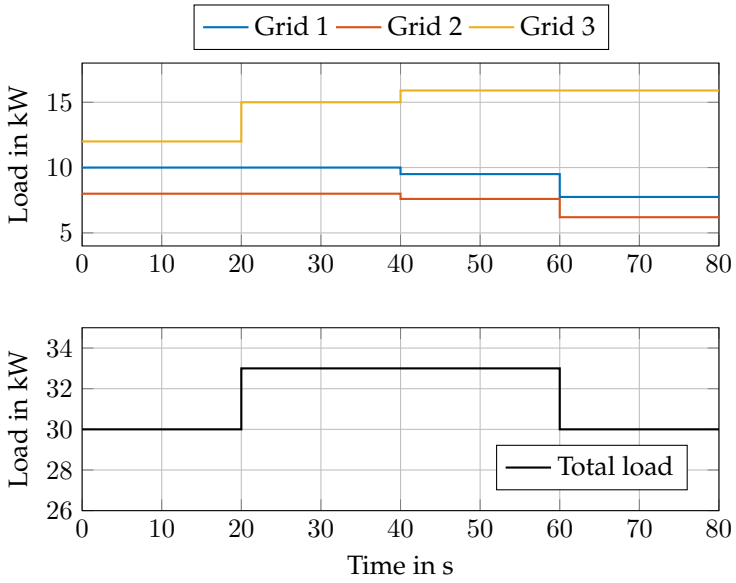

Figure 7.2: Load variations in the grids over the simulation time (top), and the sum of all loads in the three grids (bottom) over the simulation time. The loads are computed with a nominal voltage 1000 V.

ics also vary. In time period 0 - 20 s, the load is a pure impedance and thus linear. In the rest of the time steps, there is a nonlinear constant power load (see Table D.1).

In the next section, the results of applying the method proposed in Chapter 4 for regulated power systems to the scenario described above are presented.

7.2 Regulated Power System Operation

In this section, the results of a distributed setpoint-tracking and economic MPC as proposed in Chapter 4 using the distributed optimization algorithm of Chapter 5 are shown. First, in Section 7.2.1, details of the practical implementation of the distributed optimization algorithm for the regulated control framework of Chapter 4 are presented. Afterwards, in Section 7.2.2, the simulation results are presented.

7.2.1 Practical Implementation of the Distributed Optimization Algorithm for MPC

Recall that the method for regulated power systems in Chapter 4 provided an MPC framework with local stability conditions for the individual grids. However, to additionally achieve a distributed computation, a distributed optimization algorithm as

presented in Chapter 5 has to be used. Thus, this subsection is devoted to provide the details of the implementation of the distributed optimization algorithm of Chapter 5 to the approach of Chapter 4. First, the system dynamics used in Chapter 4 are discretized, and then transformed to an appropriate form.

Note that the system dynamics derived in Section 3.4 and used in Chapter 4 are in continuous time. However, to numerically solve the MPC problem (4.26), a discretization of the nonlinear system dynamics is necessary. For that, the forward Euler method

$$\boldsymbol{x}(k+1) = \boldsymbol{x}(k) + h_{\mathrm{T}} \boldsymbol{f}(\boldsymbol{x}(k), \boldsymbol{u}(k)) \tag{7.2}$$

is employed. For choosing an appropriate discretization time $h_{\mathrm{T}} \in \mathbb{R}_{>0}$, the system is linearized around an appropriate operating point and the eigenvalues of the resulting matrix are computed. With the eigenvalues, the largest discretization time h_{T} which retains the stability properties of the continuous-time system can be computed [JS+23c, Prop. 4].

The forward Euler integration method [RMD17] is used due to its sparsity preserving properties for distributed systems, i.e., it preserves the sparsity structure of the continuous-time system as in the state function $\boldsymbol{f}$ in (7.2) [Col+12; FCS13; DTS13].

As a consequence, the coupling between the grids in the system dynamics via the voltages explained in Remark 4.3 in Section 4.2.1 remains the same after discretizing the system [FCS13]. This is important, since any additional coupling between the grids implies more communication in the distributed optimization and should thus be avoided when discretizing.

Every grid $m \in \mathcal{M}$ is described by discrete-time dynamics of the form

$$\boldsymbol{x}^m(k+1) = \boldsymbol{f}_{\mathrm{T}}^m(\boldsymbol{x}^m(k)) + \boldsymbol{B}^m \boldsymbol{u}^m(k) + \sum_{l=1, l\neq m}^{n_{\mathrm{mg}}} \boldsymbol{A}^{m,l} \boldsymbol{x}^l(k), \tag{7.3}$$

where the last term describes the interconnection with other grids, and k describes the discrete-time step. According to the reduced model (4.21), the dynamics of a node in grid $m \in \mathcal{M}$ which is connected to a node in grid $l \in \mathcal{M}$ are influenced by the voltage of the corresponding node in l, which is included in the state $\boldsymbol{x}^l$. This corresponds to the term $\boldsymbol{E}_{\mathrm{int}} \boldsymbol{R}_{\pi,\mathrm{int}}^{-1} \boldsymbol{E}_{\mathrm{int}}^{\top} \boldsymbol{v}$ in (4.21a).

The system equations (7.3) of each grid $m \in \mathcal{M}$ are the private constraints for the local optimization problem of each grid. The objective function depends on whether setpoint-tracking or economic MPC is implemented. In the case of setpoint-tracking, the objective function for the MPC problem is

$$l^m(\boldsymbol{x}(k), \boldsymbol{u}(k)) = \|\boldsymbol{v}^m - \boldsymbol{v}_{\mathrm{opt}}\| + \|\boldsymbol{u}^m(k) - \boldsymbol{v}_{\mathrm{opt}}\|_{\alpha}, \tag{7.4}$$

where $\boldsymbol{v}_{\mathrm{opt}}$ is an optimal voltage reference computed via OPF (4.25) in advance, and $\alpha \in \mathbb{R}_{\geq 0}$ a constant for weighting the error of the input. Note that there exist standard

methods for computing the OPF problem in a distributed manner, see the survey in [Mol+17]. The OPF problem for the networked grids $m \in \mathcal{M}$ reads

$$\min_{p^m_{\text{ref},i}} \sum_{m\in\mathcal{M}} \sum_{i\in\mathcal{B}^m} f^m_{\text{flx},i}(p^m_{\text{ref},i}) \tag{7.5a}$$

$$\text{s.t. } \boldsymbol{Y}\boldsymbol{v} \circ \boldsymbol{v} - \boldsymbol{p} = \boldsymbol{0}, \tag{7.5b}$$

where $\boldsymbol{Y}$ is the admittance matrix of the whole grid and $\boldsymbol{p}$ the constant power loads. OPF problem (7.5) computes the setpoints such that the total cost of generation is minimized. Afterwards, the setpoint-tracking MPC ensures, with local conditions, that the nonlinear power system follows these setpoints and is asymptotically stable.

The MPC problem for an individual grid $m \in \mathcal{M}$ is, as introduced in (3.14) in continuous time,

$$\min_{\boldsymbol{u}^m(k)} \sum_{m\in\mathbb{I}_{N-1}} l^m(\boldsymbol{x}^m(k), \boldsymbol{u}^m(k)) + V_T(\boldsymbol{x}^m(n_T)) \tag{7.6a}$$

$$\text{s.t. (7.3)} \tag{7.6b}$$

$$\boldsymbol{x}^m(k) \in \mathbb{X}^m \tag{7.6c}$$

$$\boldsymbol{u}^m(k) \in \mathbb{U}^m \tag{7.6d}$$

$$\boldsymbol{x}^m(n_T) \in \mathbb{X}^m_T, \tag{7.6e}$$

where $\mathbb{I}_{N-1} = \{1, 2, \dots, n_T - 1\}$ is the set containing the discrete time steps, and $n_T = \lceil \frac{T}{h_\text{T}} \rceil$.

Note that through constraint (7.3), the MPC optimization problem of grid m is coupled with the MPC optimization problems of the other grids. To achieve global optimality, the distributed optimization algorithm proposed in Chapter 5 is used. For that, problem (7.6) is rewritten in network coordinates $\boldsymbol{z} = \text{col}\{\boldsymbol{x}^m(k), \boldsymbol{u}^m(k)\}, \forall m \in \{t, \dots, T\}$ containing all optimization variables to obtain

$$\min_{\boldsymbol{z}} F^m(\boldsymbol{z}) \tag{7.7a}$$

$$\text{s.t. (7.3)} \tag{7.7b}$$

$$\boldsymbol{z} \in \mathcal{Z}^m, \tag{7.7c}$$

where $F^m(\boldsymbol{z}) = \sum_{k=t}^{T-1} l^m(\boldsymbol{x}^m(k), \boldsymbol{u}^m(k)) + V(\boldsymbol{x}^m(T))$ and $\mathcal{Z}^m = \bigcup_{m\in\mathbb{I}_{N-1}} \{\mathbb{X}^m_k \cup \mathbb{U}^m_k\} \cup \mathbb{X}^m_T$. Note that writing problem (7.6) in network coordinates $\boldsymbol{z}$ does not change the coupling of the individual optimization problems via (7.3). It just casts the problem in the structure needed in Chapter 5, in particular with a network variable $\boldsymbol{z}$ already containing the coupling variables for grid $m \in \mathcal{M}$. This is explained in the following. Consider the global optimization problem

$$\min_{\boldsymbol{z}} \sum_{m\in\mathcal{M}} F^m(\boldsymbol{z}) \tag{7.8a}$$

$$\text{s.t. (7.3)}, \quad \forall m \in \mathcal{M} \tag{7.8b}$$

$$\boldsymbol{z} \in \mathcal{Z}^m, \forall m \in \mathcal{M}. \tag{7.8c}$$

Observe that optimization problem (7.8) has a structure as required for the distributed optimization in Chapter 5: the global objective is the sum of the objectives of the grids, and the constraints $\mathcal{Z}^m$ are private to grid $m \in \mathcal{M}$. The network variable $\boldsymbol{z}$ contains variables from all grids, but it is clear from (7.3) that only the own and coupling variables affect the objective function $F^m(\boldsymbol{z})$ and constraints $\mathcal{Z}^m$ of grid $m \in \mathcal{M}$. With the algorithm proposed in Chapter 5, the grids need to exchange only the coupling variables in every iteration, and the convergence to the global optimum is ensured by Theorem 5.14 if the objective functions are convex.

The continuous-time distributed optimization algorithm of Chapter 5 is implemented to solve (7.8) in MATLAB/SIMULINK R2022b and the variable-step size implicit solver ode15s [TM24b] is used. For solving the MPC problems, a discretization time of $10\,\mathrm{ms}$ together with an optimization horizon of 100 steps is chosen. This leads to an optimization problem with around 3300 optimization variables, which is solved in a distributed manner.

7.2.2 Simulation Results

In this subsection, the simulation results of the regulated approach of Chapter 4 together with the distributed optimization of Chapter 5, implemented as presented in the last subsection, are shown.

Setpoint-tracking MPC

The power injections of both DGUs in all grids controlled by a distributed setpoint-tracking MPC are shown in Figure 7.3. The power injections are drawn in the colors of the respective grids as in Figure 7.1, Grid 1 in blue, Grid 2 in orange, and Grid 3 in yellow. The power injections of all DGUs vary at time steps $t_1 = 20\,\mathrm{s}$, $t_2 = 40\,\mathrm{s}$ and $t_3 = 60\,\mathrm{s}$, where load steps occur. At time step t_2, the power injections remain nearly constant because the *total* load remains the constant even if it shifts among the grids (see Figure 7.2). The small variations are only to achieve fewer losses with the new load configuration such that the objective function (7.5) is minimized.

Furthermore, it can be clearly seen that the DGUs with low power generation cost inject nearly two times the power the expensive DGU inject, which corresponds to the ratio of their generation cost (see (7.1)). However, the power injections of the DGUs with low costs are between 3-4 kW and are not identical, even if they have identical cost functions. Similarly, different injections between 6-8 kW are observed for the DGUs with high generation costs. These differences arise, depending on the load configuration and location, in order to minimize the total power injection costs.

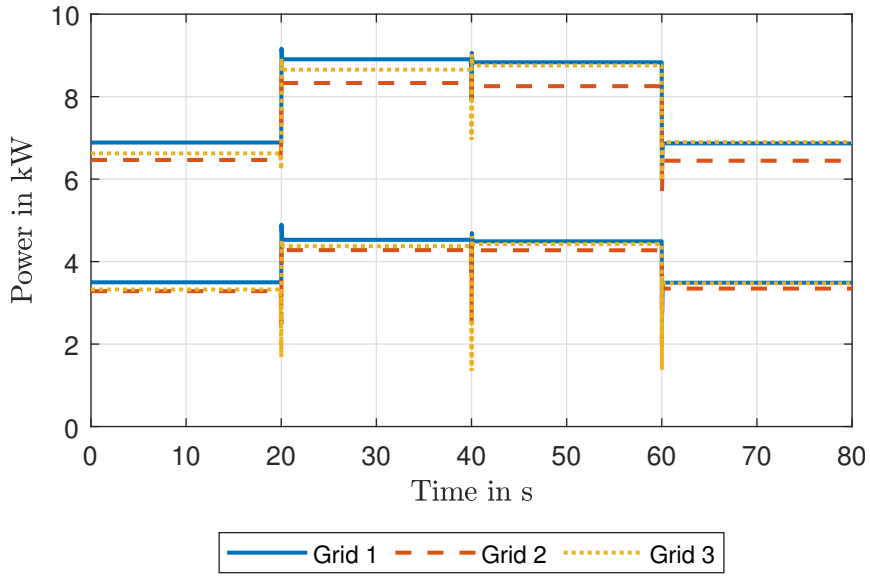

Figure 7.3: Power injection of the DGUs controlled by a distributed setpoint-tracking MPC in the three networked grids of the scenario of Figure 7.1.

The node voltages of the networked system are shown in Figure 7.4. The voltages fulfill the constraints of $\pm 10\,\%$ of the nominal voltage $1000\,\mathrm{V}$ at all times,[78] also during transients, since it is specified as a constraint for the MPC in (7.6c). When a load change occurs, the voltages vary and a new steady state which allows the power flows in Figure 7.3 arises. It can be further seen that the voltages are increasingly spreading as time increases. The voltages in the nodes of Grid 1 are the highest, and Grid 3 the lowest. This is due to the load steps, that induce increasingly high load differences between the grids at every time step, as can be seen in Figure 7.2. Grid 3 has the largest load, and has to receive power from the other grids. To allow greater power flows between grids, the voltage differences between nodes have to increase.

Lastly, the convergence properties of the distributed optimization algorithm solving the distributed setpoint-tracking MPC problem are discussed. In Figure 7.5, the error to the optimizer for the variables of Grid 1 is shown for two different time steps. The blue curve corresponds to the optimization at $t = 0\mathrm{s}$. In the first time period 0 - 20 s, which includes time step $t = 0\,\mathrm{s}$, the constant power loads are zero, and the constraint (7.6b) is affine (see Table D.1). Thus, the optimization problem is convex, and a faster convergence than in time step $t = 20.7\mathrm{s}$ is observed. Time step $t = 20.7\mathrm{s}$ is chosen because it corresponds to the time period 20 - 40 s, when there are nonzero power loads and the optimization problem is nonconvex due to the nonlinear equality constraint (7.6b). The algorithm also converges to the global optimizer in this case,[79] but slower compared

[78] Constraints of $\pm 10\,\%$ are very common in power systems, see, e.g., the North American grid code [Ass20].
[79] Note that convergence to the global optimizer is not guaranteed in general, but common in OPF problems

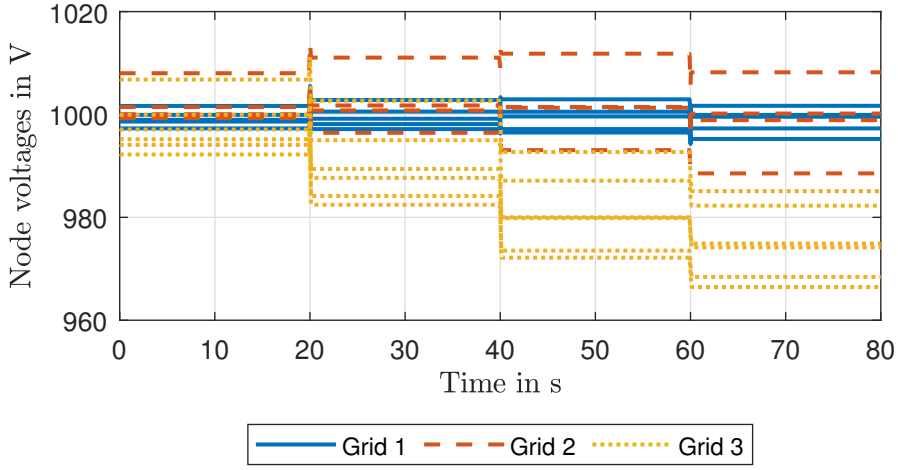

Figure 7.4: Node voltages of the networked system controlled by a distributed setpoint-tracking MPC in the three networked grids of the scenario of Figure 7.1.

to the convex problem. Note that convergence was not formally proven in the case of nonconvex optimization problems in Chapter 5, but it shows a good performance also in the nonconvex case. The number of iterations necessary to reach an accuracy of 10^{-5} and 10^{-8} is shown in Table 7.1. At $t = 20.7$s, due to the nonconvexity, around 50 more iterations are necessary. Note, that a standard initialization is used for the initial guess for both optimizations, which is in the order of 10^1 away from the optimizer, to be able to assess the effect of the nonlinearity introduced by the static loads.

Table 7.1: Number of iterations necessary for the distributed optimization to achieve an accuracy of 10^{-5} and 10^{-8}.

	$t = 0\,\mathrm{s}$	$t = 20.7\,\mathrm{s}$
10^{-5}	147	282
10^{-8}	206	318

Economic MPC

In this subsection, the results of a distributed economic MPC controller are shown. Note that, in contrast to setpoint-tracking MPC, asymptotic stability is not formally proven for this controller. However, it is subsequently shown (and has been also shown in Chapter 4) that it can achieve better performance, while not necessitating any setpoint in advance. This is an advantage when dealing with networked systems. The grids use the objective function (7.5a) for the economic MPC.

[COC+12].

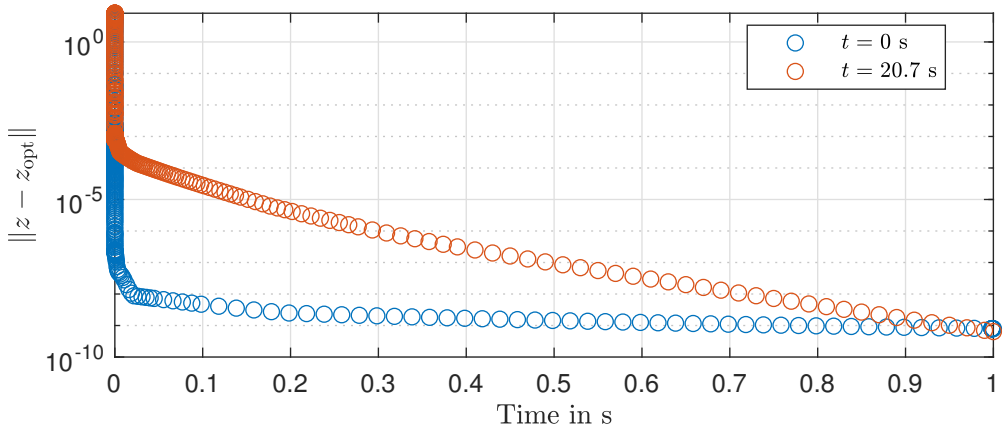

Figure 7.5: Error to the optimizer $\|\boldsymbol{z} - \boldsymbol{z}_{\text{opt}}\|$ of Grid 1 using the proposed distributed optimization algorithm. The error is plotted over the time of the continuous-time distributed optimization algorithm. The continuous-time optimization algorithm is solved numerically with ode15s [TM24b], thus yielding variable step sizes.

In Figure 7.6 the power injections of the DGUs are shown. In gray, the power injections computed by the setpoint-tracking MPC are depicted. It can be observed that the economic MPC achieves the same steady state as the setpoint-tracking MPC, but without knowing the setpoint in advance. The setpoint arises automatically from closed-loop operation. Both MPC controllers thus compute different power injections only during transients. However, observing more in detail, it can be seen that the steady state is not exactly identical. The steady-state error is inverse proportional to the length of the optimization horizon. Thus, the steady-state error can be further reduced by increasing the optimization horizon of the economic MPC. This is shown quantitatively in Figure 7.7.

Economic MPC has a great potential for the control of distributed power systems.[80] Furthermore, it is shown in Section 4.4 that it has improved performance in comparison to setpoint-tracking MPC, in particular when disturbances occur. From here on, the setpoint-tracking MPC is used for further comparison with the liberalized control framework, since only for setpoint-tracking MPC stability has been proven.

7.3 Liberalized Power System Operation

In this section, the liberalized control framework presented in Chapter 6 is studied in the same scenario as the regulated control framework (cf. Section 7.1). The grid-following DGUs represent the flexible prosumers and the loads are the inflexible prosumers.

[80] Specially, it has a great potential for general large-scale systems due to the fact that no setpoint has to be computed or known in advance.

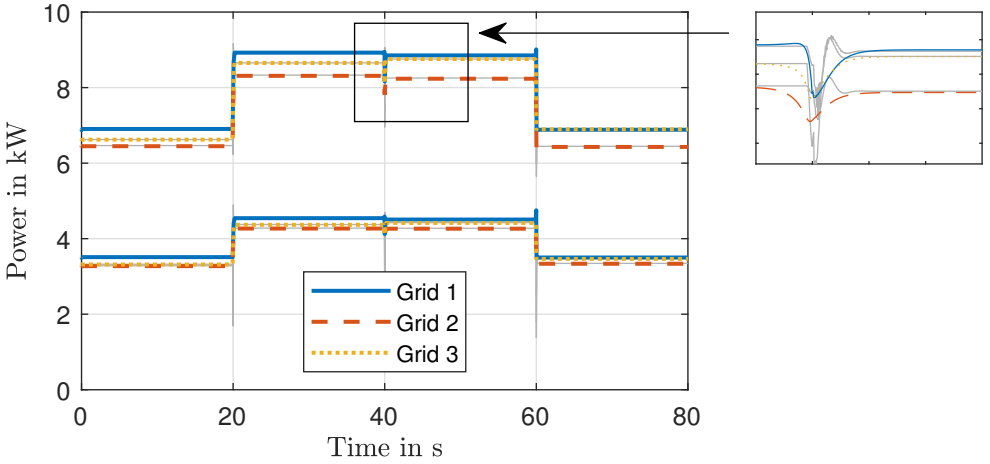

Figure 7.6: Power injection of the DGUs controlled by a distributed economic MPC in the three networked grids (blue, yellow, orange) of the scenario of Figure 7.1. In gray, the power injections computed by the setpoint-tracking MPC are depicted.

In each grid, in Node 1, a grid-forming DGU that represents the system operator is deployed. The system operator implements the price-forming mechanism (6.28). The simulation scenario including the system operators represented as red squares is shown in Figure 7.8. The load parameters and generation costs are chosen as presented in Section 7.1. Note that the controllable power generation is located in the same nodes as in the distributed MPC strategies, and all parameters are chosen identically. Hence, the simulation scenario is directly comparable to the simulation results when using the distributed MPC strategies of the previous section.

The system is implemented in MATLAB/SIMULINK R2022b and simulated numerically with the fixed time-step explicit solver ode3 [TM24a]. The standard solver parameters for fixed time-step solvers of Simulink are used.

In Figure 7.9, the power injections of the DGUs are depicted. The power injections vary when the load steps occur, at time steps $t_1 = 20\text{s}$, $t_2 = 40\text{s}$, and $t_3 = 60\text{s}$ (see Figure 7.2 in Section 7.1). It can be seen that, at steady state, after each load step, the power injections of all DGUs with the same generation costs are identical. In particular, the power injection of the DGUs with low and high generation cost are, respectively, identical at steady state even if they are located at different grids. This is a consequence of the fact that each DGU operates at the point where they maximize profit with a given price, and the price is equal at steady state for all grids, leading to UMP.

The external prices in each grid over the simulation time are shown in Figure 7.10. At steady state, all prices are identical. This is due to the distributed averaging. The external prices are formed by passing the local prices, which are all different, through a distributed averaging in order to achieve an identical price at steady state and thus

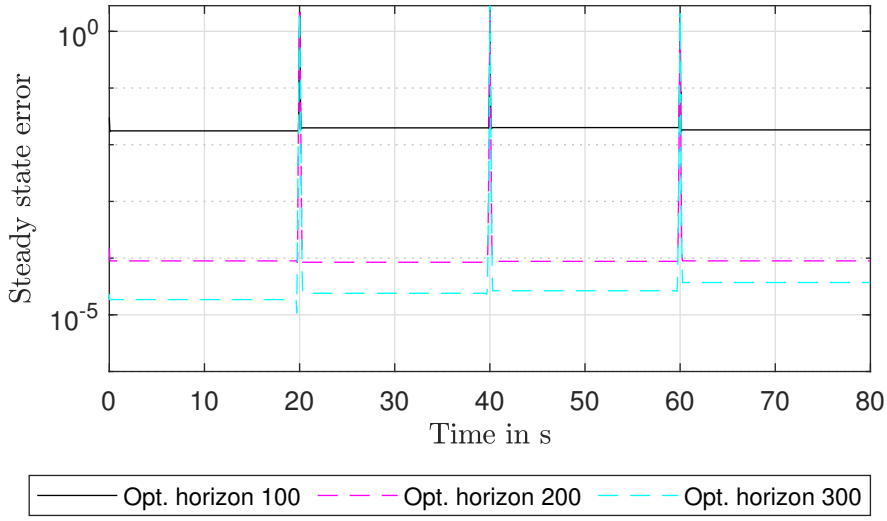

Figure 7.7: Steady-state error of the economic MPC compared to setpoint-tracking MPC.

a coordination of all flexible prosumers which inject power according to the price changes.

The price curves in Figure 7.10 arise from the price-forming mechanism (6.28). The price-forming mechanism defines that the local prices vary according to the current of the local grid-forming DGU, which in turn describes the control effort of the system operator to stabilize the system. The current of the grid-forming DGU in each grid is depicted in Figure 7.11. At time t_1, when the first load step occurs, the current of the grid-forming DGU in Grid 3 shows the largest step. This is due to the location of the load step, which is exclusively in Grid 3 (see Figure 7.2). At time step t_2, the load increases in Grid 3 but decreases in Grids 1 and 2. Thus, the currents of the grid-forming DGUs corresponding to Grids 1 and 2 are negative, whereas the current of the grid-forming DGU in Grid 3 is positive. This is because in Grid 1 and 2 there is a surplus of generation, and the control effort is to consume power from the grid, which hence lowers the price. In Grid 3 there is a lack of power and the price increases. At time step t_3, the currents of the grid-forming DGUs in Grids 2 and 3 show negative steps, since the load decreases in those two grids (see Figure 7.2). The current of the grid-forming DGU in Grid 3 also varies, but much less in magnitude, since no load step occurs in Grid 3. The current variation here is due to the load step in the other grids, which is propagated through the dynamic system. Hence, indirectly, all grids help to stabilize the system when a disturbance occurs.

The node voltages of all nodes are depicted in Figure 7.12. The voltages fulfill the constraints of $\pm 10\,\%$ of the nominal voltage $1000\,\mathrm{V}$ at all times, even if this is not explicitly taken into account in the controller design. When a load change occurs, the voltages vary and a new steady state which allows the power flows in Figure 7.9

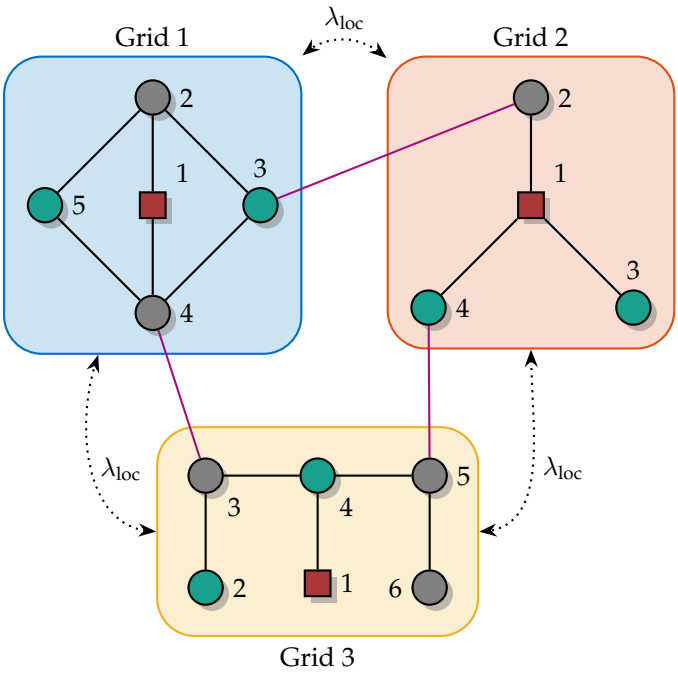

Figure 7.8: System of networked grids as described in Section 7.1 but including a grid-forming DGU in node 1 of each grid. The flexible prosumers are represented as green nodes, the inflexible prosumers as gray nodes, and system operator as a red square. The black dotted line is the communication graph for exchanging the local prices λ_{loc}^m.

arises. It can be further seen that the voltage differences between nodes increase as time increases. This is due to the load steps, that induce increasingly high load differences between the grids at every time step, as can be seen in Figure 7.2. To allow greater power flows between grids, the voltage differences between nodes have to increase.

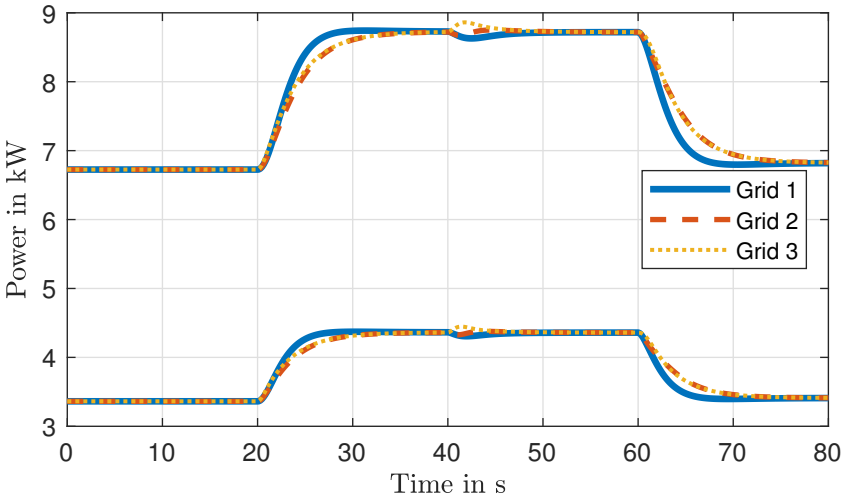

Figure 7.9: Power injection of the controlled DGUs over the simulation time when using the control framework for liberalized power systems.

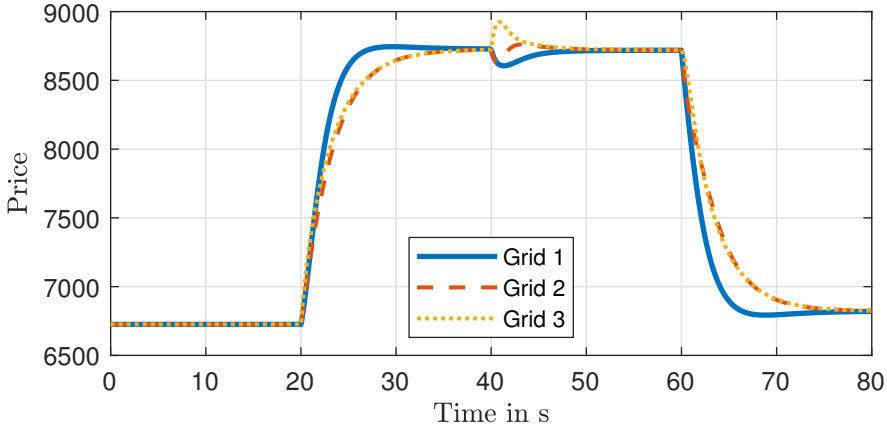

Figure 7.10: External price for each grid over the simulation time.

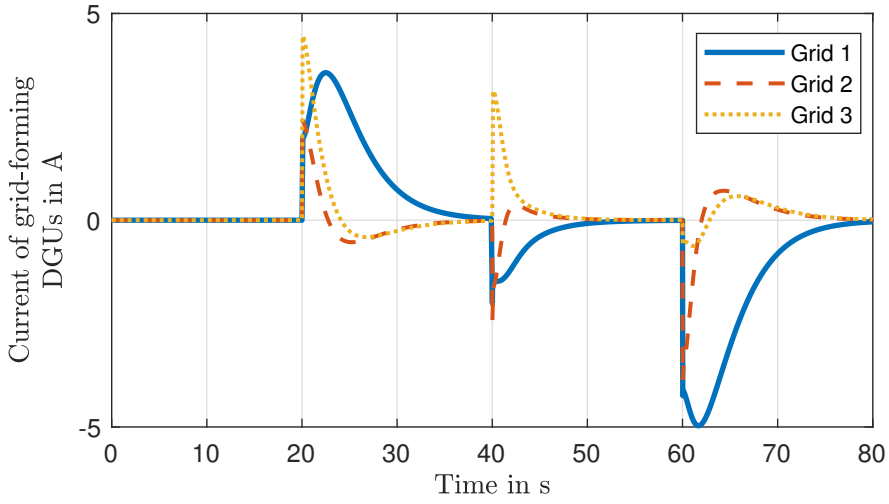

Figure 7.11: Current of the grid-forming DGU in each grid over the simulation time.

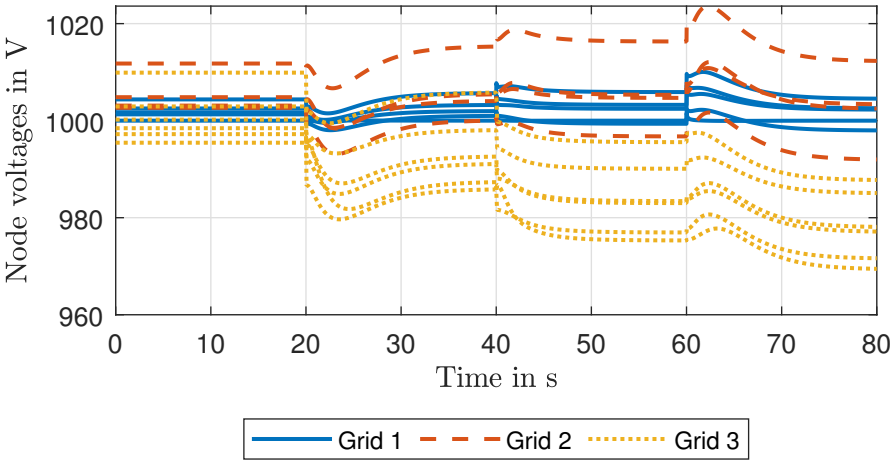

Figure 7.12: Node voltages of the networked system using the control framework for liberalized power systems.

7.4 Comparison and Discussion

In this section, the simulation results of the regulated control framework in Section 7.2 and the liberalized control framework in Section 7.3 are analyzed and compared. Special attention is paid to the interpretation of the different dynamics seen in the simulation results, the comparison of the performance, the information exchange, and the computational complexity.

Dynamics and Performance

By performance, it is meant how well the Objective of the Thesis is met. Thus, a lower power injection over time (and hence also a lower energy injection) while stabilizing the system corresponds to a better performance.

In Figure 7.13, the power injection of the DGUs in both proposed control frameworks are shown. The power generation in the liberalized framework is identical for DGUs with the same cost functions at steady state. In contrast to the liberalized approach, the power injections in the regulated framework are not identical for DGUs with identical generation costs located in different grids. This is because in the regulated framework there is no price to which the generators adapt according to its cost. The optimization problem (7.5) in the regulated framework computes the references by taking the location of the load into account. In general, two DGUs with identical cost functions may inject a different amount of power to minimize the overall costs. For instance, when one of the DGUs is located far away from the load, it should inject less power to avoid transmission losses despite having identical cost functions. This effect is seen in the power injections of the DGUs in the regulated framework, which leads to a power injection with 0.7% lower energy during the simulation time[81] than the power injection in the liberalized framework. Thus, the regulated framework shows better performance.

Furthermore, it can be observed in Figure 7.13 that the liberalized framework shows slower dynamics. This is in part due to the distributed averaging, which introduces further dynamics similar to a first order lag. On the other hand, the distributed setpoint-tracking MPC achieves a much faster regulation due to the large optimization horizon employed.

The voltage dynamics of both approaches in Figure 7.4 and Figure 7.12 also show considerable differences. Note that the steady-state node voltages arising in the liberalized framework in Figure 7.12 are similar to the node voltages arising from the distributed setpoint-tracking MPC in Figure 7.4. This is because similar power flows

[81] This number is obtained by integrating the power injections during all simulation time and comparing the energy injected in the liberalized and regulated framework. The lower injection is due to considering the global optimization problem including the losses in the regulated framework, rather than the profit-driven minimization of the own costs in the liberalized framework. The power from the stabilizing grid-forming DGU is considered for the computations in the liberalized framework, even if not shown in Figure 7.13

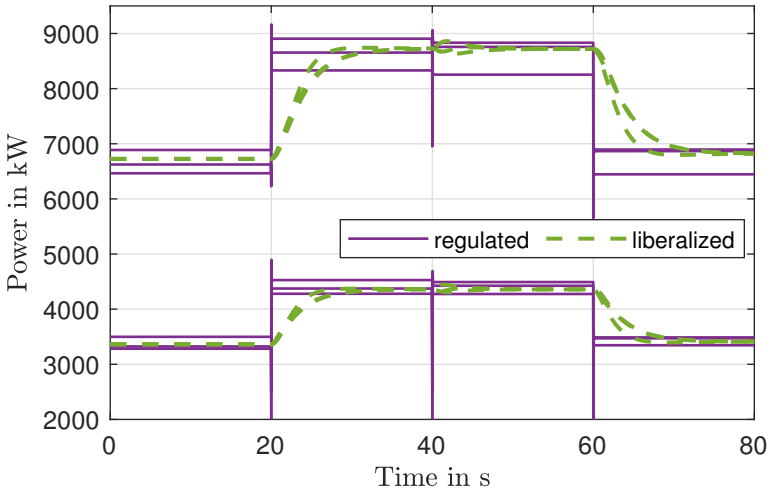

Figure 7.13: Comparison of the power injection of the DGUs in the regulated (green) and liberalized (purple) frameworks proposed in this work.

arise (see Figure 7.13), even when using completely different control frameworks where the distributed controllers exchange information of completely different nature (prices vs voltages). Note that when using the control framework for liberalized power systems, the voltage dynamics are slower, similar to the power injection in Figure 7.13. This is because, in contrast to the setpoint-tracking MPC, the voltages are not the control variables. In the liberalized framework, the voltages arise automatically in the nonlinear grid-following DGUs from the flexible prosumers in order to inject the correct amount of power. The voltages are, thus, a byproduct instead of the control variable. In addition, the distributed averaging introduces further dynamics similar to a first order lag. All in all, this also results in slower voltage dynamics.

Information Availability and Communication

Both approaches differ considerably w.r.t. the information and communication required by the controllers. The regulated approach is based on MPC strategies which use the system dynamics as a constraint. Hence, the system dynamics has to be known. Accurate knowledge about system dynamics implies accurate knowledge of the loads, which are possibly time-varying and have to be measured and/or estimated at all times. Similarly, the parameters (see Section D.1) of the power lines and DGUs have to be known. The performance of the MPC controller strongly depends, in general, on accurate knowledge of all the system parameters [Lan+24; CHM23]. In addition, during the real-time operation, the voltages have to be measured. For the underlying control, each DGU has to measure its own states to compute the state feedback as in (3.28). All in all, the regulated approach requires a large amount of measurements and system

information during operation.

In contrast to that, the liberalized framework needs less information for operation: the system operator only needs to measure the current of the grid-forming DGU in order to compute the price. The price is then forwarded to other grids according to a connected communication topology, and the distributed averaging algorithm (6.80) is performed. The averaged price is sent to the flexible prosumers, which inject an amount of power such that their profits are maximized (see Section 6.2). Via the system dynamics itself, these power injections are reflected in the current of the grid-forming DGU and, as a result, also in the price, thus closing the loop. As a consequence, the loads do not have to be known or measured. The only measurement necessary for coordination and stability is the current of the grid-following DGU.[82]

All in all, the liberalized framework requires less information about the system dynamics or system variables for operation. While the regulated framework needs to measure or estimate all the loads and voltages, the liberalized framework just requires the current of the grid-forming DGUs. This comes, however, at the price of additionally requiring a grid-forming DGU functioning as system operator, which is not required in the regulated framework.

Along with the differences regarding the information required for operation, the communication effort in the regulated framework is higher than in the liberalized framework. In the regulated framework, the information exchange is determined by the distributed optimization algorithm. With the distributed optimization proposed in Chapter 5, the grids exchange the coupling variables (i.e., voltages) in each iteration. As stated in Table 7.1, between 150 and 350 iterations are necessary at each time step, depending on the accuracy required. This then leads to 150 - 350 communication events in every time step. On the other hand, the liberalized framework relies only on the communication requirements of the distributed averaging algorithm (6.80), which is designed in continuous time in this dissertation. Thus, the communication requirements depend on the discretization time of the system dynamics.[83] In every time step, the grids need to exchange the local prices according to the communication topology of the distributed averaging once, in contrast to the 150 - 350 times per time step needed in the regulated framework.[84] However, the MPC in the regulated framework employs a reduced model, which can use discretization step sizes an order of magnitude larger than the full model.[85] Hence, the number of communication events in the regulated framework is reduced by an order of magnitude. As a result, the number of communication events of both approaches are roughly within an order of magnitude. The communication events

[82] For the underlying control, each DGU has to measure additionally its own states. This is the same in both the regulated and liberalized framework, and is thus not part of the comparison.

[83] This is only valid if the distributed averaging is discretized together with the system dynamics *after* a continuous-time-based system and control design. Larger discretization times may be possible, e.g., employing a real discrete-time controller design. However, this is not considered in this work.

[84] Since every time step, 150 - 350 iterations of the distributed optimization algorithm are necessary, and information exchange is necessary at each iteration.

[85] This is due to removing the fast dynamics of the power lines, see Section 4.2.

in the liberalized framework are around 10 times less than in the regulated framework in the same period of time. It may be possible to further reduce the discretization step size also in the liberalized framework for reducing the communication requirements, e.g., with a discrete-time system design, but this analysis lies outside the scope of this dissertation.

Computational Aspects

The computational requirements that the grids necessitate for implementing the regulated and liberalized approaches differ considerably. On the one hand, the regulated framework is based on MPC strategies which solve, in a distributed manner, a global optimization problem in *every* time step. The computational requirements strongly depend on the distributed optimization algorithm employed. As reviewed in Section 2.4, the well known ADMM approaches need to solve a nonlinear programming problem in every iteration, i.e., potentially hundreds of times within a single time step. In Chapter 5, a continuous-time primal-dual algorithm is proposed. Compared to ADMM, it reduces the computational complexity because only a gradient descent (or dual ascent, for the constraints) is performed at every iteration. However, regardless of the optimization algorithm, it holds in general for the MPC, that at each time step a global optimization problem has to be solved via the distributed optimization algorithm.

On the other hand, in the liberalized framework, no optimization problem has to be solved explicitly in every time step.[86] The price-forming mechanism and the underlying controllers perform simple integrations and multiplications. Similarly, the distributed averaging algorithm also performs basic multiplication and addition operations. Thus, the computational complexity of the controllers in the liberalized framework that the grids need to implement is significantly lower than in the regulated framework. This is an advantage of the liberalized framework.

However, despite high computational requirements, the regulated framework has an advantage in performance due to explicitly solving the global optimization problem in every time step. As explained in Section 7.4, by taking into account the location of the load,[87] a better optimization performance is possible (see Section 7.4). This is translated into 0.7% less energy injection in the simulation scenario. This may seem like a small performance increase, but it has to be taken into account that this may translate into a significant amount of energy in absolute numbers. In contrast, the steady state induced by the liberalized framework characterized in Proposition 6.8 does not take into account the location of the loads and establishes a single UMP, leading to worse performance.

[86] As a consequence, optimality is achieved only at steady state.

[87] This is possible since it has to measure or estimate all the loads, in contrast to the liberalized framework.

7.5 Summary and Outlook

In this chapter, both approaches for the optimization-based control of a future power system presented in this work have been compared using a simulation study. The regulated framework (Chapter 4) achieves better performance, at the cost of necessitating more information about the system dynamics and state, and higher computational capabilities. The liberalized framework achieves less performance. This is due to the fact that the loads are not known, measured or estimated, and thus the exact location of the load is not known. However, the computational complexity and information exchange is lower, since no global optimization problem has to be solved at every time step. Furthermore, the liberalized framework complies with the legal and operational unbundling of current power systems. As outlined in Section 6.8, there exists a clear separation of the tasks of maintaining system stability, which corresponds exclusively to the system operator, and power injection, which corresponds exclusively to the flexible and inflexible prosumers.

Moreover, the implementation details for employing the distributed optimization presented in Chapter 5 for achieving a distributed operation in the regulated framework of Chapter 4 have been presented. In Chapter 5, local stability conditions have been derived, therefore ensuring stability also when a grid connects or disconnects from the power system. However, the distributed computation of the MPC problem is necessary to fulfill Contribution 1, which contributes towards the Objective of the Thesis.

The control framework to choose in practice depends strongly on the requirements of the particular application. In power systems where the system is well known and a high quantity of states are estimated, the regulated framework may be used to increase performance if enough computational resources and a high-bandwidth communication infrastructure are available. In power systems in which the system dynamics, i.e., the loads or uncontrollable injection, are rapidly changing, the liberalized framework is more suitable, since less information has to be estimated. Furthermore, if the legal and operational unbundling is important, or if the computational resources or communication infrastructure are scarce, the liberalized framework is better suited.

All in all, this chapter illustrates the Contributions 1 - 4, which have been developed theoretically in the previous chapters, by means of a practical example. The regulated framework (Contributions 1-2) and the liberalized framework (Contributions 3-4) are compared in relevant aspects in order to showcase the strengths and requirements of each methodology. Although the computational and informational requirements of both methods are completely different, both methods fulfill the Objective of the Thesis, i.e., the design of control frameworks allowing for an optimal operation of large-scale, networked power systems based on power electronics.

8 Conclusion

The ongoing shift towards distributed, renewable generation results in power systems with small time constants that are more prone to large state deviations and instability when disturbances occur. Moreover, future power systems have an increasingly large number of *volatile* DGUs that may disconnect and reconnect, inducing frequent changes in network configuration and power generation. The current market mechanism responsible for the *optimization* of a power system is designed for systems with predictable loads and few large generators, and is thus not suitable for future power systems with a large share of *volatile* renewable generation.

The thesis at hand closes this gap by developing control frameworks for the optimization-based control of future power systems, as defined in the Objective of the Thesis in Chapter 1. To be suitable for future power systems, the individual controllers should operate in a distributed manner. Furthermore, *local stability certificates* allowing to assess stability of the interconnected power system with local conditions on the individual subsystems are necessary in power systems with a large number of power generators, since the analysis of the whole networked system becomes prohibitive. In particular, two different control frameworks for the optimal control of future power systems have been developed in this work. Both allow the optimal operation of future power systems in a distributed manner, and allow the individual grids to disconnect and reconnect without compromising stability due to local stability certificates exploiting passivity theory. All the methods proposed in this thesis are showcased on networked DC grids.

The first control framework proposed in this work (Chapter 4) creates a regulated power system as defined in Term 2.1. The approach is based on MPC strategies considering a global optimization problem over the interconnected grids. The problem is solved in a distributed manner with the novel distributed optimization algorithm proposed in Chapter 5. The main novelty is the modular Lyapunov function for MPC exploiting passivity theory and the distributed optimization, in combination allowing a plug-and-play operation of grids. In this approach, there is no distinction between different roles such as the system operator or market participants, and consequently there is no separation of tasks as in the current unbundled power system.

The second control framework proposed in this work (Chapter 6) pertains to a liberalized power system as in Term 2.2. The approach is based on a control theory-inspired price-forming mechanism implemented by the system operator that changes the price according to the control effort necessary to stabilize the power system. Therefore, the framework is specifically designed for systems with high volatility, where any disturbance that leads to a stabilizing control effort is reflected on the price of electric

power. With the novel concept of economic ports, the local prices of each grid are then exchanged in order to achieve coordination, i.e., global optimality. Economic ports do not only provide means for the coordination of grids, but also for ensuring stability via its EIP properties.

Both approaches have been compared within this thesis using an academic example. The regulated approach requires more knowledge about the system, more computation capabilities and communication, but achieves better performance. On the other hand, the liberalized approach relies on less exchange of information and simpler computations, and shows a separation of roles between system operation and energy trading compatible with current unbundled power systems. Furthermore, the liberalized approach encourages competition and can lead, combined with an appropriate legal frame, to lower prices and a greater participation in the network. Thus, both approaches have different advantages and properties, and should be chosen according to the specific needs of the power system in question.

Outlook

A natural extension of the regulated approach is to use economic MPC instead of setpoint-tracking MPC. It has been shown in this work that economic MPC achieves better performance. In addition, economic MPC does not need setpoints computed in advance, which significantly simplifies the control structure. An open question is how to design the economic MPC such that asymptotic stability is ensured while employing only local conditions for the grids.

The liberalized framework of Chapter 6 can be extended in various ways. The introduction of a price-forming mechanism and a corresponding local price opens up a wide range of possible extensions. For instance, by adequately extending the price-forming mechanism and the price consensus in Section 6.6.3, well-studied features such as congestion management can be included. Furthermore, additional incentives, e.g., to achieve long term goals, can be included. For example, price incentives for the installation of DGUs in a certain geographical area [Koe22], e.g., where a large thermal power plant is scheduled to disconnect in near future, could be included within the liberalized control framework.

Another aspect to be investigated is the utilization of predictions or priorly known information in the proposed method for liberalized power systems, in particular in the price-forming mechanism. The proposed price-forming mechanism determines the price according to the feedback control effort to stabilize the system. When a load step occurs, the grid-forming DGU stabilizes the system and this induces a price variation, until the grid-forming DGU does not have to stabilize the system anymore and hence a constant price is achieved (see Figure 8.1a). The price is, hence, formed in a feedback structure, with no information or prediction about the loads or other priorly known

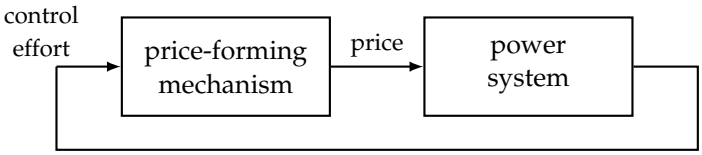

(a) Proposed price-forming mechanism

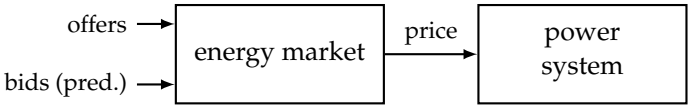

(b) Price-forming mechanism in current power systems

Figure 8.1: Comparison of the proposed novel price-forming mechanism (a) and the traditional price-forming mechanism used in power systems based on predictions (b).

information. In contrast to that, nowadays, the price is formed exclusively via predictions with a feedforward structure instead of feedback information (see Figure 8.1b and cf. Section 2.1.2). In summary, the current power system optimization uses *only* predictions, and the proposed method uses *only* feedback information. In a volatile power system, feedback control information is advantageous for forming the price rather than predictions and a feedforward structure. However, adding a feedforward part to the feedback structure proposed in this work may lead to an even more efficient price-forming mechanism. The feedforward structure then accounts for the potentially few predictable loads in the power system. This follows the doctrine *use feedforward control as much as possible, use feedback control as much as necessary*. A sketch of this idea is depicted in Figure 8.2. The price prediction could arise in an energy market similar to the one currently used. Including predictions in the novel price-forming mechanism can be seen as a trade-off between using the available information about the loads, like it has become standard in power systems, but also implementing a feedback structure that does not rely exclusively on those predictions. This may be the key for the deployment of the proposed methodology in actual power systems, paving the way towards an effective optimization in future power systems.

In summary, this thesis is the first to exploit passivity theory for the design of distributed optimization-based control methods for power systems, obtaining local conditions that guarantee both optimality and stability.

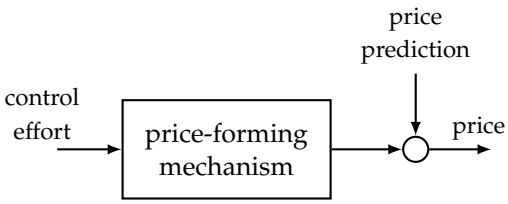

Figure 8.2: Sketch of combining the proposed price-forming mechanism with price predictions.

A Appendix to Chapter 4

A.1 Separable Functions and Constraints

In Chapter 4, separable objective functions and constraints form the basis for obtaining local stability conditions for each grid. The following definitions introduce separable functions and constraints as used in this work.

Definition A.1 (separable function)
Consider a set $\mathcal{A} = \{1, 2, \ldots, |\mathcal{A}|\}$ of agents, each having the variables $\boldsymbol{x}_1$, $\boldsymbol{x}_2$, …, $\boldsymbol{x}_{|\mathcal{A}|}$. Define $\boldsymbol{x} = \text{col}\{\boldsymbol{x}_i\} \in \mathbb{R}^n$, $i \in \mathcal{A}$ where n is the dimension of the stacked variables of all agents. A function $\boldsymbol{f} : \mathbb{R}^n \to \mathbb{R}$ is called separable, if it can be decomposed as

$$f(\boldsymbol{x}) = \sum_{i \in \mathcal{A}} f_i(\boldsymbol{x}_i). \tag{A.1}$$

A common example for a function for which the separability property is important in the context of distributed MPC is a Lyapunov function. In order to split the Lyapunov function and assign a part to each grid, it needs to be separable. If it is not separable, the Lyapunov function contains coupling terms $\boldsymbol{f}_{ij}$ between agents i and j, i.e.

$$f(\boldsymbol{x}) = \sum_{i \in \mathcal{A}} \left\{ f_i(\boldsymbol{x}_i) + \sum_{j \in \mathcal{A}} f_{ij}(\boldsymbol{x}_i, \boldsymbol{x}_j) \right\}. \tag{A.2}$$

Even if those coupling terms can be assigned to a specific agent, their evaluation requires variables from two different agents. This makes thus that the conditions for stability are not local, but have to be checked with global information about the agents.

Similarly, separable constraints can be defined.

Definition A.2 (separable constraints)
Consider a set $\mathcal{A} = \{1, 2, \ldots, |\mathcal{A}|\}$ of agents, each having the variables $\boldsymbol{x}_1$, $\boldsymbol{x}_2$, …, $\boldsymbol{x}_{|\mathcal{A}|}$. Define $\boldsymbol{x} = \text{col}\{\boldsymbol{x}_i\} \in \mathbb{R}^n$, $i \in \mathcal{A}$ where n is the dimension of the stacked variables of all agents. The constraint $\boldsymbol{x} \in \mathbb{X}$ is called separable if it can be decomposed as

$$\mathbb{X} = \mathbb{X}_1 \cup \cdots \cup \mathbb{X}_{|\mathcal{A}|}, \tag{A.3}$$

with $\boldsymbol{x}_i \in \mathbb{X}_i$.

Separable constrains are such that they can be decomposed in independent constraints for the individual agents. This is important for the terminal constraints in the context of distributed MPC, since the terminal constraints have to be chosen as the positive invariant set induced by the Lyapunov function used in the terminal costs. If the terminal constraints are not separable, global information is necessary for their evaluation, and the stability conditions cannot be local conditions.

An example of separable constraints that are commonly used in the context of MPC are polytopic constraints such that every variable is constrained by a maximum and a minimum value, i.e.

$$\mathbb{X} = \bigcup_{i \in \mathcal{A}} [\boldsymbol{x}_{i,\min}, \boldsymbol{x}_{i,\max}]. \tag{A.4}$$

Note that, with such polytopic constraints, each agent can evaluate independently of each other if the constraints are fulfilled, leading to local stability conditions for the grids when used as terminal constraints.

B Appendix to Chapter 5

B.1 Properties of the Kronecker Product

The following Kronecker product properties [Eve80, p. 107] are used in some proofs throughout the dissertation. Consider matrices $\boldsymbol{A}, \boldsymbol{B}, \boldsymbol{C}$ and $\boldsymbol{D}$ of appropriate dimension.

(P1) The mixed-product property:

$$(\boldsymbol{A} \otimes \boldsymbol{B})(\boldsymbol{C} \otimes \boldsymbol{D}) = \boldsymbol{AC} \otimes \boldsymbol{BD}. \tag{B.1}$$

(P2) Associativity:

$$\boldsymbol{A} \otimes (\boldsymbol{B} + \boldsymbol{C}) = \boldsymbol{A} \otimes \boldsymbol{B} + \boldsymbol{A} \otimes \boldsymbol{C}. \tag{B.2}$$

B.2 Auxiliary Proofs

Proposition B.1 (kernel of Kronecker product)
Consider a matrix $\boldsymbol{A} \in \mathbb{R}^{m \times n}$ with $m \geq n$, rank$(\boldsymbol{A}) = n - 1$ and a nullspace $\ker\{\boldsymbol{A}\} = \{\alpha \mathbf{1}_n \mid \alpha \in \mathbb{R}\}$. *Then, the matrix*

$$(\boldsymbol{A} \otimes \boldsymbol{I}_p) \in \mathbb{R}^{mp \times np} \tag{B.3}$$

has a nullspace which is spanned by the vectors $\mathbf{1}_n \otimes \boldsymbol{a}_p$, where $\boldsymbol{a}_p \in \mathbb{R}^p$ is an arbitrary constant vector.

Proof. Let $\boldsymbol{e}_i$, $i \in \{1, \ldots, n\}$ and $\boldsymbol{e}_j$, $j \in \{1, \ldots, p\}$ be basis vectors of $\mathbb{R}^n$ and $\mathbb{R}^p$, respectively. The vectors $\boldsymbol{e}_i \otimes \boldsymbol{e}_j$ then form a basis for $\mathbb{R}^n \times \mathbb{R}^p$, which contains the kernel of matrix (B.3). To determine the kernel of (B.3), we have to find vectors $\boldsymbol{v} \in \mathbb{R}^n \times \mathbb{R}^p$ such that

$$(\boldsymbol{A} \otimes \boldsymbol{I}_p)\, \boldsymbol{v} = 0. \tag{B.4}$$

For that, we parametrize the vector v using the basis as $\boldsymbol{v} = \sum_{i=1}^{n}\sum_{j=1}^{p} \boldsymbol{v}_{ij}(\boldsymbol{e}_i \otimes \boldsymbol{e}_j)$, with $\boldsymbol{v}_{ij} \in \mathbb{R}$. Then, (B.4) reads

$$(\boldsymbol{A} \otimes \boldsymbol{I}_p) \sum_{i=1}^{n}\sum_{j=1}^{p} \boldsymbol{v}_{ij}(\boldsymbol{e}_i \otimes \boldsymbol{e}_j) = 0. \tag{B.5}$$

Using the mixed-product and associative properties P1 and P2 of the Kronecker product as in Section B.1, (B.5) can be rearranged to

$$\sum_{i=1}^{n}\sum_{j=1}^{p} \boldsymbol{v}_{ij}(\boldsymbol{A}\boldsymbol{e}_i \otimes \boldsymbol{e}_j) = \sum_{j=1}^{p} \left(\sum_{i=1}^{n} \boldsymbol{v}_{ij}\boldsymbol{A}\boldsymbol{e}_i \right) \otimes \boldsymbol{e}_j = 0. \tag{B.6}$$

Since the vectors $\boldsymbol{e}_j$ in (B.6) are linearly independent, all the individual addends over index j have to be zero in order to fulfill the equality. The only way to achieve this is if the left-hand side of each of the Kronecker products is zero, i.e.,

$$\sum_{j=1}^{p} \boldsymbol{v}_{ij}\boldsymbol{A}\boldsymbol{e}_i = \boldsymbol{A}\sum_{j=1}^{p} \boldsymbol{v}_{ij}\boldsymbol{e}_i = 0. \tag{B.7}$$

Equation (B.7) is true if and only if $\sum_{i=1}^{n} \boldsymbol{v}_{ij}\boldsymbol{e}_i$ is a nullvector of $\boldsymbol{A}$, i.e., $\alpha_j 1_n$ for some $\alpha_j \in \mathbb{R}$. Thus, the vectors

$$\boldsymbol{v} = \sum_{j=1}^{p} \alpha_j 1_n \otimes \boldsymbol{e}_j = 1_n \otimes \left(\sum_{j=1}^{p} \alpha_j \boldsymbol{e}_j \right) = 1_n \otimes \boldsymbol{a}_p \tag{B.8}$$

span the kernel of $(\boldsymbol{A} \otimes \boldsymbol{I}_p)$. □

Proposition B.2 (semidefiniteness of special matrix product)
The matrix $\boldsymbol{M} = (\boldsymbol{I}_n + \alpha\boldsymbol{Q})^{-1}\boldsymbol{Q} \in \mathbb{R}^{n\times n}$, with $\boldsymbol{Q} \in \mathbb{R}^{n\times n}$ positive semidefinite, is positive semidefinite for any $\alpha \in \mathbb{R}_{\geq 0}$.

Proof. The proof consists of two parts. First, nonnegativity of the eigenvalues of $\boldsymbol{M}$ is proven. Afterwards, it is proven that $\boldsymbol{M}$ is symmetric, both properties proving thus positive semidefiniteness of $\boldsymbol{M}$.

For any $\alpha \geq 0$, considering that $\boldsymbol{Q}$ is positive semidefinite, the matrix $(\boldsymbol{I}_n + \alpha\boldsymbol{Q})^{-1}$ exists and is positive definite. Assume that $(\lambda, \boldsymbol{v})$ is an eigenvalue-eigenvector pair of $\boldsymbol{M}$. Then, by left multiplying $\boldsymbol{M}\boldsymbol{v} = \lambda\boldsymbol{v}$ with $(\boldsymbol{I}_n + \alpha\boldsymbol{Q})$, we obtain

$$\boldsymbol{Q}\boldsymbol{v} = \lambda(\boldsymbol{I}_n + \alpha\boldsymbol{Q})\boldsymbol{v}, \tag{B.9}$$

and regrouping the terms containing matrix Q on the left we obtain

$$\boldsymbol{Q}\boldsymbol{v} = \frac{\lambda}{1-\alpha\lambda}\boldsymbol{v}. \tag{B.10}$$

This implies that the term $\frac{\lambda}{1-\alpha\lambda}$ is an eigenvalue of $\boldsymbol{Q}$ and is nonnegative due to the semidefiniteness of $\boldsymbol{Q}$. Hence, λ needs to be such that the expression $\frac{\lambda}{1-\alpha\lambda}$ is nonnegative. This in turn implies $\lambda \geq 0$, which completes the first part of the proof.

It remains to prove that $\boldsymbol{M}$ is symmetric. This part of the proof consists in verifying that $\boldsymbol{M} = \boldsymbol{M}^\top$ holds true. Consider hence $\boldsymbol{M} = \boldsymbol{M}^\top$

$$(\boldsymbol{I}_n + \alpha\boldsymbol{Q})^{-1}\boldsymbol{Q} = \boldsymbol{Q}(\boldsymbol{I}_n + \alpha\boldsymbol{Q})^{-1}. \tag{B.11}$$

Left-multiplying the equation with $(\boldsymbol{I}_n + \alpha\boldsymbol{Q})$, it results in

$$\boldsymbol{Q} = (\boldsymbol{I}_n + \alpha\boldsymbol{Q})\boldsymbol{Q}(\boldsymbol{I}_n + \alpha\boldsymbol{Q})^{-1}. \tag{B.12}$$

Now, taking into account that $(\boldsymbol{I}_n + \alpha\boldsymbol{Q})\boldsymbol{Q} = \boldsymbol{Q}(\boldsymbol{I}_n + \alpha\boldsymbol{Q})$, it follows from (B.12) that

$$\boldsymbol{Q} = \boldsymbol{Q}. \tag{B.13}$$

Since it resulted $\boldsymbol{Q} = \boldsymbol{Q}$ from $\boldsymbol{M} = \boldsymbol{M}^\top$ only by applying equivalence relations, it can be concluded that $\boldsymbol{M} = \boldsymbol{M}^\top$ holds true, which completes the proof. □

Proposition B.3 (Limit of special function)
Consider the function $\nu(\gamma) = \text{eigmin}\{\gamma(\boldsymbol{I}_n + \gamma\boldsymbol{Q})^{-1}\}$, where $\boldsymbol{Q}$ is a positive semi-definite matrix and $\gamma \in \mathbb{R}_{\geq 0}$ a scalar. Then, it holds that

$$\lim_{\gamma\to\infty} \nu(\gamma) = \frac{1}{\text{eigmax}\{\boldsymbol{Q}\}}. \tag{B.14}$$

Proof. Since $\boldsymbol{Q}$ is symmetric, it is (unitarily) diagonalizable [HJ12, Th. 4.1.5]. Thus, consider next splitting $\boldsymbol{Q} = \boldsymbol{P}\boldsymbol{\Lambda}\boldsymbol{P}^{-1}$ into a diagonal matrix $\boldsymbol{\Lambda}$ and a unitary matrix $\boldsymbol{P}$. Recall that the eigenvalues of $\boldsymbol{Q}$ are the diagonal entries of $\boldsymbol{\Lambda}$. Note that $(\boldsymbol{I}_n + \gamma\boldsymbol{Q})^{-1}$ is the same as $\boldsymbol{P}(\boldsymbol{I}_n + \gamma\boldsymbol{\Lambda})^{-1}\boldsymbol{P}^{-1}$. Observe that

$$(\boldsymbol{I}_n + \gamma\boldsymbol{\Lambda})^{-1} = \text{diag}\{\frac{1}{1+\gamma\lambda_i}\}, \tag{B.15}$$

where λ_i are the diagonal entries of $\boldsymbol{\Lambda}$ (or, equivalently, the eigenvalues of $\boldsymbol{Q}$). Equation (B.15) follows directly from the fact that the eigenvalues of $\boldsymbol{Q}^{-1}$ are $\frac{1}{\lambda_i}$ and that the eigenvalues of $(\boldsymbol{I} + \boldsymbol{Q})$ are $1 + \lambda_i$. Next, since γ is a scalar, multiplying (B.15) by γ yields

$$\gamma(\boldsymbol{I}_n + \gamma\boldsymbol{\Lambda})^{-1} = \text{diag}\{\frac{\gamma}{1+\gamma\lambda_i}\}. \tag{B.16}$$

Then, since $\boldsymbol{P}$ is unitary, the eigenvalues of $\gamma(\boldsymbol{I}_n + \gamma\boldsymbol{Q})^{-1}$ are the eigenvalues of $\boldsymbol{P}(\boldsymbol{I}_n + \gamma\boldsymbol{\Lambda})^{-1}\boldsymbol{P}^{-1}$, which in turn are the entries in (B.16). Consider the limit

$$\lim_{\gamma\to\infty} \frac{\gamma}{1+\gamma\lambda_i} = \frac{1}{\lambda_i}. \tag{B.17}$$

Hence, the eigenvalues of $\gamma(\boldsymbol{I}_n + \gamma\boldsymbol{Q})^{-1}$ for $\gamma \to \infty$ are (B.17). The smallest eigenvalue is then the one corresponding to the largest λ_i, thus obtaining the statement (B.14), which completes the proof. □

B.3 Discontinuous Dynamic Systems

For discontinuous dynamic systems, i.e., systems that have a nonsmooth right-hand side, *classical solutions* do not necessarily exist in general. With *classical solutions*, solutions to the differential equation with the classical notion of a derivative in mathematical analysis is meant. In this dissertation, Carathéodory solutions for discontinuous dynamic systems are considered. They are defined as follows.

Definition B.1 (Carathéodory solutions [Cor08])
A Carathéodory solution of a discontinuous dynamic system is a continuous map $x : [0, t] \to \mathbb{R}^n$ that satisfied the differential equation with discontinuous right-hand side for almost all $\tau \in [0, t]$. Almost all is understood in the sense of Lebesgue measure, i.e., the solution must fulfill the differential equation except for a set of time instants that has measure zero.

Equivalently, Carathéodory solutions are continuous solutions that solve the integral version of the discontinuous differential equation [Cor08]. Thus, every classical solution is also a Carathéodory solution.

In the following, an example taken from [Cor08] of a system where classical solutions do not exist, but Carathéodory solutions do exist, is presented.

Example B.1:
Consider the system $\dot{x} = f(x)$ with discontinuous right-hand side at $x = 0$

$$f(x) = \begin{cases} 1, & x > 0 \\ \frac{1}{2}, & x = 0 \\ -1, & x < 0 \end{cases} \tag{B.18}$$

This dynamic system does not have a classical solution $x(t)$ for the initial value $x(0) = 0$. But the system has two Carathéodory solutions, i.e., $x_1(t) = t$ and

$x_2(t) = -t$. Note that both solutions violate the differential equation at $t = 0$, but not at $t > 0$ (or $t < 0$ for the case of x_2), while $t = 0$ is a set of Lebesgue measure zero.

Note that Carathéodory solutions are not the only notion of solution that has been developed for discontinuous dynamic systems. There exist, for example, the more general definition of a Fillipov solution, among others [Cor08].

B.4 Projected Dynamic Systems

Projected dynamic system theory use the concept of projecting a vector onto a closed convex set [NZ12, Ch. 2.2]. It makes use of the common (point) projection of point $\boldsymbol{z} \in \mathbb{R}^n$ onto the closed convex set $\mathcal{K}$ defined as $\text{proj}_{\mathcal{K}}(\boldsymbol{z}) = \arg\min_{\boldsymbol{x}\in\mathcal{K}} \|\boldsymbol{x} - \boldsymbol{z}\|$. The vector projection is defined as [NZ12, Eq. (2.14)]

$$\boldsymbol{\Gamma}_{\mathcal{K}}(\boldsymbol{v}, \boldsymbol{x}) = \lim_{\delta \to 0^+} \frac{\text{proj}_{\mathcal{K}}(\boldsymbol{x} + \delta \boldsymbol{v}) - \boldsymbol{x}}{\delta}. \tag{B.19}$$

The following proposition gives a geometrical interpretation of the vector projection, which is used later to establish that the system under study can be indeed casted a projected dynamic system.

The interior and boundary of a set $\mathcal{A}$ is denoted by $\text{int}\{\mathcal{A}\}$ and $\text{bnd}\{\mathcal{A}\}$, respectively.

Proposition B.4 ([NZ12, Lemma 2.1])
Let $\boldsymbol{n}(\boldsymbol{x})$ denote the set of inward normals to $\mathcal{K}$ at $\boldsymbol{x}$ on the $\text{bnd}\{\mathcal{K}\}$.

(i). If $\boldsymbol{x} \in \text{int}\{\mathcal{K}\}$, then $\boldsymbol{\Gamma}_{\mathcal{K}}(\boldsymbol{v}, \boldsymbol{x}) = \boldsymbol{v}$

(ii). If $\boldsymbol{x} \in \text{bnd}\{\mathcal{K}\}$, then $\boldsymbol{\Gamma}_{\mathcal{K}}(\boldsymbol{v}, \boldsymbol{x}) = \boldsymbol{v} + \beta(\boldsymbol{x}, \boldsymbol{v})\boldsymbol{n}^*(\boldsymbol{x})$ with $\boldsymbol{n}^*(\boldsymbol{x}) = \arg\max_{\boldsymbol{n}\in\boldsymbol{n}(\boldsymbol{x})} \boldsymbol{v}^\top(-\boldsymbol{n})$ and $\beta(\boldsymbol{x}, \boldsymbol{v}) = \max\{0, \boldsymbol{v}^\top(-\boldsymbol{n}^*(x))\}$.

Remark B.1. *It directly follows from Proposition B.4 case (ii) that if $\boldsymbol{x}$ is at the boundary and $\boldsymbol{x}$ points inwards into $\mathcal{K}$, $\boldsymbol{\Gamma}_{\mathcal{K}}(\boldsymbol{v}, \boldsymbol{x}) = \boldsymbol{v}$ since $\boldsymbol{v}^\top(-\boldsymbol{n}^*(\boldsymbol{x})) \leq 0$, which implies that $\beta(\boldsymbol{x}, \boldsymbol{v}) = 0$. Furthermore, if $\boldsymbol{x}$ is at the boundary and $\boldsymbol{v}$ points outwards and is perpendicular to $\mathcal{K}$, $\beta(\boldsymbol{x}, \boldsymbol{v})\boldsymbol{n}^*(\boldsymbol{x}) = -\boldsymbol{v}$ and $\boldsymbol{\Gamma}_{\mathcal{K}}(\boldsymbol{v}, \boldsymbol{x}) = 0$.*

With the vector projection (B.19), a special type of constrained, discontinuous system can be defined. Given a dynamic system $\dot{\boldsymbol{x}} = \boldsymbol{\phi}(\boldsymbol{x})$ and a closed and convex set $\mathcal{K}$, the projected dynamic system is defined as

$$\dot{\boldsymbol{x}} = \boldsymbol{\Gamma}_{\mathcal{K}}(\boldsymbol{\phi}(\boldsymbol{x}), \boldsymbol{x}), \quad \boldsymbol{x}(0) \in \mathcal{K}. \tag{B.20}$$

Proposition B.5 ([NZ12, Th. 2.5])

Let $\phi : \mathbb{R}^n \to \mathbb{R}^n$ be Lipschitz on a closed and convex set $\mathcal{K}$. Then,

(i) for any $\boldsymbol{x}(0) \in \mathcal{K}$, there exists a unique solution $\boldsymbol{x}(t)$ to the initial value problem (B.20)*;*

(ii) if the sequence $\boldsymbol{x}_m(0) \to \boldsymbol{x}(0)$ as $m \to \infty$, then $\boldsymbol{x}_m(t)$ converges to $\boldsymbol{x}(t)$ uniformly on every compact set of $[0, \infty)$.

C Appendix to Chapter 6

C.1 Auxiliary Propositions

Proposition C.1 (semidefiniteness of symmetric block matrix)
Consider matrices $\boldsymbol{A} \in \mathbb{R}^{n\times n}$ and $\boldsymbol{B} \in \mathbb{R}^{n\times m}$. The semidefiniteness condition on the block matrix

$$\begin{bmatrix} \boldsymbol{A} & \boldsymbol{B} \\ \boldsymbol{B}^\top & \boldsymbol{0} \end{bmatrix} \leq 0 \tag{C.1}$$

is equivalent to $\boldsymbol{A} \leq 0$ and $\boldsymbol{B} = \boldsymbol{0}$.

Proof. Matrix (C.1) is a saddle point matrix, which is indefinite whenever $\boldsymbol{B} \neq \boldsymbol{0}$ [BGL05, p. 21]. Thus, the semidefiniteness condition can only be fulfilled when $\boldsymbol{B} = \boldsymbol{0}$. This is a standard result in matrix analysis as is widely used in passivity theory, see e.g. [AMP16, p. 7]. □

D Appendix to Chapter 7

D.1 Supplementary Simulation Data

All the parameter are chosen in accordance to the literature, e.g., [Tuc+18; Mal25; Nah+20]. All lines are chosen, without loss of generality, identical with a resistance of $R_{\pi,j} = 1.5\,\Omega$ and an inductance of $L_{\pi,j} = 2\,\mathrm{mH}$. The DGU filter parameters are $R_{\mathrm{f},i} = 0.2\,\Omega$, $L_{\mathrm{f},i} = 1.8\,\mathrm{mH}$ and $C_{\mathrm{f},i} = 2.2\,\mathrm{mF}$, and the DGU control parameters are $k_1 = -0.1$, $k_2 = -2.5$, and $k_3 = 179.9$. In Table D.1, the load parameters of each node at each time period are given. The variable that changes between time steps is the constant power load. This is chosen since the constant power load introduces a strong nonlinearity, and thus is the most challenging load change. The values of Z^{-1} are given in $\frac{1}{\Omega}$, I in A, and P in W.

Table D.1: Simulation parameters of the loads in each node. The first number of the node is the grid, the second the node number. The color of the node number indicates to which grid it pertains (see Figure 7.1).

	0 - 20s			20 - 40s			40 - 60s			60 - 80s		
node number	Z^{-1}	I	P	Z^{-1}	I	P	Z^{-1}	I	P	Z^{-1}	I	P
11	0.02	2	0	0.02	2	0	0.02	2	-100	0.02	0	-450
12	0.02	2	0	0.02	2	0	0.02	2	-100	0.02	0	-450
13	0.02	2	0	0.02	2	0	0.02	2	-100	0.02	0	-450
14	0.02	2	0	0.02	2	0	0.02	2	-100	0.02	0	-450
15	0.02	2	0	0.02	2	0	0.02	2	-100	0.02	0	-450
21	0.02	0	0	0.02	0	0	0.02	0	-100	0.02	2	-450
22	0.02	0	0	0.02	0	0	0.02	0	-100	0.02	2	-300
23	0.02	0	0	0.02	0	0	0.02	0	-100	0.02	2	-450
24	0.02	0	0	0.02	0	0	0.02	0	-100	0.02	2	-450
31	0.02	5	0	0.02	5	500	0.02	5	700	0.02	5	700
32	0.02	5	0	0.02	5	500	0.02	5	700	0.02	5	700
33	0.02	5	0	0.02	5	500	0.02	5	700	0.02	5	600
34	0.02	5	0	0.02	5	500	0.02	5	600	0.02	5	700
35	0.02	5	0	0.02	5	500	0.02	5	600	0.02	5	600
36	0.02	5	0	0.02	5	500	0.02	5	600	0.02	5	600

The MPC framework consider voltage constraints for all nodes. The constraints are $\pm 10\,\%$ of the nominal value. In particular, in Chapter 7, the constraints are $[900\,\mathrm{V}, 1100\,\mathrm{V}]$.

The parameter α of setpoint-tracking MPC is chosen to be $\alpha = 1$ to penalize node voltage and input deviation equally. The discretization time of the model is $h_{\mathrm{T}} = 10\,\mathrm{ms}$.

The distributed averaging of the liberalized method uses the Laplacian matrix

$$\boldsymbol{L} = \begin{bmatrix} 2 & -1 & -1 \\ -1 & 2 & -1 \\ -1 & -1 & 2 \end{bmatrix}. \tag{D.1}$$

The voltage reference of the grid-forming DGU is set to $1000\,\mathrm{V}$.

Abbreviations and Symbols

Abbreviations

ADMM	alternating direction method of multipliers
DGD	distributed gradient descent
DGU	distributed generation unit
DiGing	distributed gradient tracking
EIO	equilibrium-independent observability
EIP	equilibrium-independent passivity
EXTRA	exact first-order algorithm
IFEIP	input feedforward EIP
KKT	Karush-Kuhn-Tucker
LMI	linear matrix inequality
MPC	Model Predictive Control
OFEIP	output feedback EIP
OPF	optimal power flow
SIOEIP	state-input-output EIP
UMP	uniform marginal pricing
ZIP	constant impedance Z, constant current I, constant power P

Latin Letters

Symbol	Description
$\boldsymbol{A}$	system matrix, name of edge
a	equality constraint parameter
$\boldsymbol{B}$	input matrix
b	input vector, equality constraint parameter
$\boldsymbol{C}$	Capacitance, output matrix, name of edge
c	output function, constant, parameter in quadratic objective function
$\boldsymbol{D}$	feedthrough matrix, name of edge
d	output of controller system
$\boldsymbol{E}$	incidence matrix, name of edge
e	control error state
$\boldsymbol{F}$	auxiliary matrix in proofs

Symbol	Description
f	objective function, frequency
$\boldsymbol{G}$	quadratic storage function
g	function of constraints
$\boldsymbol{H}$	parameter of quadratic storage function
h	
$\boldsymbol{I}$	identity matrix
i	current, index for agents / nodes
I	constant current load
$\boldsymbol{J}$	interconnection matrix in port Hamiltonian system
j	index edges / controllers, index of equality constraints
J	economic objective function of prosumers
$\boldsymbol{K}$	auxiliary matrix in proofs
$\boldsymbol{k}$	controller gain vector
k	time step
$\boldsymbol{L}$	Laplace matrix
l	stage cost, index of inequality constraints
L	Inductance, Lagrange function
$\boldsymbol{M}$	Lipschitz constant
m	strongly convex index
$\boldsymbol{N}$	auxiliary matrix in proofs
$n_{\square}$	number of elements of the set/variable/object specified in the index
o	edge index
$\boldsymbol{P}$	Lyapunov matrix (in Laypunov equation)
p	active power
P_{bal}	active balancing power
P_{gen}	active power generation
$\hat{p}$	local active power of a grid
$\boldsymbol{Q}$	parameter of quadratic objective function
q	parameter in quadratic objective function
$\boldsymbol{R}$	communication matrix with nullspace property, resistance matrix in port-hamiltonian systems
R	resistance
$\boldsymbol{S}$	matrix in storage function
s	supply rate
S	storage function
$\boldsymbol{T}$	end time
t	time
h_{T}	discretization time
U	utility function
u	system input
v	voltage
V	Lyaunov function

Symbol	Description
W	stroage function of controller systems
w	distribtued averaging state
x	system state
$\boldsymbol{Y}_{\text{ad}}$	admittance matrix
y	system output
Y	admittance
z	state of controller system

Greek Letters

Symbol	Description
α	parameter of closed-loop system, parameter of agent dynamics, number in reals
β	parameter of closed-loop system, parameter of controller dynamics
Γ	projection onto a closed convex set
γ	parameter of closed-loop system, feedthrough in agent dynamics
ζ	controller systems input
θ	number in reals
ι	feedthrough term in the economic ports
κ	parameter price-forming dynamics, stabilizing control law
λ	price, Lagrange multiplier
μ	Lagrange multiplier inequality constraints
ν	input passivity index
ξ	number in reals
Π	controller systems
ρ	output passivity index
π	correponds to power line
ϱ	strcit passivity index
Σ	sum, agent systems
σ	auxiliary passivity index
τ	time variable in integral, parameter controller in economic ports
ϕ	vector field in projected dynamic systems
χ	controller system dynamics
ψ	voltage following control parameter (scalar, diagonal matrix)
Ψ	positive definite function
Ω	sublevel set of a Lyapunov function
ω	parameter of storage function of a DGU

Calligraphic and Blackboard Bold

Symbol	Description
$\mathcal{A}$	set of agents
$\mathcal{B}$	set of nodes of a graph $\mathcal{G}$
$\mathcal{C}$	set of controllers
$\mathcal{C}_{\text{eq}}$	set of controllers
$\mathcal{C}_{\text{in}}$	set of controllers
$\mathcal{D}$	subset of the state space where passivity holds
$\mathcal{E}$	set of edges of a graph $\mathcal{G}$
$\mathcal{G}$	graph
$\mathcal{E}_{\text{eq}}$	set of equilibria
$\mathcal{F}$	set of prosumers
$\mathcal{I}$	set of active inequality constraints
$\mathbb{I}$	set of feasible currents
$\mathcal{K}$	set of configurable systems
$\mathcal{L}$	set where the derivative of the Lyapunov functions is zero
$\mathbb{L}$	load derivative bounds
$\mathcal{M}$	set of grids
$\mathcal{M}_{\text{eq}}$	equilibrium manifold
$\mathbb{N}$	set of natural numbers
$\mathbb{P}$	set of fesible power loads
$\mathbb{R}$	set of real numbers
$\mathcal{U}$	set of inflexible prosumers
$\mathbb{V}$	set of feasible node voltages
$\mathbb{U}$	input constraints
$\mathbb{X}$	state constraints
$\mathcal{Z}$	state space
$\mathfrak{e}$	element of a set of edges
$\mathfrak{v}$	element of a set of nodes

Indices and Exponents

Symbol	Description
$\square_{\mathrm{L}}$	corresponds to load
$\square_{\mathcal{A}}$	corresponds to agent systems
$\square_{\mathcal{C}}$	corresponds to controller systems
$\square_{\mathrm{cl}}$	corresponds to close-loop system
$\square_{\mathrm{flx}}$	corresponds to the flexible prosumers
$\square_{\mathrm{DA}}$	correponds to the distributed averaging algorithm
$\square_{\mathrm{DGU}}$	corresponds to a DGU
$\square^{\diamond}$	corresponds to a projected dynamic system
$\square_{\Sigma}$	aggregated value
$\square_{\mathrm{econ}}$	corresponds to the economic port
$\square_{\mathrm{ext}}$	corresponds to the electric port
$\square_{\mathrm{EQ}}$	correponds to equality constraint
$\square_{\mathrm{ext}}$	external, corresponds to other grids
$\square_{\mathrm{f}}$	relative to filter
$\square_{i}$	corresponds to node or agent i
$\square_{\mathrm{IN}}$	correponds to inequality constraint
$\square_{\mathrm{int}}$	corresponds to the interconnection between grids
$\square_{j}$	corresponds to edge or controller j
$\square_{\circ}$	expanded with the Kronecker product with identity matrix
$\square_{\mathrm{L}}$	corresponds to the load
$\square_{\mathrm{loc}}$	local, corresponds to the local grid
$\square_{\mathrm{mg}}$	corresponds to the set of grids $\mathcal{M}$
$\square^{m}$	corresponds to grid $m \in \mathcal{M}$
$\square^{*}$	optimal solution computed by a solver
$\square_{\mathrm{opt}}$	optimal
$\square_{\pi}$	relative to power line
$\square_{T}$	corresponds to the terminal cost / state / constraints
$\square^{\top}$	transpose
$\square_{\mathrm{t}}$	averaged
$\square_{\mathrm{up}}$	corresponds to the inflexible prosumers
$\square_{\Delta}$	voltge drop over power line
$\square_{\geq 0}$	set of positive real/natural numbers
$\square_{>0}$	set of strictly positive real/natural numbers
$\square_{\leq 0}$	set of negative real/natural numbers
$\square_{<0}$	set of strictly negative real/natural numbers
$\square^{-1}$	inverse of a nonsingular matrix
$\dot{\square}$	time derivative
$\dot{\overline{\square}}$	nonpathological derivative
$\bar{\square}$	equilibrium of a variable or vector

Symbol	Description
$\tilde{\square}$	error of a variable or vector with respect to its equilibrium $\bar{\square}$

List of Figures

List of Tables

References

Own Publications and Conference Proceedings

[Gie+23] GIESSLER, A.; **JANÉ-SONEIRA, P.**; MALAN, A. J.; HOHMANN, S.: Economic Dispatch for DC Microgrids: An Optimal Power Sharing Approach with Batteries. In: *2023 62nd IEEE Conference on Decision and Control (CDC)*. IEEE. 2023, pp. 1555–1562.

[Hac+18] HACKL, C. M.; **JANÉ-SONEIRA, P.**; PFEIFER, M.; SCHECHNER, K.; HOHMANN, S.: Full-and reduced-order state-space modeling of wind turbine systems with permanent magnet synchronous generator. In: *Energies* 11.7 (2018), p. 1809.

[JS+22] **JANÉ-SONEIRA, P.**; GIESSLER, A.; PFEIFER, M.; HOHMANN, S.: Distributed Suboptimal Model Predictive Control with Minimal Information Exchange. In: *2022 IEEE 61st Conference on Decision and Control (CDC)*. IEEE. 2022, pp. 3939–3946.

[JS+23b] **JANÉ-SONEIRA, P.**; MALAN, A. J.; PRODAN, I.; HOHMANN, S.: Passivity-Based Economic Ports for Optimal Operation of Networked DC Microgrids. In: *2023 62nd IEEE Conference on Decision and Control (CDC)*. 2023, pp. 1549–1554.

[JS+23c] **JANÉ-SONEIRA, P.**; PRODAN, I.; MALAN, A. J.; HOHMANN, S.: On MPC-based Strategies for Optimal Voltage References in DC Microgrids. In: *European Control Conference, Bucharest*. 2023. URL: https://arxiv.org/abs/2304.13495.

[JS+25a] **JANÉ-SONEIRA, P.**; MULLER, C.; STREHLE, F.; HOHMANN, S.: Passivity-Based Local Design Conditions for Global Optimality in Distributed Convex Optimization. In: *Arxiv* (2025). Submitted to IEEE Transactions on Automatic Control (second round of revision). URL: http://arxiv.org/abs/2503.09854.

[JS+25b] **JANÉ-SONEIRA, P.**; PRODAN, I.; MALAN, A.; HOHMANN, S.: 'Distributed Model Predictive Control Strategies for Modern Energy Systems: A Passivity-Based Approach'. In: *Energy Systems Integration for Multi-Energy Systems: From Operation to Planning in the Green Energy Context*. Ed. by OCAMPO-MARTINEZ, C.; QUIJANO, N. ISBN: 978-3-031-69014-3. Springer, 2025.

[JSDH23] **JANÉ-SONEIRA, P.**; DIKIC, M.; HOHMANN, S.: Passivity-Based Economic Ports for Optimal Operation of Networked AC Microgrids. In: *2023 FDIBA Conference, Sofia, Bulgaria*. 2023, pp. 1549–1554.

[JSH23] **JANE-SONEIRA, P.**; HOHMANN, S.: Markt- und passivitätsbasierte Regelung von vernetzten DC Microgrids. In: *VDI/VDE GMA FA 2.15*. 2023.

[JSPH22] **JANE-SONEIRA, P.**; PRODAN, I.; HOHMANN, S.: Optimal Voltage References for DC Microgrids using an Economic MPC Approach. In: *Book of abstracts PGMO DAYS 2022*. 2022, p. 67.

[Köl+21a] KÖLSCH, L.; **JANÉ-SONEIRA, P.**; STREHLE, F.; HOHMANN, S.: Optimal control of port-Hamiltonian systems: A continuous-time learning approach. In: *Automatica* 130 (2021), p. 109725.

[Köl+23] KÖLSCH, L.; **JANÉ-SONEIRA, P.**; MALAN, A. J.; HOHMANN, S.: Learning feedback Nash strategies for nonlinear port-Hamiltonian systems. In: *International Journal of Control* 96.1 (2023), pp. 201–213.

[Mal+24b] MALAN, A. J.; **JANÉ-SONEIRA, P.**; STREHLE, F.; HOHMANN, S.: Passivity-Based Power Sharing and Voltage Regulation in DC Microgrids With Unactuated Buses. In: *IEEE Transactions on Control Systems Technology* (2024), pp. 1–16.

[Mau+22] MAURER, J.; ILLERHAUS, J.; **JANÉ-SONEIRA, P.**; HOHMANN, S.: Distributed Optimization of District Heating Networks Using Optimality Condition Decomposition. In: *Energies* 15.18 (2022), p. 6605.

[MJSH22] MALAN, A. J.; **JANÉ-SONEIRA, P.**; HOHMANN, S.: Constructive analysis and design of interconnected Krasovskii passive and quadratic dissipative systems. In: *2022 IEEE 61st Conference on Decision and Control (CDC)*. IEEE. 2022, pp. 7059–7065.

[Ste+21] STEINLE, S.; RUF, J.; VAYAS, L.; ISIK, V.; MOHAN, J.; **JANE-SONEIRA, P.**; MALAN, A.; KÜCHLIN, R.; SAUERSCHELL, S.; HEROLD, L.; WALTER, J.; SURIYAH, M. R.; BAJOHR, S.; KERN, T.; KOLB, T.; HOHMANN, S.; KÖPPEL, W.; LEIBFRIED, T.: Das Verbundprojekt RegEnZell: Zellenübergreifende Regionalisierung der Energieversorgung durch betriebsoptimierte Sektorenkopplung. In: *ETG-Kongress 2021: das Gesamtsystem im Fokus der Energiewende*. 2021.

Invited Talks

[JSS22] **JANE-SONEIRA, P.**; STEINLE, S.: Das Verbundprojekt RegEnZell: Welche Möglichkeiten eröffnen zellulare Energiesysteme und deren kooperative Betriebsoptimierung? In: *12. Fachtagung Smart Grids und Virtuelle Kraftwerke Rheinland-Pfalz*. 2022.

Supervised Student Theses

[Ahl21] AHLBORN, M.: *Implementation of Primary and Secondary Control Methods for Microgrids*, Bachelor's thesis. Institute of Control Systems (IRS), Karlsruhe Institute of Technology (KIT), 2021.

[Bru22a] BRUCK, J.: *Power Flow Optimization for Microgrids Connected Through Power Electronics*, Bachelor's thesis. Institute of Control Systems (IRS), Karlsruhe Institute of Technology (KIT), 2022.

[Bru22b] BRUNNER, T.: *Stability of Networked Systems With Optimization Based Controllers*, Bachelor's thesis. Institute of Control Systems (IRS), Karlsruhe Institute of Technology (KIT), 2022.

[Dik23] DIKIC, M.: *Extension of a Price-Based Control for AC Microgrids*, Bachelor's thesis. Institute of Control Systems (IRS), Karlsruhe Institute of Technology (KIT), 2023.

[Ess23] ESSIG, J.: *Distributed Model Predictive Control for DC Microgrids*, Bachelor's thesis. Institute of Control Systems (IRS), Karlsruhe Institute of Technology (KIT), 2023.

[Feh20] FEHN, L.: *Implementation of a Distributed Model Predictive Control Algorithm for a Real Energy Grid*, Bachelor's thesis. Institute of Control Systems (IRS), Karlsruhe Institute of Technology (KIT), 2020.

[Gie21] GIESSLER, A.: *Distributed Optimization for Distributed Model Predicitve Control*, Bachelor's thesis. Institute of Control Systems (IRS), Karlsruhe Institute of Technology (KIT), 2021.

[Ham20] HAMPEL, S.: *Optimal Cooperation of Microgrids Connected on Transmission Level*, Master's thesis. Institute of Control Systems (IRS), Karlsruhe Institute of Technology (KIT), 2020.

[Ill24] ILLERHAUS, J.: *Passivity-based Reinforcement Learning*, Bachelor's thesis. Institute of Control Systems (IRS), Karlsruhe Institute of Technology (KIT), 2024.

[Mul23] MULLER, C.: *Passivity-Based Distributed Optimization*, Bachelor's thesis. Institute of Control Systems (IRS), Karlsruhe Institute of Technology (KIT), 2023.

[Mut23] MUTZ, A.: *Storage Functions for DC Microgrids with Economic Ports*, Bachelor's thesis. Institute of Control Systems (IRS), Karlsruhe Institute of Technology (KIT), 2023.

[Zha21] ZHANG, Q.: *Constrained Distributed Optimization with Diffusion Strategies*, Bachelor's thesis. Institute of Control Systems (IRS), Karlsruhe Institute of Technology (KIT), 2021.

Public References

[AAR11] ANGELI, D.; AMRIT, R.; RAWLINGS, J. B.: On average performance and stability of economic model predictive control. In: *IEEE Transactions on Automatic Control* 57.7 (2011), pp. 1615–1626.

[ACG18] ALAM, M. N.; CHAKRABARTI, S.; GHOSH, A.: Networked microgrids: State-of-the-art and future perspectives. In: *IEEE Transactions on Industrial Informatics* 15.3 (2018), pp. 1238–1250.

[Aeb+12] AEBERHARD, M.; VOLLENWYDER, R.; HAAG, C.; AEBERHARDT, B.: *Resonanzproblematik im SBB Energienetz*. de. Sept. 2012. URL: http://www.news.admin.ch/NSBSubscriber/message/attachments/34330.pdf%202012 (visited on 16/11/2024).

[Age23] AGENCY, E. E.: Greenhouse gas emission intensity of electricity generation in Europe. en. In: *Analysis and Data* (Oct. 2023). URL: https://www.eea.europa.eu/en/analysis/indicators/greenhouse-gas-emission-intensity-of-1 (visited on 21/04/2024).

[AKA07] ARNOLD, M.; KNOPFLI, S.; ANDERSSON, G.: Improvement of OPF Decomposition Methods Applied to Multi-Area Power Systems. In: *2007 IEEE Lausanne Power Tech*. July 2007, pp. 1308–1313. URL: https://ieeexplore.ieee.org/abstract/document/4538505 (visited on 03/05/2024).

[AMP16] ARCAK, M.; MEISSEN, C.; PACKARD, A.: *Networks of dissipative systems: compositional certification of stability, performance, and safety*. Springer, 2016.

[Ana+20] ANANDUTA, W.; MAESTRE, J. M.; OCAMPO-MARTINEZ, C.; ISHII, H.: Resilient distributed model predictive control for energy management of interconnected microgrids. In: *Optimal Control Applications and Methods* 41.1 (2020), pp. 146–169.

[AOM21] ANANDUTA, W.; OCAMPO-MARTINEZ, C.: Event-triggered partitioning for non-centralized predictive-control-based economic dispatch of interconnected microgrids. In: *Automatica* 132 (2021), p. 109829.

[ARA11] AMRIT, R.; RAWLINGS, J. B.; ANGELI, D.: Economic optimization using model predictive control with a terminal cost. In: *Annual Reviews in Control* 35.2 (2011), pp. 178–186.

[Arn+10] ARNOLD, M.; NEGENBORN, R. R.; ANDERSSON, G.; DE SCHUTTER, B.: 'Distributed Predictive Control for Energy Hub Coordination in Coupled Electricity and Gas Networks'. en. In: *Intelligent Infrastructures*. Ed. by NEGENBORN, R. R.; LUKSZO, Z.; HELLENDOORN, H. Dordrecht: Springer Netherlands, 2010, pp. 235–273. URL: https://link.springer.com/10.1007/978-90-481-3598-1_10 (visited on 03/05/2024).

[Arr+58] ARROW, K. J.; HURWICZ, L.; UZAWA, H.; CHENERY, H. B.; JOHNSON, S.; KARLIN, S.: *Studies in linear and non-linear programming*. Vol. 2. Stanford University Press Stanford, 1958.

[Ass20] ASSOCIATION, N. E. M.: American National Standard for Electric Power Systems and Equipment—Voltage Ratings (60 Hz) - ANSI C84 2020. In: (2020).

[Bai+17] BAIMEL, D.; BELIKOV, J.; GUERRERO, J. M.; LEVRON, Y.: Dynamic modeling of networks, microgrids, and renewable sources in the dq0 reference frame: A survey. In: *IEEE Access* 5 (2017), pp. 21323–21335.

[Bai+19] BAIDYA, R.; AGUILERA, R. P.; KARAMANAKOS, P.; ACUNA, P.; ROJAS, C.; GEYER, T.; LU, D. D.-C.: Dealing with suboptimality in multistep model predictive control for transient operations. In: *2019 IEEE energy conversion congress and exposition (ECCE)*. IEEE. 2019, pp. 3780–3785.

[Bai+20] BAIDYA, R.; AGUILERA, R. P.; ACUÑA, P.; GEYER, T.; DELGADO, R. A.; QUEVEDO, D. E.; TOIT MOUTON, H. DU: Enabling multistep model predictive control for transient operation of power converters. In: *IEEE Open Journal of the Industrial Electronics Society* 1 (2020), pp. 284–297.

[BC06] BACCIOTTI, A.; CERAGIOLI, F.: Nonpathological Lyapunov functions and discontinuous Carathéodory systems. In: *Automatica* 42.3 (2006), pp. 453–458.

[BC17] BAUSCHKE, H. H.; COMBETTES, P. L.: *Convex Analysis and Monotone Operator Theory in Hilbert Spaces*. Cham: Springer International Publishing, Jan. 2017.

[Ben62] BENDERS, J. F.: Partitioning procedures for solving mixed-variables programming problems. In: *Numerische mathematik* 4.1 (1962), pp. 238–252.

[Ber09] BERGEN, A. R.: *Power systems analysis*. Pearson Education India, 2009.

[Ber97] BERTSEKAS, D. P.: A New Class of Incremental Gradient Methods for Least Squares Problems. In: *SIAM Journal on Optimization* 7.4 (Nov. 1997), pp. 913–926. URL: https://epubs.siam.org/doi/abs/10.1137/S1052623495287022 (visited on 03/05/2024).

[Ber99] BERTSEKAS, D. P.: *Nonlinear Programming*. Athena Scientific, 1999.

[BGL05] BENZI, M.; GOLUB, G. H.; LIESEN, J.: Numerical solution of saddle point problems. In: *Acta numerica* 14 (2005), pp. 1–137.

[BH12] BROUWER, A. E.; HAEMERS, W. H.: *Spectra of Graphs*. New York, NY: Springer Science & Business Media, Jan. 2012.

[BHG07] BLATT, D.; HERO, A. O.; GAUCHMAN, H.: A Convergent Incremental Gradient Method with a Constant Step Size. en. In: *SIAM Journal on Optimization* 18.1 (Jan. 2007), pp. 29–51. URL: http://epubs.siam.org/doi/10.1137/040615961 (visited on 03/05/2024).

[BNO03] BERTSEKAS, D.; NEDIC, A.; OZDAGLAR, A.: *Convex analysis and optimization*. Vol. 1. Athena Scientific, 2003.

[Bof+18] BOF, N.; CARLI, R.; NOTARSTEFANO, G.; SCHENATO, L.; VARAGNOLO, D.: Multiagent Newton–Raphson optimization over lossy networks. In: *IEEE Transactions on Automatic Control* 64.7 (2018), pp. 2983–2990.

[Boy+11] BOYD, S.; PARIKH, N.; CHU, E.; PELEATO, B.; ECKSTEIN, J. et al.: Distributed optimization and statistical learning via the alternating direction method of multipliers. In: *Foundations and Trends® in Machine learning* 3.1 (2011), pp. 1–122.

[Boy+94] BOYD, S.; EL GHAOUI, L.; FERON, E.; BALAKRISHNAN, V.: *Linear matrix inequalities in system and control theory*. SIAM, 1994.

[Bru+14] BRUNEKREEFT, G.; GOTO, M.; MEYER, R.; MARUYAMA, M.; HATTORI, T.: *Unbundling of electricity transmission system operators in Germany: An experience report*. Tech. rep. Bremen Energy Working Papers, 2014.

[BT97] BERTSEKAS, D.; TSITSIKLIS, J.: *Parallel and distributed computation: numerical methods*. Athena Scientific, 1997.

[Buc+15] BUCHHAGEN, C.; RAUSCHER, C.; MENZE, A.; JUNG, J.: BorWin1-First Experiences with harmonic interactions in converter dominated grids. In: *International ETG Congress 2015; Die Energiewende-Blueprints for the new energy age*. VDE. 2015, pp. 1–7.

[Bun20] BUNDESNETZARGENTUR FÜR ELEKTRIZITÄT, GAS, TELEKOMMUNIKATION, POST UND EISENBAHNEN: Quartalsbericht Netz- und Systemsicherheit - Gesamtes Jahr 2019. de. In: *Press Release* (Apr. 2020). URL: https://www.bundesnetzagentur.de/SharedDocs/Mediathek/Berichte/2020/Quartalszahlen_Gesamtjahr_2019.pdf?__blob=publicationFile&v=1 (visited on 28/04/2024).

[Bun24a] BUNDESNETZARGENTUR FÜR ELEKTRIZITÄT, GAS, TELEKOMMUNIKATION, POST UND EISENBAHNEN: Quartalsbericht: Netzengpassmanagement Viertes Quartal 2023. de. In: *Press Release* (Apr. 2024). URL: https://www.bundesnetzagentur.de/SharedDocs/Downloads/DE/Sachgebiete/Energie/Unternehmen_Institutionen/Versorgungssicherheit/Engpassmanagement/QuartalszahlenQ4_2023.pdf?__blob=publicationFile&v=2 (visited on 28/04/2024).

[Bun24b] BUNDESNETZARGENTUR FÜR ELEKTRIZITÄT, GAS, TELEKOMMUNIKATION, POST UND EISENBAHNEN: *Redispatch*. de. June 2024. URL: https://www.bundesnetzagentur.de/DE/Fachthemen/ElektrizitaetundGas/Versorgungssicherheit/Netzengpassmanagement/Engpassmanagement/Redispatch/start.html (visited on 28/04/2024).

[BV04] BOYD, S. P.; VANDENBERGHE, L.: *Convex optimization*. Cambridge university press, 2004.

[BZ11] BAZMI, A. A.; ZAHEDI, G.: Sustainable energy systems: Role of optimization modeling techniques in power generation and supply - A review. en. In: *Renewable and Sustainable Energy Reviews* 15.8 (Oct. 2011), pp. 3480–3500. URL: https://linkinghub.elsevier.com/retrieve/pii/S1364032111002061 (visited on 18/04/2024).

[CA98] CHEN, H.; ALLGÖWER, F.: A quasi-infinite horizon nonlinear model predictive control scheme with guaranteed stability. In: *Automatica* 34.10 (1998), pp. 1205–1217.

[Car62] CARPENTIER, J.: Contribution a l'etude du dispatching economique. In: *Bull. Soc. Fr. Elec. Ser.* 3 (1962), p. 431.

[Che+20] CHEN, B.; WANG, J.; LU, X.; CHEN, C.; ZHAO, S.: Networked microgrids for grid resilience, robustness, and efficiency: A review. In: *IEEE Transactions on Smart Grid* 12.1 (2020), pp. 18–32.

[Che+21] CHERUKURI, A.; STEGINK, T.; DE PERSIS, C.; VAN DER SCHAFT, A.; CORTÉS, J.: Frequency-Driven Market Mechanisms for Optimal Dispatch in Power Networks. In: *Automatica* 133 (Nov. 2021), p. 109861. URL: https://linkinghub.elsevier.com/retrieve/pii/S0005109821003812 (visited on 04/05/2024).

[CHM23] CHEE, K. Y.; HSIEH, M. A.; MATNI, N.: Learning-enhanced nonlinear model predictive control using knowledge-based neural ordinary differential equations and deep ensembles. In: *Learning for Dynamics and Control Conference*. PMLR. 2023, pp. 1125–1137.

[CKG16] CHEN, Y.; KHONG, S. Z.; GEORGIOU, T. T.: On the definiteness of graph Laplacians with negative weights: Geometrical and passivity-based approaches. In: *2016 American Control Conference (ACC)*. IEEE. 2016, pp. 2488–2493.

[CKS19] CUCUZZELLA, M.; KOSARAJU, K. C.; SCHERPEN, J. M. A.: Distributed Passivity-Based Control of DC Microgrids. In: *2019 American Control Conference (ACC)*. ISSN: 2378-5861. July 2019, pp. 652–657. URL: https://ieeexplore.ieee.org/abstract/document/8814756?casa_token=BvBVkd84nfAAAAAA:5wSE0Y0K-JFjXULLtVPSaWeCPODZrAxASPG9OZwhW_9zM7Q-J_FGg7FAdqEqO_h9mbEy0LcoAQ (visited on 01/05/2024).

[CMC16] CHERUKURI, A.; MALLADA, E.; CORTÉS, J.: Asymptotic convergence of constrained primal–dual dynamics. In: *Systems & Control Letters* 87 (2016), pp. 10–15.

[CNP02] CONEJO, A. J.; NOGALES, F. J.; PRIETO, F. J.: A decomposition procedure based on approximate Newton directions. In: *Mathematical Programming* 93.3 (Jan. 2002). Num Pages: 21, pp. 495–515.

[COC+12] CAIN, M. B.; O'NEILL, R. P.; CASTILLO, A. et al.: History of optimal power flow and formulations. In: *Federal Energy Regulatory Commission* 1 (2012), pp. 1–36.

[Col+12] COLANERI, P.; FARINA, M.; SCATTOLINI, R.; SHORTEN, R.: A note on discretization of sparse linear systems. In: *IFAC Proceedings Volumes* 45.13 (2012), pp. 97–102.

[Com] COMISSION, E.: *Energy communities*. Accessed online on 02.10.2023. URL: https://energy.ec.europa.eu/topics/markets-and-consumers/energy-communities_en.

[Con+06] CONEJO, A. J.; CASTILLO, E.; MINGUEZ, R.; GARCIA-BERTRAND, R.: *Decomposition techniques in mathematical programming: engineering and science applications*. Springer Science & Business Media, 2006.

[Con+12] CONTE, C.; VOELLMY, N. R.; ZEILINGER, M. N.; MORARI, M.; JONES, C. N.: Distributed Synthesis and Control of Constrained Linear Systems. In: *2012 American Control Conference (ACC)*. June 2012, pp. 6017–6022. URL: https://ieeexplore.ieee.org/abstract/document/6314654 (visited on 05/06/2024).

[Con+16] CONTE, C.; JONES, C. N.; MORARI, M.; ZEILINGER, M. N.: Distributed synthesis and stability of cooperative distributed model predictive control for linear systems. In: *Automatica* 69 (2016), pp. 117–125.

[Con22] 117TH CONGRESS: H.R.5376 - Inflation Reduction Act of 2022. In: *Public Law 117-169, U.S. Government Publishing Office* (2022). URL: https://www.congress.gov/bill/117th-congress/house-bill/5376/text (visited on 20/04/2024).

[Cor08] CORTES, J.: Discontinuous dynamical systems. In: *IEEE Control systems magazine* 28.3 (2008), pp. 36–73.

[Cou03] COUNCIL OF THE EUROPEAN UNION: Directive 2003/87/EC of the European Parliament and of the Council. In: *Official Journal of the European Union* 275 (2003), pp. 1–15.

[Cou21] COUNCIL OF THE EUROPEAN UNION: Regulation (EU) 2021/1119 establishing the framework for achieving climate neutrality ('European Climate Law'). In: *Official Journal of the European Union* 243 (2021), pp. 1–17.

[CS12a] CHEN, J.; SAYED, A. H.: Diffusion Adaptation Strategies for Distributed Optimization and Learning Over Networks. In: *IEEE Transactions on Signal Processing* 60.8 (Jan. 2012), pp. 4289–4305.

[CS12b] CHEN, J.; SAYED, A. H.: 'On the Limiting Behavior of Distributed Optimization Strategies'. In: *2012 50th Annual Allerton Conference on Communication, Control, and Computing (Allerton)*. IEEE, Oct. 2012, pp. 1535–1542.

[CS13] CHEN, J.; SAYED, A. H.: Distributed Pareto Optimization via Diffusion Strategies. In: *IEEE Journal of Selected Topics in Signal Processing* 7.2 (Jan. 2013), pp. 205–220.

[CY19] CHENG, L.; YU, T.: Game-Theoretic Approaches Applied to Transactions in the Open and Ever-Growing Electricity Markets From the Perspective of Power Demand Response: An Overview. In: *IEEE Access* 7 (2019), pp. 25727–25762. URL: https://ieeexplore.ieee.org/document/8648326?denied= (visited on 02/06/2024).

[Dan19] DANLEY, D. R.: Defining a Microgrid Using IEEE 2030.7. In: *Business & Technology Surveillance* (2019).

[DAR10] DIEHL, M.; AMRIT, R.; RAWLINGS, J. B.: A Lyapunov function for economic optimizing model predictive control. In: *IEEE Transactions on Automatic Control* 56.3 (2010), pp. 703–707.

[DEL20] DARIVIANAKIS, G.; EICHLER, A.; LYGEROS, J.: Distributed Model Predictive Control for Linear Systems With Adaptive Terminal Sets. In: *IEEE Transactions on Automatic Control* 65.3 (Mar. 2020), pp. 1044–1056. URL: https://ieeexplore.ieee.org/abstract/document/8713880 (visited on 05/06/2024).

[Deu19] DEUTSCHER BUNDESTAG: Klimaschutzgesetz (KSG). In: *Bundesgesetzblatt I* (2019), p. 3905.

[Deu21] DEUTSCHES VERFASSUNGSGERICHT: *Beschluss des Ersten Senats vom 24. März 2021*. Karlsruhe, 2021. URL: https://www.bundesverfassungsgericht.de/SharedDocs/Downloads/DE/2021/03/rs20210324_1bvr265618.pdf?__blob=publicationFile&v=9 (visited on 18/04/2024).

[DG17] DÖRFLER, F.; GRAMMATICO, S.: Gather-and-Broadcast Frequency Control in Power Systems. In: *Automatica* 79 (May 2017), pp. 296–305. URL: https://www.sciencedirect.com/science/article/pii/S0005109817300572 (visited on 02/06/2024).

[DSPB16] DORFLER, F.; SIMPSON-PORCO, J. W.; BULLO, F.: Breaking the Hierarchy: Distributed Control and Economic Optimality in Microgrids. In: *IEEE Transactions on Control of Network Systems* 3.3 (Jan. 2016). Num Pages: 13, pp. 241–253.

[DTS13] DAAFOUZ, J.; TARBOURIECH, S.; SIGALOTTI, M.: *Hybrid systems with constraints*. John Wiley & Sons, 2013.

[DW60] DANTZIG, G. B.; WOLFE, P.: Decomposition Principle for Linear Programs. en. In: *Operations Research* 8.1 (Feb. 1960), pp. 101–111. URL: https://pubsonline.informs.org/doi/10.1287/opre.8.1.101 (visited on 04/04/2024).

[Dö+19] DÖRFLER, F.; BOLOGNANI, S.; SIMPSON-PORCO, J. W.; GRAMMATICO, S.: Distributed Control and Optimization for Autonomous Power Grids. In: *2019 18th European Control Conference (ECC)*. June 2019, pp. 2436–2453. URL: https://ieeexplore.ieee.org/abstract/document/8795974 (visited on 25/04/2024).

[EC16] ENVIRONMENT; CANADA, C. C.: *Pan-Canadian framework on clean growth and climate change: Canada's plan to address climate change and grow the economy*. 2016.

[Eng07] ENGELL, S.: Feedback control for optimal process operation. In: *Journal of process control* 17.3 (2007), pp. 203–219.

[Eur16] EUROPEAN COMISSION: COMMISSION REGULATION (EU) 2016/ 631 - of 14 April 2016 - establishing a network code on requirements for grid connection of generators. en. In: *Official Journal of the European Union* (Apr. 2016).

[Eur17a] EUROPEAN COMISSION: COMMISSION REGULATION (EU) 2017/ 1485 - of 2 August 2017 - establishing a guideline on electricity transmission system operation. en. In: *Official Journal of the European Union* (Aug. 2017).

[Eur17b] EUROPEAN COMISSION: COMMISSION REGULATION (EU) 2017/ 2195 - of 23 November 2017 - establishing a guideline on electricity balancing. en. In: *Official Journal of the European Union* (Nov. 2017).

[Eur19] EUROPEAN COMISSION: REGULATION (EU) 2019/943 of the European Parliament and of the Council - of 5 June 2019 - on the internal market for electricity. en. In: *Official Journal of the European Union* (Aug. 2019).

[Eur20] EUROPEAN NETWORK OF TRANSMISSION SYSTEM OPERATORS FOR ELECTRICITY (ENTSO-E): *Report on Deterministic Frequency Deviations*. Tech. rep. ENTSO-E, Rue de Spa 8, 1000 Brussels. 2020.

[Eur23] EUROPEAN COMMISSION: State of the Energy Union 2023. In: *Press Release* (Oct. 2023). URL: https://ec.europa.eu/commission/presscorner/detail/en/ip_23_5188 (visited on 21/04/2024).

[Eur24] EUROSTAT: *Electricity production, consumption and market overview*. 2024. URL: https://ec.europa.eu/eurostat/statistics-explained/index.php?title=Electricity_production,_consumption_and_market_overview (visited on 20/04/2024).

[Eve80] EVES, H. W.: *Elementary matrix theory*. Courier Corporation, 1980.

[Fal+20] FALSONE, A.; NOTARNICOLA, I.; NOTARSTEFANO, G.; PRANDINI, M.: Tracking-ADMM for distributed constraint-coupled optimization. In: *Automatica* 117 (2020), p. 108962.

[Far+18] FARROKHABADI, M.; CANIZARES, C.; SIMPSON-PORCO, J. W.; NASR, E.; FAN, L.; ARAYA, P. A. M.; TONKOSKI, R.; TAMRAKAR, U.; HATZIARGYRIOU, N.; LAGOS, D.: Microgrid stability, definitions, analysis, and modeling. In: *IEEE Power and Energy Society, Piscataway, NJ, USA, Tech. Rep. PES-TR66* (2018).

[FCS13] FARINA, M.; COLANERI, P.; SCATTOLINI, R.: Block-wise discretization accounting for structural constraints. In: *Automatica* 49.11 (2013), pp. 3411–3417.

[FGM+18] FAULWASSER, T.; GRÜNE, L.; MÜLLER, M. A. et al.: Economic nonlinear model predictive control. In: *Foundations and Trends® in Systems and Control* 5.1 (2018), pp. 1–98.

[FYL06] FREEMAN, R. A.; YANG, P.; LYNCH, K. M.: Stability and convergence properties of dynamic average consensus estimators. In: *Proceedings of the 45th IEEE Conference on Decision and Control*. IEEE. 2006, pp. 338–343.

[Gao+19] GAO, F.; KANG, R.; CAO, J.; YANG, T.: Primary and secondary control in DC microgrids: a review. In: *J. of Modern Power Systems and Clean Energy* 7.2 (2019), pp. 227–242.

[GC13] GHARESIFARD, B.; CORTÉS, J.: Distributed continuous-time convex optimization on weight-balanced digraphs. In: *IEEE Transactions on Automatic Control* 59.3 (2013), pp. 781–786.

[GECC18] GÓMEZ-EXPÓSITO, A.; CONEJO, A. J.; CAÑIZARES, C. A., eds.: *Electric Energy Systems: Analysis and Operation*. 2nd. Boca Raton, Florida, U.S.: CRC Press, 2018.

[Gey+11] GEYER, T.; OIKONOMOU, N.; PAPAFOTIOU, G.; KIEFERNDORF, F. D.: Model predictive pulse pattern control. In: *IEEE Transactions on Industry Applications* 48.2 (2011), pp. 663–676.

[GP14] GRÜNE, L.; PALMA, V. G.: Robustness of performance and stability for multistep and updated multistep MPC schemes. In: (2014).

[GR01] GODSIL, C.; ROYLE, G.: *Algebraic Graph Theory*. Vol. 207. Graduate Texts in Mathematics. New York, NY: Springer, 2001. URL: http://link.springer.com/10.1007/978-1-4613-0163-9 (visited on 10/05/2024).

[Gue+10] GUERRERO, J. M.; VASQUEZ, J. C.; MATAS, J.; DE VICUÑA, L. G.; CASTILLA, M.: Hierarchical control of droop-controlled AC and DC microgrids—A general approach toward standardization. In: *IEEE Transactions on Industrial Electronics* 58.1 (2010), pp. 158–172.

[Gui+18a] GUI, Y.; LI, M.; LU, J.; GOLESTAN, S.; GUERRERO, J. M.; VASQUEZ, J. C.: A Voltage Modulated DPC Approach for Three-Phase PWM Rectifier. In: *IEEE Transactions on Industrial Electronics* 65.10 (Oct. 2018), pp. 7612–7619. URL: https://ieeexplore.ieee.org/document/8281061/ (visited on 03/06/2024).

[Gui+18b] GUI, Y.; WEI, B.; LI, M.; GUERRERO, J. M.; VASQUEZ, J. C.: Passivity-based coordinated control for islanded AC microgrid. In: *Applied energy* 229 (2018), pp. 551–561.

[Hah31] HAHN, G.: Load division by the increment method. In: *Power* 73 (1931), pp. 910–911.

[Han22] HAN, D.-R.: A Survey on Some Recent Developments of Alternating Direction Method of Multipliers. en. In: *Journal of the Operations Research Society of China* 10.1 (Mar. 2022), pp. 1–52. URL: https://link.springer.com/10.1007/s40305-021-00368-3 (visited on 03/05/2024).

[HAP11] HINES, G. H.; ARCAK, M.; PACKARD, A. K.: Equilibrium-Independent Passivity: A New Definition and Numerical Certification. In: *Automatica* 47.9 (Jan. 2011), pp. 1949–1956.

[Hap77] HAPP, H.: Optimal power dispatch: A comprehensive survey. In: *IEEE Transactions on Power Apparatus and Systems* 96.3 (May 1977). Conference Name: IEEE Transactions on Power Apparatus and Systems, pp. 841–854. URL: https://ieeexplore.ieee.org/document/1601999 (visited on 16/04/2024).

[Har+16] HARNEFORS, L.; WANG, X.; YEPES, A. G.; BLAABJERG, F.: Passivity-Based Stability Assessment of Grid-Connected VSCs—An Overview. In: *IEEE Journal of Emerging and Selected Topics in Power Electronics* 4.1 (Mar. 2016). Conference Name: IEEE Journal of Emerging and Selected Topics in Power Electronics, pp. 116–125. URL: https://ieeexplore.ieee.org/abstract/document/7298361 (visited on 18/03/2024).

[Hat+07] HATZIARGYRIOU, N.; ASANO, H.; IRAVANI, R.; MARNAY, C.: Microgrids. In: *IEEE power and energy magazine* 5.4 (2007), pp. 78–94.

[Hat+18] HATANAKA, T.; CHOPRA, N.; ISHIZAKI, T.; LI, N.: Passivity-based distributed optimization with communication delays using PI consensus algorithm. In: *IEEE Transactions on Automatic Control* 63.12 (2018), pp. 4421–4428.

[Hau+16] HAUSWIRTH, A.; BOLOGNANI, S.; HUG, G.; DÖRFLER, F.: Projected Gradient Descent on Riemannian Manifolds with Applications to Online Power System Optimization. In: *2016 54th Annual Allerton Conference on Communication, Control, and Computing (Allerton)*. Sept. 2016, pp. 225–232. URL: https://ieeexplore.ieee.org/abstract/document/7852234 (visited on 08/04/2024).

[Hau+21] HAUSWIRTH, A.; BOLOGNANI, S.; HUG, G.; DÖRFLER, F.: Timescale Separation in Autonomous Optimization. In: *IEEE Transactions on Automatic Control* 66.2 (Feb. 2021), pp. 611–624. URL: https://ieeexplore.ieee.org/abstract/document/9075378 (visited on 08/04/2024).

[Hau+24] HAUSWIRTH, A.; HE, Z.; BOLOGNANI, S.; HUG, G.; DÖRFLER, F.: Optimization Algorithms as Robust Feedback Controllers. In: *Annual Reviews in Control* 57 (2024), p. 100941. URL: https://linkinghub.elsevier.com/retrieve/pii/S1367578824000105 (visited on 08/04/2024).

[He+24] HE, X.; DUARTE, J.; HÄBERLE, V.; DÖRFLER, F.: Grid-Forming Control of Modular Dynamic Virtual Power Plants. In: *arXiv preprint arXiv:2410.14912* (2024).

[HJ12] HORN, R. A.; JOHNSON, C. R.: *Matrix analysis*. Cambridge university press, 2012.

[HLJ14] HERMANS, R.; LAZAR, M.; JOKIĆ, A.: Stabilization of Interconnected Dynamical Systems by Online Convex Optimization. In: *International Journal of Robust and Nonlinear Control* 24.10 (2014), pp. 1467–1487. URL: https://onlinelibrary.wiley.com/doi/abs/10.1002/rnc.2939 (visited on 05/06/2024).

[HMDB21] HOMAN, S.; MAC DOWELL, N.; BROWN, S.: Grid frequency volatility in future low inertia scenarios: Challenges and mitigation options. In: *Applied Energy* 290 (2021), p. 116723.

[Hos+24] HOSSEINABADI, F.; CHAKRABORTY, S.; BHOI, S. K.; PROCHART, G.; HRVANOVIC, D.; HEGAZY, O.: A Comprehensive Overview of Reliability Assessment Strategies and Testing of Power Electronics Converters. In: *IEEE Open Journal of Power Electronics* (2024).

[Hu+21] HU, J.; SHAN, Y.; GUERRERO, J. M.; IOINOVICI, A.; CHAN, K. W.; RODRIGUEZ, J.: Model predictive control of microgrids–An overview. In: *Renewable and Sustainable Energy Reviews* 136 (2021), p. 110422.

[Hu+24] HU, J.; SHAN, Y.; YANG, Y.; PARISIO, A.; LI, Y.; AMJADY, N.; ISLAM, S.; CHENG, K. W.; GUERRERO, J. M.; RODRÍGUEZ, J.: Economic Model Predictive Control for Microgrid Optimization: A Review. en. In: *IEEE Transactions on Smart Grid* 15.1 (Jan. 2024), pp. 472–484. URL: https://ieeexplore.ieee.org/document/10098893/ (visited on 02/05/2024).

[HWL23] HALLINAN, L.; WATSON, J. D.; LESTAS, I.: Inverse Optimal Control and Passivity-Based Design for Converter-Based Microgrids. In: *2023 62nd IEEE Conference on Decision and Control (CDC)*. Singapore: IEEE, Dec. 2023, pp. 1245–1250. URL: https://ieeexplore.ieee.org/document/10384101/ (visited on 10/05/2024).

[HZZ20] HE, X.; ZHANG, H.; ZAHAR, A.: *Climate Change Law in China in Global Context*. Vol. 120. Routledge, 2020.

[Hä+23] HÄBERLE, V.; TAYYEBI, A.; HE, X.; PRIETO-ARAUJO, E.; DÖRFLER, F.: Grid-forming and spatially distributed control design of dynamic virtual power plants. In: *IEEE Transactions on Smart Grid* (2023).

[Int20] INTERNATIONAL ENERGY AGENCY: *India 2020 Energy Policy Review*. Paris: OECD Publishing, 2020.

[IYA21] ISLAM, M.; YANG, F.; AMIN, M.: Control and optimisation of networked microgrids: A review. In: *IET Renewable Power Generation* 15.6 (2021), pp. 1133–1148.

[Jia+19a] JIA, Y.; DONG, Z. Y.; SUN, C.; CHEN, G.: Distributed economic model predictive control for a wind–photovoltaic–battery microgrid power system. In: *IEEE Transactions on Sustainable Energy* 11.2 (2019), pp. 1089–1099.

[Jia+19b] JIA, Y.; DONG, Z. Y.; SUN, C.; MENG, K.: Cooperation-based distributed economic MPC for economic load dispatch and load frequency control of interconnected power systems. In: *IEEE Transactions on Power Systems* 34.5 (2019), pp. 3964–3966.

[Jia+20] JIA, Y.; MENG, K.; WU, K.; SUN, C.; DONG, Z. Y.: Optimal load frequency control for networked power systems based on distributed economic MPC. In: *IEEE Transactions on Systems, Man, and Cybernetics* 51.4 (2020), pp. 2123–2133.

[JS+23a] JANÉ-SONEIRA, P.; MALAN, A. J.; PRODAN, I.; HOHMANN, S.: Passivity-based economic ports for optimal operation of networked DC microgrids. In: 2023.

[JSS22] **JANE-SONEIRA, P.**; STEINLE, S.: Das Verbundprojekt RegEnZell: Welche Möglichkeiten eröffnen zellulare Energiesysteme und deren kooperative Betriebsoptimierung? In: *12. Fachtagung Smart Grids und Virtuelle Kraftwerke Rheinland-Pfalz*. 2022.

[KA17] KOELN, J. P.; ALLEYNE, A. G.: Stability of decentralized model predictive control of graph-based power flow systems via passivity. In: *Automatica* 82 (2017), pp. 29–34.

[Kal+60] KALMAN, R. E. et al.: Contributions to the theory of optimal control. In: *Bol. soc. mat. mexicana* 5.2 (1960), pp. 102–119.

[Kar72] KARP, R. M.: 'Reducibility Among Combinatorial Problems'. en. In: *Complexity of Computer Computations*. Ed. by MILLER, R. E.; THATCHER, J. W. New York: Plenum Press, 1972, pp. 85–103.

[KCM15] KIA, S. S.; CORTÉS, J.; MARTINEZ, S.: Distributed convex optimization via continuous-time coordination algorithms with discrete-time communication. In: *Automatica* 55 (2015), pp. 254–264.

[KCRC24] KRAVIS, R.; COLÓN-REYES, G. E.; CALLAWAY, D. S.: Small-signal stability in inverter-dominated grids: exploring the role of gains, line dynamics, and operating conditions. In: *2024 IEEE Power & Energy Society General Meeting (PESGM)*. IEEE. 2024, pp. 1–5.

[Kha02] KHALIL, H. K.: *Nonlinear systems third edition*. Vol. 115. Prentice Hall, 2002.

[Kha+20] KHAYAT, Y.; SHAFIEE, Q.; HEYDARI, R.; NADERI, M.; DRAGICEVIC, T.; SIMPSON-PORCO, J. W.; DÖRFLER, F.; FATHI, M.; BLAABJERG, F.; GUERRERO, J. M.; BEVRANI, H.: On the Secondary Control Architectures of AC Microgrids: An Overview. In: *IEEE Transactions on Power Electronics* 35.6 (June 2020), pp. 6482–6500. URL: https://ieeexplore.ieee.org/abstract/document/8892668 (visited on 24/04/2024).

[Kia+19] KIA, S. S.; VAN SCOY, B.; CORTES, J.; FREEMAN, R. A.; LYNCH, K. M.; MARTINEZ, S.: Tutorial on Dynamic Average Consensus: The Problem, Its Applications, and the Algorithms. In: *IEEE Control Systems Magazine* 39.3 (June 2019), pp. 40–72. URL: https://ieeexplore.ieee.org/abstract/document/8716798 (visited on 11/07/2024).

[KM22] KUNDUR, P. S.; MALIK, O. P.: *Power system stability and control*. McGraw-Hill Education, 2022.

[Koe22] KOELSCH, L.: *Dynamic Incentives for Optimal Control of Competitive Power Systems*, phdthesis. Karlsruher Institute of Technology, 2022.

[Köl+20a] KÖLSCH, L.; DUPUIS, M.; BHATT, K.; KREBS, S.; HOHMANN, S.: Distributed frequency regulation for heterogeneous microgrids via steady state optimal control. In: *2020 IEEE Green Technologies Conference (GreenTech)*. IEEE. 2020, pp. 92–99.

[Köl+20b] KÖLSCH, L.; WIENINGER, K.; KREBS, S.; HOHMANN, S.: Distributed frequency and voltage control for ac microgrids based on primal-dual gradient dynamics. In: *IFAC-PapersOnLine* 53.2 (2020), pp. 12229–12236.

[Köl+21b] KÖLSCH, L.; ZELLMANN, L.; VYAS, R.; PFEIFER, M.; HOHMANN, S.: Optimal Distributed Frequency and Voltage Control for Zonal Electricity Markets. In: *IEEE Transactions on Power Systems* 37.4 (2021), pp. 2666–2678.

[KS04] KIRSCHEN, D.; STRBAC, G.: *Fundamentals of Power System Economics*. en. 1st ed. Wiley, Mar. 2004. URL: https://onlinelibrary.wiley.com/doi/book/10.1002/0470020598 (visited on 19/04/2024).

[KSW21] KRUSE, J.; SCHÄFER, B.; WITTHAUT, D.: Exploring deterministic frequency deviations with explainable AI. In: *2021 IEEE International Conference on Communications, Control, and Computing Technologies for Smart Grids (SmartGridComm)*. Oct. 2021, pp. 133–139.

[Lai+21] LAIB, K.; WATSON, J.; OJO, Y.; LESTAS, I.: Decentralized Stability Conditions in DC Microgrids. In: *2021 60th IEEE Conference on Decision and Control (CDC)*. IEEE. 2021, pp. 5659–5664.

[Lai+23] LAIB, K.; WATSON, J.; OJO, Y.; LESTAS, I.: Decentralized stability conditions for DC microgrids: Beyond passivity approaches. In: *Automatica* 149 (2023), p. 110705.

[Lan+24] LANGTRY, M.; WICHITWECHKARN, V.; WARD, R.; ZHUANG, C.; KREITMAIR, M. J.; MAKASIS, N.; CONTI, Z. X.; CHOUDHARY, R.: Impact of data for forecasting on performance of model predictive control in buildings with smart energy storage. In: *Energy and Buildings* 320 (2024), p. 114605.

[Las02] LASSETER, R. H.: Microgrids. In: *2002 IEEE power engineering society winter meeting. Conference proceedings*. Vol. 1. IEEE. 2002, pp. 305–308.

[LCF16] LEI, J.; CHEN, H.-F.; FANG, H.-T.: Primal–dual algorithm for distributed constrained optimization. In: *Systems & Control Letters* 96 (2016), pp. 110–117.

[LCH20] LI, M.; CHESI, G.; HONG, Y.: Input-feedforward-passivity-based distributed optimization over jointly connected balanced digraphs. In: *IEEE Transactions on Automatic Control* 66.9 (2020), pp. 4117–4131.

[Lei74] LEITMANN, G.: *Cooperative and non-cooperative many players differential games*. Vol. 190. Springer, 1974.

[Les22] LESSARD, L.: The analysis of optimization algorithms: A dissipativity approach. In: *IEEE Control Systems Magazine* 42.3 (2022), pp. 58–72.

[LHK19] LEHMANN, N.; HUBER, J.; KIESSLING, A.: Flexibility in the context of a cellular system model. In: *2019 16th International Conference on the European Energy Market (EEM)*. IEEE. 2019, pp. 1–6.

[Li+10] LI, L.; CHAMBERS, J. A.; LOPES, C. G.; SAYED, A. H.: Distributed Estimation Over an Adaptive Incremental Network Based on the Affine Projection Algorithm. en. In: *IEEE Transactions on Signal Processing* 58.1 (Jan. 2010), pp. 151–164. URL: http://ieeexplore.ieee.org/document/5071198/ (visited on 03/05/2024).

[Lon+23] LONG, B.; SHEN, D.; CAO, T.; RODRIGUEZ, J.; GUERRERO, J. M.; CHONG, K. T.; TENG, Y.: Passivity-based partial sequential model predictive control of T-type grid-connected converters with dynamic damping injection. In: *IEEE Transactions on Power Electronics* 38.7 (2023), pp. 8262–8281.

[Lou+17] LOU, G.; GU, W.; XU, Y.; CHENG, M.; LIU, W.: Distributed MPC-Based Secondary Voltage Control Scheme for Autonomous Droop-Controlled Microgrids. In: *IEEE Transactions on Sustainable Energy* 8.2 (2017), pp. 792–804.

[LSL20] LI, M.; SU, L.; LIU, T.: Distributed optimization with event-triggered communication via input feedforward passivity. In: *IEEE Control Systems Letters* 5.1 (2020), pp. 283–288.

[LSM21] LAWRENCE, L. S. P.; SIMPSON-PORCO, J. W.; MALLADA, E.: Linear-Convex Optimal Steady-State Control. In: *IEEE Transactions on Automatic Control* 66.11 (Jan. 2021), pp. 5377–5384.

[Lun13] LUNZE, J.: *Regelungstechnik 1*. Vol. 10. Springer, 2013.

[Lun19] LUNZE, J.: *Networked control of multi-agent systems: Consensus and synchronisation, communication structure design, self-organisation in networked systems, event-triggered control*. Rotterdam: Bookmundo, 2019.

[LW15] LIU, Q.; WANG, J.: A Second-Order Multi-Agent Network for Bound-Constrained Distributed Optimization. In: *IEEE Transactions on Automatic Control* 60.12 (2015), pp. 3310–3315.

[LY16] LUENBERGER, D. G.; YE, Y.: *Linear and Nonlinear Programming*. Vol. 228. Cham: Springer International Publishing, Jan. 2016.

[MA17] MÜLLER, M. A.; ALLGÖWER, F.: Economic and distributed model predictive control: Recent developments in optimization-based control. In: *J. of Control, Measurement, and Systems Integration* 10.2 (2017), pp. 39–52.

[Mac+20] MACHOWSKI, J.; LUBOSNY, Z.; BIALEK, J. W.; BUMBY, J. R.: *Power system dynamics: stability and control*. John Wiley & Sons, 2020.

[Mal+23] MALAN, A. J.; JANE-SONIERA, P.; STREHLE, F.; HOHMANN, S.: Passivity-based power sharing and voltage regulation in DC microgrids with unactuated buses. In: *ArXiv* (2023). URL: https://arxiv.org/abs/2301.13533.

[Mal+24a] MALAN, A. J.; FERGUSON, J.; CUCUZZELLA, M.; SCHERPEN, J.; HOHMANN, S.: Passivation of Clustered DC Microgrids with Non-Monotone Loads. In: *arXiv preprint arXiv:2404.19520* (2024).

[Mal25] MALAN, A. J.: *Stabilisation and Coordination in Networked Multi-Energy Systems using Dissipativity Theory*, phdthesis. Karlsruher Institute of Technology, 2025.

[Mar+17] MARTINI, L.; BRUNNER, H.; RODRIGUEZ, E.; CAERTS, C.; STRASSER, T. I.; BURT, G. M.: Grid of the future and the need for a decentralised control architecture: the web-of-cells concept. In: *CIRED-Open Access Proceedings Journal* 2017.1 (2017), pp. 1162–1166.

[Mar+21] MARKOVIC, U.; STANOJEV, O.; ARISTIDOU, P.; VRETTOS, E.; CALLAWAY, D.; HUG, G.: Understanding small-signal stability of low-inertia systems. In: *IEEE Transactions on Power Systems* 36.5 (2021), pp. 3997–4017.

[May+00] MAYNE, D. Q.; RAWLINGS, J. B.; RAO, C. V.; SCOKAERT, P. O. M.: Constrained model predictive control: Stability and optimality. In: *Automatica* 36.6 (2000), pp. 789–814.

[MB11] MATEI, I.; BARAS, J. S.: Performance Evaluation of the Consensus-Based Distributed Subgradient Method Under Random Communication Topologies. In: *IEEE Journal of Selected Topics in Signal Processing* 5.4 (Aug. 2011), pp. 754–771. URL: https://ieeexplore.ieee.org/abstract/document/5720506 (visited on 04/05/2024).

[MC76] MIDDLEBROOK, R. D.; CUK, S.: A General Unified Approach to Modelling Switching-Converter Power Stages. In: *1976 IEEE Power Electronics Specialists Conference*. June 1976, pp. 18–34. URL: https://ieeexplore.ieee.org/abstract/document/7072895 (visited on 27/05/2024).

[MCWG+95] MAS-COLELL, A.; WHINSTON, M. D.; GREEN, J. R. et al.: *Microeconomic theory*. Vol. 1. Oxford university press New York, 1995.

[Mil+18] MILANO, F.; DÖRFLER, F.; HUG, G.; HILL, D. J.; VERBI, G.: Foundations and challenges of low-inertia systems. In: *2018 power systems computation conference (PSCC)*. IEEE. 2018, pp. 1–25.

[MK22] MORADIAN, H.; KIA, S. S.: A distributed continuous-time modified Newton–Raphson algorithm. In: *Automatica* 136 (2022), p. 109886.

[Mol+17] MOLZAHN, D. K.; DÖRFLER, F.; SANDBERG, H.; LOW, S. H.; CHAKRABARTI, S.; BALDICK, R.; LAVAEI, J.: A survey of distributed optimization and control algorithms for electric power systems. In: *IEEE Transactions on Smart Grid* 8.6 (2017), pp. 2941–2962.

[MS20] MACHADO, J. E.; SCHIFFER, J.: A passivity-inspired design of power-voltage droop controllers for DC microgrids with electrical network dynamics. In: *2020 59th IEEE Conference on Decision and Control (CDC)*. ISSN: 2576-2370. Dec. 2020, pp. 3060–3065. URL: https://ieeexplore.ieee.org/abstract/document/9303758?casa_token=y9AOwG72N1MAAAAA:JWrdnKpNaH19RqanoVEgD5wFVZ3wrI73zinRlMigddMbNciGYi7RuyEunyI2cOKcIgPmqpYXDg (visited on 01/05/2024).

[Nah+20] NAHATA, P.; SOLOPERTO, R.; TUCCI, M.; MARTINELLI, A.; FERRARI-TRECATE, G.: A passivity-based approach to voltage stabilization in DC microgrids with ZIP loads. In: *Automatica* 113 (2020), p. 108770.

[Nah+21] NAHATA, P.; BELLA, A. L.; SCATTOLINI, R.; FERRARI-TRECATE, G.: Hierarchical Control in Islanded DC Microgrids With Flexible Structures. en. In: *IEEE Transactions on Control Systems Technology* 29.6 (Nov. 2021), pp. 2379–2392. URL: https://ieeexplore.ieee.org/document/9284559/ (visited on 30/04/2024).

[Nav+20] NAVON, A.; BEN YOSEF, G.; MACHLEV, R.; SHAPIRA, S.; ROY CHOWDHURY, N.; BELIKOV, J.; ORDA, A.; LEVRON, Y.: Applications of Game Theory to Design and Operation of Modern Power Systems: A Comprehensive Review. In: *Energies* 13.15 (Jan. 2020), p. 3982. URL: https://www.mdpi.com/1996-1073/13/15/3982 (visited on 02/06/2024).

[NB01] NEDIC, A.; BERTSEKAS, D. P.: Incremental subgradient methods for nondifferentiable optimization. In: *SIAM Journal on Optimization* 12.1 (2001), pp. 109–138.

[Nes18] NESTEROV, Y.: *Lectures on convex optimization*. Vol. 137. Springer, 2018.

[NFT19] NAHATA, P.; FERRARI-TREEATE, G.: Passivity-based voltage and frequency stabilization in AC microgrids. In: *2019 18th European Control Conference (ECC)*. IEEE. 2019, pp. 1890–1895.

[NI23] NISHINO, T.; ISHIZAKI, T.: Estimation of Domain of Attraction Based on Equilibrium-Independent Passivity of Power Systems. In: *IFAC-PapersOnLine* 56.2 (2023), pp. 2299–2304.

[NO09] NEDIC, A.; OZDAGLAR, A.: Distributed subgradient methods for multi-agent optimization. In: *IEEE Transactions on Automatic Control* 54.1 (2009), pp. 48–61.

[Nor17] NORWEGIAN MINISTRY OF CLIMATE AND ENVIRONMENT: *Norways Climate Strategy for 2030: a transformational approach within a European cooperation framework*. 2017. URL: https://www.regjeringen.no/contentassets/7d3c209f821248da8d4727713ab9619c/en-gb/pdfs/stm201620170041000engpdfs.pdf (visited on 20/04/2024).

[NOS17] NEDIC, A.; OLSHEVSKY, A.; SHI, W.: Achieving geometric convergence for distributed optimization over time-varying graphs. In: *SIAM Journal on Optimization* 27.4 (2017), pp. 2597–2633.

[Not+23] NOTARNICOLA, I.; BIN, M.; MARCONI, L.; NOTARSTEFANO, G.: The Gradient Tracking Is a Distributed Integral Action. In: *IEEE Transactions on Automatic Control* (2023).

[NPC03] NOGALES, F. J.; PRIETO, F. J.; CONEJO, A. J.: A Decomposition Methodology Applied to the Multi-Area Optimal Power Flow Problem. en. In: *Annals of Operations Research* 120 (2003), pp. 99–116.

[NTG18] NOROOZI, N.; TRIP, S.; GEISELHART, R.: Model predictive control of DC microgrids: current sharing and voltage regulation. In: vol. 51. 23. IFAC-PapersOnLine, 2018, pp. 124–129.

[NW99] NOCEDAL, J.; WRIGHT, S. J.: *Numerical optimization*. Springer, 1999.

[NZ12] NAGURNEY, A.; ZHANG, D.: *Projected dynamical systems and variational inequalities with applications*. Vol. 2. Springer Science & Business Media, 2012.

[Oli+14] OLIVARES, D. E.; MEHRIZI-SANI, A.; ETEMADI, A. H.; CAÑIZARES, C. A.; IRAVANI, R.; KAZERANI, M.; HAJIMIRAGHA, A. H.; GOMIS-BELLMUNT, O.; SAEEDIFARD, M.; PALMA-BEHNKE, R. et al.: Trends in microgrid control. In: *IEEE Transactions on Smart Grid* 5.4 (2014), pp. 1905–1919.

[Par+17] PARISIO, A.; WIEZOREK, C.; KYNTÄJÄ, T.; ELO, J.; STRUNZ, K.; JOHANSSON, K. H.: Cooperative MPC-Based Energy Management for Networked Microgrids. In: *IEEE Transactions on Smart Grid* 8.6 (Nov. 2017), pp. 3066–3074. URL: https://ieeexplore.ieee.org/document/8004502 (visited on 02/05/2024).

[PB14] PARIKH, N.; BOYD, S.: Proximal algorithms. In: *Foundations and trends® in Optimization* 1.3 (2014), pp. 127–239.

[Pey+19] PEYGHAMI, S.; DAVARI, P.; ZHOU, D.; MAHMUD, F.; BLAABJERG, F. et al.: Wear-out failure of a power electronic converter under inversion and rectification modes. In: *2019 IEEE Energy Conversion Congress and Exposition (ECCE)*. IEEE. 2019, pp. 1598–1604.

[PFV16] PEREIRA, S.; FERREIRA, P.; VAZ, A.: Optimization modeling to support renewables integration in power systems. en. In: *Renewable and Sustainable Energy Reviews* 55 (Mar. 2016), pp. 316–325. URL: https://linkinghub.elsevier.com/retrieve/pii/S1364032115011958 (visited on 18/04/2024).

[Pin23] PINSON, P.: What May Future Electricity Markets Look Like? In: *Journal of Modern Power Systems and Clean Energy* 11.3 (May 2023). Conference Name: Journal of Modern Power Systems and Clean Energy, pp. 705–713. URL: https://ieeexplore.ieee.org/abstract/document/10049815 (visited on 19/04/2024).

[Pol64] POLYAK, B. T.: Some methods of speeding up the convergence of iteration methods. In: *Ussr computational mathematics and mathematical physics* 4.5 (1964), pp. 1–17.

[PZP10] PRITCHARD, G.; ZAKERI, G.; PHILPOTT, A.: A Single-Settlement, Energy-Only Electric Power Market for Unpredictable and Intermittent Participants. In: *Operations Research* 58.4 (2010). Publisher: INFORMS, pp. 1210–1219. URL: https://www.jstor.org/stable/40793317 (visited on 19/04/2024).

[QL17] QU, G.; LI, N.: Harnessing smoothness to accelerate distributed optimization. In: *IEEE Transactions on Control of Network Systems* 5.3 (2017), pp. 1245–1260.

[Raw+08] RAWLINGS, J. B.; BONNÉ, D.; JORGENSEN, J. B.; VENKAT, A. N.; JORGENSEN, S. B.: Unreachable setpoints in model predictive control. In: *IEEE Transactions on Automatic Control* 53.9 (2008), pp. 2209–2215.

[Raz+20] RAZZANELLI, M.; CRISOSTOMI, E.; PALLOTTINO, L.; PANNOCCHIA, G.: Distributed Model Predictive Control for Energy Management in a Network of Microgrids Using the Dual Decomposition Method. In: *Optimal Control Applications and Methods* 41.1 (Jan. 2020), pp. 25–41. URL: https://onlinelibrary.wiley.com/doi/10.1002/oca.2504 (visited on 04/06/2024).

[RMD17] RAWLINGS, J. B.; MAYNE, D. Q.; DIEHL, M.: *Model predictive control: theory, computation, and design*. Vol. 2. Nob Hill Publishing, 2017.

[Roc+12] ROCABERT, J.; LUNA, A.; BLAABJERG, F.; RODRIGUEZ, P.: Control of power converters in AC microgrids. In: *IEEE Transactions on Power Electronics* 27.11 (2012), pp. 4734–4749.

[Rud+06] RUDION, K.; ORTHS, A.; STYCZYNSKI, Z. A.; STRUNZ, K.: Design of benchmark of medium voltage distribution network for investigation of DG integration. In: *IEEE Power Eng. Soc. General Meeting*. 2006, 6–pp.

[RW98] ROCKAFELLAR, R. T.; WETS, R. J. B.: *Variational Analysis*. Ed. by BERGER, M.; DE LA HARPE, P.; HIRZEBRUCH, F.; HITCHIN, N. J.; HÖRMANDER, L.; KUPIAINEN, A.; LEBEAU, G.; RATNER, M.; SERRE, D.; SINAI, Y. G.; SLOANE, N. J. A.; VERSHIK, A. M.; WALDSCHMIDT, M. Vol. 317. Grundlehren Der Mathematischen Wissenschaften. Berlin, Heidelberg: Springer Berlin Heidelberg, 1998. URL: http://link.springer.com/10.1007/978-3-642-02431-3 (visited on 17/07/2024).

[Say14] SAYED, A.: Adaptation, Learning, and Optimization over Networks. In: *Foundations and Trends® in Machine Learning* 7.4-5 (Jan. 2014), pp. 311–801.

[SB09] SCHRÖDER, D.; BÖCKER, J.: *Elektrische antriebe-regelung von antriebssystemen*. Vol. 2. Springer, 2009.

[Sch+14] SCHIFFER, J.; ORTEGA, R.; ASTOLFI, A.; RAISCH, J.; SEZI, T.: Conditions for stability of droop-controlled inverter-based microgrids. In: *Automatica* 50.10 (Oct. 2014), pp. 2457–2469. URL: https://www.sciencedirect.com/science/article/pii/S0005109814003100 (visited on 24/04/2024).

[Sch+16] SCHIFFER, J.; ZONETTI, D.; ORTEGA, R.; STANKOVIĆ, A. M.; SEZI, T.; RAISCH, J.: A survey on modeling of microgrids—From fundamental physics to phasors and voltage sources. In: *Automatica* 74 (2016), pp. 135–150.

[SDPS16a] STEGINK, T.; DE PERSIS, C.; SCHAFT, A. VAN DER: A unifying energy-based approach to stability of power grids with market dynamics. In: *IEEE Transactions on Automatic Control* 62.6 (2016), pp. 2612–2622.

[SDPS16b] STEGINK, T.; DE PERSIS, C.; SCHAFT, A. VAN DER: Optimal power dispatch in networks of high-dimensional models of synchronous machines. In: *2016 IEEE 55th Conference on Decision and Control (CDC)*. IEEE. 2016, pp. 4110–4115.

[SGV14] SHAFIEE, Q.; GUERRERO, J. M.; VASQUEZ, J. C.: Distributed Secondary Control for Islanded Microgrids—A Novel Approach. In: *IEEE Transactions on Power Electronics* 29.2 (Feb. 2014), pp. 1018–1031. URL: https://ieeexplore.ieee.org/document/6507301 (visited on 24/04/2024).

[Shi+15] SHI, W.; LING, Q.; WU, G.; YIN, W.: Extra: An exact first-order algorithm for decentralized consensus optimization. In: *SIAM Journal on Optimization* 25.2 (2015), pp. 944–966.

[SJK12] SEPULCHRE, R.; JANKOVIC, M.; KOKOTOVIC, P. V.: *Constructive nonlinear control*. Springer Science & Business Media, 2012.

[SNG20] SADOLLAH, A.; NASIR, M.; GEEM, Z. W.: Sustainability and Optimization: From Conceptual Fundamentals to Applications. en. In: *Sustainability* 12.5 (Jan. 2020). Number: 5 Publisher: Multidisciplinary Digital Publishing Institute, p. 2027. URL: https://www.mdpi.com/2071-1050/12/5/2027 (visited on 18/04/2024).

[SP+15] SIMPSON-PORCO, J. W.; SHAFIEE, Q.; DÖRFLER, F.; VASQUEZ, J. C.; GUERRERO, J. M.; BULLO, F.: Secondary Frequency and Voltage Control of Islanded Microgrids via Distributed Averaging. In: *IEEE Transactions on Industrial Electronics* 62.11 (2015), pp. 7025–7038.

[SP17] SIMPSON-PORCO, J. W.: A theory of solvability for lossless power flow equations—Part I: Fixed-point power flow. In: *IEEE Transactions on Control of Network Systems* 5.3 (2017), pp. 1361–1372.

[SP18] SIMPSON-PORCO, J. W.: Equilibrium-independent dissipativity with quadratic supply rates. In: *IEEE Transactions on Automatic Control* 64.4 (2018), pp. 1440–1455.

[SPDB12] SIMPSON-PORCO, J. W.; DÖRFLER, F.; BULLO, F.: Droop-Controlled Inverters are Kuramoto Oscillators*. In: *IFAC Proceedings Volumes*. 3rd IFAC Workshop on Distributed Estimation and Control in Networked Systems 45.26 (Sept. 2012), pp. 264–269.

[SPDB13] SIMPSON-PORCO, J. W.; DÖRFLER, F.; BULLO, F.: Synchronization and power sharing for droop-controlled inverters in islanded microgrids. In: *Automatica* 49.9 (Sept. 2013), pp. 2603–2611. URL: https://www.sciencedirect.com/science/article/pii/S0005109813002884 (visited on 24/04/2024).

[SPDB17] SIMPSON-PORCO, J. W.; DÖRFLER, F.; BULLO, F.: Voltage Stabilization in Microgrids via Quadratic Droop Control. In: *IEEE Transactions on Automatic Control* 62.3 (Mar. 2017). Conference Name: IEEE Transactions on Automatic Control, pp. 1239–1253. URL: https://ieeexplore.ieee.org/abstract/document/7500071.

[SS+43] STEINBERG, M. J.; SMITH, T. H. et al.: Economy loading of power plants and electric systems. In: (1943).

[Sta30] STAHL, E. C.: Load division in interconnections. In: *Electrical World* 95 (1930), pp. 434–438.

[Sta31] STAHL, E. C.: Economic loading of generating stations. In: *Electrical Engineering* 50.9 (1931), pp. 722–727.

[Ste+18] STEGINK, T.; CHERUKURI, A.; DE PERSIS, C.; VAN DER SCHAFT, A.; CORTES, J.: Stable Interconnection of Continuous-Time Price-Bidding Mechanisms with Power Network Dynamics. In: *2018 Power Systems Computation Conference (PSCC)*. June 2018, pp. 1–6. URL: https://ieeexplore.ieee.org/document/8443005 (visited on 05/05/2024).

[Ste+19] STEGINK, T.; CHERUKURI, A.; DE PERSIS, C.; SCHAFT, A. VAN DER; CORTÉS, J.: Hybrid Interconnection of Iterative Bidding and Power Network Dynamics for Frequency Regulation and Optimal Dispatch. In: *IEEE Transactions on Control of Network Systems* 6.2 (June 2019), pp. 572–585. URL: https://ieeexplore.ieee.org/abstract/document/8411329 (visited on 04/05/2024).

[Str+19] STREHLE, F.; MALAN, A. J.; KREBS, S.; HOHMANN, S.: A port-Hamiltonian approach to plug-and-play voltage and frequency control in islanded inverter-based AC microgrids. In: *2019 IEEE 58th Conference on Decision and Control (CDC)*. IEEE. 2019, pp. 4648–4655.

[Str+20] STREHLE, F.; PFEIFER, M.; MALAN, A. J.; KREBS, S.; HOHMANN, S.: A Scalable Port-Hamiltonian Approach to Plug-and-Play Voltage Stabilization in DC Microgrids. In: *IEEE Conf. on Control Technology and Applications*. 2020.

[Str+21] STREHLE, F.; NAHATA, P.; MALAN, A. J.; HOHMANN, S.; FERRARI-TRECATE, G.: A unified passivity-based framework for control of modular islanded AC microgrids. In: *IEEE Transactions on Control Systems Technology* 30.5 (2021), pp. 1960–1976.

[Str24] STREHLE, F.: *A Framework for Decentralized Stabilization in Networked Energy Systems: A Passivity-Based Approach*, phdthesis. Karlsruher Institute of Technology, 2024.

[Sul+17] SULTANA, W. R.; SAHOO, S. K.; SUKCHAI, S.; YAMUNA, S.; VENKATESH, D.: A review on state of art development of model predictive control for renewable energy applications. In: *Renewable and sustainable energy reviews* 76 (2017), pp. 391–406.

[SW00] SCHERER, C.; WEILAND, S.: Linear matrix inequalities in control. In: *Lecture Notes, Dutch Institute for Systems and Control, Delft, The Netherlands* 3.2 (2000).

[Tay15] TAYLOR, J. A.: *Convex optimization of power systems*. Cambridge University Press, 2015.

[Teg+16] TEGLING, E.; ANDREASSON, M.; SIMPSON-PORCO, J. W.; SANDBERG, H.: Improving performance of droop-controlled microgrids through distributed PI-control. In: *2016 American Control Conference (ACC)*. ISSN: 2378-5861. July 2016, pp. 2321–2327.

[TFT20] TUCCI, M.; FERRARI-TRECATE, G.: A scalable, line-independent control design algorithm for voltage and frequency stabilization in AC islanded microgrids. In: *Automatica* 111 (2020), p. 108577.

[TM24a] THE MATHWORKS, I.: *Fixed Step Solvers in Simulink*. en. Sept. 2024. URL: https://de.mathworks.com/help/simulink/ug/fixed-step-solvers-in-simulink.html (visited on 01/12/2024).

[TM24b] THE MATHWORKS, I.: *Variable Step Solvers in Simulink*. en. Sept. 2024. URL: https://de.mathworks.com/help/simulink/ug/variable-step-solvers-in-simulink-1.html#bsc6i4i (visited on 01/12/2024).

[TRFT17] TUCCI, M.; RIVERSO, S.; FERRARI-TRECATE, G.: Line-independent plug-and-play controllers for voltage stabilization in DC microgrids. In: *IEEE Transactions on Control Systems Technology* 26.3 (2017), pp. 1115–1123.

[Tuc+16] TUCCI, M.; RIVERSO, S.; VASQUEZ, J. C.; GUERRERO, J. M.; FERRARI-TRECATE, G.: A Decentralized Scalable Approach to Voltage Control of DC Islanded Microgrids. In: *IEEE Transactions on Control Systems Technology* 24.6 (2016), pp. 1965–1979.

[Tuc+18] TUCCI, M.; MENG, L.; GUERRERO, J. M.; FERRARI-TRECATE, G.: Stable current sharing and voltage balancing in DC microgrids: A consensus-based secondary control layer. In: *Automatica* 95 (2018), pp. 1–13.

[Umw25] UMWELTBUNDESAMT: Kraftwerke: konventionelle und erneuerbare Energieträger in Deutschland. de. In: *Daten zur Umwelt und Energie* (Apr. 2025). URL: https://www.umweltbundesamt.de/daten/energie/kraftwerke-konventionelle-erneuerbare#kraftwerkstandorte-in-deutschland (visited on 03/08/2025).

[Var+15] VARAGNOLO, D.; ZANELLA, F.; CENEDESE, A.; PILLONETTO, G.; SCHENATO, L.: Newton-Raphson consensus for distributed convex optimization. In: *IEEE Transactions on Automatic Control* 61.4 (2015), pp. 994–1009.

[Var92] VARIAN, H. R.: *Microeconomic analysis*. Vol. 3. Norton New York, 1992.

[vdS17] VAN DER SCHAFT, A.: *L2-Gain and Passivity Techniques in Nonlinear Control*. 3rd. Communications and control engineering. Cham: Springer, 2017.

[Vel+19a] VELASQUEZ, M. A.; BARREIRO-GOMEZ, J.; QUIJANO, N.; CADENA, A. I.; SHAHIDEHPOUR, M.: Distributed model predictive control for economic dispatch of power systems with high penetration of renewable energy resources. In: *Int. Journal of Electrical Power & Energy Systems* 113 (2019), pp. 607–617.

[Vel+19b] VELASQUEZ, M. A.; BARREIRO-GOMEZ, J.; QUIJANO, N.; CADENA, A. I.; SHAHIDEHPOUR, M.: Intra-hour microgrid economic dispatch based on model predictive control. In: *IEEE Transactions on Smart Grid* 11.3 (2019), pp. 1968–1979.

[Ven+08] VENKAT, A. N.; HISKENS, I. A.; RAWLINGS, J. B.; WRIGHT, S. J.: Distributed MPC strategies with application to power system automatic generation control. In: *IEEE Transactions on Control Systems Technology* 16.6 (2008), pp. 1192–1206.

[VRW05] VENKAT, A. N.; RAWLINGS, J. B.; WRIGHT, S. J.: 'Stability and Optimality of Distributed Model Predictive Control'. In: *Proceedings of the 44th IEEE Conference on Decision and Control*. 2005, pp. 6680–6685.

[VSZ95] VENKATASUBRAMANIAN, V.; SCHATTLER, H.; ZABORSZKY, J.: Fast time-varying phasor analysis in the balanced three-phase large electric power system. In: *IEEE Transactions on Automatic Control* 40.11 (1995), pp. 1975–1982.

[Vu+15] VU, T. V.; PARAN, S.; DIAZ, F.; EL MEYZANI, T.; EDRINGTON, C. S.: Model predictive control for power control in islanded DC microgrids. In: *Ann. Conf. of the IEEE Industrial Electronics Soc.* 2015, pp. 001610–001615.

[WA04] WEN, J. T.; ARCAK, M.: A unifying passivity framework for network flow control. In: *IEEE Transactions on automatic control* 49.2 (2004), pp. 162–174.

[Wat+19] WATSON, J.; OJO, Y.; LESTAS, I.; SPANIAS, C.: Stability of power networks with grid-forming converters. In: *2019 IEEE Milan PowerTech*. IEEE. 2019, pp. 1–6.

[Wat+21] WATSON, J. D.; OJO, Y.; LAIB, K.; LESTAS, I.: A scalable control design for grid-forming inverters in microgrids. In: *IEEE Transactions on Smart Grid* 12.6 (2021), pp. 4726–4739.

[WB06] WÄCHTER, A.; BIEGLER, L. T.: On the implementation of an interior-point filter line-search algorithm for large-scale nonlinear programming. In: *Mathematical programming* 106 (2006), pp. 25–57.

[WE10] WANG, J.; ELIA, N.: Control approach to distributed optimization. In: *2010 48th Annual Allerton Conference on Communication, Control, and Computing (Allerton)*. IEEE. 2010, pp. 557–561.

[Wil72] WILLEMS, J. C.: Dissipative dynamical systems part I: General theory. In: *Archive for rational mechanics and analysis* 45.5 (1972), pp. 321–351.

[WL20] WANG, J.; LU, X.: Sustainable and resilient distribution systems with networked microgrids. In: *Proceedings of the IEEE* 108.2 (2020), pp. 238–241.

[WRL18] WEISSBACH, T.; REMPPIS, S.; LENS, H.: Impact of Current Market Developments in Europe on Deterministic Grid Frequency Deviations and Frequency Restauration Reserve Demand. In: *2018 15th International Conference on the European Energy Market (EEM)*. ISSN: 2165-4093. June 2018, pp. 1–6.

[XXM19] XING, X.; XIE, L.; MENG, H.: Cooperative Energy Management Optimization Based on Distributed MPC in Grid-Connected Microgrids Community. In: *International Journal of Electrical Power & Energy Systems* 107 (May 2019), pp. 186–199. URL: https://linkinghub.elsevier.com/retrieve/pii/S0142061518325997 (visited on 04/06/2024).

[Yan+19] YANG, T.; YI, X.; WU, J.; YUAN, Y.; WU, D.; MENG, Z.; HONG, Y.; WANG, H.; LIN, Z.; JOHANSSON, K. H.: A survey of distributed optimization. In: *Annual Reviews in Control* 47 (2019), pp. 278–305.

[Yan+22] YANG, Y.; GUAN, X.; JIA, Q.-S.; YU, L.; XU, B.; SPANOS, C. J.: *A Survey of ADMM Variants for Distributed Optimization: Problems, Algorithms and Features*. Tech. rep. Aug. 2022. URL: http://arxiv.org/pdf/2208.03700v2.

[Yao+18] YAO, L.; YUAN, Y.; SUNDARAM, S.; YANG, T.: Distributed finite-time optimization. In: *2018 IEEE 14th International Conference on Control and Automation (ICCA)*. IEEE. 2018, pp. 147–154.

[Zan+11] ZANELLA, F.; VARAGNOLO, D.; CENEDESE, A.; PILLONETTO, G.; SCHENATO, L.: Newton-Raphson consensus for distributed convex optimization. In: *2011 50th IEEE Conference on Decision and Control and European Control Conference*. IEEE. 2011, pp. 5917–5922.

[ZB15] ZELAZO, D.; BÜRGER, M.: On the robustness of uncertain consensus networks. In: *IEEE Transactions on Control of Network Systems* 4.2 (2015), pp. 170–178.

[ZD15] ZHAO, J.; DÖRFLER, F.: Distributed control and optimization in DC microgrids. In: *Automatica* 61 (2015), pp. 18–26.

[ZDMK12] ZIVIC DJUROVIC, M.; MILACIC, A.; KRSULJA, M.: A simplified model of quadratic cost function for thermal generators. In: *Proceedings of the 23rd International DAAAM Symposium, Zadar, Croatia*. 2012, pp. 24–27.

[Zei+13] ZEILINGER, M.; PU, Y.; RIVERSO, S.; FERRARI-TRECATE, G.; JONES, C.: Plug and Play Distributed Model Predictive Control Based on Distributed Invariance and Optimization. In: *52nd IEEE Conference on Decision and Control*. Dec. 2013, pp. 5770–5776. URL: https://ieeexplore.ieee.org/abstract/document/6760799 (visited on 05/06/2024).

[Zhe+24] ZHENG, T.; LOIZOU, N.; YOU, P.; MALLADA, E.: Dissipative Gradient Descent Ascent Method: A Control Theory Inspired Algorithm for Min-max Optimization. In: *IEEE Control Systems Letters* (2024).

[ZMD15] ZHAO, C.; MALLADA, E.; DÖRFLER, F.: Distributed Frequency Control for Stability and Economic Dispatch in Power Networks. In: *2015 American Control Conference (ACC)*. July 2015, pp. 2359–2364. URL: https://ieeexplore.ieee.org/document/7171085 (visited on 02/06/2024).

[ZP15] ZHANG, X.; PAPACHRISTODOULOU, A.: A real-time control framework for smart power networks: Design methodology and stability. In: *Automatica* 58 (2015), pp. 43–50.

[ZW10] ZHONG, Q.-C.; WEISS, G.: Synchronverters: Inverters that mimic synchronous generators. In: *IEEE Transactions on Industrial Electronics* 58.4 (2010), pp. 1259–1267.

[ZYH17] ZENG, X.; YI, P.; HONG, Y.: Distributed Continuous-Time Algorithm for Constrained Convex Optimizations via Nonsmooth Analysis Approach. In: *IEEE Transactions on Automatic Control* 62.10 (2017), pp. 5227–5233.